Universitat Autònoma de Barcelona

# Genomic Analyses of the CUP-SHAPED COTYLEDON1 Network

**Mariana Bustamante Montoya**

Universitat Autònoma de Barcelona

Doctoral Thesis

# Genomic Analyses of the *CUP-SHAPED COTYLEDON1* Network

*Author:*
Mariana Bustamante Montoya

*Supervisor:*
Dr. José Luis Riechmann

*Tutor:*
Dra. Roser Tolrà

*A thesis submitted in fulfillment of the requirements for the degree of Doctor of Philosophy*

*in the*

Facultat de Biociències
Universitat Autònoma de Barcelona

November 1, 2017

# Declaration of Authorship

I, Mariana Bustamante Montoya, declare that this thesis titled, "Genomic Analyses of the *CUP-SHAPED COTYLEDON1* Network" and the work presented in it are my own. I confirm that:

- This work was done wholly or mainly while in candidature for a research degree at this University.
- Where any part of this thesis has previously been submitted for a degree or any other qualification at this University or any other institution, this has been clearly stated.
- Where I have consulted the published work of others, this is always clearly attributed.
- Where I have quoted from the work of others, the source is always given. With the exception of such quotations, this thesis is entirely my own work.
- I have acknowledged all main sources of help.
- Where the thesis is based on work done by myself jointly with others, I have made clear exactly what was done by others and what I have contributed myself.

Signed:

_____

Date:

_____

*"Sólo viviendo absurdamente se podría romper alguna vez este absurdo infinito."*

Julio Cortázar

# *Abstract*

Flower development has been an active field of research for many years and the thorough analysis of genetic interactions provided a general framework to understand how floral organs are specified. More recently, the introduction of genome-wide technologies helped confirm and expand the existing models about organ identity establishment and other important events during flower formation. Still, there are other aspects of flower development for which general models are lacking, such as the formation of floral organ boundaries.

The *Arabidopsis thaliana CUP-SHAPED COTYLEDON1* (*CUC1*) gene is a key transcription factor involved in the regulation of flower development by controlling boundary formation. In plants, proper boundaries are fundamental for meristem maintenance and to coordinate organogenesis. This occurs throughout plant development, from the early separation of cotyledons in dicots to the formation of boundaries between ovules during the reproductive phase.

CUC1 suppresses growth in the boundary regions that it helps to delimit, and it has been proposed that it does so by affecting cell division. Despite the crucial role of CUC1, the molecular mechanisms by which it controls boundary formation are still poorly understood.

Here, CUC1 regulatory network is characterized at the genome-wide level, using state-of-the-art genomic technologies. In this work, several aspects of CUC1 function were analyzed for the first time through the combination of complementary genome-wide approaches including transcriptomics, transcription factor binding profiles and protein interactome analyses. The results obtained from such techniques allowed to elucidate a set of transcriptional targets, molecular pathways and CUC1 interactors that help delineate the mechanisms by which this NAC transcription factor contributes to the establishment of floral organ boundaries.

These results represent a substantial advance in the understanding of the molecular events that are controlled by CUC1 in this key developmental stage of plant development. In this regard, this Thesis provides a foundational body of work that can be used to further explore CUC1's regulatory network.

# *Resumen*

El desarrollo de la flor ha sido un importante campo de investigación por muchos años y el análisis extensivo de interacciones genéticas resultó en un marco de referencia que permitió entender cómo se produce la especificación de los órganos florales. Recientemente, la introducción de tecnologías de nivel genómico permitió confrimar y expandir los modelos existentes sobre el establecimiento de la identidad de los órganos florales y otros eventos importantes que ocurren durante la formación de la flor. A pesar de esto, hay otros aspectos del desarrollo floral para los cuales no existen modelos generales, como el caso de la formación de los límites entre los órganos de la flor.

El gen *CUP-SHAPED COTYLEDON1* (*CUC1*) de *Arabidopsis thaliana* es un factor de transcripción clave involucrado en la regulación del desarrollo floral mediante el control de la formación de estos límites o fronteras. En las plantas, la separación correcta entre distintos tejidos es fundamental para el mantenimiento de los meristemos y para coordinar la formación de nuevos órganos. Esto ocurre a través de todo el desarrollo de la planta, desde la separación temprana de cotiledones en las dicotiledóneas, hasta la fromación de límites entre óvulos durante la fase reproductiva.

CUC1 reprime el crecimiento en la zona de los límites que contribuye a establecer y se propuso que lo hace afectando la división celular. A pesar de este rol crucial de CUC1, los mecanismos moleculares a través de los cuales controla la formación de límites no están descriptos de manera extensiva.

Aquí, la red regulatoria de CUC1 es caracterizada a nivel genómico, usando tecnologías de última generación. En este trabajo, varios aspectos de la función de CUC1 fueron analizados por primera vez mediante la combinación de enfoques complementarios que incluyen la transcriptómica, el perfil de unión al DNA del factor de transcripción y el análisis de interacción entre proteínas. Los resultados obtenidos por estas técnicas permitieron dilucidar un set de dianas transcripcionales, vías moleculares e interactores proteicos de CUC1 que ayudan a delinear los mecanismos por los cuales este factor de transcipción del tipo NAC contribuye al establecimiento de los límites entre órganos florales.

Estos resultados representan un avance sustancial para la comprensión de los eventos moleculares controlados por CUC1 en esta etapa fundamental del desarrollo de una planta. En este sentido, esta Tesis provee un cuerpo de trabajo fundacional que puede utilizarse para explorar la red regulatoria de CUC1 más profundamente.

# *Acknowledgements*

I would like to acknowledge the Spanish Ministerio de Economía, Industria y Competitividad for my PhD scholarship and the European Molecular Biology Organization for funding for my short stay in Germany.

I specially thank my PhD supervisor, José Luis, for having guided me in this path throughout the years, during good and bad moments, and for always encouraging me to learn new things and follow my interests.

Also thanks to all the Riechmann lab, past and present: Thilia and Jin, and now Tomás and Laura.

A big thanks to the CRAG services, specially the plant growth facilities and the genomic area for all the help to make my research possible.

# Contents

# List of Figures

# List of Tables

# List of Abbreviations

| | |
|---|---|
| Ab | Antibody |
| ChIP | Chromatin immunoprecipitation |
| DEG | Differentially expressed gene |
| DEX | Dexamethasone |
| dpi | Days post induction |
| FM | Floral meristem |
| IM | Inflorescence meristem |
| miRNA | microRNA |
| MS | Mass spectrometry |
| SAM | Shoot apical meristem |
| seq | Sequencing |
| TF | Transcription factor |
| TRR | Transcription regulatory region |
| WB | Western blot |
| WT | Wild type |

*a mamá y papá*

# *Objectives*

The main aim of this Thesis is to characterize the gene regulatory network and molecular mechanisms underlying the function of the *CUP-SHAPED COTYLEDON1* transcription factor during early flower development. To this end, three complementary approaches were the specific goals of the project:

- Characterize the transcriptomic response to elevated levels of CUC1 during early flower development.
- Identify the genome-wide binding regions of CUC1 in order to find its direct target genes.
- Infer the mechanism by which CUC1 modulates transcription through the characterization of the its protein interactome.

A summary of the selected experimental design is depicted in Figure 1.

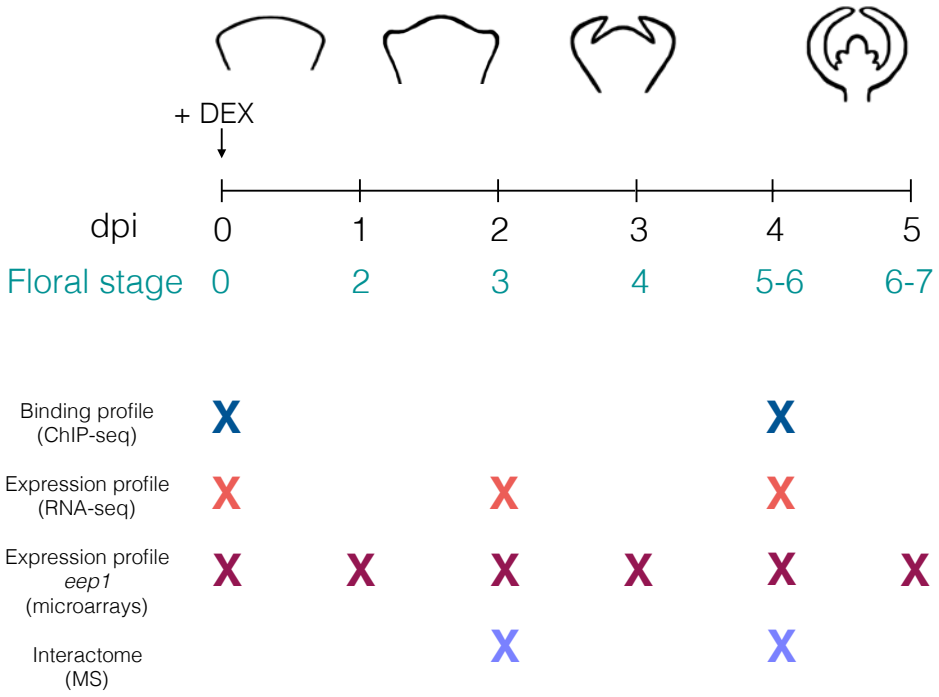


FIGURE 1: **Experimental design.** General diagram of the experimental design used for this Thesis. Crosses indicate the time points at which samples were collected and analyzed for each type of experiment: ChIP-seq (Chapter 4), RNA-seq (Chapter 3), microarrays (Chapter 2) and proteomics (Chapter 5). dpi: days post induction. Floral stages according to Smyth, Bowman, and Meyerowitz, 1990.

# Chapter 1

# Introduction

## 1.1 Flower development

The transition from vegetative to reproductive development is a key event in the life cycle of a plant. An array of environmental factors influence this transition and include temperature, light, nutrient availability and others. Endogenous signals are also required and the combination of both are reflected in the complex regulatory network of genes and pathways that control floral initiation (reviewed in Andrés and Coupland, 2012).

The reproductive capability of angiosperms, the largest group of land plants, is contained in flowers and thus understanding their development is of great interest. Even though inflorescence development and architecture can vary widely among plant species, the basic organization of floral structure is largely conserved, providing valuable insights into the evolutionary mechanisms that acted upon these structures.

In dicots, flowers begin to be formed when the shoot apical meristem (SAM) is transformed into an inflorescence meristem (IM) after the transition from vegetative to reproductive growth. Floral meristems (FM) arise from the flanks of the IM (Long and Barton, 2000; Grbić and Bleecker, 2000) and will give rise to individual flowers with four types of organs organized in concentrical whorls. The sepals arise at specific positions in the first outermost whorl, the second whorl will contain the petals, the third has the pollen-producing stamens, and the final fourth whorl contains the carpels.

A central question in biology is how different types of floral organs are produced from these meristems. The proper development of a flower requires sepals, petals, stamens and carpels to be formed in a sequential manner, respecting a canonical pattern. This requires orchestrated changes in the expression of a vast array of genes, and the characterization of the gene regulatory networks underlying these changes, despite impressive progress in the recent years, is still far from being comprehensive.

### 1.1.1 Arabidopsis and the ABC model

Flower development has been an active field of research for many years, which resulted in a richness of knowledge that makes it one of the best understood developmental processes in plants. The classic ABC model, postulated based on genetic studies performed in *Arabidopsis thaliana* and *Antirrhinum majus* (snapdragon), explained how floral organs are specified by the combinatorial activity of three functional classes of genes (Coen and Meyerowitz, 1991). These genes were initially identified in floral homeotic mutants (those in which a type of floral organ is converted into another) and the analysis of genetic interactions between them led to the creation of the ABC model (Figure 1.1).

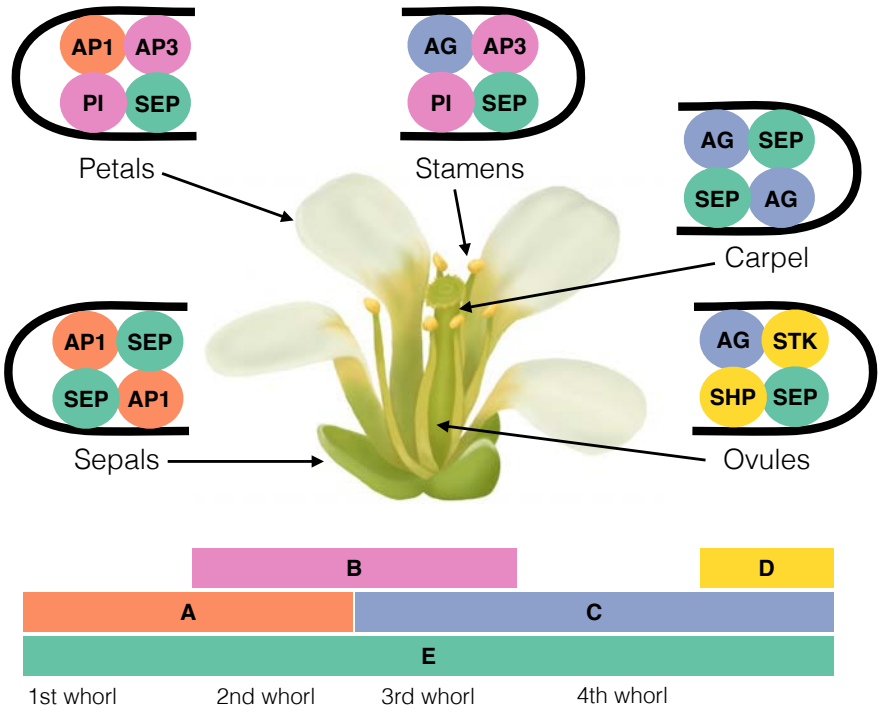


FIGURE 1.1: **Organ identity determination in *Arabidopsis thaliana*.** The upper part of the figure depicts the tetrameric protein complexes described in the floral quartet model interact with DNA (black line). The underlying ABCDE model is depicted in the bottom part, indicating the classes of genes that give rise to the different organ types from each whorl. Colors in the proteins indicate the class to which they belong. Adapted from Theissen and Saedler, 2001

According to this model, sepal identity is specified by class A genes. The combined activity of class A and class B genes specifies petal identity, while the combination of B and C activities result in stamen formation. Carpels are established through the action of class C genes. A key aspect of the ABC model is the that class A and class C genes are able to repress each other.

The subsequent cloning of the identified *Arabidopsis* genes that form

part of the ABC model allowed a more thorough investigation. Their expression patterns were observed through *in-situ* hybridization experiments that mostly confirmed the predictions of the ABC model and, together with other type of approaches, allowed to better understand their functions.

In *Arabidopsis*, the master regulators that belong to the A class are *APETALA1* (*AP1*) and *APETALA2* (*AP2*), and their mutants show organ identity defects in the first and second whorl (sepals and petals). *APETALA3* (*AP3*) and *PISTILLATA* (*PI*) are included in the B class, so their mutation leads to defects in the second and third whorls (petals and stamens). *AGAMOUS* (*AG*) belongs to the C class and the *ag* mutants lack stamens and carpels and lose floral determinacy, leading to flowers that can have more than 100 sepals and petals.

Later, this model was expanded to include class D and E genes. Class E genes are the partially redundant *SEPALLATA1* (*SEP1*), *SEP2*, *SEP3* and *SEP4*, and are involved in the formation of all floral organ types (Pelaz et al., 2000; Ditta et al., 2004). The D-class proteins, SEEDSTICK (STK), SHATTERPROOF1 (SHP1) and SHP2, interact in larger complexes with the E-class proteins to specify ovule identity (Favaro et al., 2003; Pinyopich et al., 2003).

The thorough analysis of the genetic interactions led to the development of the floral quartet model (Theissen and Saedler, 2001), which functions as the molecular framework of the ABCDE model postulating that organs are specified by tetramers of MADS domain proteins, a group of TFs to which all of the class A-E transcription factors (TFs) (except AP2) belong to (Figure 1.1). Mass-spectrometry analyses demonstrated the *in planta* existence of the all major binary interactions proposed in the floral quartet model and provided clues towards deciphering the specificity of their interaction with DNA (Smaczniak et al., 2012a).

### 1.1.2 Introduction of genomic tools

Even though a complex network of interactions underlying floral development could be uncovered by traditional genetic analyses such as the described above, a more detailed understanding of the dynamic basis of molecular events taking place was long hindered by the difficulty to obtain precise "molecular snapshots" that included all factors involved. Furthermore, the level of genetic redundancy between important regulators of development presented a problem that in many cases could not be solved by genetic approaches. The introduction of techniques that could assess the genome-wide transcriptional response to changes (with microarrays and more recently RNA-seq) facilitated the identification of TF downstream genes, although in general they could not distinguish direct or indirect interactions. This distinction has been enabled by technologies that allow the identification of genomic sites bound by specific TFs, such as chromatin immunoprecipitation followed by next-generation sequencing (ChIP-seq) or by hybridization to tilling arrays (ChIP-chip).

All these advances have boosted our knowledge of the molecular basis of flower development and revolutionized the ability to describe and understand gene regulatory networks. They have been applied to many key transcription factors, such as SEP3 (Kaufmann et al., 2009), AP1 (Kaufmann et al., 2010b; Pajoro, Alice et al., 2014), LEAFY (LFY) (Winter et al., 2011), AP3/PI (Wuest et al., 2012), AG (Ó'Maoiléidigh et al., 2013). The growing array of results clearly indicates that gene regulatory networks that control organ identity are very complex and feature interaction loops the simple hierarchical structure once proposed cannot explain by itself.

### 1.1.3 Plant morphology and boundaries

The introduction of genome-wide technologies has been a most valuable tool to confirm and expand the existing models about organ identity establishment and other important events during flower formation. Still, there are other aspects of flower development for which general models are lacking that could take advantage of these advances. One crucial process that is still poorly understood is how flowers establish their general morphology.

It is known that floral organs arise in an organized manner from the flower primordia, and the distinct morphological structures that are developed require the formation of areas where growth is repressed and therefore can act as a physical boundary between contiguous tissues (Figure 1.2).

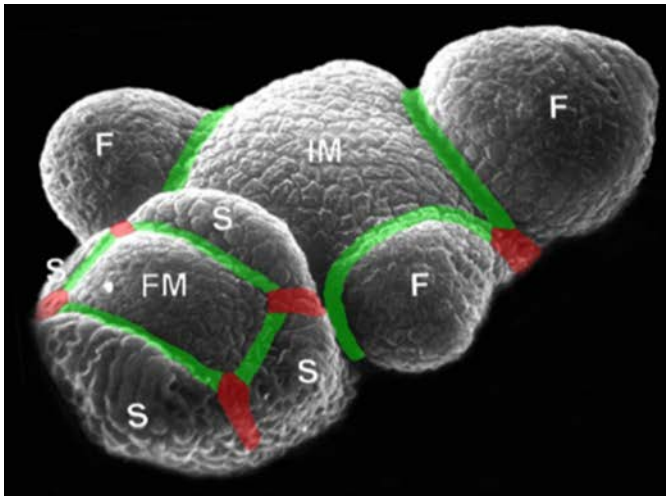


FIGURE 1.2: **Boundaries in the inflorescence meristem.** The *Arabidopsis* inflorescence meristem with organ-organ (red) and meristem-organ (green) boundaries depicted on it. IM, inflorescence meristem; FM, floral meristem; S, sepal; F, floral primordia. Adapted from (Ding et al., 2015)

Boundaries between different gene expression domains are essential for the development of multicellular organisms. The establishment of organ boundaries is a major developmental process and it occurs not only during plant development but across species during animal development also (Dahmann, Oates, and Brand, 2011; Rast and Simon, 2008; Aida and Tasaka, 2006).

In plants, proper boundaries are fundamental for meristem maintenance and to coordinate organogenesis. This occurs throughout plant development, from the early separation of cotyledons in dicots to the formation of boundaries between ovules during the reproductive phase.

Boundary cells express a particular array of transcription factors that are able to repress growth and/or cell division, which gives rise to the physical border between different cell populations, allowing cells from either side of the functional frontier to act distinctively according to their lineage fate. Different cell groups that have different gene expression profiles and will subsequently produce completely different morphologies.

Boundary gene mutants have phenotypes that show tissue fusions at different developmental stages (i.e. cotyledons, flowers) due to the lack of growth repression between arising structures. *Arabidopsis* mutants lacking the activity of boundary genes such as *CUP-SHAPED COTYLEDON1* (*CUC1*, Aida et al., 1997), *LATERAL ORGAN BOUNDARIES* (*LOB*, Bell et al., 2012), *LATERAL ORGAN FUSION1* (*LOF1*, Lee, Geisler, and Springer, 2009), *PETAL LOSS* (*PTL*, Lampugnani, Kilinc, and Smyth, 2012), *RABBIT EARS* (*RBE*, Takeda, Matsumoto, and Okada, 2004) all show fusion defects. Changes in the phlyllotactic patterning of the whole organism also occur, revealing the importance of boundary regions as organizing centers (Dahmann, Oates, and Brand, 2011).

## 1.2 The CUP-SHAPED COTYLEDON genes

The *CUP-SHAPED COTYLEDON* (*CUC*) genes (Aida et al., 1997; Vroemen et al., 2003) are key transcription factors controlling boundary formation in *Arabidopsis thaliana*. In 1997, Aida et al. found an *Arabidopsis* mutant that lacked a shoot apical meristem (SAM) and had cotyledons that failed to separate, giving rise to a goblet shaped structure (Figure 1.3). The two genes that caused this phenotype were named *CUP-SHAPED COTYLEDON1* and *2* (*CUC1* and *CUC2*).


FIGURE 1.3: **Seedling phenotypes.** Wild type (Ler) with two normal cotyledons and the cup-shaped *cuc1 cuc2* mutants.

*CUC* genes resembled a mutant from petunia characterized by Souer et al. on the previous year, that had no SAM (Souer et al., 1996). The gene

responsible, named *NO APICAL MERISTEM* (*NAM*), was expressed in the boundary regions between meristems and primordia. The transcription factors encoded by the *CUC* genes shared a conserved N-terminal domain with the petunia NAM and, together with other TFs identified thereafter with varied functions, form the NAC (petunia **N**AM and *Arabidopsis* **A**TAF1, **A**TAF2, and **C**UC) family of transcription factors. This plant-specific family is large and more than a hundred genes in *Arabidopsis* code for its members (Riechmann et al., 2000; Zhu et al., 2012; Welner et al., 2015), although the majority are involved in other biological processes and not specifically in the establishment of boundaries (Kim, Nam, and Lim, 2016; Tweneboah and Oh, 2017).

### 1.2.1 CUP-SHAPED COTYLEDON are NAC transcription factors

In *Arabidopsis*, there are three CUP-SHAPED COTYLEDON transcription factors: the more closely related CUC1 and CUC2, and the most divergent CUC3 (Figure 1.4). They share a common ancestor and the family to which they belong consists of 21 subfamilies with a similar NAC domain (Zhu et al., 2012; Wikström, Savolainen, and Chase, 2001).

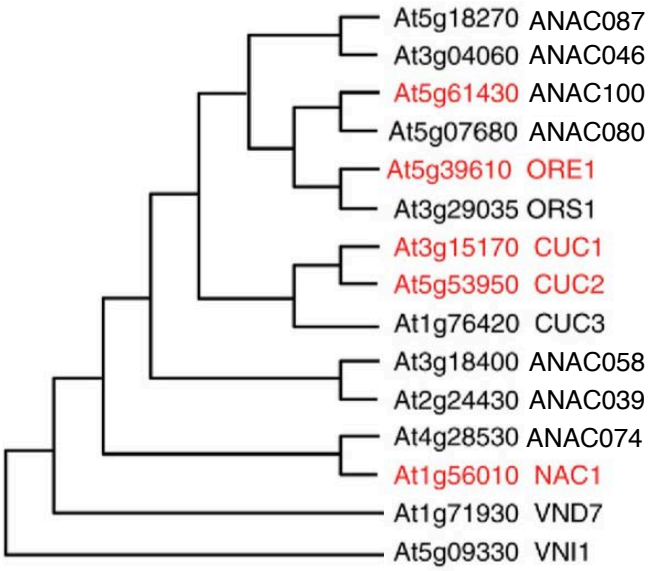


FIGURE 1.4: **CUC1 phylogeny.** Phylogeny of the subgroup of Arabidopsis thaliana NAC proteins containing the CUC1, CUC2 and CUC3 proteins. The genes targeted by the microRNA 164 (miR164) are indicated in red. Adapted from Maugarny et al., 2016 and Zhu et al., 2012.

NAC proteins typically have two domains. The N-terminal DNA binding NAC domain, which consists of approximately 160 amino acids in *Arabidopsis*, and a more variable C-terminal transcription regulatory region (TRR, Ernst, Heidi A et al., 2004; Olsen et al., 2005; Welner et al., 2015). There are five subdomains, termed A-E. The A, C and D subdomains are the most highly conserved and are involved in the formation of functional

dimers, DNA binding, and contain putative nuclear localization signals (NLSs) (Ooka et al., 2003; Olsen et al., 2005).

The NAC domain is involved in dimerization and DNA binding and the TRRs are involved in the activation or repression of transcription (reviewed in Puranik et al., 2012). The DNA binding mechanism of NAC proteins has been studied and different but similar consensus sites were found for different members of the family (Lindemose et al., 2014). The differences in the preference for the particular binding sites is largely correlated to the phylogenetic dissimilarity of the analyzed NAC proteins.

The functions of the different NAC subfamilies are very diverse. There are members involved in a wide range of biological processes such as biotic and abiotic stress response, secondary metabolism, control of flowering time, hormonal signaling pathways and more (Zhu et al., 2012; Tweneboah and Oh, 2017).

*CUC3* (Vroemen et al., 2003) appears in a separate clade from *CUC1* and *CUC2* in monocots and dicots, suggesting that their divergence occurred more than 150 million years ago (Wikström, Savolainen, and Chase, 2001).

*CUC1* and *CUC2* were generated by a gene duplication event. Afterwards they followed different evolutionary patterns in the Brassicaceae and CUC1 acquired new functionality, diverging more substantially from its ancestor (Wikström, Savolainen, and Chase, 2001; Hasson et al., 2011). Even though both genes are required for a subset of functions (ie. floral organ separation), there is certain level of specialization in others (ie. CUC2 in the control of leaf serration, where CUC1 is not involved) (Hasson et al., 2011; Nikovics et al., 2006) (see Section 1.3.3).

## 1.3 CUC genes in plant development

### 1.3.1 Expression of CUP-SHAPED COTYLEDON1

During early development, *CUC1* is expressed in the area between the arising cotyledons. Later it will be present in the axillary meristems when branching occurs and in inflorescences its expression is detected in the meristem-organ and organ-organ boundary regions.

In stage 1 flowers, *CUC1* expression is localized in the boundary region between the inflorescence meristem and the flower meristem (Figure 1.5 A). Stage 4 flowers show *CUC1*'s expression concentrated in between the sepal primordia (Figure 1.5 B, E). Later, in stages 5, 6 and 7, the highest level of *CUC1* expression is localized in the boundary between stamen primordia (Figure 1.5 B, C, F). When the gynecium is formed after stages 10-11, expression of CUC1 can be observed in between ovules, in the carpel margins (Figure 1.5 D).

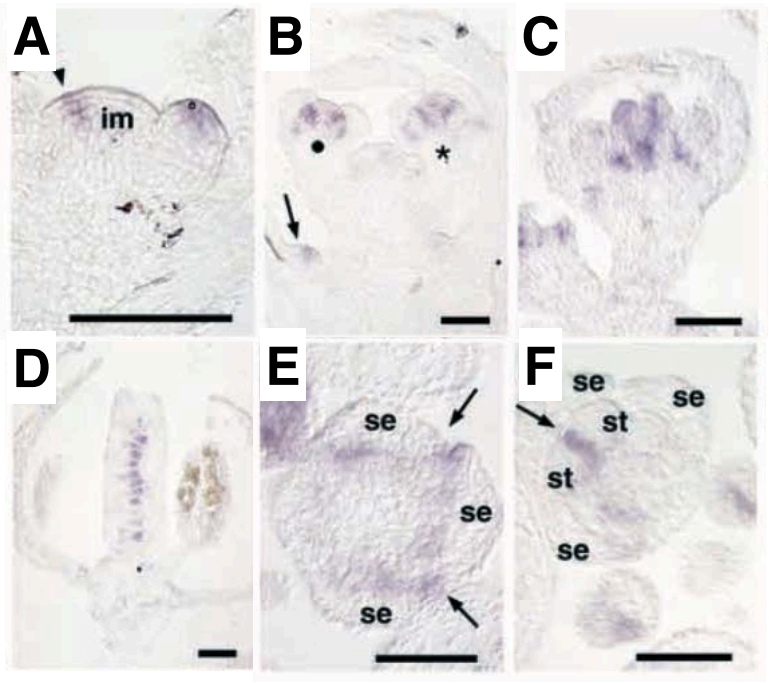


FIGURE 1.5: **CUC1 expression.** *In situ* hybridization using CUC1 anti-sense probe in inflorescences. (A) Longitudinal section through the inflorescence meristem. Arrowhead indicates boundary region between the inflorescence meristem (im) and a stage 1 floral meristem. (B) Longitudinal section through an inflorescence shoot. Filled circle, stage 4 flower; asterisk, stage 6 flower; arrow, axillary meristem. (C) Longitudinal section through a stage 7 flower. (D) Longitudinal section through a stage 10-11 flower. (E) Transverse section through a stage 4 floral meristem. Arrows indicate boundaries between individual sepal primordia. (F) Oblique transverse section through a stage 5-6 floral meristem. Arrow indicates the boundary between stamen primordia. Floral stages according to Smyth, Bowman, and Meyerowitz, 1990. se, sepal; st, stamen primordia; g, gynoecium. Scale bars, 50 $\mu$m. Adapted from (Takada et al., 2001).

### 1.3.2 CUP-SHAPED COTYLEDON in shoot apical meristem establishment and maintenance

The earliest developmental time at which CUC1 activity has been shown to be essential is in the establishment of the SAM (Aida et al., 1997; Aida, Ishida, and Tasaka, 1999). CUC1 is required during embryogenesis for the activation of SHOOT MERISTEMLESS (STM), a homeodomain transcription factor that is essential for normal meristem initiation and maintenance (Long et al., 1996; Aida, Ishida, and Tasaka, 1999).

As in *cuc* mutants, cotyledons in *stm* mutants appear fused . STM can bind *CUC1*'s promoter and is able to induce its expression, while it can also indirectly upregulate *CUC2* and *CUC3* (Spinelli et al., 2011).

The distinct mechanism between STM's action on *CUC1*, *CUC2* and *CUC3* is a factor that contributes to the idea that strict regulation of the expression *CUC1* is extremely important and very specific, to the extent that

it can be differentiated from that of its close homologs (see Section 1.4.1).

Overexpression of *CUC1* can induce adventitious shoots on cotyledons through *STM* expression (Takada et al., 2001; Hibara, Takada, and Tasaka, 2003). STM can in turn activate *miR164a*, a member of the microRNA 164 (miR164) family, which could be part of a regulatory loop to fine-tune the levels of CUC1 (Section 1.4.1, Spinelli et al., 2011).

### 1.3.3 CUP-SHAPED COTYLEDON genes in vegetative development

#### Leaf development

Later in development, *CUC* genes become involved in the development of leaves. Wild-type leaves in *Arabidopsis* are simple and feature shallow serrations on their margins. If *CUC2* is overexpressed, either by introducing a transgene or by impairment of downregulation by miR164, these serrations become deeper and bigger. On the contrary, the absence of *CUC2* expression leads to smooth leaf margins where the normal serrations are not present (Nikovics et al., 2006).

If the expression pattern of *CUC2*, usually confined to a few cells inside the leaf teeth sinuses, is altered and the protein is expressed along the whole leaf margin, the normal serrations disappear, also resulting in smooth leaf margins (Bilsborough et al., 2011)

These phenotypic modifications also appear in plants overexpressing or lacking *CUC3*, but not in *CUC1* mutants or overexpressors. This is likely because in the wild-type *CUC1* is not expressed in leaves. When CUC1 protein is expressed in *cuc2* mutants under the control of the *CUC2* promoter (pCUC2:CUC1 *cuc2*), leaf serration is restored, although in an enhanced manner in comparison with CUC2 (pCUC2:CUC2 *cuc2*) (Hasson et al., 2011).

This suggests that the CUC1 protein can functionally replace CUC2 and that the specific function that each TF will carry out depends, at least partially, in the spatial domain in which the protein is expressed. It also highlights the importance of the precise regulation of *CUC* genes expression during plant development (see Section 1.4.1).

#### Axillary meristem initiation

Axillary meristems (AMs) are primordia that give rise to shoots during vegetative growth and are developmentally analogous to FMs (Long and Barton, 2000). The developmental stage of the plant will determine whether one or the other is formed.

*CUC* genes are required for axillary meristem formation, which develop from the boundary regions between leaf primordia and the shoot apex (Raman et al., 2008). In this case, the key regulator is *CUC3*, with *CUC2* also playing a prominent role, and *CUC1* participating to a lesser extent (Raman et al., 2008).

### 1.3.4 CUP-SHAPED COTYLEDON1 in flower development

Establishment of boundaries is a critical part of floral development. When flowers are initiated by the action of key floral identity genes, such as LFY and AP1, the formation of the meristem-organ (M-O) boundary between the central zone and the peripheral zone in the inflorescence meristem occurs (Rast and Simon, 2008).

The process of M-O boundary formation is related to a local depletion of auxin that causes a reduction of the growth and division of boundary cells (Žádníková and Simon, 2014; Murray et al., 2012). After the flower begins to form, organ-organ (O-O) boundaries between the same and different whorls (intra-whorl and inter-whorl) are created.

*CUC* genes are key nodes in the genetic networks that control the formation of both types of boundaries (M-O and O-O). The mechanism by which this occur is not completely understood. The control of floral organ boundary formation is quite complex and many other factors are involved in this process in addition to *CUC* genes (see Sections 1.4.2 and 1.4.3).

In *cuc1 cuc2* mutants, there are very severe organ fusions between sepals and stamens and they often show a reduced number of petals or stamens. The fusion defects are much less severe in single mutants, which indicates a certain level of functional redundancy between *CUC* genes in floral organ establishment, in accordance to what has been observed at other developmental stages (Aida et al., 1997; Ishida et al., 2000; Takada et al., 2001; Vroemen et al., 2003; Hibara, Ken-ichiro et al., 2006; Sieber et al., 2007).

As described in Section 1.4.1, *CUC* genes are subject to regulation by the miR164 family, and the *mir164c* mutant (*early extra petals1*, *eep1*) shows extra petals in early arising flowers due to the higher level of *CUC1* and *CUC2* expression (Baker et al., 2005).

### 1.3.5 CUP-SHAPED COTYLEDON in gynoecium development

The gynoecium is the female reproductive structure of flowering plants, and *CUC* genes are also required during its development (Ishida et al., 2000). They are expressed in carpel tissues around developing ovules and *cuc* mutants have fewer ovules than the wild-type (Ishida et al., 2000; Takada et al., 2001; Vroemen et al., 2003; Kamiuchi et al., 2014). This is due to the failure to establish the medial ridge meristems (or carpel margin meristems, *CMM*s) that will form the placenta, which results in severe septum fusion defects, ultimately leading to a smaller number of ovules (Ishida et al., 2000; Nahar et al., 2012; Galbiati et al., 2013; Kamiuchi et al., 2014; Gonçalves et al., 2015).

In an analogous way to what happens during SAM development (Section 1.3.2), *STM* expression is greatly reduced in the *cuc1 cuc2* double mutant gynoecia, indicating that *CUC1* and *CUC2* are also required for its expression in the CMM (Kamiuchi et al., 2014). On the other hand, plants with miRNA resistant versions of *CUC1* and *CUC2* show an expanded pattern of

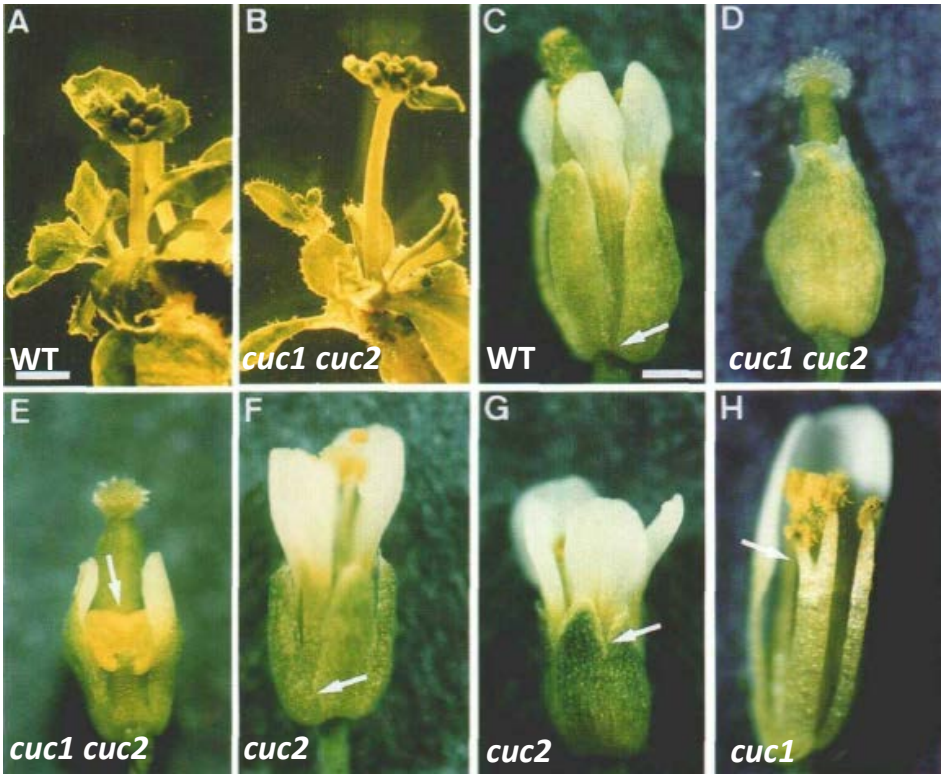


FIGURE 1.6: **Floral phenotypes in *cuc* mutants.** (A) and (B) Shoots regenerated from wild-type (A) and *cuc* mutant (B) calli. (C) Wild-type flower. Sepals are separated from the basalmost part (arrow). (D) and (E) *cuc1 cuc2* double mutant flower. A part of the fused sepals in (E) was removed to show the fused stamens (arrow). (F) and (G) *cuc2* single mutant (F) and *cuc1*/+ *cuc2*/*cuc2* (G) flowers. Arrows indicate the uppermost points of the fused sepals. (H) *cuc1* single mutant flower. The sepals and petals in the front were removed to show the fused stamens (arrow). Bar in (A) and (B) = 5 mm; bar in (C) to (H) = 1 mm. Adapted from Aida et al., 1997.

STM expression and more CMMs (normal and ectopic) are formed (Kamiuchi et al., 2014).

### 1.3.6 CUP-SHAPED COTYLEDON1 homologs in other plant species

*CUC* gene homologs are present in other plant species, and genetic analysis demonstrate that these homologs carry out functions similar or identical to those of the *CUC* genes in *Arabidopsis*.

For instance, *GOBLET* (*GOB*) is a *CUC* homolog in tomato (*Solanum lycopersicum*). *gob* mutants show defects similar to those observed in *cuc* mutants in *Arabidopsis*, such as cotyledon fusions and absence of SAM (Berger et al., 2009), as well as defects in leaf patterning (Brand et al., 2007; Blein et al., 2008) (Figure 1.7). The same type of defects are present in *Medicago truncatula NO APICAL MERISTEM* (*NAM*) mutants (Cheng et al., 2012). The *CUPULIFORMIS* (*CUP*) gene in *Antirrhinum majus* was identified through its fusion phenotypes in mutants and the severity of these

mutations suggest that the redundancy level for genes involved in boundary establishment can vary across species (Figure 1.7 Weir et al., 2004).

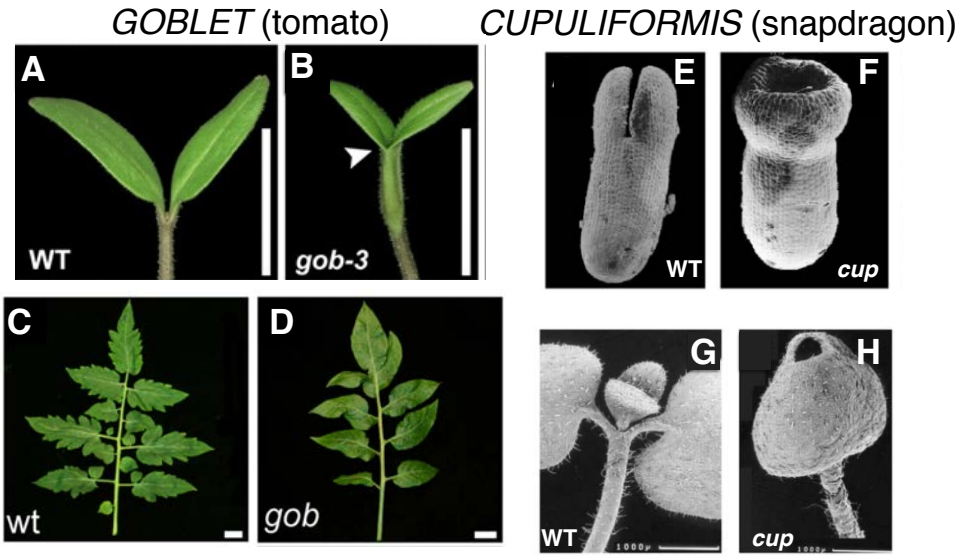


FIGURE 1.7: ***CUC* homolog phenotypes in tomato and snapdragon.** (A) Wild-type tomato seedling. (B) *gob* mutant seedling. Arrow points to the fused cotyledons. (C) Wild-type tomato leaflet with normal serrations. (D) *gob* mutant leaflets with smooth leaf margins. The serration of the leaves is lost. (E, G) Wild type *Antirrhinum majus* embryo and seedling. (F, H)*cup* mutant embryo and seedling with severe fusions. Adapted from Berger et al., 2009; Brand et al., 2007; Blein et al., 2008; Weir et al., 2004; Wang et al., 2015.

In all of the mentioned mutants floral organ fusion phenotypes were found and *CUC*'s homologs were expressed in floral organ boundaries, suggesting that their role during reproductive development is also conserved across species(Weir et al., 2004; Berger et al., 2009; Cheng et al., 2012).

In monocots, the oil palm *EgNAM1* and *EgCUC3* genes, and the maize *ZmNAM1*, *ZmNAM2* and *ZmCUC3* genes have similar spatial expression patterns to those of *CUC* genes in *Arabidopsis*, but some differences are observed with dicots. The monocot proteins have not been fully functionally characterized yet and the temporal patterns of expression are not exactly coincident with their *Arabidopsis* counterparts (Zimmermann and Werr, 2005; Adam et al., 2011).

## 1.4 Control of CUP-SHAPED COTYLEDON1 expression

### 1.4.1 Regulation of CUP-SHAPED COTYLEDON1 by microRNA164

Failure to establish proper *CUC* expression domains leads to severe phenotypes (Laufs et al., 2004; Mallory et al., 2004; Nikovics et al., 2006; Sieber et al., 2007). *CUC1* and *CUC2* are negatively regulated by the miR164 family, which is composed of three members: miR164a, miR164b and miR164c.

The downregulation of *CUC* genes by miR164 is essential for normal development.

These miRNAs are able to recognize a specific sequence in mRNA and recruit the molecular machinery that will ultimately result in mRNA cleavage, leading to a reduced amount of protein being produced. The miR164 family also regulates other genes from the *Arabidopsis* NAC family such as *NAC DOMAIN CONTAINING PROTEIN 1* (*NAC1*) (Guo, Hui-Shan et al., 2005) and *ORESARA* (*ORE1*) (Schwab et al., 2005).

Outside of the NAC domain CUC1 and CUC2 are not highly conserved except from specific motifs, called the S, L and V motifs, that are also found in other members of the NAC family. This suggests that these motifs are relevant for CUC1 and CUC2 function (Taoka et al., 2004). The V motif coding sequence contains the recognition site for miR164 (Taoka et al., 2004; Mallory et al., 2004; Laufs et al., 2004).

Interestingly, miR164 does not regulate the expression of *CUC3*. The importance of mir164 mediated regulation of *CUC1* and *CUC2* expression is demonstrated in experiments in which it is either overexpressed or mutated.

The single mutation of the miR164c locus causes a phenotype where early arising flowers produce extra petals and a have a slight reduction in sepal size, caused by the higher level of CUC1 and CUC2 present in this mutant (Baker et al., 2005). It is referred to as the *early extra petals1* (*eep1*) mutant.

The modification of the miR164 recognition site in the mRNA from CUC1 and CUC2 without altering their protein sequences results in transcripts that are insensitive to the regulation by the miRNA (Mallory et al., 2004; Baker et al., 2005). Thus, plants expressing the resistant versions of *CUC1* (*CUC1m*) or *CUC2* (*CUC2m*) mRNAs show an increased level of these proteins (Figure 1.8 B-C).

The overexpression of members of the miR164 family phenocopies the cuc1 cuc2 mutants and, conversely, plants that express (*CUC1m*) or (*CUC2m*) produce extra petals and have enlarged sepal boundaries, phenotypes associated with the overexpression of *CUC* genes (Laufs et al., 2004; Mallory et al., 2004).

Plants expressing *CUC1m* showed heterogeneous phenotypes that included cotyledon orientation defects, rosette leaf abnormalities, extra petals and missing sepals in anomalous positions. They also showed delayed sepal formation and exposed floral buds due to the proliferation of petals, and resembled the phenotype of the *eep1* mutant (Mallory et al., 2004; Baker et al., 2005).

The regulation of CUC genes by the miR64 family is conserved in other species. In tomato, expression of the *CUC* gene homolog, *GOB*, is also regulated by SlmiR164, and expression of a modified *GOB* gene that is insensitive to this regulation results in flowers with phenotypic changes that consist on extra petals and ectopic carpels (Berger et al., 2009).

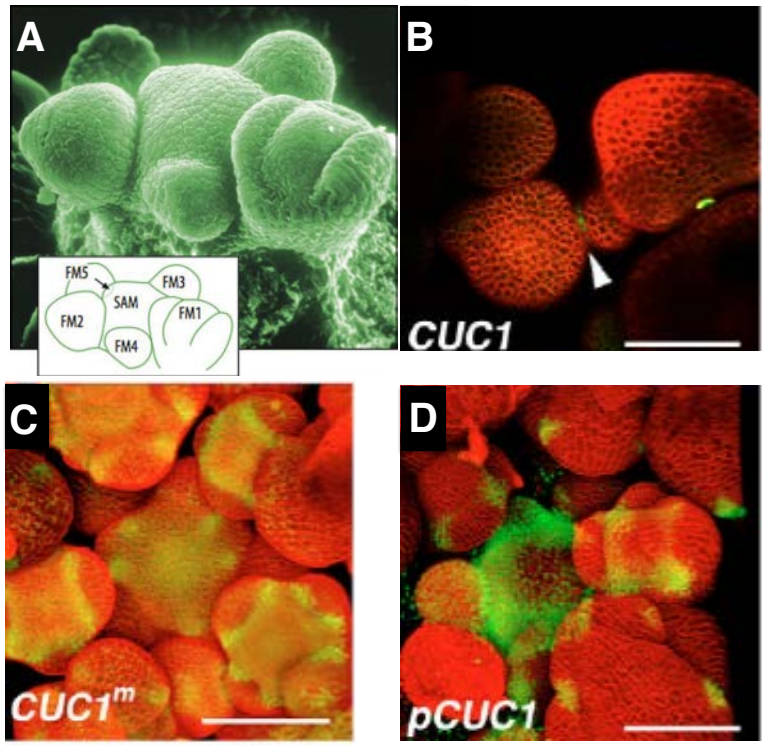


FIGURE 1.8: **CUC1 expression.** (A) Inflorescence meristem. The diagram in the bottom left indicates the position of the shoot apical meristem (SAM) and the different floral meristems (FM). The numbers indicate the order in which they arose. (B) Expression of CUC1-GFP is maintained at very low levels in boundary regions. (C) Modified version of CUC1 insensitive to regulation by miR164 (CUC1m) tagged with GFP. (D) Transcriptional reporter of CUC1 expression (pCUC:GFP). Adapted from Sieber et al., 2007.

### 1.4.2 Regulation of CUP-SHAPED COTYLEDON genes

Expression of *CUC* genes is regulated from embryogenesis and throughout plant development by different transcription factors.

SHOOT MERISTEMLESS (STM), a TF essential for the establishment of the SAM, induces the expression of *CUC1* directly by binding to its promoter (Spinelli et al., 2011), as described in Section 1.3.2. During embryogenesis, STM contributes to the localization of CUC genes in the center of the embryo.

When cotyledons start to form, two members of the *WUSCHEL-RELATED HOMEOBOX* (*WOX*) family, *WOX2* and *STIMPY-LIKE* (*STPL*) (also known as *WOX8*), restrict the expression of *CUC1* in the boundaries between the forming cotyledons. At the same time, they positively regulate the transcription of *CUC2* and *CUC3*, promoting the symmetry in *CUC2* and *CUC3* expression domains (Lie, Kelsom, and Wu, 2012). These regulations are likely indirect, and the mechanism by which they occur is yet to be elucidated.

Later, during axillary meristem initiation, LATERAL ORGAN FUSION1 (LOF1) and REGULATOR OF AXILLARY MERISTEM1 (RAX1) induce the

expression of *CUC* genes (Keller et al., 2006; Lee, Geisler, and Springer, 2009). They are MYB transcription factors and are required for the early induction of axillary meristems.

There are other factors that are able to regulate *CUC* genes by controlling the expression of miR164, such as RABBIT EARS (RBE) and SUPERMAN (SUP).

RBE is a zinc-finger protein that holds similarity with SUP and is expressed in organ boundaries. RBE is able to repress the expression of miR164b and miR164c and upregulate miR164A in floral buds (Huang et al., 2012). It is required for the correct positioning of boundaries in the second whorl and *rbe* mutants show defects in petals and sepals (Takeda, Matsumoto, and Okada, 2004; Krizek, Lewis, and Fletcher, 2006). Due to the balance between the different effects of RBE in the miR164 family, the overall effect in the *rbe* mutant is an increase in miR164a/b and miR164c. This results in a decrease in the level of *CUC1* and *CUC2* in *rbe* in comparison to WT (Huang et al., 2012), so the effect of RBE on *CUC1* is an indirect upregulation.

SUP, like RBE, is also a zinc-finger protein and regulates boundary formation between the stamen and carpel whorls by controlling the expression of miR164 (Sakai, Medrano, and Meyerowitz, 1995; Huang et al., 2012).

Another plant specific TF from the TCP family (TEOSINTE BRANCHED/ CYCLOIDEA/ PROLIFERATING CELL FACTOR), TCP3, is able to upregulate the transcription of miR164a. Plants with lower levels of TCP3 show enhanced serrations in their rosette leaves and lobed cotyledons with ectopic shoot meristems (Koyama et al., 2007). Since not all of these phenotypical characteristics were found in plants with single mutations of miR164a, it is thought that TCP3 might control the expression of CUC1 both transcriptionally and post-transcriptionally.

The regulation of *CUC* gene expression is influenced not only by TFs that bind directly to its promoter and affect their expression, but also through the modulation of chromatin availability for the access of those TFs. These epigenetic mechanisms, including DNA and histone covalent modifications and adjustment of histone-DNA interactions, are mediated by proteins and complexes of proteins that can alter chromatin state and will ultimately have an effect in the overall transcription of CUC genes.

BRAHMA (BRM), an adenosine triphosphatase of the Switch/sucrose nonfermentable (SWI/SNF) family of chromatin-remodeling factors, induces the expression of *CUC1-3* at the epigenetic level (Kwon et al., 2006).

RELATIVE OF EARLY FLOWERING 6 (REF6) is a demethylase that counteracts polycomb-mediated gene silencing by removing methyl groups from trimethylated histone H3 lysine 27 (H3K27me3) (Lu et al., 2011).

*CUC1* is targeted by REF6 through sequence-specific binding to its promoter. As a result, H3K27me3 is demethylated and *CUC1* is maintained at a transcriptionally active state (Cui et al., 2016). REF6 regulates organ boundary formation mainly through *CUC1*, and to a lesser extent through *CUC3*, but it does not target *CUC2*. This level of specificity in the regulation

of particular *CUC* genes is also found in the miR164 mediated control over them, where only CUC1 and CUC2 are targeted by these microRNAs (Cui et al., 2016, Section 1.4.1).

### 1.4.3 Hormone mediated regulation of CUP-SHAPED COTYLEDON1

The expression of *CUC1-3* genes is modulated by several plant hormones, including auxin and brassinosteroids, and the interplay between hormone signaling and boundary gene expression seems to be crucial to establish and maintain proper boundaries. A complex regulatory network between hormonal cues and CUC genes is in place but the molecular links between the main factors are still poorly understood.

In embryogenesis *CUC1* is activated in between the arising cotyledons, in a narrow band where auxin is depleted (Aida, Ishida, and Tasaka, 1999; Takada et al., 2001; Benkova et al., 2003). Complementary, auxin polar localization points to the incipient cotyledon tips. These gradients of auxin accumulation are mediated by PIN-FORMED1 (PIN1), a cellular efflux carrier that is localized asymmetrically within cells (Benkova et al., 2003; Friml et al., 2003). *PIN1* activity is required for the establishment of the proper expression of *CUC1* in the embryo; in *pin1* mutants the expression of *CUC1* is extended to the entire apical region (Aida et al., 2002).

Polar auxin transport leads to localized auxin maxima in the inflorescence meristem, where floral primordia starts to form (Benkova et al., 2003; Heisler et al., 2005). After flower formation, auxin directionality reverses towards the meristem and the local depletion of auxin between the meristem and the flower allows the formation of the boundary zone (Heisler et al., 2005).

The same type of auxin minimum is required in boundary formation at different developmental stages, as in organ abscission (Estornell et al., 2013) and axillary meristem formation (Tian et al., 2014; Wang et al., 2014).

The involvement of auxin in the *CUC* gene regulation is also illustrated by the serine/threonine kinase PINOID (PID) which is localized mainly in the boundaries between cotyledon primordia. It modulates intracellular localization of PIN1 and therefore polar auxin transport; *pid* mutants have abnormal auxin distribution (Wang et al., 2014). In *pin1 pid* double mutants the disruption of auxin polar distribution is enhanced and *CUC* gene expression is broadened (Furutani et al., 2004). The localized growth repression caused by the expanded domain of *CUC* genes represses the formation of cotyledons and causes the lack of bilateral symmetry. This does not occur in *pin1 pid cuc1 cuc2* mutants, and cotyledons are small in *pin1 pid cuc1* mutants, suggesting that CUC1 is the main responsible for this repression. The involvement of PID during flower development has not been observed, which may be due to functional specialization or to the fact that the effects might be subtle and only noticeable by thorough molecular marker evaluation.

MONOPTEROS (MP) is an auxin-responsive transcription factor that has an overlapping expression pattern with *CUC1* and *CUC2*. In *mp* mutants

auxin signaling is disrupted and *CUC1* expression is expanded outside the boundary area (Aida et al., 2002). It has been reported that in inflorescences and leaves, on the contrary, *CUC1* and *CUC2* expression is reduced in *mp* mutants, and MP binds to their promoters, suggesting that it directly activates them (Galbiati et al., 2013).

These results suggest that there is an interplay between auxin signaling and *CUC1* expression. Moreover, auxin depletion appears to be necessary to allow *CUC1* expression.

Brassinosteroids (BRs) are growth promoting steroidal hormones able to regulate cell division, elongation, differentiation, and a broad range of developmental processes throughout the plant. Their complex signaling pathway has been characterized and starts with the binding of the hormone to the BRI1 receptor kinase. A series of signaling events finally activates BZR1 and BES1, the TFs that are able to regulate the expression of hundreds of genes (reviewed in Kim and Wang, 2010).

BRs act in an antagonistic way to *CUC* genes by promoting growth, so an increased level of the hormone or its signaling events lead to fusions in axillary shoots, cotyledons and stamens, that result from the failure to establish proper boundaries (Gendron et al., 2012). On the contrary, low BR abundance or response results in the formation of ectopic boundaries and *CUC* transcript abundance is higher than in high BR zones (Gendron et al., 2012).

BZR1 directly represses *CUC* gene expression and is excluded from boundary regions, through interactions between LATERAL ORGAN BOUNDARIES (LOB) and the BR-inactivating enzyme BAS1 (Bell et al., 2012). BLADE-ON-PETIOLE1 (BOP1) and BOP2 reinforce the BR minimum that is observed in the boundary (Ha et al., 2007).

Cytokinins have also been reported to be linked to *CUC* genes by promoting their expression. They also appear to modulate polar auxin transport (Li et al., 2010; Marhavý, Peter et al., 2014), but the interplay between auxin, cytokinins and *CUC* genes is not yet fully understood.

## 1.5 CUC1 downstream events

### 1.5.1 CUP-SHAPED COTYLEDON1 and cell division

Genetic and phenotypic analyses have shown that *CUC* genes repress growth in boundary regions, but the molecular mechanisms by which they do it are still poorly understood.

At the cellular level, growth repression can be due to a reduction in cell division, cell expansion or both. To test how *CUC1* expression affects growth, Sieber et al., 2007 overexpressed it and found that sepal length was dramatically reduced but the number of cells per area remained the same. They also found that the mir164abc triple mutant plants had cell division repressed in the internodes at separate individual flowers, affecting phylotaxis, but cell size remained similar to the wild-type. These results

showed that the mechanisms by which CUC1 is able to repress growth in boundary regions by affecting cell division, but not cell expansion.

### 1.5.2 CUP-SHAPED COTYLEDON1 target genes

Despite the importance of CUC1 in plant development, only two potential direct downstream targets have been identified so far: *LIGHT-DEPENDENT SHORT HYPOCOTYLS 4* (*LSH4*) and its homolog *LSH3* (also known as *ORGAN BOUNDARY1*, *OBO1*, Takeda et al., 2011).

Both LSH3 and LSH4 were found to be upregulated in seedlings when CUC1 was overexpressed (Takeda et al., 2011). The authors used microarray experiments to assess the genome-wide expression profile of plants that had CUC1 fused to the 35S promoter of the cauliflower mosaic virus (35S) and compared it to a wild-type background.

They also fused the miR164 insensitive version of *CUC1* (*CUC1m*) to the GR receptor and put it under the control of the RIBOSOMAL PROTEIN S5A (RPS5A) promoter, which induces strong and constitutive expression in the whole embryo, SAM and organ primordia. This system (pRPS5A:CUC1m-GR) allows for the chemical induction of *CUC1m* activity by the application of dexamethasone.

This upregulation was deemed to be direct since it was maintained after the application of the protein synthesis inhibitor cycloheximide (CHX) (Takeda et al., 2011). CHX is a protein synthesis inhibitor that blocks translation once applied. Hence, CUC1 primary response genes are not able to produce any protein. As a result, the observed changes in gene transcript levels are assumed to be a product of the direct action of CUC1.

Expression of *LSH4* in embryos and young seedlings largely overlaps with expression of *CUC1* (Figure 1.9 A, B). Later in development, *LSH4* mRNA is detected in boundary cells between the SAM and flower primordia and between the floral meristem and sepal primordia (Figure 1.9 C, D).

*LSH3* is expressed at the base of petal and stamen primordia and along stamen filaments. It is also expressed at the boundary between the SAM and lateral organs and in the boundary region between cotyledons in heart shaped embryos and in young seedlings (Figure 1.10, Takeda et al., 2011; Cho and Zambryski, 2011). Ablation of cells that express *LSH3* leads to the loss of the SAM and lateral organs and overexpression cause petal-stamen fusions, indicating that it plays a role in meristem maintenance and organogenesis (Cho and Zambryski, 2011).

Constitutive expression of *LSH4* and *LSH3* in the SAM and organ primordia resulted in the suppression of leaf development and formation of ectopic meristems. Flowers showed pleiotropic phenotypes, with altered number of sepals and chimeric floral organs, and flowers that had extra floral organs or shoots within them. These phenotypic defects were similar in both *LSH4* and *LSH3* transgenic lines, but more pronounced in the case of *LSH4* (Takeda et al., 2011).

These results indicate that normal expression of *LSH4* and *LSH3*, where they are restricted to boundary cells and excluded from the SAM and organ

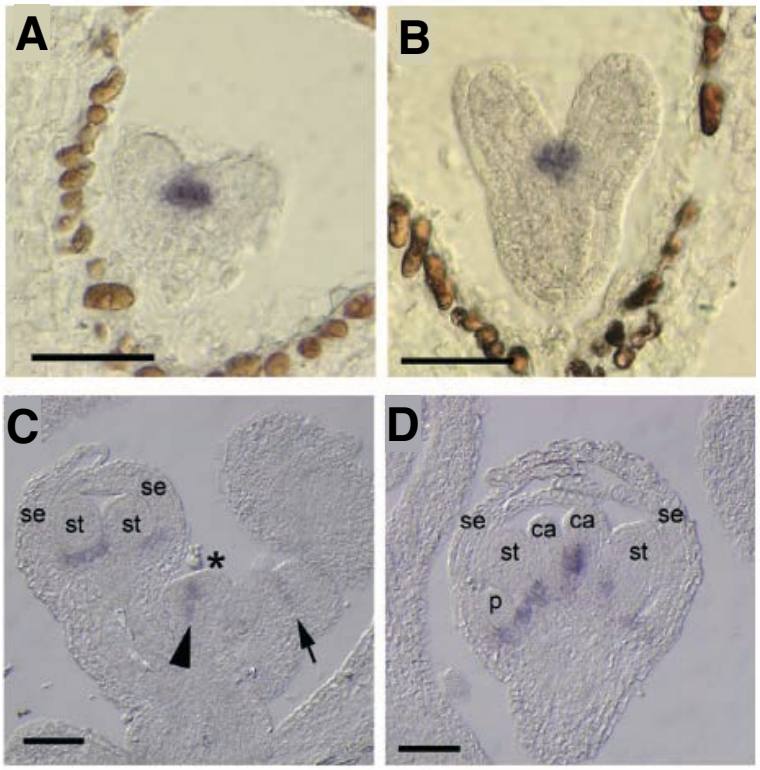


FIGURE 1.9: ***LSH4* expression.** (A) Frontal section of an early-heart embryo. (B) Frontal section through a late-heart embryo. (C) Longitudinal section through an inflorescence apex, showing LSH4 expression in the boundary regions between the SAM (asterisk) and flower primordia (arrowhead), and the floral meristem and sepal primordia (arrow). (D) Longitudinal section of a stage 7 flower. co, cotyledon; se, sepal; st, stamen; p, petal; ca, carpel. Scale bars = 50 $\mu$m. Adapted from Takeda et al., 2011.

primordia, is required for normal development (Takeda et al., 2011). The fact that developmental defects are caused when expression of *LSH3* and *LSH4* is not confined to the boundary region highlights the importance of the spacial specificity of this local activation by CUC1.

The mutant phenotype of *cuc1 cuc2* mutants cannot be rescued by constitutive *LSH4* overexpression, indicating that other factors must be involved in the formation of boundaries downstream of *CUC1* (Takeda et al., 2011).

*LSH4* and *LSH3* are two members of the ALOG plant-specific gene family, which is characterized by the presence of a single small domain (133 amino acids, Cho and Zambryski, 2011). The ALOG family is conserved in angiosperms, gymnosperms, the lycophyte *Selaginella moellendorffii* and the moss *Physcomitrella patens*, but not in algae, fungi or animals (Yoshida et al., 2009). ALOG proteins are predicted to bind DNA and modulate transcriptional activity (Iyer and Aravind, 2012). LSH4 is localized in the nucleus and its closest homolog is LSH3, that is also localized in the nucleus (Takeda et al., 2011).

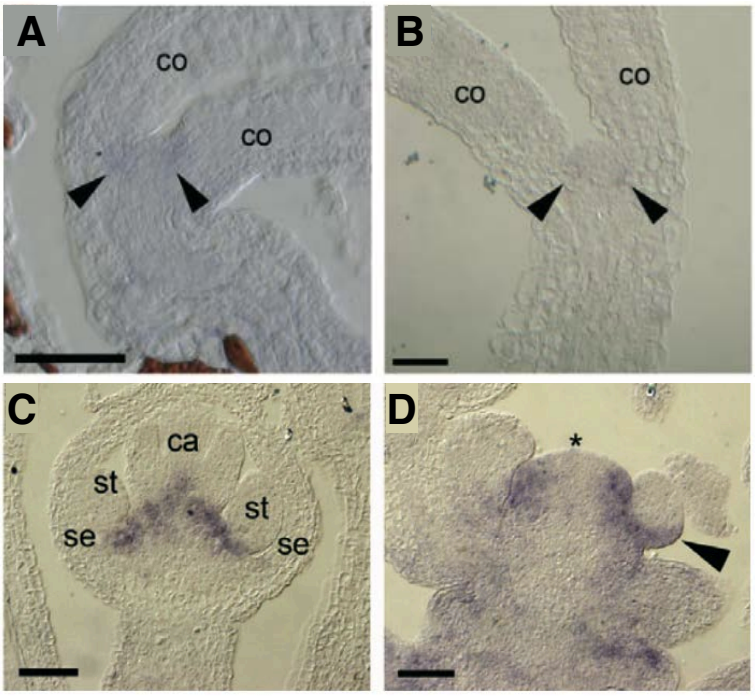


FIGURE 1.10: ***LSH3* expression.** (A) LSH3 expression is weakly detected in the boundary cells between the SAM and cotyledons in a bent-cotyledon stage embryo (arrowheads). (B) LSH3 expression in the boundary cells of the leaf primordia of a 4-day-old seedling (arrowheads). (C) Longitudinal section of a stage 7 flower. (D) Longitudinal section of an inflorescence apex. The signal is detected in an early stage 1 flower and in the cryptic bracts of a stage 2 flower (arrowhead), but not in the SAM (asterisk) or floral meristems at later stages. co, cotyledon; se, sepal; st, stamen; ca, carpel. Scale bars = 50 $\mu$m (C, D) and 100 $\mu$m (A, B).Adapted from Takeda et al., 2011.

Even though only two putative direct targets have been identified, genetic studies have shown that *cuc* mutant phenotypes can be enhanced by mutations in other genes. For instance, mutation in the BELL-type *ARABIDOPSIS THALIANA HOMEOBOX GENE1* (*ATH1*), which is required for proper boundary formation, enhanced the floral phenotype in *cuc* mutants and it is thought to act downstream of *CUC1* (Gómez-Mena and Sablowski, 2008). *BRM* (see Section 1.4.2) enhances *cuc1*, *cuc2* and *cuc3* mutant phenotypes while *SPLAYED* (*SYD*), its closest homologue, enhances only the *cuc1* phenotype (Kwon et al., 2006).

Likewise, the KNOXI genes *STM* (see Section 1.3.2 and *BREVIPEDICELLUS* (*BP*) are expressed ectopically when *CUC1* is overexpressed (Hibara, Takada, and Tasaka, 2003). *LATERAL SUPRESSOR* (*LAS*) is a member of the GRAS family of putative TFs that is expressed at the SAM boundary and is downregulated when *CUC1* is expressed at lower levels and upregulated in *CUC1* overexpressing plants (Greb et al., 2003; Raman et al., 2008).

Put together, these results suggest that there are several regulatory and response events that take place downstream of CUC1, but the molecular

links that underlie these processes is yet to be understood.

## 1.6 Genome-wide studies for dissecting gene regulatory networks

### 1.6.1 The APETALA1 study

The experimental approach used in this Thesis is derived from the work carried out by our group and published in Kaufmann et al., 2010b, that focused in the search of downstream transcriptional targets of APETALA1 (AP1).

*AP1*'s network had been extensively delineated by using genetic studies. The result was a dense network that contained many interactions (Ferrier et al., 2011). However, the gene regulatory networks that underlie the events that take place after AP1's activation were not fully understood. This occurred in part because, despite its central role in flower development, only a few downstream AP1 targets were known.

In that study, a genome-wide identification of the transcriptional targets of AP1 was performed, through a combination of chromatin immunoprecipitation followed by next-generation sequencing (ChIP-seq) and transcriptomic experiments using microarrays. By combining the results of the aforementioned experiments, the researchers were able to obtain a set genes that were bound by AP1 in vivo and that responded transcriptionally to its activation, and considered these genes to be high confidence targets (HCT) of AP1.

In the case of the study of CUC1's network presented here, the strategy was analogous, although RNA-seq was also performed in place of microarrays to obtain the transcriptomic landscape.

## 1.7 Transgenic lines used in this Thesis

In the sections that follow, the transgenic lines used in this Thesis are described.

### 1.7.1 The ap1 cal floral induction system and the AP1 line

The adopted experimental approach involves the use of the floral induction system first developed in Wellmer et al., 2006 and improved as described in Ó'Maoiléidigh et al., 2013. This system facilitates the collection of sufficient amount of tissue from flowers that are developing synchronously in the early stages of development.

Since the experimental design involves a time-course, the tissue collected at each time point should be enriched in flowers at a particular stage of development. Harvesting sufficient floral material in an homogeneous

developmental stage is very challenging due to the minute size of *Arabidopsis* flowers and the fact that they arise in a spiral way, so that in any given plant flowers will be in different stages.

The system uses the *ap1 cal* cauliflower mutant background described in Kempin, Savidge, and Yanofsky, 1995. In brief, when both *AP1* and *CAULIFLOWER* (*CAL*) are mutated, flower development arrests and inflorescence-like meristems accumulate, leading to a phenotype that resembles a cauliflower. In Wellmer et al., 2006, *AP1* was expressed in the *ap1 cal* background under the control of the 35S promoter, and in Ó'Maoiléidigh et al., 2013 under *AP1*'s endogenous promoter. In turn, the AP1 protein was fused to the hormone-binding domain of the rat glucocorticoid receptor (GR). Applying dexamethasone (DEX) activates the AP1-GR fusion protein, triggering flower formation synchronously throughout the whole cauliflower (Wellmer et al., 2006).

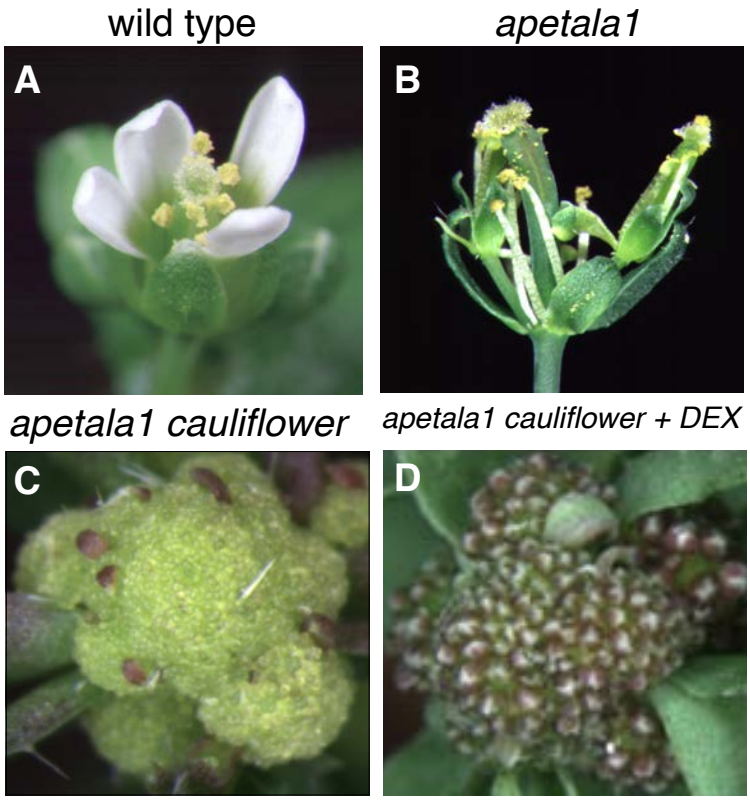


FIGURE 1.11: **Floral Induction in *ap1 cal* double mutants by AP1-GR activation.** (A) wild type flower. (B) *apetala1* single mutant. Petals are missing. (C) Floral induction system in the *apetala1 cauliflower* double mutant before induction. Inflorescence-like meristems accumulate forming a "cauliflower" phenotype. (C) Activation of AP1-GR with dexamethasone triggers the massive induction of flower primordia. (Wellmer et al., 2006).

The pAP1:AP1-GR *ap1 cal* line (from now on the *AP1 line*) is the genetic background of the *CUC line* used for ChIP-seq, RNA-seq and proteomic experiments of this Thesis, and serves as a control for some of these experiments. Similarly, 35S:AP1-GR *ap1 cal* is the background of the *eep1*

*line.*

### The CUC line

The ideal line to perform CUC1 ChIP-seq and transcriptomic experiments needs to posses a set of characteristics in order to be suitable for the chosen experimental design. It should:

(i) express a tagged version of CUC1 to facilitate ChIP-seq: the immunoprecipitation of TF requires the availability of a specific antibody to allow its immunoprecipitation. This can be achieved by designing a new antibody against the TF of interest or by using a tag, in this case GFP.

(ii) have low levels of endogenous CUC1: the aim is to have most genomic regions where CUC1 can bind occupied by the tagged version of the TF so they can be recovered when immunoprecipitation is performed. Hence, since CUC1 tagged with GFP and the untagged endogenous CUC1 will be competing to bind to the same genomic regions, the ratio between the tagged protein and the endogenous one should be high.

Because of the regulation by miR164 (Section 1.4.1), the endogenous level of CUC1 is low (Figure 1.8 B). Using the modified version (CUC1m) that is insensitive to miR164 regulation in the transgenic line results in higher levels of CUC1 in comparison to the control background (Figure 1.8 C). Taking advantage of this characteristic, CUC1m can be tagged with GFP to obtain the necessary high ratio of CUC1m-GFP/CUC1.

(iii) feature the possibility to synchronize flower development to facilitate the collection of enough material for performing time-course experiments: hence, the use of the *ap1 cal* floral induction system (Section 1.7.1).

(iv) produce enough seeds: due to the importance of CUC1, the modification of its activity can cause severe developmental defects leading to the lack of seeds in the mature plant.

(v) use the TF's native promoter to preserve its endogenous spatio-temporal expression properties.

Therefore, the *CUC line* used in the experiments described in this Thesis contains the *CUC1* endogenous promoter directing the expression of the modified version of *CUC1* (*CUC1m*), in the *ap1 cal* floral induction system (pCUC1:CUC1m-GFP, pAP1:AP1-GR, *ap1 cal*).

# Chapter 2

# eep1 microarray analyses

## 2.1 Background

The *early extra petals1* (*eep1*) mutant is a knock-out of *mir164c* (see Introduction, Section 1.4.1). As a consequence of the absence of this miRNA-mediated regulation, levels of *CUC1* and *CUC2* transcripts and proteins are higher in *eep1* plants than in wild-type (Figure 2.1 A-F, Baker et al., 2005; Sieber et al., 2007).

The single mutation of the miR164c locus and consequent increase in *CUC1* and *CUC2* levels causes an expansion in the growth suppression domain between sepals, where extra petals are able to form (Figure 2.1 H-I). The *eep1* mutant presents a phenotype where early arising flowers produce extra petals and a have a slight reduction in sepal size, (Figure 2.1 G, Baker et al., 2005).

In addition to controlling the expression levels of *CUC1* and *CUC2*, the *miR164* family regulates other four transcription factors in *Arabidopsis*: *NAC1*, involved in the regulation of lateral root induction, *ORESARA1* (*ORE1*), involved in leaf senescence, *NAC4*, involved in the nitrogen metabolic network and pathogen-induced cell death, and another NAC member that has not been characterized, *NAC100* (At5G61430) (Laufs et al., 2004; Schwab et al., 2005; Vidal et al., 2013; Lee et al., 2017).

In particular, *miR164c* is expressed in early stage floral buds throughout the entire primordia until they reach stages 3-4, and shows a more restricted pattern in older flowers that partially overlaps with that of *CUC1* and *CUC2* at those stages (Baker et al., 2005). Overexpression of miR164c led to floral phenotypes that resembled those of *cuc1 cuc2* mutants, although fusions in cotyledons or in axillary meristems were never observed. Moreover, no significant differences in transcript accumulation of the different *mir164* target TFs was detected in *eep1* other that the increase in *CUC1* and *CUC2* transcript levels. Put together, this evidence indicates that *miR164c* activity might be specific for *CUC1* and *CUC2* regulation and its scope might be restricted to later developmental stages (Baker et al., 2005).

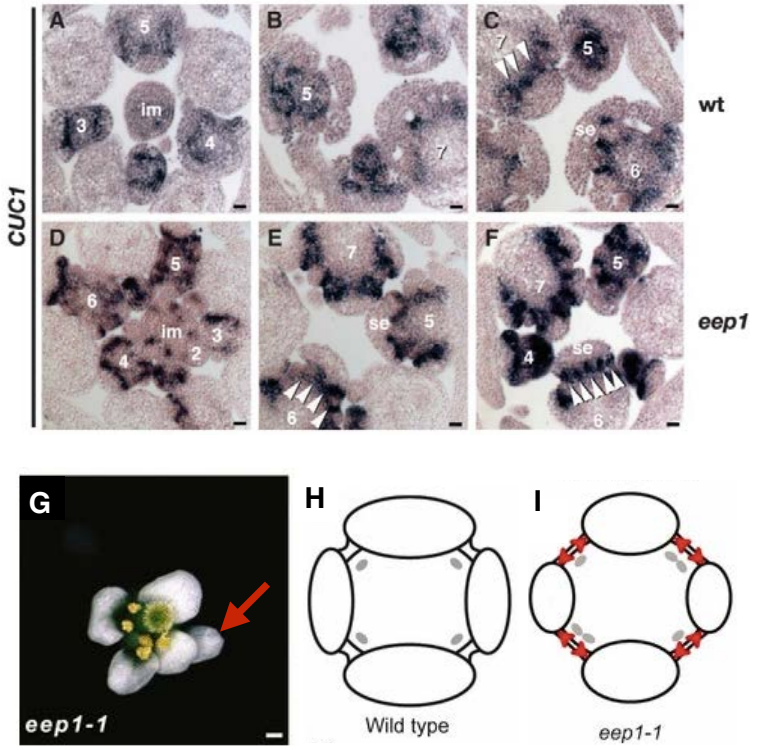


FIGURE 2.1: **The *eep1* mutant.** (A-F) In situ hybridization with CUC1 probe in wild type and *eep1* inflorescence tissue. The signal is higher in the *eep1* mutant and the white arrowheads indicate ectopic boundaries. The numbers indicate floral stages (according to Smyth, Bowman, and Meyerowitz, 1990). Abbreviations: se, sepal; im, inflorescence meristem. The scale bars represent 20 $\mu$m. (G) Floral phenotype in the *eep1* mutant. The red arrow indicates an extra petal. (H, I) Diagrams of growth patters in stage 4 wild type and eep1 buds. Grey shading represents petal anlagen. Red arrows represent the expansion of growth suppression. (Baker et al., 2005; Lampugnani, Kilinc, and Smyth, 2012)

### The eep1 line

The *eep1* mutant was crossed with a version of the floral induction system (see 1.7.1) that contains the 35S promoter fused to AP1-GR in the *ap1 cal* mutant background (Wellmer et al., 2006). The resulting line, 35S:AP1-GR *ap1 cal eep1*, is referred to hereafter as the "*eep1 line*". The 35S:AP1-GR *ap1 cal* line serves as a background control in the presented experimental conditions.

The application of dexamethasone initiates flower development by activating AP1, which is then transported to the nucleus and is able to trigger flower development throughout the inflorescence-like tissue in the cauliflower both in the *eep1 line* and the control.

Before dexamethasone induction (0 dpi) miR164c level is already lower in the *eep1 line* in comparison to the control, and hence *CUC1* and *CUC2* are elevated. After induction, all the changes in the transcriptome that are related exclusively to the onset of flower development and the activation of

AP1, and that are independent of the levels of *CUC1* and *CUC2* present in the system, will occur in both genotypes and, hence, be corrected for.

Therefore, by comparing the genome-wide gene expression in the *eep1 line* (35S:AP1-GR *ap1 cal eep1*) using 35S:AP1-GR *ap1 cal* as a control, the effect that is being evaluated is that caused durieng the early stages of flower development by the elevated levels of *CUC1* and *CUC2* resulting from the lack of miRNA-mediated regulation.

In the study performed in Kaufmann et al., 2010b (Section 1.6.1) the transcriptional response to AP1 is assessed in the 35S:AP1-GR *ap1 cal* line after dexamethasone treatment. In that case, the protein of interest (AP1) only becomes active after dexamethasone is applied and flower development is simultaneously triggered. In the experiment presented here, however, the elevated levels of *CUC1* and *CUC2* are present in the *eep line* during the whole life cycle of the plant. This means that at 0 dpi the *eep line* and the control are already different, and some changes in genome-wide gene expression between them are expected.

## 2.2 Experimental design

Microarrays were employed to assess the stage-specific genome-wide gene expression profile in plants from the *eep1 line* (35S:AP1-GR *ap1 cal eep1*), and the 35S:AP1-GR *ap1 cal* line was used as a control background. The experimental setup is summarized in Figure 2.2 and details about the hybridization and conditions are detailed in Materials and Methods (Section 7.10). Plants of both genotypes were treated with dexamethasone and inflorescence tissue from the cauliflower was collected right before the treatment and at 24 hour intervals for the following 5 days. Four biological replicates were used for each time and genotype.

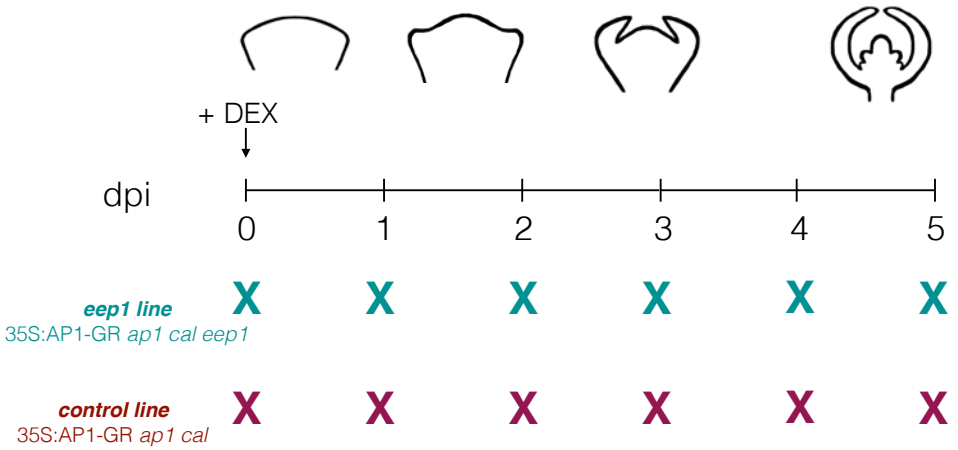


FIGURE 2.2: **Experimental design.** Two-color Agilent microarrays were used to obtain the differences in the transcriptome of the *eep1 line* and the *control line*.

## 2.3 Results and Discussion

RNA derived from both genotypes was co-hybridized to two-color custom Agilent microarrays (Kaufmann et al., 2010b). Chips were scanned with an Agilent SureScan Microarray Scanner and the obtained images were processed with Agilent's Feature Extraction Software. Raw data was imported into R (R Core Team, 2017). Bioinformatic analysis was performed with the `limma` package (Ritchie et al., 2015) and is described in depth in Section 7.14.5.

Complete tables of results for all time points can be obtained in the online Supplementary information.

In this Chapter, genes for which the adjusted p-value (FDR) was below 0.05 and the absolute fold change was above 1.8 ($\log_2$FC above ~0.85) in at least one of the time points were considered to be differentially expressed.

There were 1228 genes that had an adjusted p-value below 0.05 in at least one time point. Of those, 843 had an absolute fold change above 1.8 and are considered to be differentially expressed (Supplementary table 2.1).

Figure 2.3 shows the number of DEG at the different time points. It can be noted that at every given time point there are both downregulated and upregulated genes. At day 0 only 15 genes passed the cutoff that was set to be considered as differentially expressed, suggesting that the differences in the transcriptomes of both genotypes at this stage are not substantial.

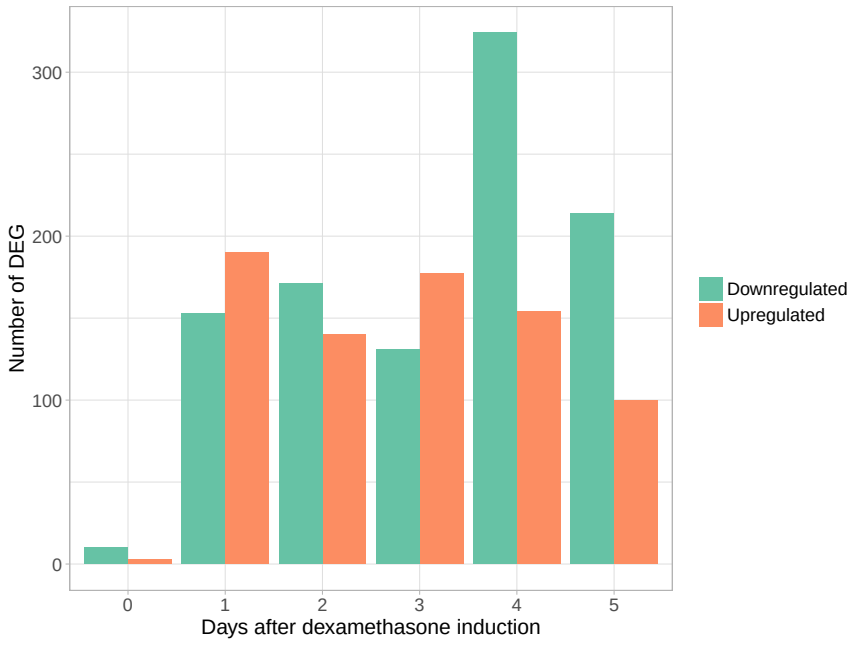


FIGURE 2.3: **Gene expression changes.** Number of differentially expressed genes from the *eep1 line* vs. the *AP1 line* over time. Green bars represent downregulated genes in the *eep1 line* while orange bars represent the upregulated genes.

In the first four time points analyzed, the number of genes that are up and downregulated is more or less equivalent, and the ratio remains

stable within a small margin through these early stages of development. Later, at 4 and 5 dpi, the absence of mir164c, that is, the increased levels of *CUC1* and *CUC2*, seem to have a predominant repressive effect in gene transcription, where the number of genes that are downregulated is twice as large as the number of upregulated genes.

A heatmap showing the differential expression values of the genes that show an absolute value of logFC higher than 0.85 and FDR below 0.05 is depicted in Figure 2.4.

Hierarchical clustering of these genes based on their logFC is shown in the dendrogram on the left, where the colors indicate the 8 most dissimilar clusters.

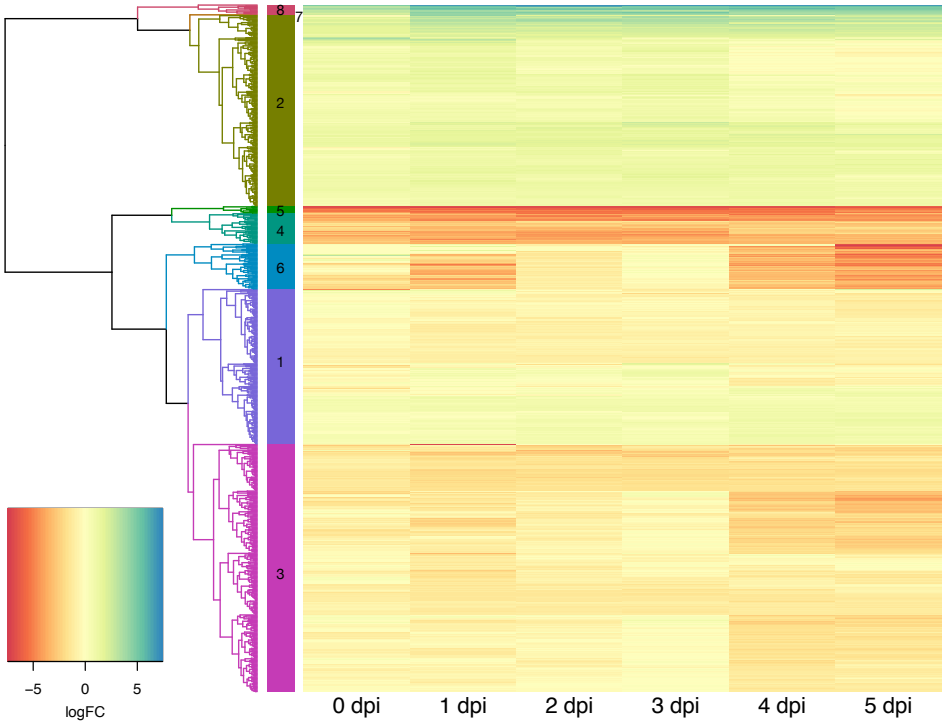


FIGURE 2.4: **Heatmap of expression changes.** Filtered by absolute value of FC > 1.8.

Figure 2.5 shows the expression dynamics of each of the genes separated by the cluster they belong to. The colored dots in Figure 2.5 indicate the color of the corresponding branches in the dendrogram in Figure 2.3.

Cluster 1 corresponds to the purple colored cluster where the expression changes are not very extreme, finding values between -2 and 2 logFC. Within this cluster there is LATERAL SUPPRESSOR (LAS), a member of the GRAS family of putative TFs, appearing upregulated at 3 and 4 dpi. It had been previously shown that (*LAS*) is downregulated when *CUC1* is expressed at lower levels and upregulated in *CUC1* overexpressing plants (Greb et al., 2003; Raman et al., 2008).

*RABBIT EARS* (*RBE*), which upregulates *CUC1* and *CUC2* indirectly by repressing mir164 in floral buds (Huang et al., 2012), appears in the same cluster as upregulated at 4 dpi.

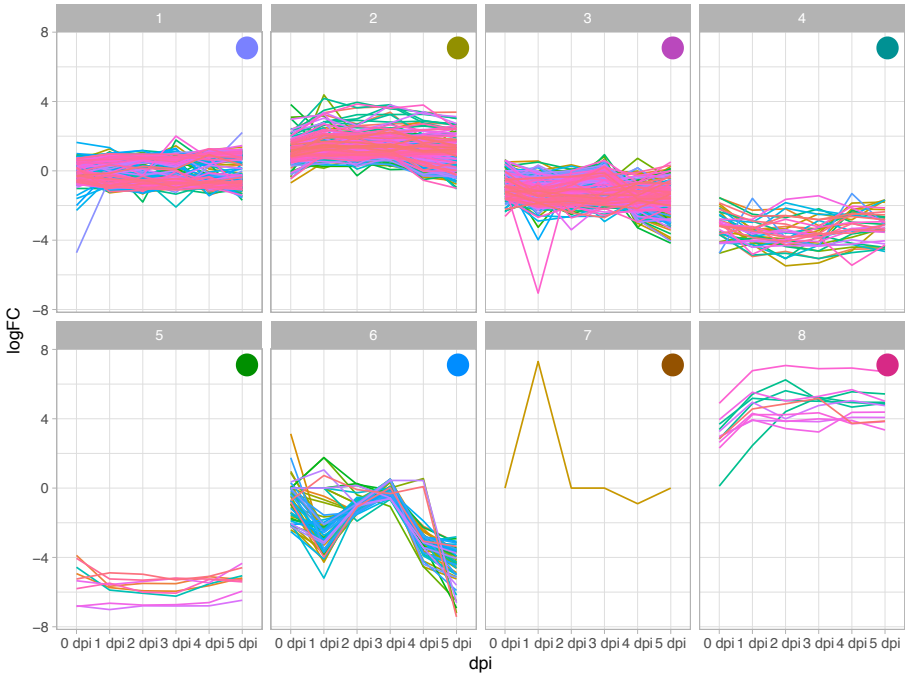


FIGURE 2.5: **Cluster expression dynamics.** Expression dynamics of genes separated according to the clusters they belong to in Figure 2.4.

Cluster 2 is colored in pale green and the genes in this group are in general upregulated, with the majority of logFC values ranging between 0 and 3.5. *CUC1* and *CUC2* are included in this group. Conversely, most of the genes in cluster 3 are downregulated with values of logFC between -3.5 and 0.

It is worth noticing that the observed changes are due only in part to the higher levels of CUC1, as CUC2 final abundance is also elevated in the absence of mir164c regulation (Figure 2.6). In fact, the fold change of the transcript level of *CUC2* is higher than that of *CUC1* in the earliest stages in the *eep line* vs. the control, in an analogous way to what was described when analyzing their expression in the *eep1* mutant compared to the wild-type in Baker et al., 2005.

The transcript levels of *CUC1* and *CUC2* assessed by microarray analysis are higher in the *eep line* in comparison to the control (except for CUC1 at 0 dpi, although the p-value is very high for this comparison). *CUC2* passes the cutoffs set to be considered differentially expressed from 1 dpi onwards, while *CUC1* does from 2 dpi (Figure 2.6, Supplementary table 2.1).

Also in agreement to what was observed in Baker et al., 2005, the other targets of the mir164 family (*NAC1*, *ORE1*, *NAC4* and *NAC100*) do not appear to be differentially expressed in the *eep1 line* vs the control line comparison at any of the time points (Supplementary table 2.1).

Using the DEG from each time point, a gene ontology analysis was performed in order to determine if there were overrepresented categories in

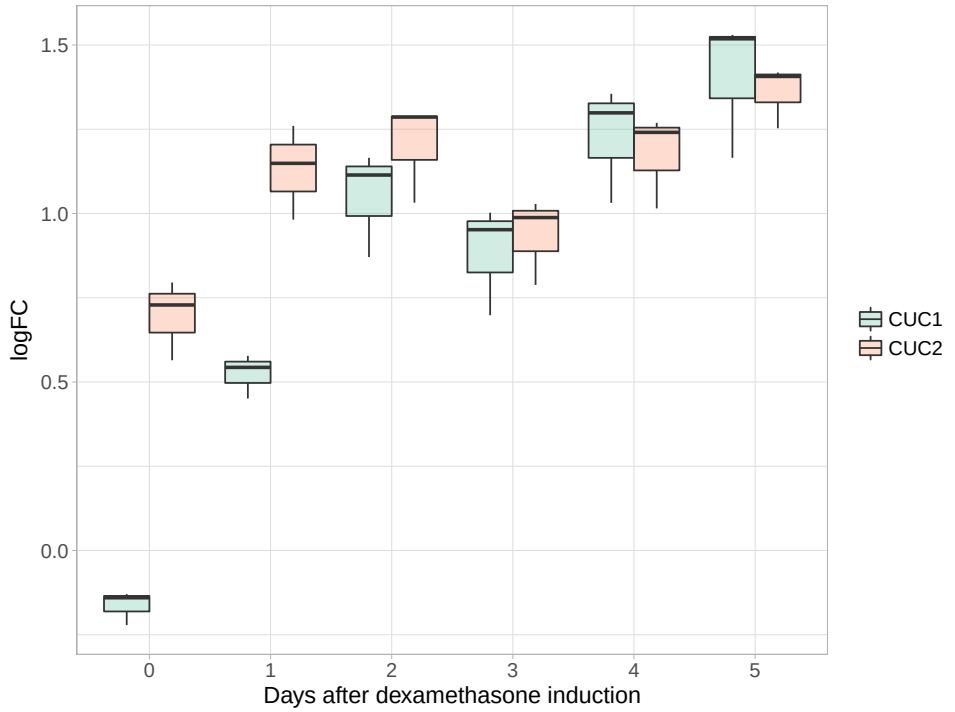


FIGURE 2.6: **CUC1 and CUC2 expression changes.** Logarithmic fold change of CUC1 (green) and CUC2 (orange) expression from the *eep1 line* vs. the *AP1 line* over time. The central black line in the boxplots represents the median from the 3 probes for each gene.

these sets of genes. The results indicated that there are several categories enriched at the different time points, and many of them are found to be relevant repeatedly (Figure 2.7). At time 0 dpi no GO categories were found to be overrepresented.

A category that was overrepresented in all of the time points was post-embryonic development. Flower development also appears significant in all but one time point, while the response to stimulus related categories seem to be enriched at 1 dpi only. Interestingly, given the involvement of *CUC* genes in gynoecium development (see Introduction, section 1.3.5), the categories related to reproductive development appear overrepresented at 4 and 5 dpi, when these structures begin to be formed.

The fact that both *CUC1* and *CUC2* do not pass the cutoff to be considered DE in 0 and 1 dpi could be due to a lower level of regulation by mir164c at these stages of development. As shown in Baker et al., 2005, the expression pattern of mir164c can be detected throughout the floral primordia in the first stages of floral development, while it overlaps more accurately with that of *CUC1* and *CUC2* after stages 3-4, that correspond to approximately 3-4 dpi (Figure). If mir164c is not acting to repress *CUC1* and *CUC2* post-transcriptionally at the beginning of development as hypothesized in Baker et al., 2005, the difference between their expression in the *eep1 line* compared to the control line would be negligible. Also, the level of expression of *CUC1* and *CUC2* at early stages of flower development is very low (Figure

1.5, Figure 2.1), so changes in levels between both genotypes might not be detected in our experimental setup.

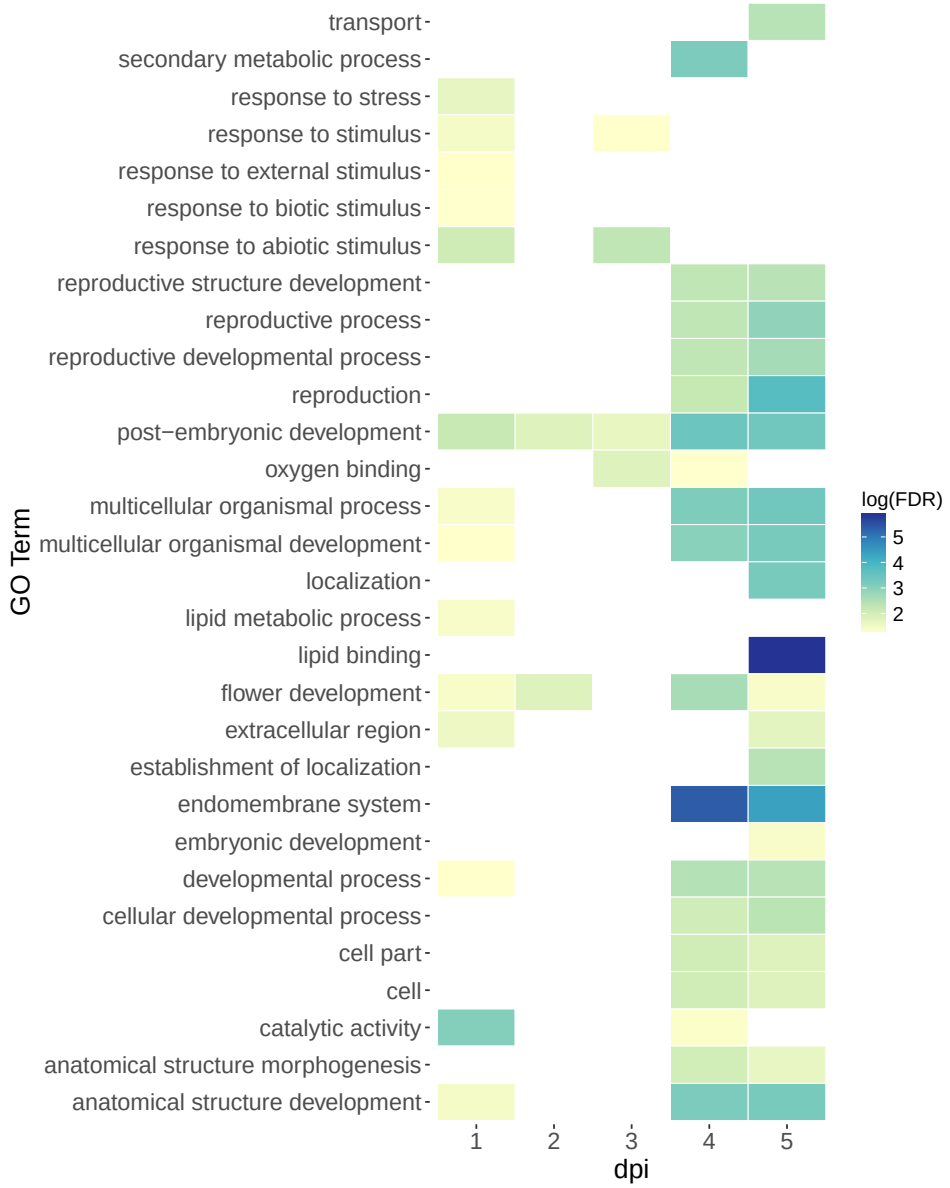


FIGURE 2.7: **Gene ontology analysis.** Gene ontology categories overrepresented in the differentially expressed genes from the *eep1 line* vs. the *AP1 line* over time. Color represents the level of significance.

# Chapter 3

# RNA-seq

## 3.1 Background

Genetic interaction studies have shown that CUC1 is able to affect the expression of several genes. The enhancement of the *cuc* mutant phenotypes by mutations in other genes such as *ATH1* (Gómez-Mena and Sablowski, 2008), *BRM* or *SYD* (Kwon et al., 2006) suggest that they act downstream of CUC1. Overexpression of *CUC1* leads to mis-regulation of *STM*, *BP* (Hibara, Takada, and Tasaka, 2003) and *LAS* (Raman et al., 2008), also suggesting that they are subject to CUC1 regulation (see Section 1.5.2 in the Introduction for more detail).

The existence of functional redundancy between *CUC1* and *CUC2* has hampered the the identification of a wider set of transcriptional targets. Hence, the genes that are affected by CUC1 activity at a genome-wide level during flower development are yet largely unknown.

In order to shed light into the molecular events that are regulated by CUC1, RNA-seq experiments were carried out. Comparing the *CUC line* (pCUC1:CUC1m-GFP pAP1:AP1-GR *ap1 cal*), that contains elevated levels of CUC1, with its background, allows the characterization the transcriptomic landscape related to CUC1's activity.

Genes that appear as differentially expressed in the RNA-seq experiments and are also bound by CUC1 *in vivo* are potential direct transcriptional targets of CUC1.

## 3.2 Experimental design

The chosen experimental setup (Figure 3.1) aims to characterize the genome wide response at a transcriptomic level to the elevated level of *CUC1* during early flower development, while controlling for the variations that are due exclusively to the activation of AP1 and the triggering of flower development along time.

As in the case of the microarray assays (Chapter 2), in this setup the application of dexamethasone initiates flower development by activating AP1

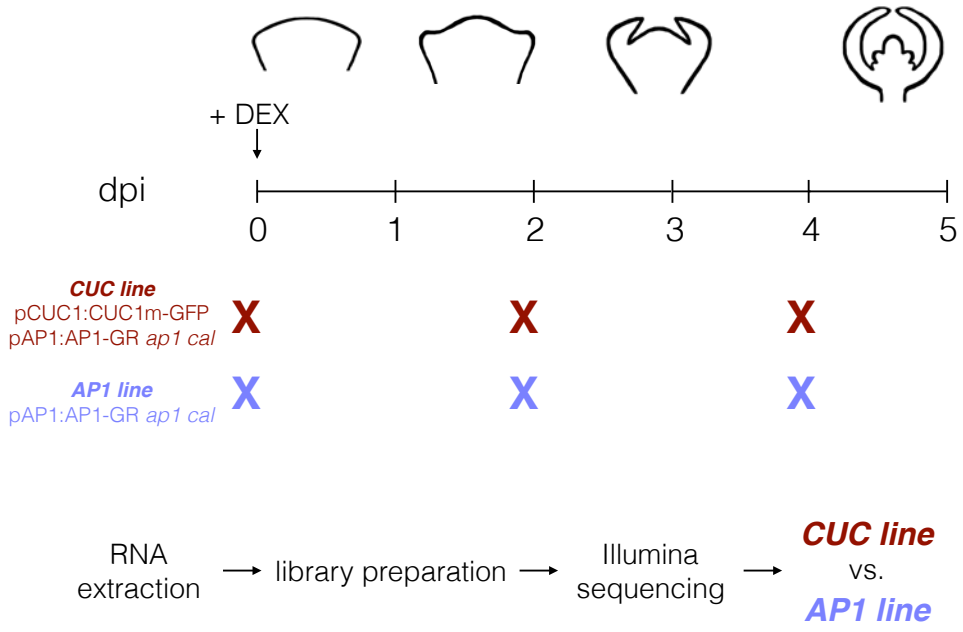


FIGURE 3.1: **Experimental design.** Libraries prepared with RNA extracted from the *CUC line* and the *AP1 line* at 0, 2 and 4 dpi were sequenced and analyzed.

which is able to trigger flower development throughout the inflorescence-like tissue in the cauliflower both in the *CUC line* and the control line *AP1 line*. Consequently, the genes detected as differentially expressed in this configuration are the ones that respond to the elevated levels of *CUC1*.

RNA was obtained from inflorescence tissue of both lines before treatment and at 2 and 4 dpi (Figure 3.1). Before treatment is the initial point, where floral induction has not been triggered yet. At 2 dpi (corresponding to Stage 3 or *Arabidopsis* flower development; Stages defined in Smyth, Bowman, and Meyerowitz, 1990) sepals are starting to arise and CUC1 acts to create boundaries between adjacent organs. Then, 4 dpi (Stages 5-6) is a key moment for CUC1's function, since boundaries are also created when petals and stamen primordia arise and sepals enclose the floral bud (Smyth, Bowman, and Meyerowitz, 1990).

### 3.2.1 Expression level of CUC1 in the experimental lines

The expression levels of *CUC1* were first assessed by RT-qPCR at 2 and 4 dpi using two different sets of primers spanning exon 1 and 3 respectively (Figure 3.2). The results are normalized to the levels of CUC1 in wild-type Ler (the background ecotype of both lines).

It can be noted that *CUC1* transcript level both in the *AP1 line* samples and the *CUC line* samples is higher than in samples derived from WT Ler. This can be explained by the disparate characteristics of the tissue being analyzed, since in the case of the WT normal inflorescences are used, while

in the ones that use the floral induction system the cauliflowers are collected. In the latter, there is an accumulation of inflorescence- like meristems higher than in the WT and consequentially there are more developing flowers with boundary regions where *CUC1* is expressed per sample.

The level of *CUC1* in the *CUC line* both at 2 and 4 dpi is close to two fold higher than in the control, as evidenced by the use of two different sets of primers and expected from the presence of the pCUC1:CUC1m-GFP transgene.

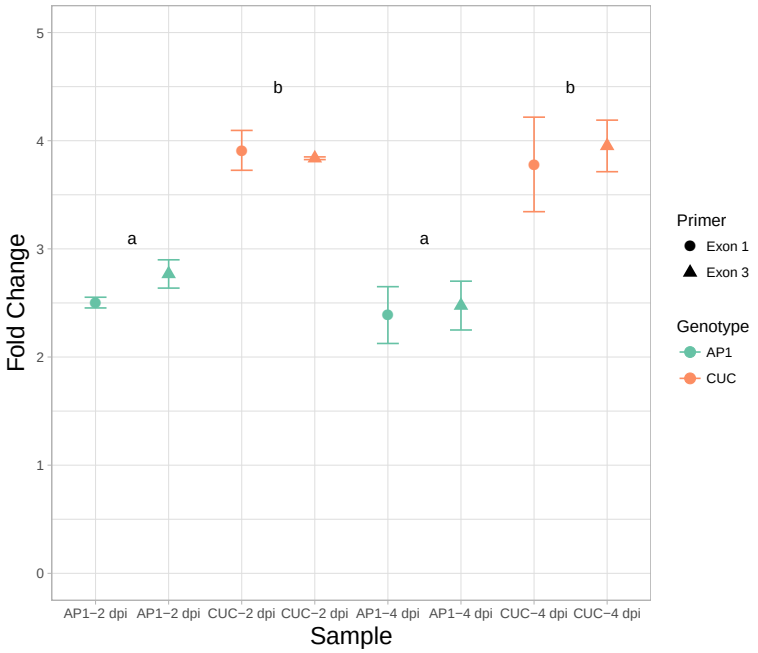


FIGURE 3.2: **CUC1 expression in the *CUC line*.** Relative transcript levels of CUC1 in the *CUC line* and *AP1 line* normalized to expression in WT Ler. Bars indicate the standard error and letters (a and b) indicate the t-test result.

### 3.2.2 RNA-seq setup and analysis

Three biological replicates were used for each time point and genotype for the RNA-seq experiment for a total of eighteen libraries that were constructed and sequenced. Details about the extraction and processing of the samples and sequences can be obtained in Materials and Methods.

In short, reads were aligned to the *Arabidopsis* genome of reference (TAIR10) and a count table was obtained. This table was used as the input for analysis in R with `DESeq2` (Love, Huber, and Anders, 2014). The presented fold changes are in the logarithmic scale and always refer to *CUC vs AP1 lines* (so a positive fold change means that gene is expressed in the *CUC line* at a higher level than in the *AP1 line*, and vice versa).

The variance between biological replicates used for RNA-seq was found to be larger than initially expected. Of the three biological replicates, two had grown at the same time in the growth chambers while the third one

grew after the first batch had been collected. When the reads were obtained, a principal component analysis (PCA) revealed that there were batch effects present in the samples (ie. the two replicates grown at the same time clustered together and the third one was not placed within this cluster).

This was taken into account when performing the bioinformatic analyses by including batch information into the design formula of the differential expression algorithm (`DESeq2`). By doing this, the batch effect is modeled in the regression step so `DESeq2` is able to estimate its size and to substract it when performing all other tests (with a consequent reduction in the residual degrees of freedom to reflect this).

As a consequence, the results are expected to be more conservative (or robust) in comparison with what would be obtained if the analysis was based only on the samples that grew together.

## 3.3 Results and Discussion

The online Supplementary Material contains a table with the identification, names, and values of logarithmic fold change and FDR of all the genes that were identified as differentially expressed: genes for which the adjusted p-value (FDR) was below 0.05 in at least one of the time points, with no cutoff set for fold change (Supplementary table 3.1). Another table includes that information and adds the names and descriptions of these genes (Supplementary table 3.2).

In accordance to the results obtained by qPCR, the levels of CUC1 assessed by RNA-seq reflect a similar level of overexpression in the *CUC line* (Figure 3.3) compared to the *AP1 line*. *CUC1* passes the set cutoff to be considered as a DEG at 0 and 4 dpi (see Supplementary table 3.2, Figure 3.3).

### 3.3.1 Differentially expressed genes

There were 216 genes that were differentially expressed in at least one time point. Figure 3.4 shows the number of DEG at each time point and whether they are downregulated or upregulated.

At 0 and 2 dpi there is a higher number of genes that respond to the elevated levels of CUC1 by increasing their expression level (51 upregulated and 28 downregulated at 0 dpi; and 39 upregulated and 25 downregulated at 2 dpi). Meanwhile, at 4 dpi downregulation is somewhat more frequent (58 downregulated genes vs. 42 upregulated, Figure 3.4).

A gene ontology analysis was performed in order to determine if there were overrepresented functional categories among the DEG from each time point (Figure 3.5). Several categories were enriched. Among the categories with a higher level of enrichment there are the response to stimulus and response to stress categories. Transcription factor activity appears enriched at 0 dpi, which could indicate that CUC1 may be triggering a cascade of responses after the onset of flower development by AP1's activation. The

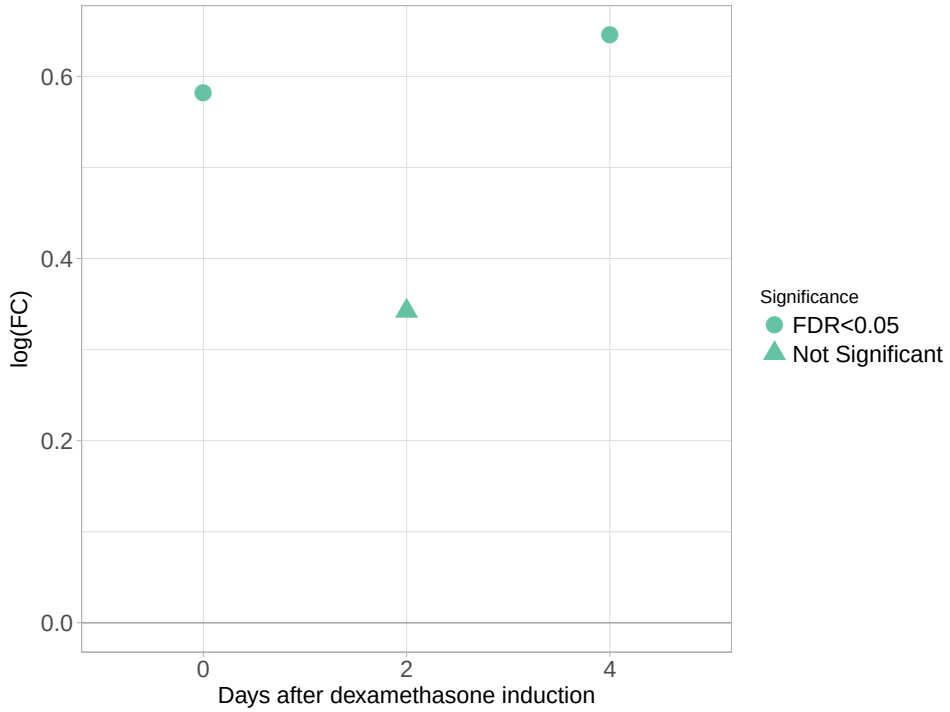


FIGURE 3.3: **CUC1 expression changes.** Logarithmic fold change of CUC1 expression from the *CUC line* vs. the *AP1 line* over time. The shape of the points shows whether the measure passed the set significance cutoff value.

secondary metabolic category appears to be important at 2 and 4 dpi, which might provide a link between CUC1 activity and the biosynthesis of different plant hormones.

Figure 3.6 shows a heatmap constructed with all the differentially expressed genes. The dendrogram on the left shows the hierarchical clustering of these genes based on their expression profile, and the colors indicate the 8 most dissimilar clusters.

The expression profiles of individual genes grouped by the cluster they belong to are depicted in Figure 3.7. The numbers and colored dots indicate the corresponding branches of the dendrogram in Figure 3.6.

Gene ontology analyses were performed with the genes that belong to each cluster and significant enrichment in any category was found for clusters 1 to 6 (but not in 7 and 8, which happen to be clusters with a relative low number of genes). The gene ontology categories enriched in each one of the clusters are depicted in Figure 3.8.

*CUC1* is included in cluster 7 (pale green branches), where all genes are upregulated at all time points. *WUSCHEL-RELATED HOMEOBOX12* (*WOX12*), *EMBRYO SAC DEVELOPMENT ARREST 31* (*EDA31*) and *ARGONAUTE3* (*AGO3*) are also included within this cluster.

WOX12 promotes root primordia initiation and organogenesis and has been shown to be upregulated by auxin (Liu et al., 2014; Hu and Xu, 2016). It is able to activate the expression of *LATERAL ORGAN BOUNDARIES DOMAIN16* (*LBD16*) and *LBD29*, which in turn are involved in the regulation

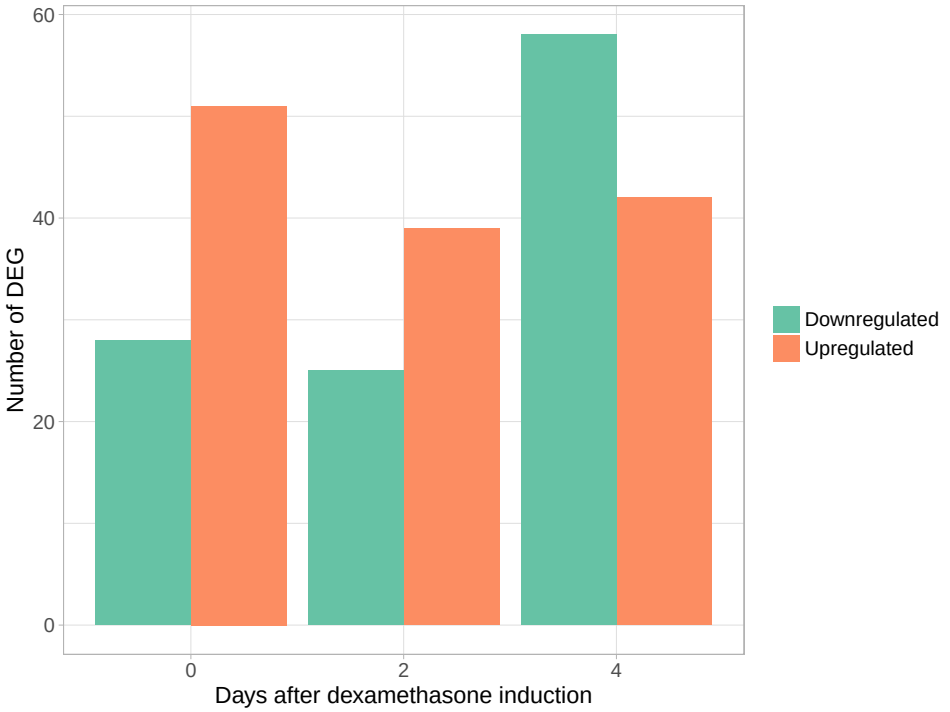


FIGURE 3.4: **Gene expression changes.** Number of differentially expressed genes from the *CUC line* vs. the *AP1 line* over time. Green bars represent downregulated genes in the *CUC line* while orange bars represent the upregulated genes.

of cell division and cell wall metabolism (Pagnussat et al., 2005; Lee et al., 2009a; Berckmans et al., 2011). WOX12 has been detected in early developing flowers (Supplementary information in Wellmer et al., 2006).

*EDA31* (AT3G10000) is upregulated at all time points and is the closest relative to *PETAL LOSS* (*PTL*). PTL represses growth in boundary regions of early developing flowers; its absence causes fusions in sepals and defects in the number of petals, along with other developmental abnormalities (Brewer, P B, 2004; Lampugnani, Kilinc, and Smyth, 2012). It is a transcriptional activator and *ptl* mutants show increased cell proliferation without changes in cell size. Replacing the PTL N-terminal trihelix with that of EDA31 can complement *ptl* mutants (Kaplan-Levy et al., 2014).

Argonaute (AGO) proteins recruit 21–24-nucleotide small RNAs (sRNAs) to constitute RNA-induced silencing complexes (RISCs) to regulate gene expression at transcriptional or post-transcriptional levels (Rogers and Chen, 2013). AGO3 is also involved in the regulation of epigenetic silencing (Zhang et al., 2016).

Cluster 6 contains genes that are downregulated at all time points. The GO categories enriched the most in this group are secondary metabolic process, response to biotic stimulus, oxygen binding, response to stress and reproduction (Figure 3.8).

The genes in this cluster include 4 members of the cytochrome p450 family (*CYP79B2*, *CYP79B3*, *CYP83B1* and *CYP710A2*). The first three are involved in the metabolism of auxin precursors (Kim et al., 2015). *CYP710A2*

encodes a C22 sterol desaturase involved in brassinosteroid metabolism. It catalyzes the final step in the biosynthesis of brassicasterol and stigmasterol (Morikawa et al., 2006).

Another gene also related to auxin homeostasis in cluster 6 is the UDP-glucose: thiohydroximate S-glucosyltransferase, *UGT74B1* (Grubb et al., 2004; Grubb et al., 2014). Plants with mutations on this gene accumulate higher levels of auxin.

*CUC2* is also placed within cluster 6, as is *AGAMOUS-LIKE6* (*AGL6*, reviewed in Dreni and Zhang, 2016). AGL6 is involved in floral meristem regulation, floral organs, ovule and seed development, and has possible roles in both male and female germline and gametophyte development.

Other genes that might be of interest based on their functional relationship to CUC1 were also found as differentially expressed. For example, *LATERAL ORGAN FUSION1* (*LOF1*), which is involved in organ separation through regulation of cell division (Lee, Geisler, and Springer, 2009), is upregulated at 2 dpi (cluster 1). *SPATULA* (*SPT*), which represses *CUC1* in the apical region of the gynoecial primordium and promotes medial ridge growth (Nahar et al., 2012), also appears in cluster 1, upregulated at 4 dpi.

Takeda et al., 2011 found *LIGHT-DEPENDENT SHORT HYPOCOTYLS 4* (*LSH4*) to be upregulated in seedlings when *CUC1* was overexpressed and is one of the two putative CUC1 direct targets (together with *LSH3*, see Section 1.5.2 in the Introduction). Here it appears upregulated at 0 dpi and is included in cluster 3.

### 3.3.2 Other considerations

It can be noted that the number of DEG is much smaller to that observed in thee *eep line* vs. the *AP1 line* Chapter 2. This could be a real biological effect or a consequence of the experimental setup chosen.

If it was a real biological effect it could be due to the fact that the genes that appear as DE in the *eep line* come from the increased level of *CUC1* and *CUC2* in comparison to the control, while in the *CUC line* only *CUC1*'s expression is elevated.

On the other hand, the observed FCs for *CUC1* are not very high, as it was assessed by qPCR too. It is possible that, since CUC1 is expressed from its own promoter, the resulting expression level is relatively low, as it is in the wild-type. Furthermore, even if the modification in the *CUC1m* sequence prevents the downregulation from *miR164*, this regulation might not be fully taking place during early developmental stages, as described in Section 2.3 and Baker et al., 2005.

In Chapter 2 the overall effect of the miR164c mutation was repressive at 0, 2 and 4 dpi. The reversal of that trend at 0 and 2 dpi could also be due to the sole upregulation of CUC1 or to high biological variability between samples.

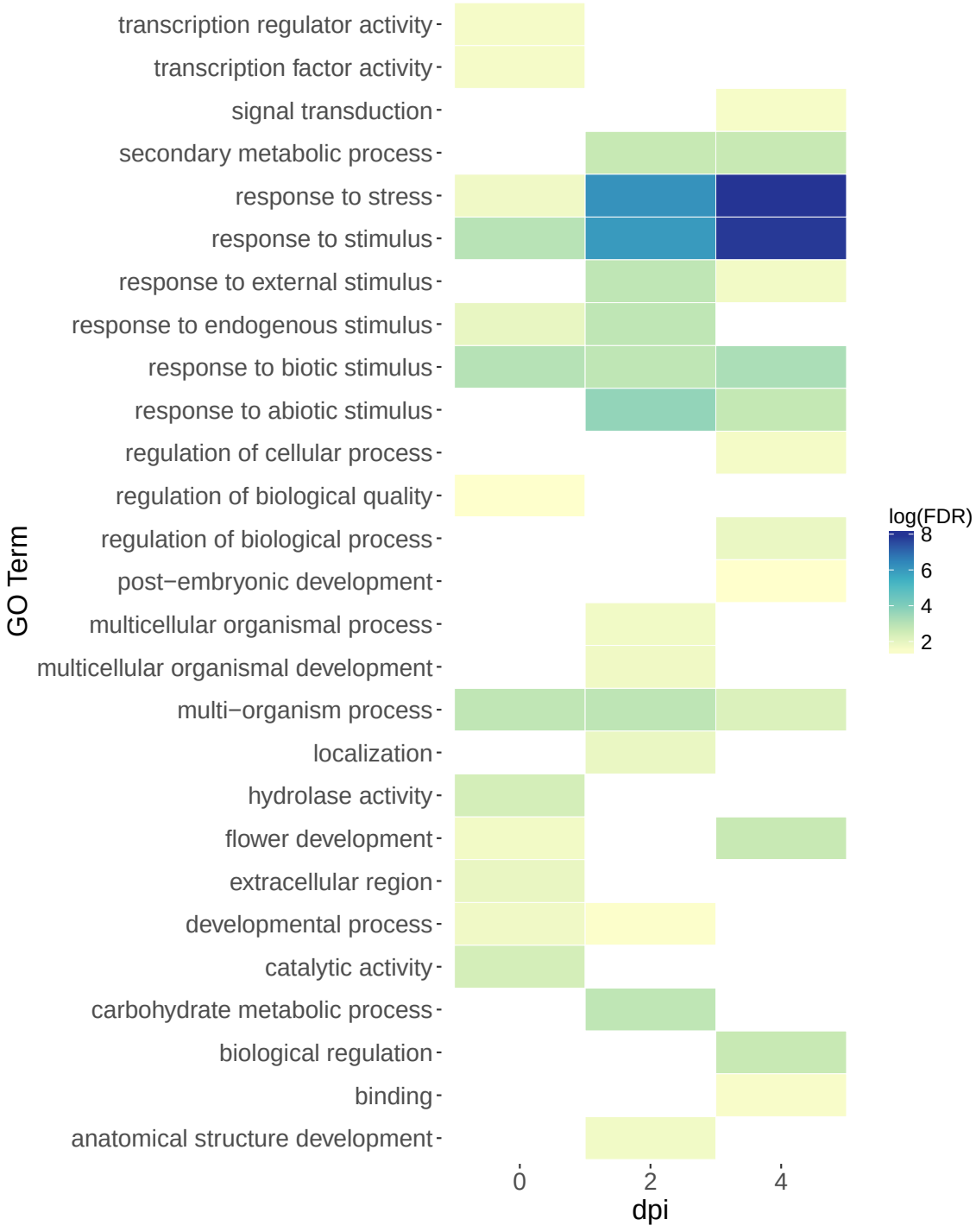


FIGURE 3.5: **Gene ontology analysis.** Gene ontology categories overrepresented in the differentially expressed genes from the *CUC line* vs. the *AP1 line* over time. Color represents the level of significance.

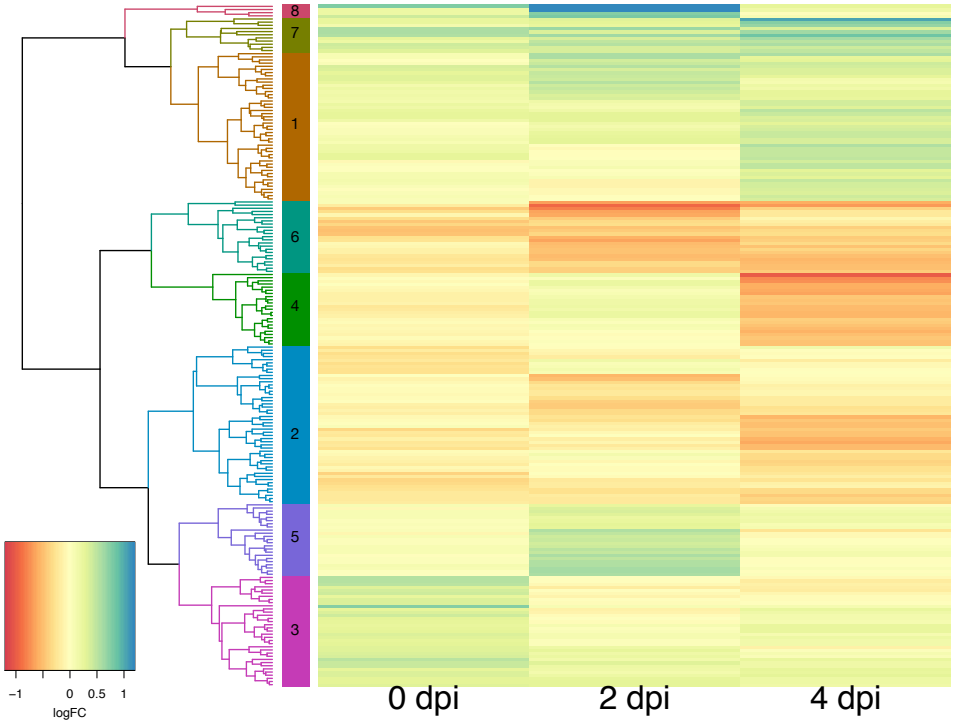


FIGURE 3.6: **Heatmap of DEGs.** Heatmap using the logarithmic fold change of the DEGs. The dendrogram is constructed using hierarchical clustering and the colors and numbers indicate the 8 most dissimilar clusters.

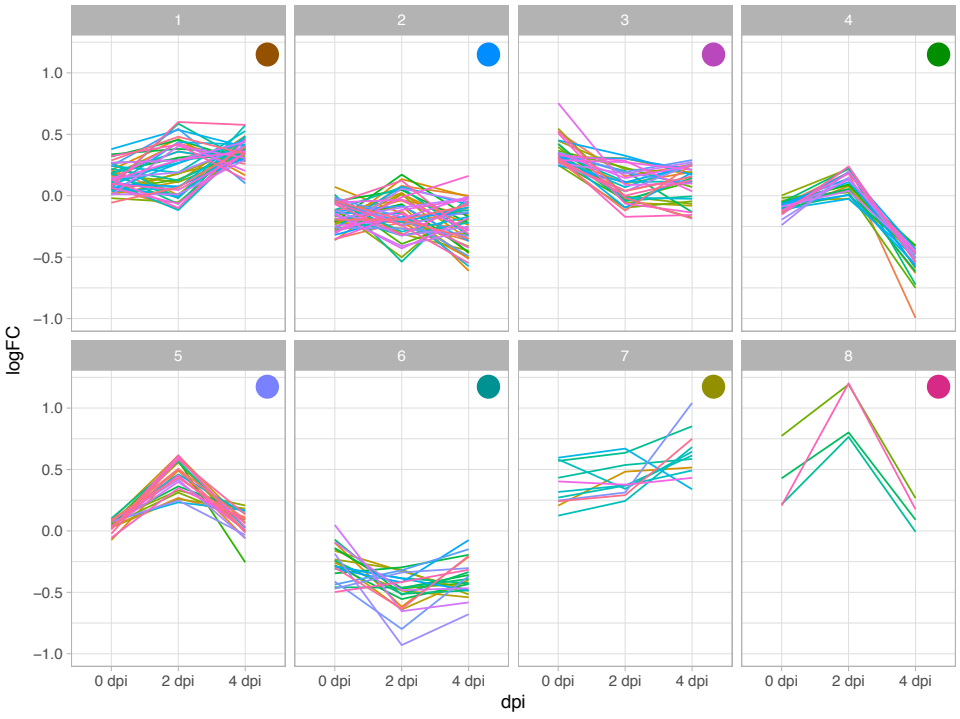


FIGURE 3.7: **Cluster expression dynamics.** Expression dynamics of genes separated according to the clusters they belong to in Figure 3.6.

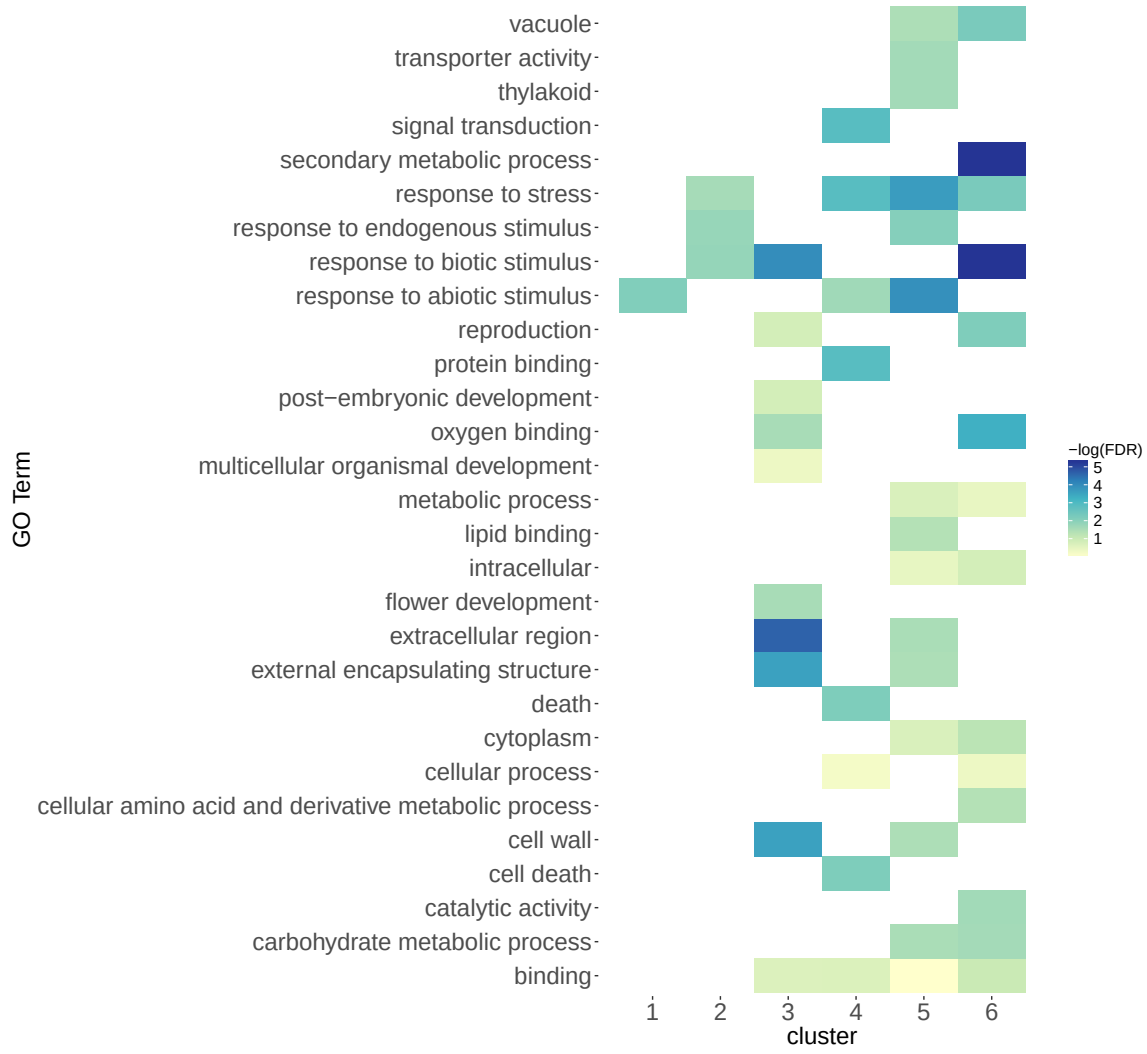


FIGURE 3.8: **Cluster gene ontology analysis.** Enriched GO categories in each of the clusters from Figure 3.6.

# Chapter 4

# ChIP-seq

## 4.1 Background

Gene expression is regulated through the integrated action of many processes and the binding of transcription factors to DNA is one of the most important ones. TFs are able to control gene expression by binding to sequences in the DNA, frequently regulatory regions in the vicinity of the genes they control, such as their promoters. TFs typically recognize 6-12 bp long sequences that are more or less degenerate and their impact on gene expression is influenced by different mechanisms which give rise to a robust, concerted action.

Finding the genomic regions to which transcription factors bind is paramount to understanding their function. Chromatin immunoprecipitation followed by next-generation sequencing (ChIP-seq) or by hybridization to arrays (ChIP-chip) is the standard method used to uncover *in vivo* protein-DNA interactions and to locate the DNA-binding sites of TFs in the genome.

The ChIP methodology has been successfully used to locate the direct target genes of different TFs involved in flower and plant development. The use of this and other genome-wide technologies allowed advances in the understanding of gene regulatory networks underlying flower development that had remained elusive through the use of genetic approaches (see Section 1.1.2, Ferrier et al., 2011; Bustamante, Matus, and Riechmann, 2016).

For example, the regulatory landscape controlled by WUSCHEL (WUS), a key TF required for stem cell specification and maintenance, was studied in Busch et al., 2010 using ChIP-chip combined with gene expression analyses. The study revealed that WUS is capable of binding to two motifs in over a hundred genome sites while affecting the expression of genes related to hormone signaling, metabolism, and development. Key direct targets were *CLAVATA1* (*CLV1*), which is repressed by WUS and in turn downregulates it in a negative feedback loop and the TOPLESS family of transcriptional repressors, which are involved in auxin signaling. Overall, a better understanding of the molecular mechanisms underlaying the maintenance of the stem cell niche was achieved.

In Ó'Maoiléidigh et al., 2013, the molecular mechanisms by which AGAMOUS (AG) participates in the control of meristem determinacy and the formation of reproductive floral organs were studied using ChIP-seq and microarrays. The authors found that AG is capable of controlling the expression of numerous genes that have regulatory functions, and so is able to indirectly regulate a myriad of developmental processes.

The study of AP1 gene regulatory network (see Section 1.6.1 for more details), on which this thesis is based on, also used ChIP-seq in combination with microarrays to characterize the genome-wide interactions of this key regulator of flower initiation and development with DNA (Kaufmann et al., 2010b).

There are several more examples of the ChIP methodology being applied in plant tissues (i.e. Winter et al., 2011; Wuest et al., 2012; Merelo, Paz et al., 2013; Nagel et al., 2015), and the results have been varied. The number of direct target genes found range from less than a couple of hundred, as is the case with WUS, Busch et al., 2010 to several thousands, as in the case of KANADI1 (KAN1), Merelo, Paz et al., 2013.

To determine CUC1 binding sites genome-wide, ChIP-seq was performed on the *CUC line* (pCUC1:CUC1m-GFP pAP1:AP1-GR *ap1 cal*).

The genes associated to the genomic regions where CUC1 is bound are putative CUC1 direct targets. Binding events may result in a transcriptional response in some cases, but it has been observed that only a minority of genes with TFs bound in their vicinity show a change in their expression activity (Kaufmann et al., 2010b; Wuest et al., 2012; Merelo, Paz et al., 2013).

Genes that are bound by CUC1 and that respond transcriptionally to it are direct transcriptional targets. Using the results of ChIP-seq experiments described in this Chapter and overlapping the list of genes obtained with the ones that appear as differentially expressed in response to the elevated levels of CUC1 (as assessed in the RNA-seq Chapter) is a way to obtain CUC1's direct targets.

### 4.1.1 Experimental design

The ChIP-seq protocol consists of a series of steps that include *in vivo* cross-linking of proteins to DNA with formaldehyde, isolation of the chromatin complex, shearing DNA along with bound proteins into small fragments using sonication, immunoprecipitation with an antibody specific against the tag (GFP) fused to CUC1, release of the co-precipitated DNA, and preparation of libraries to be sequenced by Illumina technology (see Materials and Methods for the detailed experimental protocol).

Normalization to a control sample is essential for the processing of the obtained reads to make experiments comparable, and as a control for background signal and non-specific binding. Different types of controls can be used to this end. The most common methods are the use of mock ChIP, ChIP in tissue from wild type or mutants for the studied TF, or input DNA.

Mock ChIP uses the same procedure for processing the samples and controls but employs a non-specific antibody (e.g. IgG) instead of the specific one against the protein of interest or its tag. Another option is the use of wild type tissue (without the tagged protein of interest) or mutants (without the protein of interest) and maintaining the rest of the protocol identical in samples and controls.

In this case, input samples were used, as described in several studies of the same type (e.g. Kaufmann et al., 2010b, Ó'Maoiléidigh et al., 2013 and Nagel et al., 2015). This control is tissue from the same transgenic line that has been subject to the same processes as the IP samples, except for the immunoprecipitation with anti-GFP, so it is essentially sonicated chromatin.

Using this approach, it is expected that the IP samples will be enriched in DNA regions that are bound by CUC1, as opposed to the input samples where the reads are derived from randomly shredded chromatin and the abundance of reads mapped in different regions should reflect background signal or differences related to chromatin accessibility and not to specific TF binding.

Tissue from inflorescences at 0 and 4 days post induction (dpi) was collected from the *CUC line* (pCUC1:CUC1m-GFP pAP1:AP1-GR *ap1 cal*, Figure 4.1) and samples were processed as described in Materials and Methods. 0 dpi is the starting point where floral induction has not been triggered yet. Then, 4 dpi (Stages 5-6 according to Smyth, Bowman, and Meyerowitz, 1990) is a key moment for CUC1's function, since boundaries are created when petals and stamen primordia arise and sepals enclose the floral bud (Smyth, Bowman, and Meyerowitz, 1990).

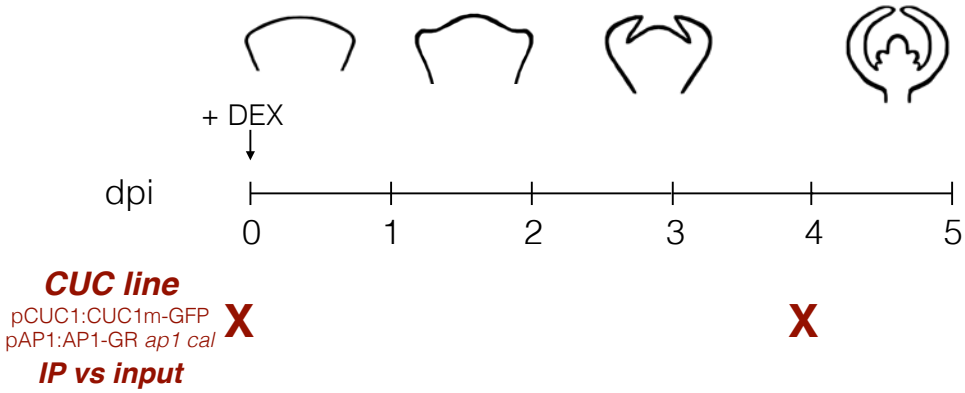


FIGURE 4.1: **Experimental design.** Samples were collected at 0 and 4 dpi from the *CUC line* and libraries were prepared with IP and input samples.

Three biological replicates were used for each time point. Since each biological replicate consists of one IP sample and one input (control) sample, a total of twelve libraries were constructed and sequenced (6 IP, 6 input).

After sequences were trimmed and filtered by quality, peaks were called using MACS2 (Zhang et al., 2008), using the sequences derived from IP

samples versus the input control. Peak calling algorithms are able to identify regions of the genome where there is a statistically significant higher abundance of mapped reads in the IP samples vs. the controls.

## 4.2 Results and Discussion

### 4.2.1 Peaks

A table with all peak coordinates in each library can be obtained in the online Supplementary information (Supplementary table 4.1). A total of 6611 peaks were found in at least one library.

Coordinates for peaks grouped by day are in Supplementary table 4.2.

#### Peak positions

The position of the peaks with respect to the transcriptional start site (TSS) of the closest gene in any library is depicted in Figure 4.2. The data used to construct this plot includes all peaks regardless of the library it appears on and whether it is present in more than one library or not.

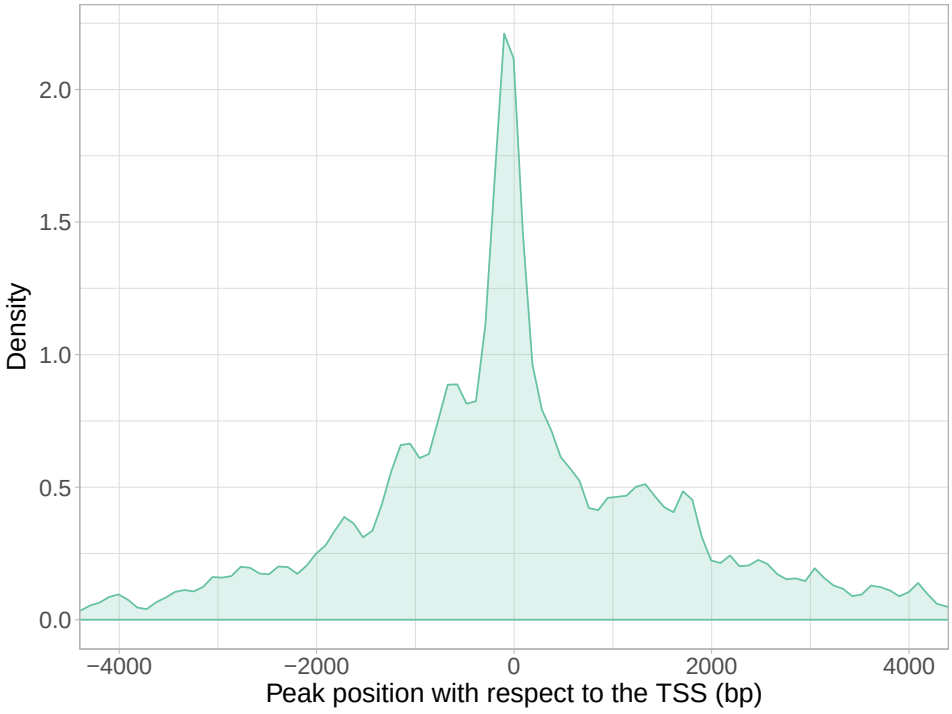


FIGURE 4.2: **Peak position.** Position of ChIP-seq peaks with respect to the closest associated gene in all samples (TSS: Transcription start site).

Using the same data, the distribution of peak positions with respect to the closest gene according to the dpi the sample was taken on can be observed in Figure 4.3. The peak positions according to the library they are found in and the dpi is shown in Figure 4.4.

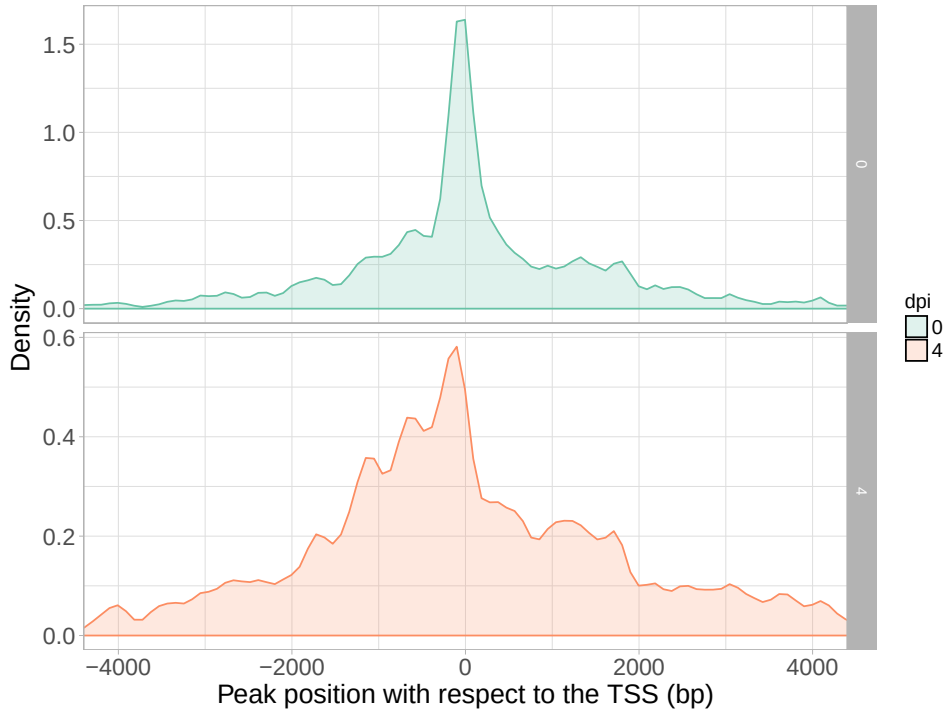


FIGURE 4.3: **Peak position.** Position of ChIP-seq peaks with respect to the closest associated gene in all samples, separated by dpi (TSS: Transcription start site).

### Shared ChIP peaks between libraries

All available ChIP library biological replicates for each time point were analyzed. Results obtained for each time point were first assessed using the Irreproducible Discovery Rate (IDR) (Li et al., 2011).

The IDR measures the reproducibility of the peaks from replicate experiments. It assesses the rank consistency of identified peaks between replicates and can be use to detect low quality experiments. The IDR method is independent from peak-calling algorithms and produces results that are consistent in experiments from diverse origins (e.g. different laboratories, protocols, antibodies, etc).

This approach was used in the samples for each time point and the results indicated that there was a good correlation between the different replicates that were included in the downstream analysis.

In order to have a way to estimate the level of reproducibility of peaks, a system of *tiers* was created. Each peak was assigned a score according to the number of libraries it appeared in. So, a score of 3 means that a peak was found in 3 different libraries. Peaks with score of 1 or more are referred to as *tier 1 peaks*, and so on. The higher the tier, the more reproducible a peak is considered to be.

For example, a region that is consistently bound by CUC1 and consistently detected in all replicates for a time point would result on a peak with a score of 3. In contrast, a region that is detected in only 2 of the replicates will have a score of 2, or a score of 1 if it is detected in a single replicate.

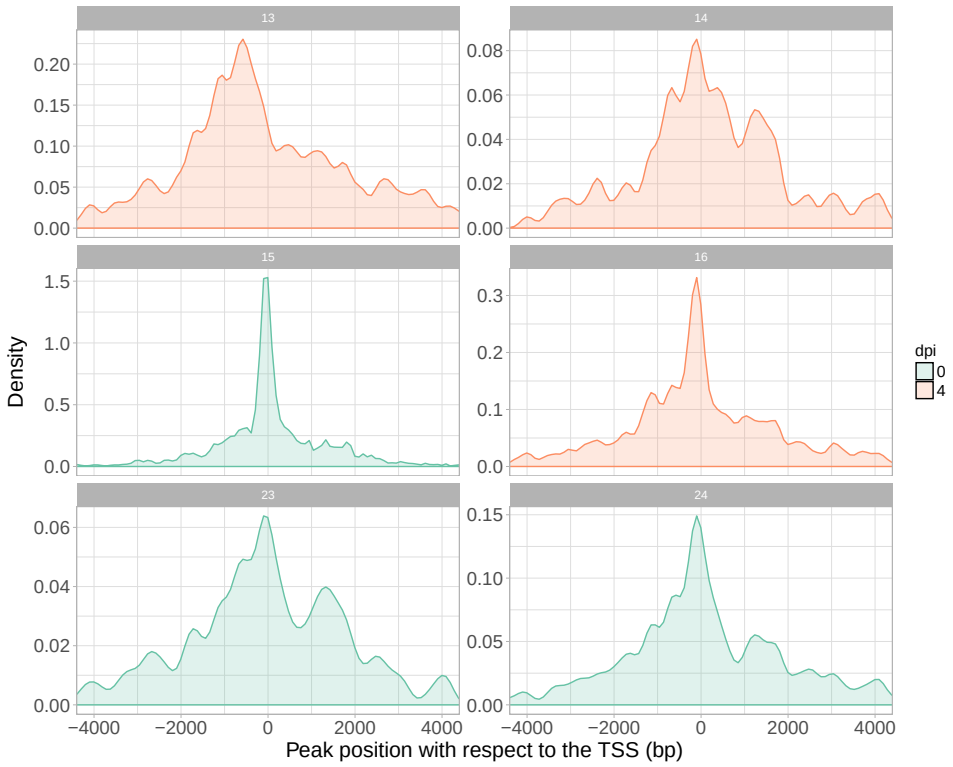


FIGURE 4.4: **Peak position.** Position of ChIP-seq peaks with respect to the closest associated gene in all samples, separated by library. Color indicates the dpi (TSS: Transcription start site).

In order to be able to assign these scores to a peak, the genomic regions of the *original peaks* in different replicates were compared. When there was an overlap (of at least 1 bp), the 2 or 3 peaks that are found in those overlapping genomic regions in different biological replicates were merged (using BEDTools `merge`, Quinlan and Hall, 2010). This way, a *combined peak* that would now span from the beginning of the most 5' original peak to the end of the most 3' one was obtained.

The majority of peaks appear in only one library. Out of 4836 peaks that come from the dataset divided by days, 3766 peaks have a score of 1, while 1070 peaks have a score of at least 2 in the complete dataset (both time points). A table of the peaks with score of at least 2 can be found in the Supplementary table 4.3. Using the data for each time point separately, the frequency of peaks with scores 2 or 3 is shown in Figure 4.5.

### Genes associated to peaks

A peak is considered to be associated to a gene if it falls in a genomic region within 3 kb upstream of the transcription start (TSS) site and 1 kb downstream of the transcription termination site (TTS). Note that, using this criteria, one peak can be associated to more than one gene, and one gene can be associated to more than one peak.

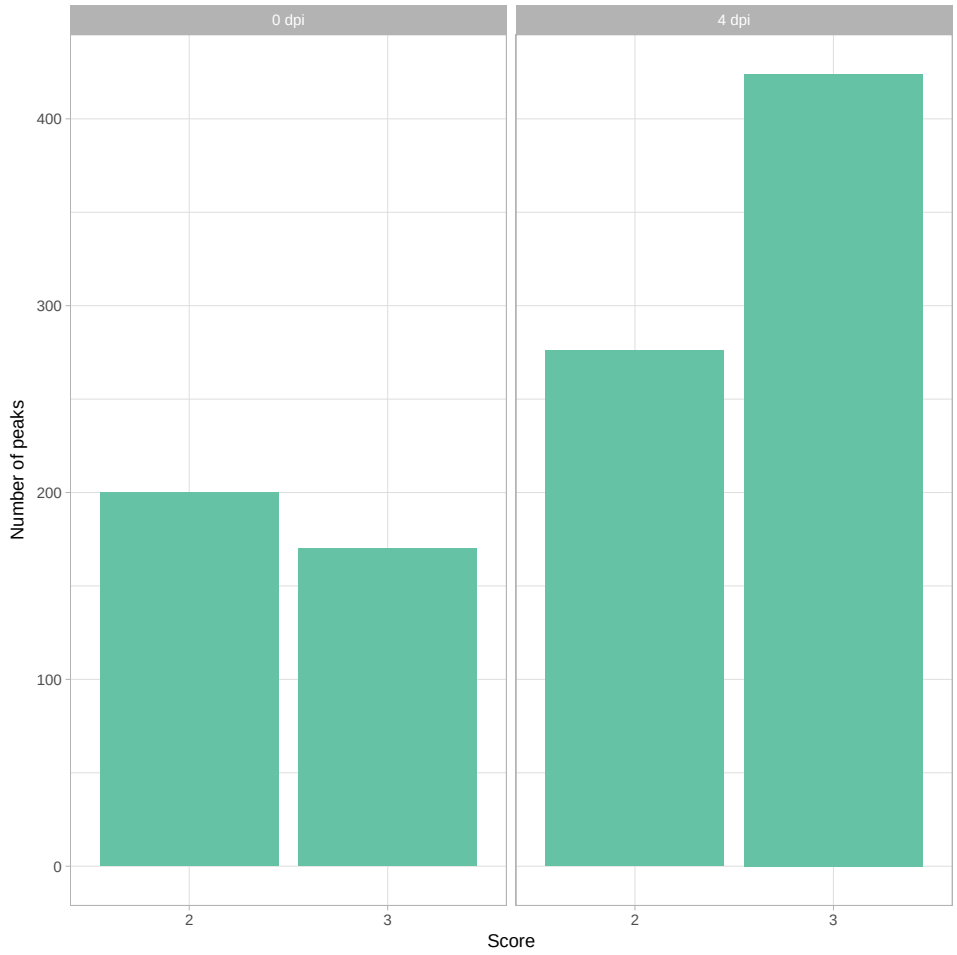


FIGURE 4.5: **ChIP-seq peaks at 0 dpi.** Distribution of number of peaks with score of at least 2 in all libraries separated by dpi.

Out of the 4836 peaks that were identified, 4665 were within the 3 kb upstream and 1 kb downstream cutoff that was set. The other 171 peaks were located in intergenic regions at greater distances from annotated genes. Out of the 4665 peaks, 1000 peaks had a score of 2 or higher. Within the -3kb/+1kb range of these 1000 peaks, 327 genes were found.

The 1000 tier 2 *combined peaks* are originated from 2641 *original peaks*. The position of the 2641 peaks with respect to the features of their associated genes is depicted in Figure 4.6. To associate the peaks to a feature, the summit of each original peak was considered.

The vast majority of peaks are located in the defined promoter region (3 kb upstream of the TSS). This suggests that CUC1 is more likely to bind to regulatory regions in the genome, as it is expected for transcription factors.

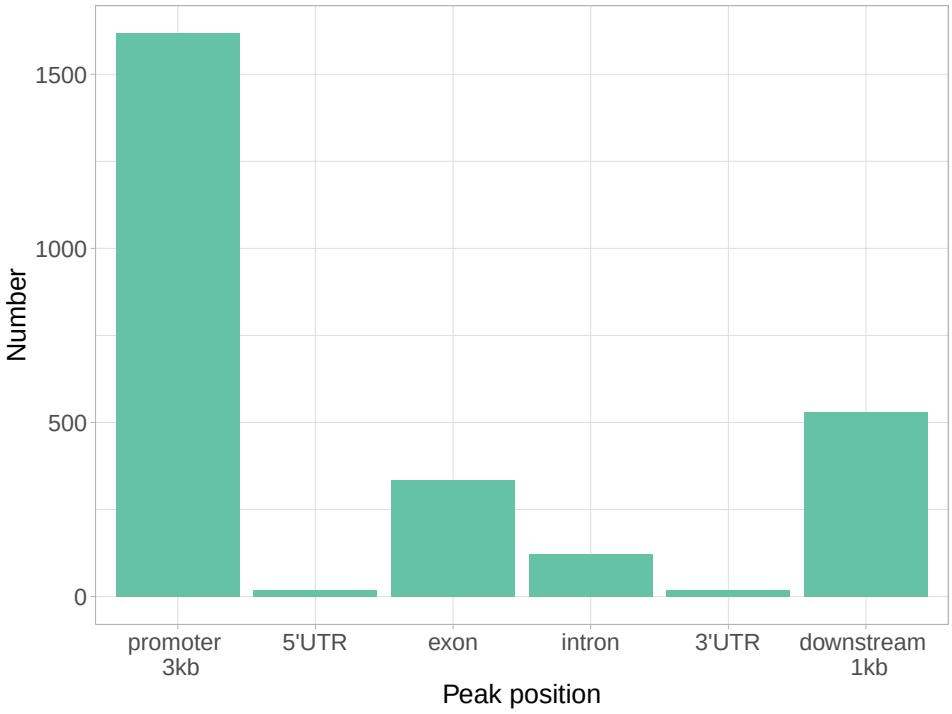


FIGURE 4.6: **Original peak position.** Position of ChIP-seq original peaks in tier 2 group with respect to their associated genes, separated by dpi. The associated feature is where the summit is located.

### Gene Ontology analysis

A gene ontology (GO) analysis was performed with the genes associated to tier 2 peaks and an enrichment in categories related to translation, biosynthetic process, generation of precursor metabolites and energy, RNA binding and ribosome was found (Figure 4.7).

Five peaks were found in the promoter of CUC1. This indicates that CUC1 is able bind directly to its own promoter.

Another TF that has several peaks in its promoter is APETALA1 (AP1). Despite this, AP1 does not appear to be differentially expressed in our experimental conditions in the RNA-seq experiments of the same line or the microarray experiments with the *eep line* (Chapter 2).

The AUXIN RESPONSE FACTOR 6 (ARF6) has been shown to interact with BRASSINAZOLE-RESISTANT 1 (BZR1) and they share 51% of their targets (Oh et al., 2014). There is a peak with a score of 3 at 0 dpi and 2 at 4 dpi present in the ARF6 promoter. This could provide a link between CUC1 and the auxin and brassinosteroid hormonal pathways. ARF6 does not appear as a DEG in the RNA-seq or microarrays carried out.

## 4.2.2 ChIP vs RNA-seq

In order to obtain a list of CUC1 direct transcriptional targets (genes that are bound by CUC1 and that respond transcriptionally to it), the genes associated to peaks in the ChIP-seq experiments can be compared to the

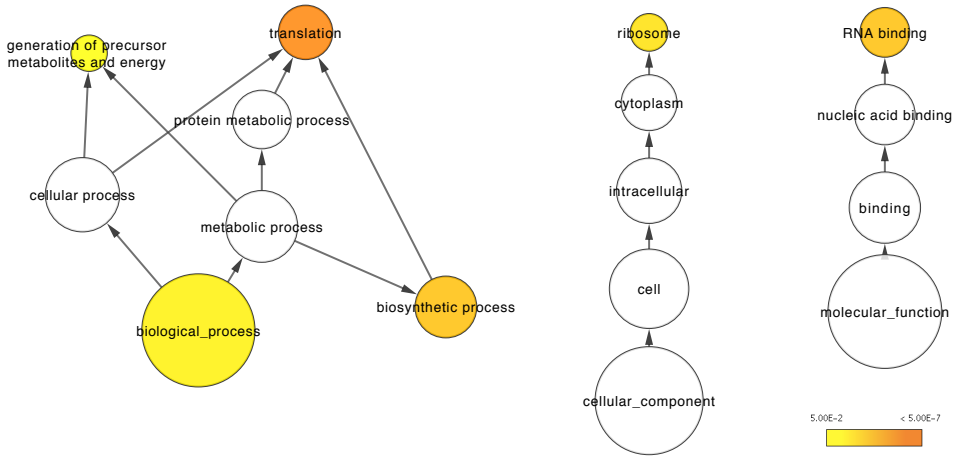


FIGURE 4.7: **Gene ontology analysis.** Gene ontology categories overrepresented in the genes associated to peaks with a score of at least 3. Color represents the level of significance.

| Gene ID | Gene name | Gene symbol | Position of peak | Peak score |
|---|---|---|---|---|
| AT2G33480 | NAC DOMAIN CONTAINING PROTEIN 41 | NAC041 | promoter-3kb | 3 |
| AT3G15170 | CUP-SHAPED COTYLEDON1 | CUC1 | promoter-3kb | 2 |
| AT3G16180 | NITRATE TRANSPORTER 1.12 | NRT1.12 | promoter-3kb | 3 |

TABLE 4.1: **Genes that appear in RNA-seq and ChIP-seq datasets.** The peak score and position is included.

ones that are differentially expressed in the RNA-seq experiments (Chapter 3).

The genes associated to the genomic regions where CUC1 is bound are putative CUC1 direct targets. Binding events may result in a transcriptional response in some cases, but it has been observed that only a minority of genes with TFs bound in their vicinity show a change in their expression activity (Kaufmann et al., 2010b; Wuest et al., 2012; Merelo, Paz et al., 2013).

Genes that respond trasncriptionally to CUC1 and have peaks in their vicinity with an *inter-day* score of 2 or higher are listed in Table 4.2.

Among those is CUC1 itself. As stated before, since the transgenic line used for the experiments (the *CUC line*) is an overexpressing line in practice, it is impossible to know whether the binding of CUC1 to its own promoter is affecting its expression in this experimental conditions.

### 4.2.3 CUC1 binding sequence

In order to establish CUC1's binding sequence, 100 bp sequences centered in the summit from the 2641 peaks that gave origin to the score 2 peaks were used to do a MEME-chip analysis. The three most enriched motifs are shown in Figure 4.8.

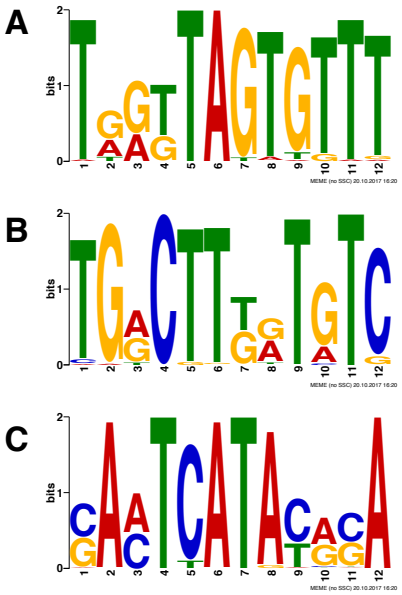


FIGURE 4.8: **CUC1 binding sequences.** Motifs found by MEME-chip analysis of the peaks with score 2 or higher.

The proteins that had sequences most similar to these motifs are WRKY7 (B motif), a Ca-dependent calmodulin binding protein with sequence similarity to the WRKY transcription factor gene family, and CRABS CLAW (CRC, motif A and C), a transcription factor with zinc finger and helix-loop-helix domains involved in the specification of abaxial cell fate in the carpel.

The fact that the majority of the peaks are located in regulatory regions (mainly promoters) suggests that the ChIP-seq experiments have been successful and shows the potential regulatory function of CUC1. Despite this, the correlation with genes that appear as differentially expressed in the RNA-seq experiments performed in the same line and time point is quite low. This has been observed for other TFs. For instance, in Busch et al., 2010, only about 1% of the WUS response genes are direct targets. This is about the same ratio obtained at 4 dpi. At 0 dpi it is about 5%.

On the other hand, if the comparison is done without taking into account the time point at which the experiment was made, a higher number of putative direct transcriptional targets is obtained. About 15% of the genes that respond transcriptionally to the elevated levels of CUC1 have a binding site in their vicinity (tier 1 peaks). If peaks with scores of at least 2 are used, the overlap is about 2%.

One reason for this could be that, as explained in the RNA-seq Chapter, the number of differentially expressed genes obtained in this experimental setup is likely underestimated due to the high variability between biological replicates and to the fact that CUC1's overexpression is not very strong and restricted to a specific domain. If this is the case, the overlap with the direct

targets found by ChIP-seq is going to be small too.

In order to test this it would be useful to have a different transgenic like overexpressing CUC1 at a higher level and maybe in a broader domain, ie. using a 35S promoter.

## 4.3 Peak profiles

Profiles of some of the peaks obtained are depicted in Figures 4.9, 4.10, 4.11.

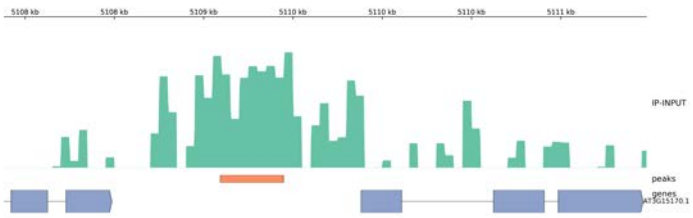


FIGURE 4.9: **CUC1 LM15.** Peak.

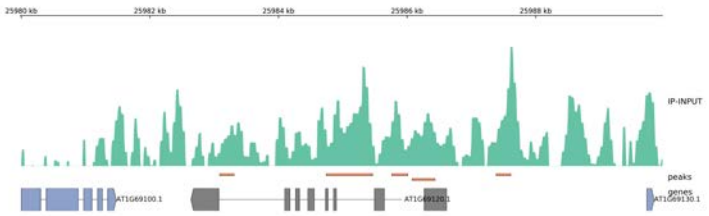


FIGURE 4.10: **AP1 LM15.** Peak.

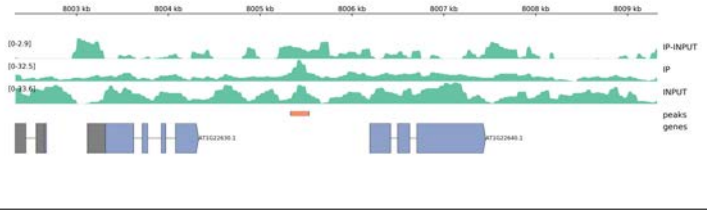


FIGURE 4.11: **SAC1 LM15.** Peak.

| Gene ID | Gene name | Gene symbol | Position of peak | Peak score |
|---|---|---|---|---|
| AT2G33480 | NAC DOMAIN CONTAINING PROTEIN 41 | NAC041 | promoter-3kb | 3 |
| AT3G15170 | CUP-SHAPED COTYLEDON1 | CUC1 | promoter-3kb | 2 |
| AT3G16180 | NITRATE TRANSPORTER 1.12 | NRT1.12 | promoter-3kb | 3 |

TABLE 4.2: **Genes that appear in RNA-seq and ChIP-seq datasets.** The peak score and position is included.

# Chapter 5

# Proteomics

## 5.1 Background

Plants are sessile organisms and as such they are forced to adjust their metabolism, growth and development to a highly dynamic environment. Many signaling processes converge at the level of gene regulation, where transcription factors can modulate gene expression.

Protein-protein interaction is important to fine-tune the activity of TFs. Multimeric protein complexes are often required for the execution of specific biological functions (Immink, Kaufmann, and Angenent, 2010; Smaczniak et al., 2012a; Pajoro et al., 2014). TF DNA binding specificity and mechanisms of gene regulation can depend on the interaction with cofactors or on the recruitment of other TFs or other types of transcriptional regulators, such as chromatin remodelers.

Results obtained by ChIP-seq, RNA-seq and microarray analysis have shown that CUC1 can act as an activator and a repressor of transcription (Chapter 3, Chapter 2, Chapter 4). The identification of CUC1 protein partners would aid to shed light on the mechanisms by which CUC1 can modulate the transcription of its target genes.

For a long time, only targeted methods to detect protein complexes, such as the traditional Western blot method, were available. The obvious disadvantage of this approach is the need of obtaining antibodies for the proteins of interest or their tags. This is often time and resource consuming and it requires previous knowledge of potential interactions, thus not resulting appropriate for the discovery of novel connections between previously unknown protein partners. To overcome this obstacle, large-scale methods have been developed, using liquid chromatography coupled to tandem mass spectrometry (LC-MS/MS), a highly sensitive procedure.

Smaczniak et al., 2012b described a method that combines affinity-based protein complex isolation of endogenously expressed, fluorophore-tagged proteins from intact plant tissues and is coupled to the identification of interaction partners by label-free MS-based analysis. This approach was successfully applied to characterize MADS-domain TF complexes in

Smaczniak et al., 2012a using the floral induction system described before (Wellmer et al., 2006, Section 1.7.1).

In the work presented in this Chapter this is the approach that has been taken in order to characterize CUC1's interactome.

### 5.1.1 CUC1 known interactors

It has been reported that CUC1 is able to interact in yeast and in planta with itself, forming homodimers, and with CUC2 and CUC3, forming heterodimers (Gonçalves et al., 2015). The dimerization occurs through the N-terminal highly conserved NAC domain, although it can be influenced by the C-terminal regions. Two residues that allow the formation of salt bridges (arginine-19 and glutamate-26) are essential for dimerization (Ernst, Heidi A et al., 2004; Olsen et al., 2005).

To this date, no other CUC1 interactors have been described.

## 5.2 Results and discussion

### 5.2.1 Experimental design

The goal of this section is to identify proteins that are interacting with CUC1 in vivo. In order to achieve this, the *CUC line* (pCUC1:CUC1m-GFP pAP1:AP1-GR *ap1 cal*) and the *AP1 line* (pAP1:AP1-GR *ap1 cal*) were used. The experimental design is analogous to the one used for RNA-seq (Figure 5.1).

In this case, IP samples were obtained from the *CUC line* using anti-GFP antibody. Suitable IP controls are essential for obtaining reliable results. In order to correct for nonspecific binding of the GFP antibody to other proteins, the *AP1 line* (pAP1:AP1-GR *ap1 cal*) was used.

Samples from the *CUC line* and the *AP1 line* were collected at 2 and 4 dpi. Protein extracts were immunoprecipitated with anti-GFP antibody and processed in parallel throughout the experiment (detailed in Materials and Methods).

Using this approach, proteins that are enriched in the IP samples from the *CUC line* in comparison to the IP controls and their relative abundance could be identified. In order to reliably estimate protein abundance ratios, biological replicates were used. Table 5.1 indicates the number of replicates for each time point and genotype.

| Genotype | Time (dpi) | Number of biological replicates |
|---|---|---|
| CUC line | 2 | 3 |
| AP1 line | 2 | 2 |
| CUC line | 4 | 6 |
| AP1 line | 4 | 3 |

Table 5.1: Proteomics sample information

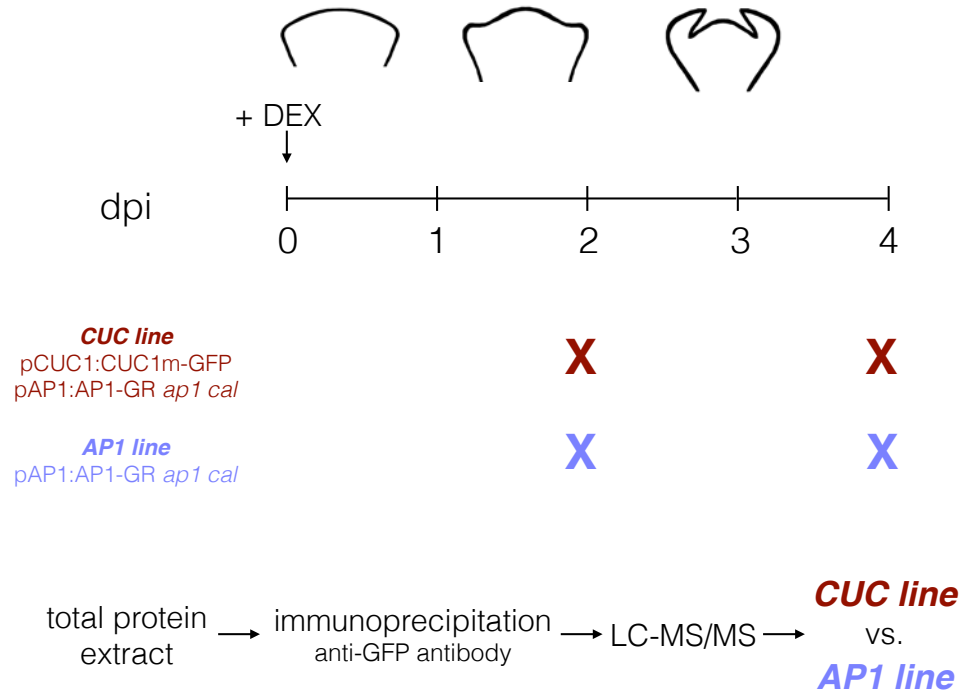


FIGURE 5.1: **Experimental design.** Protein extracts from the *CUC line* and the *AP1 line* at 2 and 4 dpi were immunoprecipitated and analyzed by mass spectrometry.

The presence of CUC1m-GFP was assessed through confocal microscopy in the *CUC line* and the spatial specificity of its expression in the boundary regions was confirmed (Figure 5.2).

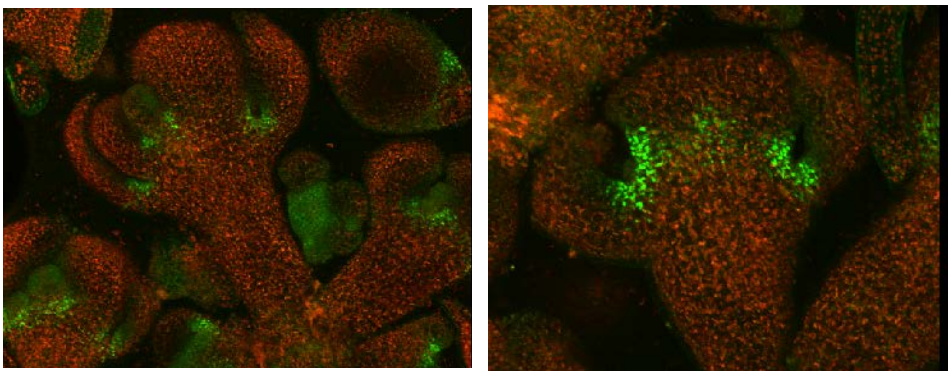

FIGURE 5.2: **CUC1 expression in the CUC line.** CUC1m-GFP expression in pCUC1:CUC1m-GFP pAP1:AP1-GR *ap1 cal* (*CUC line*) at 4 dpi.

It is important to note that the high sensitivity of the LTQ-Orbitrap XL mass spectrometer used in this method permits the detection of low abundance proteins in complex mixtures, as CUC1 protein is present mainly in the boundary cells, which represent a small proportion of the inflorescence tissue collected (Sieber et al., 2007, Figure 5.2).

### 5.2.2 CUC1 immunoprecipitation

In order to assess the IP process, both total and nuclear extracts were obtained from inflorescences of the *CUC line* at 4 dpi, as described in Smaczniak et al., 2012b.

Immunoprecipitation with anti-GFP antibody (Abcam Ab290) was followed by Western blotting (Figure 5.3). Pellets and flow through fractions were also loaded to check if CUC1m-GFP was being lost during the IP process.

A single band of the expected molecular weight corresponding to the CUC1m-GFP fusion protein (51 kDa) was detected in the immunoprecipitated nuclear extract with the anti-GFP antibody (IP), whereas no protein was detected in the pellet (P1) or flow-through samples (FT). This indicates that there is no apparent loss of CUC1m-GFP protein during the IP procedure (Figure 5.3).

Similarly, CUC1m-GFP is specifically detected in the sample derived from the IP performed on total extract, although in this case additional bands are detected. There is no detectable loss of protein in the pellets (P1 and P2) and flow-through (FT) fractions (Figure 5.3) from total extract.

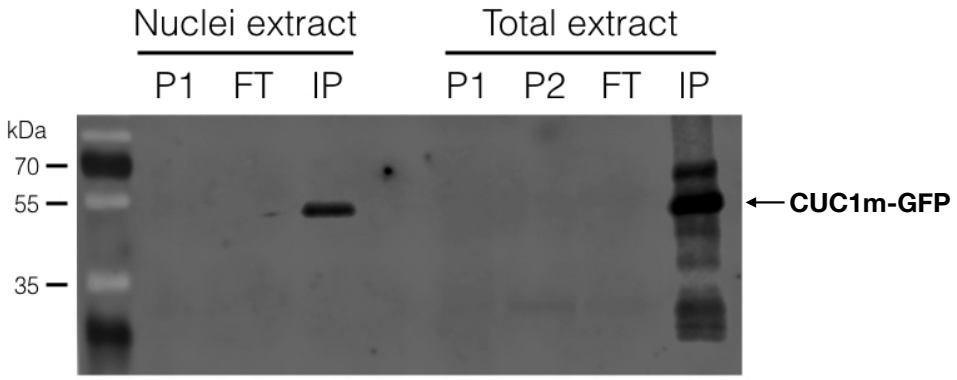


FIGURE 5.3: **Western Blot of CUC1m-GFP IP.** Western Blot against immunoprecipitated CUC1m-GFP (anti-GFP Ab) from total extract and nuclear extract (IP). Controls for first (P1) and second (P2) pellets are shown, as well as for flow through (FT). CUC1m-GFP has a molecular weight of 51 kDa.

Both extracts were analyzed by MS as a first assessment to determine the best experimental approach. The results of this test showed that a higher number of peptides could be recovered with better protein coverage (how much of each protein can be identified) in the total extract compared to the nuclear extract. This might be because the biochemical process of isolating the nuclei can result in protein degradation or loss. Also, some transcription factors do not localize exclusively in the nucleus and might form complexes in the cytoplasm too.

To minimize a lengthy isolation process, get a better quality of peptide mapping and to avoid loss of potential complexes, the results shown in this

Chapter (5) come from experiments performed with IP samples from total extracts.

### 5.2.3 Data analysis

After samples were analyzed in the LTQ-Orbitrap mass spectrometer, the acquired LC-MS/MS raw data was loaded into the MaxQuant software and analyzed as described in Smaczniak et al., 2012b.

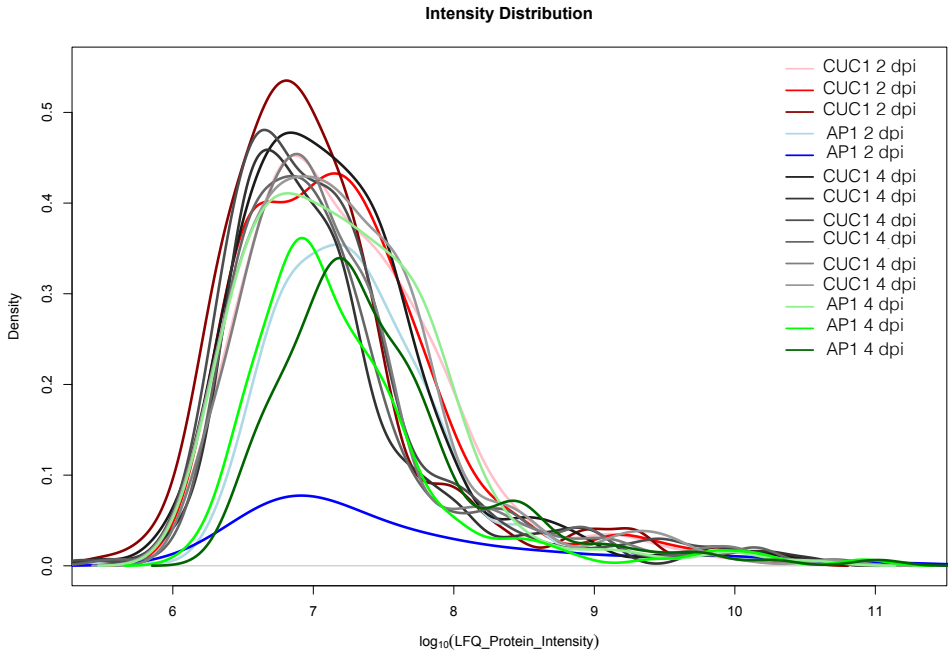


FIGURE 5.4: **Intensities distribution.** Density plots of proteomics samples detailed in Table 5.1 according to normalized protein intensity.

The normalized intensity distribution shows that a comparable amount of protein was detected for samples at 4 dpi (Figure 5.4). Since there are more biological replicates for this time point (Table 5.1), statistical analyses were performed to obtain a list of proteins that are detected in the *CUC line* at a higher level in comparison to the control line (Materials and Methods). In this Chapter, proteins that are more abundant in the *CUC line* with a FDR below 0.1 are considered to be significantly enriched.

On the other hand, very little amount of protein could be detected in the sample that corresponds to the *AP1 line* at 2 dpi (Figure 5.4, blue line). Since there was only one other replicate of this sample, the statistical significance of the differential detection of proteins at 2 dpi could not be calculated. Therefore, the data obtained from the 2 dpi analysis was used only to reinforce the evidence of presence of putative CUC1 interactors found in the 4 dpi time point analysis.

### 5.2.4 CUC1 putative interactors

An indication that this kind of experiment is technically performing adequately is to find the bait protein (CUC1) and its tag (GFP) amongst the most enriched proteins in the line of interest in comparison to the control. As expected, CUC1 and GFP appeared in the top 3 most enriched proteins both at 2 and 4 dpi.

There were 38 proteins identified to be more abundant in the CUC line at 4 dpi with a FDR below 0.1, of which 20 also passed the 0.05 FDR threshold (Figure 5.5, Table 5.2).

For downstream analysis, the predicted localization of the 38 proteins that passed the 0.1 FDR cutoff was retrieved from the TAIR website (Download > TAIR10 Genome Release > TAIR10-Subcellular_Predictions.xlsx).

| Gene ID | Symbol | Description | Significance | Predicted Localization |
|---|---|---|---|---|
| AT3G15170 | CUC1 | NAC transcription factor involved in SAM and boundary formation | FDR<0.05 | Nucleus |
| Tag | GFP | Green fluorescent protein | FDR<0.05 | NA |
| AT1G79930 | HSP91 | heat shock protein 91 | FDR<0.05 | Cytoplasm |
| AT5G56500 | | TCP-1/cpn60 chaperonin family protein | FDR<0.05 | Chloroplast |
| AT3G13470 | | | FDR<0.05 | Chloroplast |
| AT1G79920 | HSP70-15 | Heat shock protein 70 family protein | FDR<0.05 | Nucleus |
| AT2G28000 | CPN60A | chaperonin-60alpha | FDR<0.05 | Chloroplast |
| AT1G55490 | CPN60B,LEN1 | chaperonin 60 beta | FDR<0.05 | Unknown |
| AT2G20580 | RPN1A | 26S proteasome regulatory subunit S2 1A | FDR<0.05 | Nucleus |
| AT3G11130 | | NA | FDR<0.05 | Unknown |
| AT2G21060 | GRP2B | glycine-rich protein 2B | FDR<0.05 | Unknown |
| AT2G38040 | CAC3 | | FDR<0.05 | Chloroplast |
| ATCG00500 | ACCD | acetyl-CoA carboxylase carboxyl transferase subunit beta | FDR<0.05 | Chloroplast |
| AT4G20360 | | RAB GTPase homolog E1B | FDR<0.1 | Chloroplast |
| AT2G39730 | RCA | | FDR<0.05 | Chloroplast |
| AT3G42170 | DAYSLEEPER | Transposase-like gene with conserved domains from the family of hAT transposases | FDR<0.05 | Nucleus |
| AT1G09100 | RPT5B | 26S proteasome AAA-ATPase subunit RPT5B | FDR<0.05 | Nucleus |
| AT2G29550 | | tubulin beta-7 chain | FDR<0.1 | Cytoplasm |
| AT5G19780 | | tubulin alpha-5 | FDR<0.1 | Cytoplasm |
| AT4G18850 | | | FDR<0.1 | Unknown |
| AT4G16155 | | dihydrolipoyl dehydrogenases | FDR<0.05 | Mitochondrion |
| AT3G13920 | | | FDR<0.1 | Nucleus |
| AT3G26650 | | | FDR<0.1 | Chloroplast |
| AT3G44110 | ATJ3, ATJ | homologous to the co-chaperon DNAJ protein from E coli | FDR<0.05 | Cytoplasm |
| AT5G26210 | AL4 | Member of the Alfin1-like family of plant homeodomain containing proteins. Binds to di- or trimethylated histone H3 (H3K4me3/2). | FDR<0.05 | Nucleus |
| AT5G18380 | | Ribosomal protein S5 domain 2-like superfamily protein | FDR<0.1 | Cytoplasm |
| AT4G15802 | | heat shock factor binding protein | FDR<0.1 | Nucleus |
| AT2G42520 | | | FDR<0.1 | Unknown |
| AT1G20200 | RPN3A | 26S proteasome regulatory subunit S3 homolog A | FDR<0.05 | Nucleus |
| AT3G61430 | | plasma membrane intrinsic protein 1A | FDR<0.1 | Cell membrane |
| AT1G18210 | | Calcium-binding EF-hand family protein | FDR<0.1 | Cell membrane |
| AT5G62700 | | tubulin beta chain 3 | FDR<0.1 | Cytoplasm |
| AT1G62940 | | acyl-CoA synthetase 5 | FDR<0.1 | Unknown |
| AT1G53750 | RPT1A | 26S proteasome AAA-ATPase subunit RPT1A | FDR<0.1 | Nucleus |
| AT4G35100 | | plasma membrane intrinsic protein 3 | FDR<0.1 | Cell membrane |
| AT1G20010 | | tubulin beta-5 chain | FDR<0.1 | Cytoplasm |
| AT1G20620 | | catalase 3 | FDR<0.1 | Unknown |
| AT5G44340 | | tubulin beta chain 4 | FDR<0.1 | Cytoplasm |

TABLE 5.2: Putative CUC1 interactors with a FDR below 0.1.

There are 57 possible isoforms that correspond to the 38 proteins that are enriched in the CUC line. During the MS data analysis, the fragments obtained from the spectrometer are assigned to the proteins from which

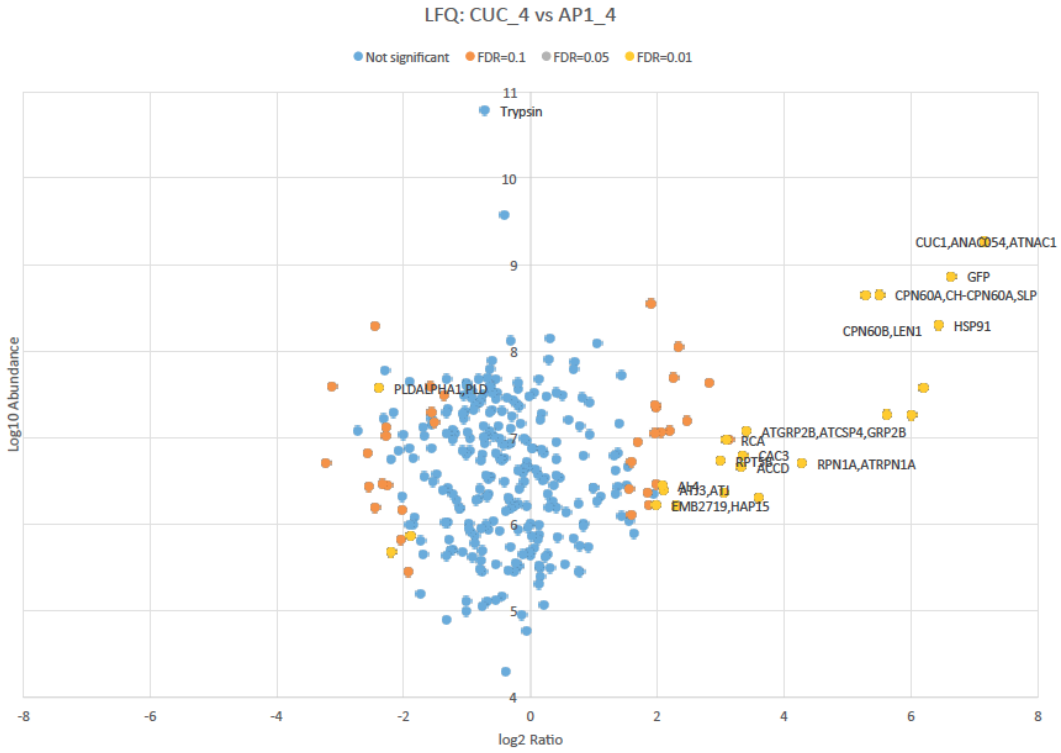


FIGURE 5.5: **Relative protein abundance.** Logarithmic abundance of proteins according to their ratio in the *CUC line* vs. the *AP1 line*. Color represents the level of significance.

they derive, but fragments from different isoforms cannot always be unequivocally assigned to one of the variants within the same protein.

In the majority of cases, the predicted localization of these isoforms that correspond to one protein are the same, but in some instances it can be different. Thus, Figure 5.6 shows the predicted localization of each of these 57 isoforms.

### Nuclear putative interactors

Since CUC1 is localized in the nucleus, further investigation was initially focused in nuclear localized putative interactors (the ones that pass the 0.1 cutoff and are nuclear, Table 5.3).

There are 10 putative interactors that matched this criteria, which can be grouped in three categories according to their function: 26S proteasome subunits, transcriptional regulators, and others.

First, four subunits of the 26S proteasome were found: RPT1A, RPT5B (from regulatory particle triple-A ATPases), RPN1A and RPN3A (from regulatory particle non-triple-A ATPases).

The ubiquitin (Ub)/ 26S proteasome pathway is the predominant proteolytic system in plants. Selective degradation of proteins is essential for plant physiology. This process is required in different situations, such

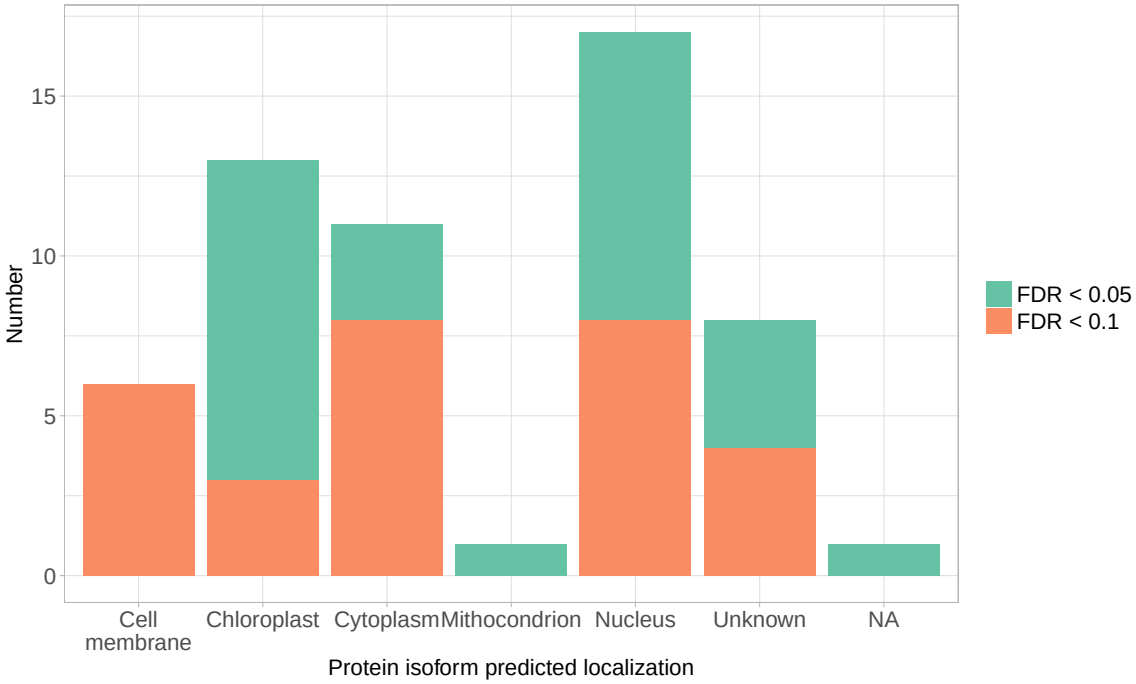


FIGURE 5.6: **Protein predicted localization.** Predicted localizations of all the detected isoforms at 4 dpi. Color indicates the level of significance. NA corresponds to GFP.

as the removal of misfolded or abnormal proteins, or the degradation of short-lived regulatory proteins. In the 26S proteasome, ubiquitin acts a a recyclable recognition signal to make protein turnover selective and specific (Smalle and Vierstra, 2004).

The 26S proteasome is a 2 MDa ATP-dependent proteolytic complex that is divided into 2 subcomplexes: the 20S core protease (CP) and the 19S regulatory particle (RP) (for a review, see Sadanandom et al., 2012). The RP associates with the CP and regulates it, conferring ATP and Ub dependence to the otherwise ATP and Ub independent CP. The RP itself is divided into two subcomplexes, called Lid and Base, composed of 17 subunits. The Base comprises six related AAA-ATPases (RTP1-6) and three non-ATPase subunits (RPN 1, 2 and 10). The lid is formed by the RPN 3, 5-9 and 11-12 nonATP-ase subunits (Figure 5.7).

The RPT subunits are thought to facilitate substrate unfolding and opening of the CP pore gating. The RPN subunits are presumed to act as receptors for poly-Ub carrier proteins and other complexes from the Ub proteasome cascade.

The subunits that appear as CUC1's putative interactors form part of the regulatory particle and are both ATPases (RPT1 and RPT5) and nonATPases (RPN1 and RPN3). All of these subunits have been associated with cell cycle related events.

In particular, RPN1 has been shown to interact with ubiquitin-binding shuttle proteins, which suggests a role in substrate recognition. RPN1a is essential for embryogenesis and showed cell division defects, where cyclin

| Gene ID | Symbol | Description | Significance |
|---|---|---|---|
| AT3G15170 | CUC1 | NAC transcription factor involved in SAM and boundary formation | FDR<0.05 |
| AT2G20580 | RPN1A | 26S proteasome regulatory subunit S2 1A | FDR<0.05 |
| AT1G20200 | RPN3A | 26S proteasome regulatory subunit S3 homolog A | FDR<0.05 |
| AT1G53750 | RPT1A | 26S proteasome AAA-ATPase subunit RPT1A | FDR<0.1 |
| AT1G09100 | RPT5B | 26S proteasome AAA-ATPase subunit RPT5B | FDR<0.05 |
| AT4G15802 | HSBP | Heat shock factor binding protein | FDR<0.1 |
| AT1G79920 | HSP70-15 | Heat shock protein 70 (Hsp 70) family protein | FDR<0.05 |
| AT5G26210 | AL4 | Member of the Alfin1-like family of plant homeodomain containing proteins. Binds to di- or trimethylated histone H3 (H3K4me3/2). | FDR<0.05 |
| AT3G42170 | DAYSLEEPER | Transposase-like gene with conserved domains from the family of hAT transposases | FDR<0.05 |
| AT3G13920 | EIF4A1 | EUKARYOTIC TRANSLATION INITIATION FACTOR 4A1. RNA helicase. | FDR<0.1 |

TABLE 5.3: Nuclear localized CUC1 putative interactors with a FDR below 0.1

B1 was not properly degraded and irregular division panes were observed (Brukhin et al., 2005)

RPN3 is essential for cell cycle progression in yeast (Bailly and Reed, 1999). In *Nicotiana tabacum*, NtRPN3 interacts with NtCDPK1, a calcium-dependent protein kinase that is involved in the control of cell division and differentiation (Lee et al., 2003).

The mutation of RPT1 in yeast caused strong growth alterations and displayed a $G_1$ cell cycle defect (Rubin et al., 1998). RPT5 is essential for cell viability during gametophyte development, as its mutation fails to degrade mitotic cyclin and causes gametophytic lethality (Gallois et al., 2009).

Other members of the proteasome are involved in the specification of leaf polarity (Huang et al., 2006). RPN5A is essential for gametogenesis; its mutants show severely dwarfed phenotypes and other defects are associated to alterations in the number of cells (Book et al., 2009). Two RP members, RPN8a and RPT2a also participate in the repression of class-1 KNOX genes during leaf development (Huang and Huang, 2007).

It is worth noting that, even if more informative statistical analysis could not be performed for the results at 2 dpi, several members of the 26S proteasome also appear to be more abundant in the *CUC line* in comparison to the control at this time point.

There is evidence that other TFs can interact with different members of the proteasome and regulate the degradation of other proteins. In mammals, the HOXA2 TF from the homeodomain HOX gene family is involved in embryonic development and patterning and has been shown to interact with two core proteasome subunits (PSMA3 and PSMB2) (Bergiers et al., 2013).

Among the nuclear putative interactors (Table 5.3), two proteins potentially involved in transcriptional regulation were found: DAYSLEEPER and ALFIN-LIKE4 (AL4).

DAYSLEEPER is a transposase-derived protein resembling members of the hAT-superfamily (Bundock and Hooykaas, 2005) that is predominantly expressed in meristems, developing flowers and siliques (Knip et al., 2013)

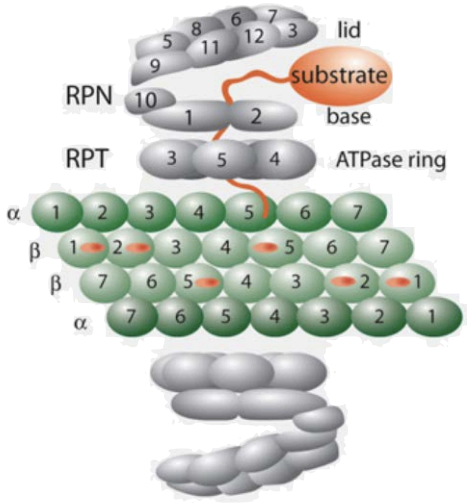


FIGURE 5.7: **The 26S proteasome.** The proteasome 20S core protease is depicted in green and the 19S regulatory particle in gray (Raasi and Wolf, 2007).

and is essential for plant development (Bundock and Hooykaas, 2005). It is involved in gene regulation and its mutants show severe growth defects, with slow growing seedlings, impaired cotyledon expansion and failure to form normal leaves and floral organs (Bundock and Hooykaas, 2005).

ALFIN-LIKE4 is a member of the Alfin1-like family of nuclear-localized PHD (plant homeodomain) domain containing proteins, and can bind to di- or trimethylated histone H3 (H3K4me3/2), acting as a transcription co-activator (Lee et al., 2009b)

The EUKARYOTIC TRANSLATION INITIATION FACTOR 4A (eIF4A) is also a CUC1 nuclear putative interactor (Table 5.3) that is not included in the previous two groups. eIF4A is coded by two *Arabidopsis* genes, *eIF4A1* (AT3G13920) and *eIF4A2* (AT1G54270), and the two proteins share a 97% similarity at the primary sequence level.

eIF4A is a highly conserved ATPase and helicase involved in the initiation of mRNA translation, a key target of post-transcriptional regulation (Browning and Bailey-Serres, 2015; Bush et al., 2015). It is highly expressed in growing tissues, specially in meristems and flowers. eIF4A physically interacts with the cell cycle regulator CDKA (Hutchins et al., 2004; Bush et al., 2016) and its mutants show defects in cell division and growth in *Brachypodium distachyon* (Vain et al., 2011) and *Arabidopsis* (Bush et al., 2015).

The mechanism by which eIF4A affects cell growth remains to be elucidated, although the eIF4A-CDKA interaction could provide a molecular

pathway for controlling translation in proliferating tissues and thus contributing to cell size homeostasis in mersitems (Bush et al., 2016).

Another translation initiation factor, eIF3, has been shown to interact with the RP of the 26S proteasome (Paz-Aviram, Yahalom, and Chamovitz, 2008) and this interaction could be responsible for the regulation cell division (Yen, Gordon, and Chang, 2003; Yahalom et al., 2001).

# JOSE: I could not find other TFs interacting with eif4A. Pdcd4 is a tumor suppressor (nuclear/cytoplasmatic shuttling protein) and does interact (couldnt access paper to get more specific info)

As in the case of the proteasomal subunits, it has been observed that TFs from the HOX family can interact with another translation initiation factor in mammals, eIF4E, to stimulate translation efficiency and regulate cell proliferation (Topisirovic et al., 2005).

There were two heat shock-related proteins in the nuclear putative interactor group: HSP70-16 and HSBP.

The tissue specific localization of the transcripts of some of the genes encoding for CUC1's nuclear putative partners coincides with the boundary region defined as the area where the pLAS promoter is active (Figure 5.8, image obtained from the eFP Browser, Winter et al., 2007). This indicates that these putative interactors are expressed in the same region as CUC1 and reinforces the evidence for their physical interaction.

Using the list of CUC1 putative nuclear interactors, a protein-protein database was queried and the first order interactors for each of these proteins were obtained (Figure 5.9). The broken orange lines represent the interactions that have not been observed previously and were found through the experiments presented in this Chapter.

### Cytoplasmatic putative interactors

Table 5.4 contains the proteins that appear as putative CUC1 interactors and are predicted to be localized in the cytoplasm, although CUC1 is localized in the nucleus. Several tubulin subunits appear in this list.

| Gene ID | Symbol | Description | Significance |
|---|---|---|---|
| AT1G79930 | HSP91 | heat shock protein 91 | FDR<0.05 |
| AT2G29550 | TUB7 | tubulin beta-7 chain | FDR<0.1 |
| AT5G19780 | TUA5 | tubulin alpha-5 | FDR<0.1 |
| AT3G44110 | ATJ3, ATJ | homologous to the co-chaperon DNAJ protein from E coli | FDR<0.05 |
| AT5G18380 | NA | Ribosomal protein S5 domain 2-like superfamily protein | FDR<0.1 |
| AT5G62700 | TUB3 | tubulin beta chain 3 | FDR<0.1 |
| AT1G20010 | TUB5 | tubulin beta-5 chain | FDR<0.1 |
| AT5G44340 | TUB4 | tubulin beta chain 4 | FDR<0.1 |

TABLE 5.4: Cytoplasm localized proteins with an FDR below 0.1

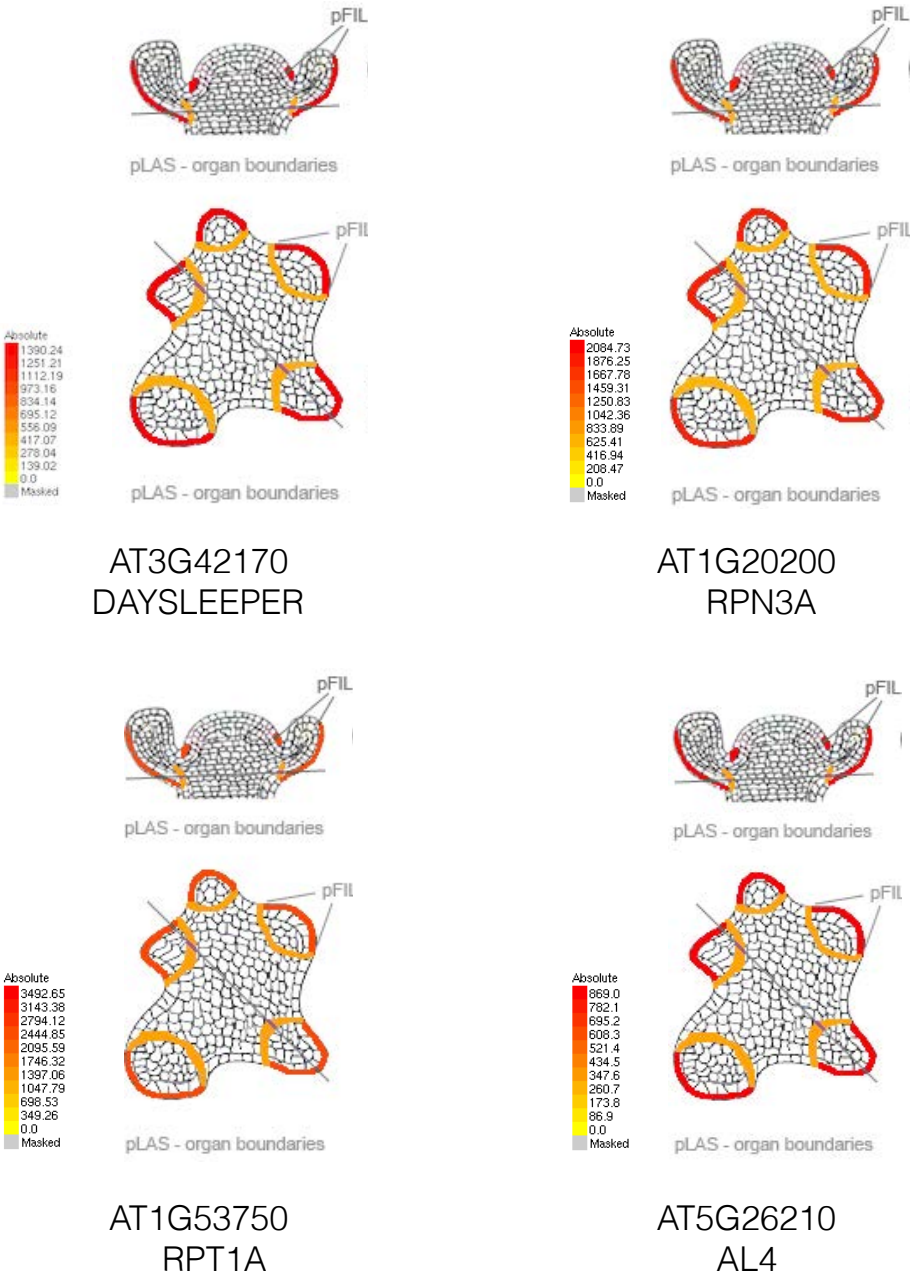


FIGURE 5.8: **Expression profile of CUC1 putative interactors.** Images depicting the expression levels of CUC1 putative interactors according to the eFP Browser, particularly in boundary regions(pLAS promoter).

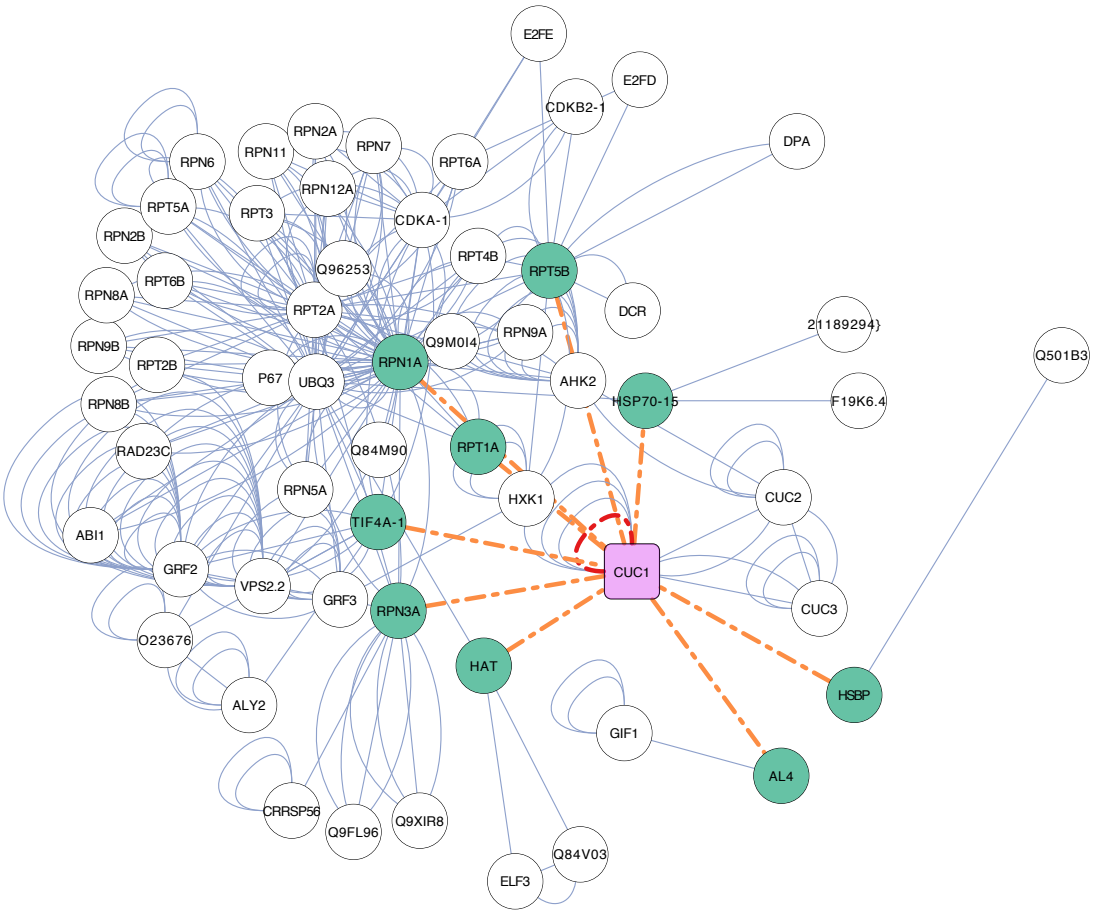


FIGURE 5.9: **Protein Network of CUC1 putative interactors.** First neighbors of CUC1 putative nuclear interactors (marked in color). Interactions that were previously unknown are shown in orange broken lines.

# Chapter 6

# Discussion and Conclusions

## 6.1 CUP-SHAPED COTYLEDON1 regulatory network

The main goal of this Thesis was to determine the transcriptional and post transcriptional events related to the role of CUC1 during the early stages of flower development. Several aspects of CUC1 function were analyzed through the combination of complementary genome-wide approaches including transcriptomics, transcription factor binding profiles and protein interactome analyses. The results obtained from such techniques allowed to elucidate a set of transcriptional targets, molecular pathways and CUC1 interactors with the intention of delineating the mechanisms by which this NAC transcription factor contributes to the establishment of floral organ boundaries. These results represent a substantial advance in the understanding of the molecular events that are controlled by CUC1 in this key developmental stage of plant development. In this regard, this Thesis provides a foundational body of work that can be used to further explore CUC1's regulatory network.

## 6.2 Transcriptomic response to elevated levels of CUC1 during early flower development.

The transcriptomic landscapes associated to the role of CUC1 during early flower development were defined by using different genetic backgrounds, all of which shared the increased levels of *CUC1* in meristematic tissues. By both comparing the *eep1* and the *CUC1 lines* to their controls (eep1 control and AP1 lines, respectively), it was possible to distinguish an increased rate of upregulation of the downstream genes at early stages after floral initiation. In the case of the eep1 line it was even more clear that a shift towards downregulation occurred at later stages. Among the shared DEGs between both datasets (microarrays and RNA-seq), approximately 25% corresponded to nuclear proteins mostly consisting of transcriptional regulators (transcription factors belonging to different TF families). In addition to these, ARGONAUTE 3, which is present in ribonucleoprotein complexes in

the cytosol, was also found. Altogether, these findings suggest that CUC1 may exert its control of organ boundaries by regulating other regulators of transcriptional or post-transcriptional processes.

*CUC1* expression is governed by the action of several hormone response pathways, including auxins, cytokinins and brassinosteroids. The transcriptomic analyses using both genomic platforms suggest that CUC1 may also regulate some hormone responses downstream. This is the case of the ABA signaling pathway, as CUC1 downregulates the expression of the ABA receptor PYL5.

## 6.3 Genome-wide binding landscape of CUC1 in floral tissues

The role of *CUC1* and its gene regulatory network was tested through the analysis of transcriptomic data correlated with transcription factor genome-wide binding (ChIP-Seq) data. This combined analysis is a powerful strategy for the identification of transcription factor targets and the elucidation of gene regulatory network circuitry. This approach has been recently illustrated by several recent studies in Arabidopsis including processes such as floral transition (e.g. to define the mechanism of action of AP1 and SEP3) and shoot apical stem cell maintenance (deciphering the regulatory network of WUSCHEL).

CUC1 binds preferentially to regulatory regions (i.e. gene promoters) very close to the transcriptional start site, confirming the main role of CUC1 as a transcription factor. Among bound genes, CUC1 seems to regulate translation-related processes. This may impact translation efficiency by altering the abundance of ribosomal proteins.

## 6.4 Elucidation of the CUC1 protein interactome

Through the use of protein-protein interaction analyses, it was possible to define a set of CUC1 interactors in vivo, including several cytosolic and nuclear proteins with diverse functions. Among these, it is worth highlighting the identification of several heat shock proteins, proteasome units and transcriptional and translational regulators. Further experiments are required to confirm the observed interactions. This should be addressed by in vivo experiments, such as co-immunoprecipitation or bimolecular fluorescence complementation (BiFC), and the validation of the nuclear interactions should be approached first.

As previously described, it has been shown that CUC1 is able to repress cell division (Sieber et al., 2007). While the mechanisms by which this occur are not fully understood, hormonal factors are thought to be involved. The presence of several members of the 26S proteasome as putative CUC1 interactors is noteworthy, since it is well known that these factors are involved in the regulation of the cell cycle. Another of the identified nuclear

putative interactors, eIF4A, also affects cell division. This raises the possibility that the interactions with translational and post-translational related proteins could mediate CUC1's effects on cell division.

## 6.5 Future perspectives

For both the transcriptomic and ChIP-seq experiments, a possibility to improve the results would be to use a single-cell approach, for instance using fluorescent-tagged cell sorting (FACS).

When comparing the *CUC line* or the *eep line* with the controls, the whole inflorescence-like tissue is being assessed. This means that the source of RNA that is used for transcriptomic experiments derives from functionally heterogeneous groups of cells. The effects of CUC1 (and CUC2) on boundary formation are very specific to a finite group of cells and there are mechanisms in place to ensure that they are restrained to these spacial domains so that the surrounding tissues are able to grow normally. The consequences of the alteration of the levels of these boundary genes is likely to be subject to some kind of regulation in the surrounding cell types, where a different set of transcriptional regulators is expressed and may provide a feedback mechanism to prevent fluctuations that alter normal development. In consequence, by comparing the transcriptomes of the whole inflorescence tissue, some of the changes caused by CUC1 may be masked in this experimental setup.

The possible problem is that this would not be done in intact tissues, but would require the preparation of protoplasts and, hence, some of the particular developmental context would be missed.

It is possible that the low correlation observed between the genome-wide binding of CUC1 and the transcriptional response to its elevated levels could be due to the presence of other modulating factors. These may act by either physically interacting with CUC1 or by affecting the context in its vicinity, for example by altering chromatin structure in a way that prevents the translational machinery to activate the expression of downstream genes. By this or other means, this possibility could have a repressive effect on CUC1's transcriptional regulatory potential.

Considering this in the biological context of the activity of CUC1, it would make sense that its potential is limited. Even if at the level of its own expression CUC1 is very restricted, it is of utmost importance to restrain its capacity to affect growth exclusively to the boundary regions. Some of the discovered protein-protein interactions, in particular those related to the 26S proteasome, would be good candidates to further analyze this possibility and try to advance our knowledge about CUC1.

# Chapter 7

# Materials and Methods

## 7.1 Plant materials and growth conditions

The *Arabidopsis thaliana* accession used for all the lines employed in this PhD thesis was Landsberg *erecta* (Ler). Ler is referred to as wild type (WT) throughout the thesis.

### 7.1.1 Transgenic lines

Details about the transgenic lines are discussed in the Introduction.

#### The AP1 line : pAP1:AP1-GR ap1 cal

The *AP1 line* was obtained from Dr. Frank Wellmer and is described in Ó'Maoiléidigh et al., 2013.

#### The CUC line: pCUC1:CUC1m-GFP pAP1:AP1-GR ap1 cal

The *CUC line* was obtained in our laboratory by Dr. Jian Jin (former post-doc). The *AP1 line* was transformed with a plasmid containing pCUC1:CUC1m-GFP using Agrobacterium transformation and selected until a single insertion line was obtained.

#### The eep1 line: 35S:AP1-GR ap1 cal eep1

The *eep1 line* was obtained from Dr. Frank Wellmer, from Trinity College Dublin.

### 7.1.2 Growth conditions

Seeds were sown directly on soil mixed with vermiculite and perlite (5:1:1) for RNA-seq and ChIP-seq, microarrays and proteomic experiments. After a 3 to 5 day vernalization period, plants were grown under long day photoperiods (16 h light, 8 h dark, 20-23°C) in growth chambers.

## 7.2 Dexamethasone induction

Cauliflower buds were treated with dexamethasone (10$\mu$M, Sigma-Aldrich) with 0.01 % v/v ethanol and 0.015 % Silwet L-77 (De Sangosse) when the main inflorescence stem was between 0 and 2 cm. Treatment was performed using a plastic Pasteur pipette and placing drops over each bud to cover them completely. Dexamethasone was applied once (at day 0, after collecting the corresponding 0 dpi sample) and for every biological replicate, always at the same time of the day (between 14:30 and 15:30 hs, or 5.5-6.5 ZT).

## 7.3 Tissue collection from inflorescences

Tissue from the inflorescences was collected using jewelers forceps (Dumont, #55) and immediately frozen in liquid nitrogen. Collection before treatment with dexamethasone constitutes samples referred to as "0 dpi". After collecting 0 dpi samples, floral buds were treated with dexamethasone as described in Section 7.2 and subsequent time points were collected in the same way at their respective time after treatment.

## 7.4 RNA extraction

Plant material was collected in liquid nitrogen and stored at $-80°C$ until further processing. The tissue was then ground in liquid nitrogen using a mortar and pestle or an electric drill and polypropylene pellet pestles (Sigma-Aldrich). Total RNA was extracted using Spectrum total RNA kit (Sigma-Aldrich) according to the manufacturer's recommendations. RNA was resuspended in 50 $mu$l of Milli-Q water. The same method was used for RNA-seq experiments and RT-qPCR presented in Results. Total RNA preparations used for RNA-seq analysis were treated with DNase I (Ambion) to reduce contamination with genomic DNA.

## 7.5 qPCR

LightCycler® 480 SYBR Green PCR Master Mix (Roche) was used for qPCR experiments in a LightCycler 480 II Instrument (Roche). Both in ChIP-qPCR and RT-qPCR at least 3 technical replicates were used to obtain mean values and perform subsequent calculations.

Relative abundance of mRNA transcripts (RT-qPCR) or chromatin fragments (ChIP-qPCR) was calculated using the $\Delta\Delta$ Ct method (Livak and Schmittgen, 2001). *Reference1* (AT4G26930) and *Reference2* (AT4G17740) were used as reference/ housekeeping genes (see 7.12).

The qPCR reaction mix composition is detailed in Table 7.1 and the amplification conditions in Table 7.2.

| Reagent | Volume ($\mu$l) |
|---|---|
| SYBR Green PCR Master Mix | 10 |
| Primer Forward | 100 |
| Primer Reverse | 100 |
| Template | 1-5 |
| Water | to 20 |

TABLE 7.1: qPCR mix per reaction

| Step | Temperature (°C) | Time (min:sec) | Cycles |
|---|---|---|---|
| Initial Taq activation | 95 | 10 | 1 |
| Denaturation | 95 | 0:10 | 45 |
| Annealing and extension | 60 | 0:30 | |

TABLE 7.2: qPCR program

## 7.6 Chromatin immunoprecipitation

Chromatin immunoprecipitation was carried out as described in Kaufmann et al., 2010a with some modifications, as follows.

Around 1.5 g of inflorescence tissue was used for each biological replicate. Tissue was fixed for 30 minutes under vacuum with 1 % formaldehyde and frozen in liquid nitrogen. 9 $mu$ ul of GFP antibody (Abcam AB290) was used for each ChIP.

The full protocol can be found in the online Supplementary information.

### 7.6.1 Library preparation for ChIP-seq

Libraries were prepared using NEBNext® Ultra™ II DNA Library Prep Kit for Illumina ® (#E7645S, New England Biolabs) with NEBNext® Multiplex Oligos for Illumina® (Index Primers Set 1, #E7335S, New England Biolabs).

For input libraries 1 $\mu$l of input ChIP was used. For IP libraries 40 $\mu$l were used. The protocol for preparation was followed according to manufacturer's instructions. Adaptors were diluted 1/25 and 1/10 for IP and input samples respectively. 15 PCR cycles were used for ChIP-seq libraries.

In the size selection step with SPRI magnetic beads 40 $\mu$l and 20 $\mu$l were used for the first and second step respectively.

## 7.7 Library preparation for RNA-seq

RNA extracted as described in Section 7.4 from the *CUC line* and the *AP1 line* was collected at 0, 2 and 4 dpi and frozen at -80°C until library preparation.

Libraries were prepared at the Millard and Muriel Jacobs Genetics and Genomics Laboratory from the California Institute of Technology.

## 7.8 Bioanalyzer

To assess ChIP-seq libraries size range, samples were loaded undiluted and in a 1:5 dilution in Bioanalyzer High Sensitivity DNA chips (Agilent).

RNA samples for microarrays and RNA-seq were loaded on RNA Bioanalyzer chips to determine their purity and integrity. Only RNA samples with RIN values over 8 were used for subsequent experiments.

## 7.9 Sequencing

All RNA-seq and ChIP-seq and RNA-seq libraries were sequenced at the Millard and Muriel Jacobs Genetics and Genomics Laboratory from the California Institute of Technology using a HiSeq2500 (Illumina) high throughput sequencer.

## 7.10 Microarrays

Custom microarrays (Agilent) described in Kaufmann et al., 2010b were used in Chapter 2 following manufacturer's instructions.

RNA samples from inflorescences of about ~25 plants was extracted as described in 7.4 and labeled with fluorescent dyes using the Quick Amp Labeling Kit (Agilent). Microarray hybridizations (65°C, 16h) and washes were performed with Agilent reagents and following standard protocols. Microarrays were scanned using an Agilent DNA Microarray Scanner G2565CA, and data was acquired using Agilent's Feature Extraction Software. Data analysis is described in 7.14.5.

Four independent sets of biological samples were used for the experiments. In each of the biological replicates of the time course experiment, two samples derived from the *eep1 line* were labeled with one dye (i.e., Cy3), and two samples derived from *ap1 line* plants were labeled with the alternative dye (i.e., Cy5). The dyes used for labeling RNA from a given genotype (*eep1* and *AP1 lines*) were switched for the two other biological replicates to reduce dye- related artifacts. *eep1 line* and *AP1 line*-derived samples for each time point and biological replicate were co-hybridized. This experimental setup resulted in a total of 6 hybridizations per set (0d, 1d, 2d, 3d, 4d and 5d; eep1 vs. AP1 at each time point), and two biological replicate sets labeled with each dye polarity (eep1-Cy3/ AP1-Cy5, and vice versa).

Data analysis is described in 7.14.5.

## 7.11 Microscopy

Confocal microscopy images from the *CUC line* were obtained using an FV 1000 confocal microscope (Olympus). Images were processed and Z stacks were assembled using Olympus FV software. To obtain the images, the apices from the cauliflowers in the *CUC line* were dissected using sharp

tweezers and then flattened and spread on glass slides. A drop of water was poured over the tissue and a cover slide was placed on top of it.

## 7.12 Primers

All primers were designed using Primer3 online tool (http://bioinfo.ut.ee/primer3).

Primers used for ChIP-qPCR were designed surrounding the peak center in the corresponding peak identified in preliminary ChIP-Seq experiments.

## 7.13 Proteomics

Proteomics experiments were carried out during a short stay at the University of Potsdam in the laboratory led by Dr. Kerstin Kaufmann.

The protocol used for the identification of CUC1 protein complexes is outlined thoroughly in Smaczniak et al., 2012b. All steps were followed as described unless otherwise specified.

### 7.13.1 Plant material

About 0.75 g of cauliflower tissue from the *CUC line* was used for each sample. Samples proceed from plants that were pooled according to the time of collection after DEX treatment, and each biological replicate was independent from each other (pools for each sample came from different sets of plants) . It was stored at $-80°C$ until the start of the experiments.

### 7.13.2 Protein extraction

Total protein extract was used, so steps 7-12 of Smaczniak et al., 2012b for nuclear isolation were skipped. Step 15 was repeated twice more to make sure no particles were left in the supernatant.

### 7.13.3 Protein immunoprecipitation

Incubation at $4°C$ was done for 90 minutes with anti-GFP antibody (Abcam 290).

### 7.13.4 LC-MS/MS analysis

LC-MS/MS analysis was performed on a LTQ-Orbitrap mass spectrometer as described in Smaczniak et al., 2012b.

### 7.13.5 Statistical analysis of results from MaxQuant

After initial peak intensities were determined and normalized using MaxQuant software (Cox and Mann, 2008; Cox, Jürgen et al., 2011), statistical analysis was performed to identify proteins that were differentially identified in

the *CUC line* as compared to the control (*AP1 line*) as described in Smaczniak et al., 2012b.

### 7.13.6 Protein extraction and Western blot

Western blot was performed on total protein extract and nuclei protein extract using cauliflowers from the *CUC line* at 4dpi. Both extracts were obtained as described in Smaczniak et al., 2012b and 7.13.2.

About 50 $\mu$g of protein were denatured in loading buffer (100 mM Tris-HCl pH 6.8, 4 % SDS , 200 mM DTT , 20 % glycerol, 0.002 % Bromophenol Blue) at 95°C for 10 min. The SDS-PAGE gel was prepared with acrylamide at 12 % for the resolving gel and 4 % for the the stacking gel. Samples were ran at 20 mA for about 1 hour using the PageRuler™ Prestained Protein Ladder (Thermo Fisher Scientific). Proteins were transferred on a Nitrocellulose membrane (Optitran BA-S 83, Whatman) by blotting for 1 hour at 100 V with agitation at 4°C. Membrane was blocked with 3 % milk in TBS-T (TBS with 0.25 % Tween) for 2 hours at room temperature followed by 2 hours at 4 °C and then rinsed with TBS-T. Membrane was then incubated with anti-GFP primary antibody (ab290, Abcam) in TBS-T (1/2000) overnight at 4°C. Membrane was washed 3 times with TBS-T and secondary antibody (IRDye® 800CW Donkey anti-Rabbit IgG H + L, Li-Cor) was incubated in 3 % milk in TBS-T for 2 hours with agitation. Finally membranes were washed 3 times with TBS-T and protein was detected by infrared fluorescence using an Odyssey® Imaging System (Li-Cor).

Gel was stained for 2 hours with Coomassie Brilliant Blue (0.1 %) and destained using a methanol/acetic acid solution overnight.

## 7.14 Bioinformatic analyses

### 7.14.1 RNA-seq analysis

Raw reads from the eighteen libraries prepared were obtained in FastQ format from Caltech and were analyzed using a custom pipeline, as follows.

First the quality of the reads was assessed using FastQC (`http://www.bioinformatics.babraham.ac.uk/projects/fastqc`). Potential adaptor contamination and low quality trailing sequences were removed using Trimmomatic (Bolger, Lohse, and Usadel, 2014). The trimmed reads were then aligned to the Arabidopsis reference genome (TAIR10) using STAR aligner (Dobin et al., 2013). To obtain the number of reads that were assigned to each gene, `featureCounts` was used (Liao, Smyth, and Shi, 2014). Downstream differential expression analysis was performed using DESeq2 (Love, Huber, and Anders, 2014).

### 7.14.2 ChIP-seq analyses

A custom pipeline was used after obtaining raw reads from the sixteen libraries in FastQ format.

First the quality of the reads was assessed using FastQC (`http://www.bioinformatics.babraham.ac.uk/projects/fastqc`). Potential adaptor contamination and low quality trailing sequences were removed using Trimmomatic (Bolger, Lohse, and Usadel, 2014). The trimmed reads were then aligned to the Arabidopsis reference genome (TAIR10) using STAR aligner (Dobin et al., 2013). Read duplicates from the PCR amplification step in the sequencing process were removed using Picard `MarkDuplicates` and only those uniquely mapped reads having a mapping score equal or higher than 30 (probability equal to or lower than 0.001 that a read is mismapped) were kept. The resulting bam files from the IP and input samples were used to call peaks using MACS2 (Zhang et al., 2008). Annotation of the peaks was performed using HOMER (Heinz et al., 2010) and Bedtools (Quinlan and Hall, 2010).

### 7.14.3 Gene Ontology analysis

Several tools were used to asses the enrichment of gene ontology categories in different gene sets.

- Cytoscape (Shannon et al., 2003), BiNGO app (Maere, Heymans, and Kuiper, 2005).
- AgriGO (Du et al., 2010).

### 7.14.4 CUC1 binding sequence analysis

The MEME-ChIP tool from the MEME-suite was used to find the motifs that were enriched in the vicinity of CUC1's binding sites. The fasta files of the sequences spanning 100 bp around the tier 2 peak summits was used. The Arabidopsis DAP motifs database was used to find similar motifs (O'Malley et al., 2016) and default options were used except for the maximum with of the motifs to search for, that was set to 12.

### 7.14.5 eep1 microarrays

Raw data from scans was imported into R (R Core Team, 2017) and analyzed with the `limma` package (Ritchie et al., 2015). Background correction was performed using the `backgroundCorrect` function using the `normexp` method with maximum likelihood estimation of the background (Silver et al., 2009). Within-array normalization was performed using the loess method and between-array normalization using quantile normalization (Smyth and Speed, 2003). The linear model was fit using the `lmFit` function and the `ebayes` function, which uses empirical Bayes moderation of the standard errors towards a common value. The p-values were corrected for multiple testing using the `BH` method (Benjamini, Hochberg, and Yekutieli, Yekutieli and Benjamini, 2001), which is the false discovery rate (FDR).

# Appendix A

# Full tables

Full tables of results and complete protocols can be obtained in Supplementary information (URL: https://drive.google.com/drive/folders/0B_FLIzlQvlygYmNvOUtseGwxR3M?usp=sharing).

The PDF version of this Thesis contains links that can be used to open the specified online document or folder.

# Appendix B

# Publications

In the next pages the publications have been reproduced.

- Bustamante, M., J. Jin, O. Casagran, T. Nolan, and J. L. Riechmann. 2014. "Gene Expression Analysis by Quantitative Real-Time PCR for Floral Tissues.." Methods in molecular biology (Clifton, N.J.) 1110(Chapter 21):363–82.
- Bustamante, M., J. T. Matus, and J. L. Riechmann. 2016. "Genome-Wide Analyses for Dissecting Gene Regulatory Networks in the Shoot Apical Meristem.." Journal of Experimental Botany 67(6):1639–48.

# Chapter 21

# Gene Expression Analysis by Quantitative Real-time PCR for Floral Tissues

**Mariana Bustamante, Jian Jin, Oriol Casagran, Tania Nolan, and José Luis Riechmann**

## Abstract

Real-time, or quantitative, reverse transcription polymerase chain reaction (qRT-PCR), is a powerful method for rapid and reliable quantification of mRNA abundance. Although it has not featured prominently in flower development research in the past, the availability of novel techniques for the synchronized induction of flower development, or for the isolation of cell-specific mRNA populations, suggests that detailed quantitative analyses of gene expression over time and in specific tissues and cell types by qRT-PCR will become more widely used. In this chapter, we discuss specific considerations for studying gene expression by using qRT-PCR, such as the identification of suitable reference genes for the experimental setup used. In addition, we provide protocols for performing qRT-PCR experiments in a multiwell plate format (with the LightCycler® 480 system, Roche) and with nanofluidic arrays (BioMark™ system, Fluidigm), which allow the automatic combination of sets of samples with sets of assays, and significantly reduce reaction volume and the number of liquid-handling steps performed during the experiment.

**Key words** Real-time PCR, qRT-PCR, Quantitative PCR (qPCR), SYBR Green I dye

## 1 Introduction

Differential gene expression, over time or among different cell and tissue types, is central to the developmental processes of all organisms. In flower development studies, this aspect of gene function has usually been approached by using methods to characterize spatial patterns, or domains, of gene expression, such as in situ hybridization (*see* Chapter 14) and promoter–reporter gene fusions (*see* Chapter 15). In contrast, real-time, or quantitative, reverse transcription polymerase chain reaction (qRT-PCR), which is a powerful method for rapid and reliable quantification of mRNA abundance, has not featured prominently in flower development research. However, the development of techniques for the synchronized induction of flower development (*see* Chapter 16), or for the isolation of cell-specific mRNA populations (*see* Chapters 17–19),

José Luis Riechmann and Frank Wellmer (eds.), *Flower Development: Methods and Protocols*, Methods in Molecular Biology, vol. 1110, DOI 10.1007/978-1-4614-9408-9_21, 

suggests that detailed quantitative analyses of gene expression over time and in specific tissues and cells will become more broadly used (not the least because such data will be needed for the characterization and ultimate modeling of the molecular gene regulatory networks that control the development of the flower).

The qRT-PCR method involves three processes: The conversion of mRNA into cDNA via reverse-transcription; the amplification of the resulting cDNA by PCR; and the detection and quantification in real time of the synthesized PCR amplification products [1–3]. The reliability of the data obtained in qRT-PCR experiments can be affected by several factors that impact on those processes, including template quality (RNA integrity [3, 4]), purity [3, 5] and quantity, efficiency of the RT reaction, PCR primer design, and efficiency of the PCR amplification [3]. To compensate for between-sample variations in the amount of starting material and in the efficiency of the qRT-PCR process, expression levels of the genes of interest are reported relative to one or more reference genes that are presumed to be uniformly and stably expressed across the tissues or conditions tested in the experiment, and whose abundance reflects the total amount of mRNA present in each sample. Thus, the reliability of qRT-PCR analyses is largely affected by the suitability of the gene (or genes) that is selected as a reference, i.e., by whether or not such a gene really fulfills the requirements of a normalization control [6, 7].

Housekeeping genes, which function in basic cellular processes and are expressed in all cells of an organism, have often been used as reference genes to normalize the data in qRT-PCR experiments (e.g., genes such as glyceraldehyde-3-phosphate dehydrogenase (*GAPDH*), elongation factor-1α (*EF-1α*), actin (*ACT*), or tubulin (*TUB*)). However, the initial evidence indicating that housekeeping genes are stably expressed was obtained using methods that are mostly qualitative (for instance, RNA gel-blots and end-point RT-PCR), and subsequent studies have demonstrated that in some circumstances their expression may be regulated, or be unstable, and thus show changes in transcript levels throughout development or among different conditions or tissues. In addition, housekeeping genes are usually expressed at higher levels than the typical genes of interest. For these reasons, using them as reference genes may introduce biases in the results obtained by qRT-PCR [6, 7]. For example, in a series of experiments designed to assess traditional *Arabidopsis* reference genes (including *ACT2*, *ACT7*, *ACT8*, *ADENINE PHOSPHORIBOSYLTRANSFERASE 1* (*APT1*), *EF1α*, *EUKARYOTIC TRANSLATION INITIATION FACTOR 4A1* (*eIF4A*), *TUB2*, *TUB6*, *TUB9*, *UBIQUITIN 4* (*UBQ4*), *UBQ5*, *UBQ10*, and *UBQ11*), it was found that *eIF4A* would appear to be stably expressed over the course of silique development when *APT1*, *UBQ5*, or *eF1α* were used to normalize the data, whereas its expression would appear quite variable when *TUB6* was used as reference gene [6].

In summary, the validity of "housekeeping" reference genes is not universal, and is highly dependent on the experimental conditions [7]. Thus, the selection of appropriate reference genes for the normalization of qRT-PCR data has emerged as a crucial component for successful expression studies carried out with this technology, and statistical algorithms like *geNorm* [8] or *BestKeeper* [9] have been developed for that purpose (*see* **Note 1**).

Concomitantly, the use of genome-wide technologies (i.e., DNA microarrays) to characterize gene expression changes across many different tissues and developmental stages, environmental conditions, or in response to biotic and abiotic stresses or perturbations, has resulted in very rich datasets (for instance, [10]) that can be mined to identify novel, better suited reference genes for the desired experimental setup. For instance, Czechowski et al. [11] analyzed a very large set of Arabidopsis data obtained with Affymetrix ATH1 GeneChip arrays to identify several hundred genes that outperform traditional reference genes in terms of expression stability throughout development and under a range of environmental conditions. Subsequent qRT-PCR experiments performed with a subset of those novel reference genes confirmed that they showed superior expression stability and lower absolute expression levels [11] (*see* Table 1) (*see* **Note 2**). The results obtained in *Arabidopsis* have informed the selection of reference genes in other plant species, as the corresponding orthologous genes may also show stable expression (for an example in Leafy spurge, *see* ref. 12). If candidate reference genes are selected based on orthology, however, their suitability needs to be confirmed experimentally, as such character is not always maintained across all experimental conditions in all organisms [3] (for instance, *see* ref. 13).

The approach of using genome-wide data to select reference genes has been further expanded and refined with *RefGenes*, an online tool that allows easy identification of condition-specific reference genes [14]. *RefGenes* is based on the Genevestigator database of normalized and well-annotated microarray experiments, and is accessible through the Genevestigator Web page (www.genevestigator.com). The appropriateness of using condition-specific reference genes is based on the observation that for each biological context a subset of stable genes exists that has a smaller variance than either commonly used reference genes or genes that were selected for their stability across all conditions [14]. In other words, there is no gene that is universally stable, and for each biological context and specific experimental condition, the most appropriate set of reference genes does vary.

Through *RefGenes*, users are able to select the microarray experiments that are most similar to their chosen experimental conditions (including tissue, developmental stage, treatment, etc.). Afterwards, the user indicates the set of target genes of interest (up to ten genes can be tested at once). A search is then triggered to identify those genes that have the lowest variance within the

**Table 1**
**Traditional and novel Arabidopsis general reference genes, from Czechowski et al. [11]**

| Gene | Annotation | Forward primer (5′–3′) | Reverse primer (5′–3′) |
|---|---|---|---|
| *Traditional reference genes* | | | |
| *AT1G13440* | GAPDH | TTGGTGACAACAGGTCAAGCA | AAACTTGTCGCTCAATGCAATC |
| *AT3G18780* | ACT2 | CTTGCACCAAGCAGCATGAA | CCGATCCAGACACTGTACTTCCTT |
| *AT4G05320* | UBQ10 | GGCCTTGTATAATCCCTGATGAATAAG | AAAGAGATAACAGGAACGGAAACATAGT |
| *AT5G25760* | UBC | CTGCGACTCAGGGAATCTTCTAA | TTGTGCCATTGAATTGAACCC |
| *AT5G60390* | EF-1α | TGAGCACGCTCTTCTTGCTTTCA | GGTGGTGGCATCCATCTTGTTACA |
| *Novel reference genes* | | | |
| *AT1G13320* | PP2A subunit *PDF2* | TAACGTGGCCAAAATGATGC | GTTCTCCACAACCGCTTGGT |
| *AT1G47770* | Hypothetical protein | GTTCAATAAAATGGCGCATCTTG | GAAAAGGTGCAAAACGATCTCAC |
| *AT1G58050* | Helicase | CCATTCTACTTTTTGGCGGCT | TCAATGGTAACTGATCCACTCTGATG |
| *AT1G62930* | PPR gene | GAGTTGCGGGTTTGTTGGAG | CAAGACAGCATTTCCAGATAGCAT |
| *AT2G07190* | Hypothetical protein | CCGTCCAATCCAACAGATCAG | CGTCATCTAAAGACATTAGGTCCTGTAC |
| *AT2G28390* | SAND family | AACTCTATGCAGCATTTGATCCACT | TGATTGCATATCTTTATCGCCATC |
| *AT2G32170* | Expressed protein | ATCGAGCTAAGTTTGGAGGATGTAA | TCTCGATCACAAACCCAAAATG |
| *AT3G01150* | Polypyrimidine-tract-binding protein | GATCTGAATGTTAAGGCTTTTAGCG | GGCTTAGATCAGGAAGTGTATAGTCTCTG |
| *AT3G32260* | Hypothetical protein | CTGTTTGCCGAAGTTCCAGAGT | TTAAATCAGCAAGAACGTCGGATA |
| *AT3G53090* | Ubiquitin-transferase | TTCAAATACTTGCAGCCAACCTT | CCCAAAGAGAGGTATCACAAGAGACT |
| *AT4G26410* | Expressed protein | GAGCTGAAGTGGCTTCCATGAC | GGTCCGACATACCCATGATCC |
| *AT4G27960* | UBC9 | TCACAATTTCCAAGGTGCTGC | TCATCTGGGTTTGGATCCGT |
| *AT4G33380* | Expressed protein | TTGAAAATTGGAGTACCGTACCAA | TCCCTCGTATACATCTGGCCA |
| *AT4G34270* | TIP41-like | GTGAAAACTGTTGGAGAGAAGCAA | TCAACTGGATACCCTTTCGCA |
| *AT4G38070* | bHLH | GAAAGCAAAGGCGGTGAGAG | CAAGGCACACTTGGTTCTTCC |
| *AT5G08290* | Mitosis protein | TTACTGTTTCGGTTGTTCTCCATTT | CACTGAATCATGTTCGAAGCAAGT |
| *AT5G12240* | Expressed protein | AGCGGCTGCTGAGAAGAA^GT | TCTCGAAAGCCTTGCAAAATCT |
| *AT5G15710* | F-box protein | TTTCGGCTGAGAGGTTCGAGT | GATTCCAAGACGTAAAGCAGATCAA |
| *AT5G46630* | Clathrin adaptor complex subunit | TCGATTGCTTGGTTTGGAAGAT | GCACTTAGCGTGGACTCTGTTTGATC |
| *AT5G55840* | PPR gene | AAGACAGTGAAGGTGCAACCTTACT | AGTTTTTGAGTTGTATTTGTCAGAGAAAG |

selected set of microarray experiments and a range of expression that is similar to that of the target gene set. The result of the search is graphically displayed, showing the top 25 best candidate reference genes for the selected conditions. The behavior of these candidate genes in the chosen (or in additional) tissues or experimental conditions can then be explored using the *Conditions* tool of Genevestigator. In addition, the novel candidate reference genes that are identified using *RefGenes* should be validated for the specific biological conditions (tissue type, treatment, etc.) of the experiments to be performed, by using one of the aforementioned algorithms (*geNorm* or *BestKeeper*) and preferably together with commonly used reference genes.

The use of *RefGenes* to select reference genes for flower development studies is illustrated in Figs. 1 and 2 and in Table 2. A set of ten genes that participate in and/or are expressed at early stages of Arabidopsis flower development was used as the target set (including *SUPERMAN -SUP*, At3g23130-, *LEAFY -LFY*, At5g61850-, *AGL24*-At4g24540-, *YABBY3*-*YAB3*, At4g00180-, *APETALA2 -AP2*, AT4g36920-, *AGL42* -At5g62165-, *SHATTERPROOF2 -SHP2*, At2g42830-, *AGAMOUS -AG*, AT4g18960-, *SEPALLATA3*-*SEP3*, At1g24260-, and *APETALA3 -AP3*, At3g54340-, *see* ref. 15) to search for reference genes using a subset of the genome-wide expression profiling data available in Genevestigator (in particular, experiments under the Anatomy-Inflorescence category). *RefGenes* returns a list of candidate novel reference genes (Fig. 1, Table 2), which are then compared to traditional reference genes (*see* Fig. 2).

The detection of product formation in real time during the amplification reaction of qRT-PCR experiments is carried out by measuring the emission signal from either fluorescent double-stranded DNA-binding dyes (such as SYBR® Green I and EvaGreen®, see below), or template-specific fluorescent probes (such as the TaqMan® probe technology). A general protocol for using SYBR Green I dye in a qRT-PCR experiment performed in a LightCycler® 480 Real-Time PCR system (Roche) is provided below (equally suited real-time PCR machines are available from various manufacturers). In addition to standard real-time PCR systems, in which reactions are performed either in thin-wall PCR tubes or in multiwell plates, new systems for high-throughput analyses have been developed, which are based on nanofluidic arrays (such as the BioMark™ system, Fluidigm). These arrays contain nanofluidic networks that allow the automatic combination of sets of samples with sets of assays, and significantly reduce reaction volume (and thus the amount of material needed to perform an assay) and the number of liquid-handling steps performed during the experiment. A protocol for a qRT-PCR experiment using EvaGreen® and the BioMark™ system is also provided.

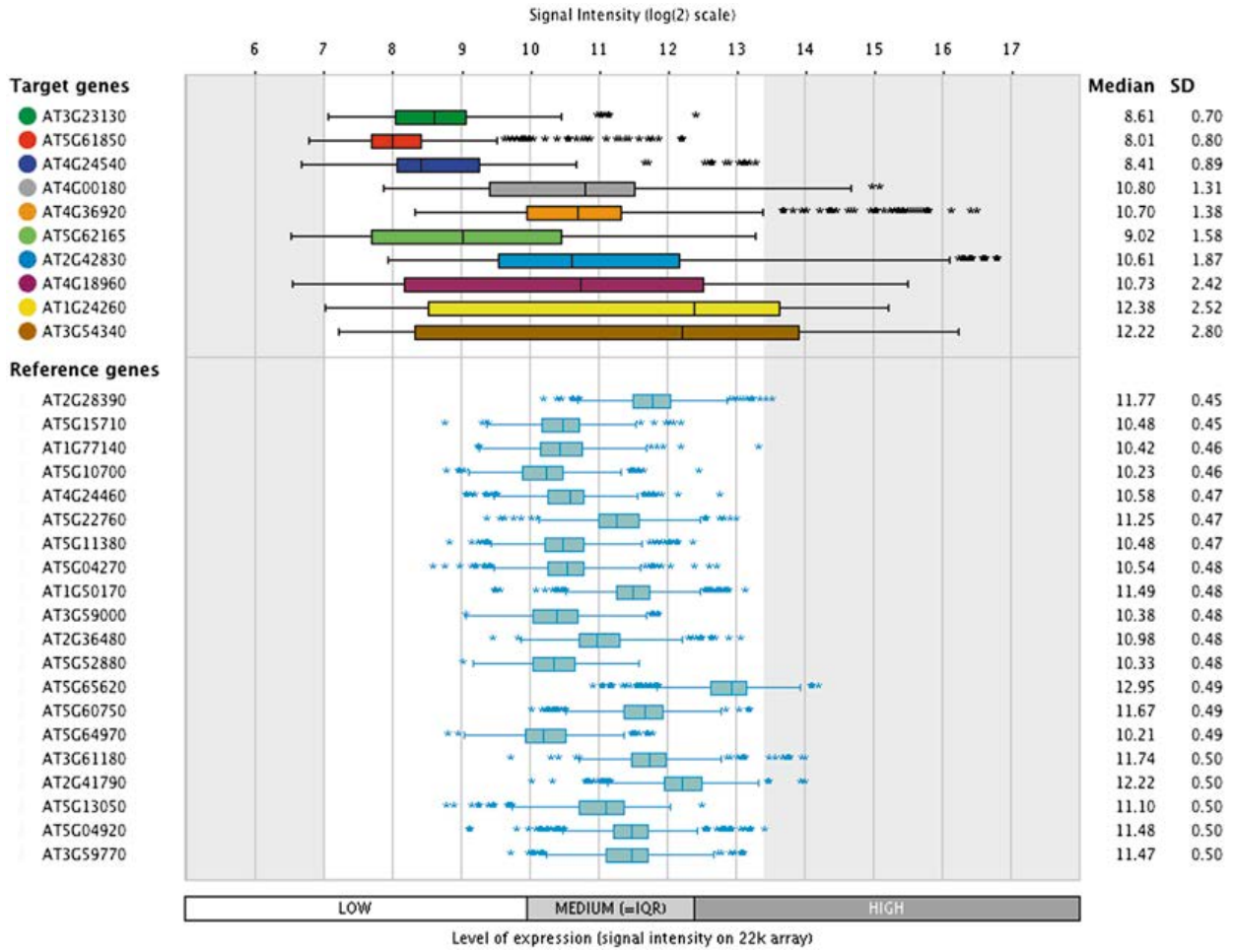


**Fig. 1** Example of output results obtained when using the *RefGenes* tool with the indicated set of floral regulatory genes (*SUP* (AT3G23130), *LFY* (AT5G61850), *AGL24* (AT4G24540), *YAB3* (AT4G00180), *AP2* (AT4G36920), *AGL42* (AT5G62165), *SHP2* (AT2G42830), *AG* (AT4G18960), *SEP3* (AT1G24260), and *AP3* (AT3G54340)) and microarray experiments under the Anatomy-Inflorescence category in Genevestigator

## 2 Materials

### 2.1 Tissue Collection and RNA Extraction

1. RNase-free microcentrifuge tubes (1.5 mL).
2. Plastic pellet pestles for 1.5 mL microcentrifuge tubes (optional: a mixer motor or an electric drill).
3. Forceps (e.g., Dupont size #5).
4. Liquid nitrogen.
5. Vortex.
6. Microcentrifuge.
7. Spectrum Plant Total RNA Kit (Sigma-Aldrich) or an equivalent total RNA isolation kit or reagents (*see* **Note 3**).
8. Spectrophotometer (such as a NanoDrop).
9. Agilent Bioanalyzer and associated reagents (Agilent RNA 6000 Nano kit).

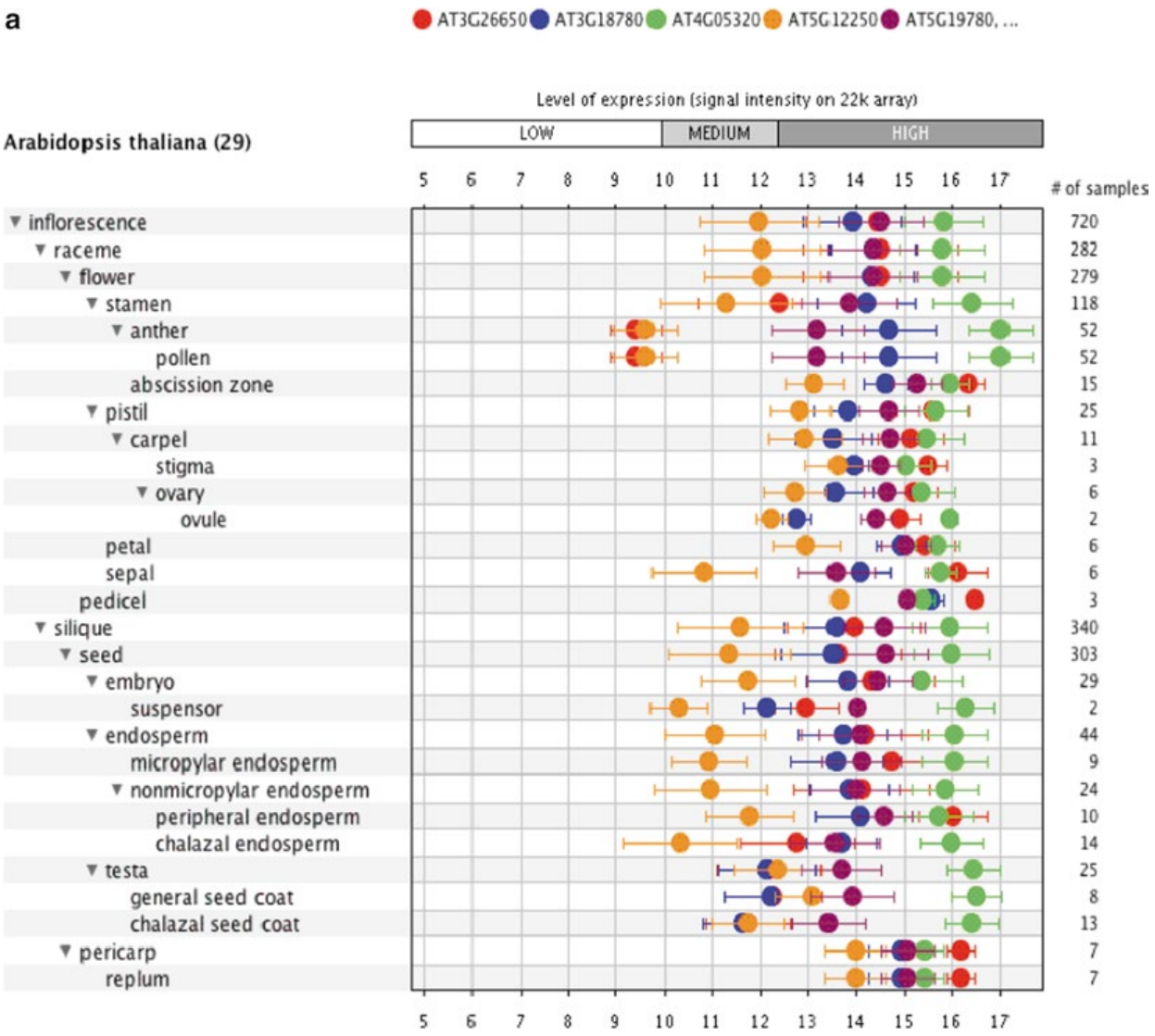


**Fig. 2** Expression characteristics of some commonly used and novel reference genes in Arabidopsis inflorescences (Genevestigator; Inflorescence category microarray experiments). (**a**) Traditional reference genes: *GAPDH* (AT3G26650), *ACT2* (AT3G18780), *UBQ10* (AT4G05320), *TUB6* (AT5G12250), *TUA5* (AT5G19780). (**b**) Novel reference genes: AT2G28390, AT5G15710, AT1G77140, AT5G10700, and AT4G24460. The novel reference genes are more stably expressed throughout the experimental series, and their mean expression level is generally lower than that of traditional reference genes, and thus closer to that of the typical genes of interest

### *2.2 Reverse Transcription Reaction*

1. High Capacity cDNA Reverse Transcription Kit (e.g., Applied Biosystems; other commercial kits are available, but the protocols provided below are based on this kit) containing dNTPs (100 mM), MultiScribe reverse transcriptase (50 U/mL), reverse transcription Random Primers, reverse transcription buffer (10×), RNase inhibitor (20 U/mL).
2. RNase-free PCR-tubes.
3. Nuclease-free water.

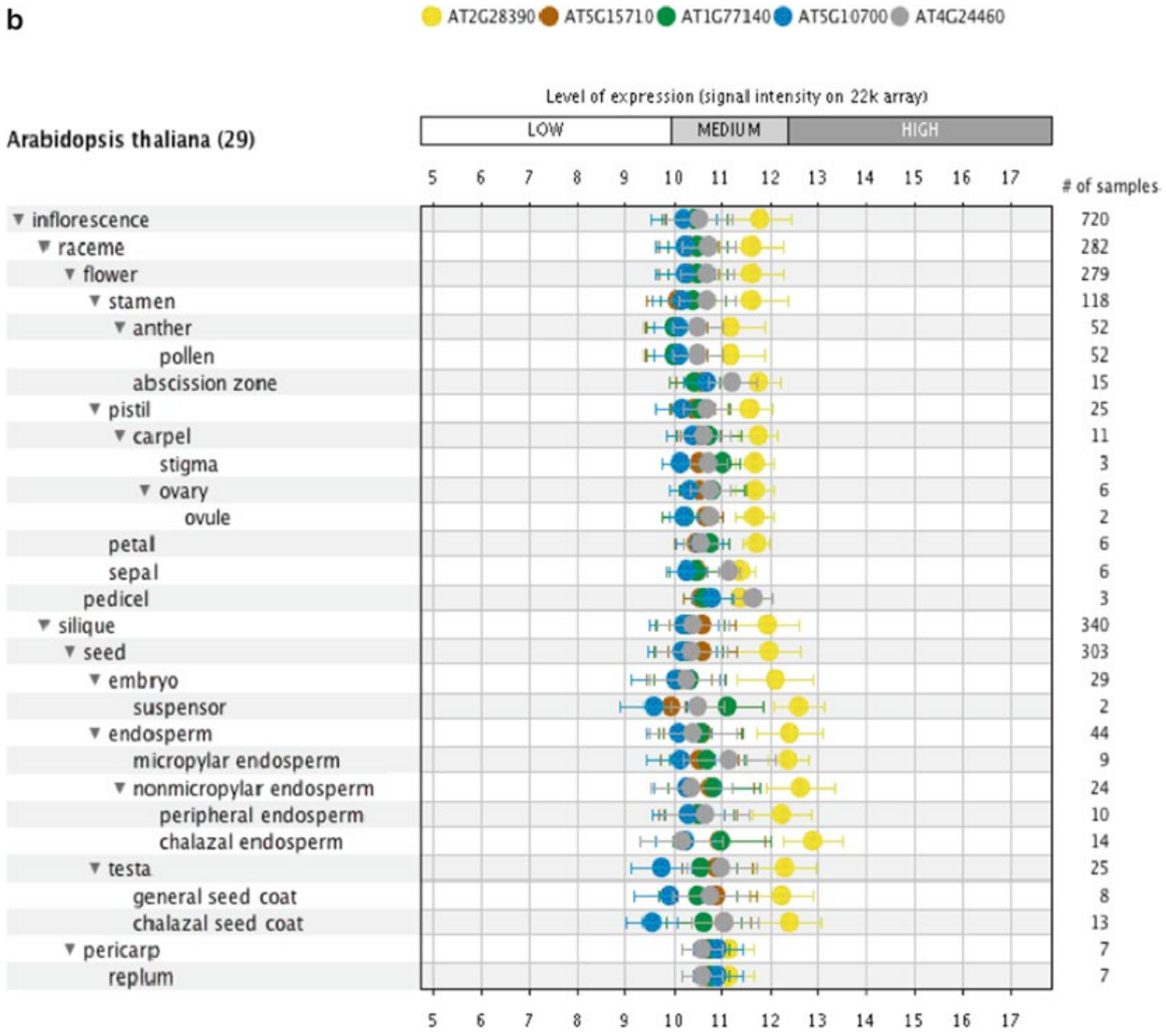


**Fig. 2** (continued)

### 2.3 Quantitative Real-time PCR: LightCycler® 480 System

1. LightCycler® 480 SYBR Green I Master (Roche Diagnostics; other commercial kits are available, but the protocols provided below are based on this kit): ready-to-use hot-start PCR mix containing FastStart Taq DNA Polymerase, reaction buffer, dNTP mix (with dUTP, instead of dTTP), SYBR Green I dye, and $MgCl_2$.
2. LC 480 Multiwell Plate 96 (Roche Diagnostics) (*see* **Note 4**).
3. Forward and reverse PCR primers at 100 μM each.
4. Nuclease-free water.

### 2.4 Quantitative Real-time PCR: BioMark™ System

1. TaqMan PreAmp Master Mix 2× (Applied Biosystems).
2. SsoFast EvaGreen SuperMix with Low ROX (Bio-Rad): 2× real-time PCR mix, containing dNTPs, Sso7d fusion polymerase, $MgCl_2$, ROX passive reference dye and stabilizers.
3. 2× Assay Loading Reagent (Fluidigm).

**Table 2**
**Candidate novel reference genes for Arabidopsis floral tissues identified using *RefGenes***

| Gene | Annotation |
|---|---|
| *AT2G28390* | SAND family protein |
| *AT5G15710* | Galactose oxidase/kelch repeat superfamily protein |
| *AT1G77140* | Vacuolar protein sorting 45 |
| *AT5G10700* | Peptidyl-tRNA hydrolase II (PTH2) family protein |
| *AT4G24460* | CRT (chloroquine-resistance transporter)-like transporter 2 |
| *AT5G22760* | PHD finger family protein |
| *AT5G11380* | 1-deoxy-d-xylulose 5-phosphate synthase 3 |
| *AT5G04270* | DHHC-type zinc finger family protein |
| *AT1G50170* | Sirohydrochlorin ferrochelatase B |
| *AT3G59000* | F-box/RNI-like superfamily protein |
| *AT2G36480* | ENTH/VHS family protein |
| *AT5G52880* | F-box family protein |
| *AT5G65620* | Zincin-like metalloproteases family protein |
| *AT5G60750* | CAAX amino terminal protease family protein |
| *AT5G64970* | Mitochondrial substrate carrier family protein |
| *AT3G61180* | RING/U-box superfamily protein |
| *AT2G41790* | Insulinase (Peptidase family M16) family protein |
| *AT5G13050* | 5-formyltetrahydrofolate cycloligase |
| *AT5G04920* | EAP30/Vps36 family protein |
| *AT3G59770* | sacI homology domain-containing protein/WW domain-containing protein |

4. 20× DNA Binding Dye Sample Loading Reagent (Fluidigm).
5. Exonuclease I (*E. coli*) (20,000 U/mL; New England Biolabs).
6. Exonuclease I Reaction Buffer 10× (New England Biolabs).
7. Forward and reverse PCR primers at 100 μM each.
8. Nuclease-free water.
9. TE Buffer: 10 mM Tris–HCl, pH 8.0, 1.0 mM EDTA (TEKnova).
10. DNA Suspension Buffer; 10 mM Tris–HCl, pH 8.0, 0.1 mM EDTA (TEKnova).
11. 48.48 Dynamic Array IFC (Fluidigm).

## 3 Methods

The performance of the primers that are used in a qRT-PCR experiment is crucial for obtaining high-quality results, and there are several aspects that have to be considered for successful primer design (*see* **Note 5**). There are public, searchable databases of primer and probe sequences that have been used and validated in real-time PCR assays, and can thus be an alternative to the time-consuming primer design and experimental optimization steps (e.g., RTPrimerDB; http://medgen.ugent.be/rtprimerdb/). In addition, there are many online resources for primer design, some of which also provide access to a consultative design service, such as:

- Oligoarchitect: www.sigma.com/oligoarchitect
- RealTimeDesign: https://www.biosearchtech.com/display.aspx?pageid=54
- QuantPrime: http://www.quantprime.de/
- IDT-qPCR: http://eu.idtdna.com/scitools/Applications/RealTimePCR/
- Primer3: http://primer3.sourceforge.net/
- Primer-BLAST: http://www.ncbi.nlm.nih.gov/tools/primer-blast/

### 3.1 Tissue Collection and RNA Extraction

RNA quality (integrity and purity) is a critical factor for qRT-PCR experiments.

1. Harvest at least 100 mg of the desired plant tissue (e.g., inflorescences), into a 1.5 mL RNase-free microcentrifuge tube containing liquid nitrogen.
2. Grind the tissue to a fine powder with the pellet pestles (and a mixer motor), keeping the bottom of the tube immersed in liquid nitrogen throughout the grinding process in order to avoid RNA degradation (*see* **Notes 6** and **7**).
3. Follow the manufacturer's instructions for the RNA extraction kit.
4. Analyze the integrity of the isolated RNA using a Bioanalyzer (or by using the 3′/5′ integrity assay, *see* ref. 3) and determine the concentration by absorption at 260 nm (e.g., with a NanoDrop spectrophotometer).

### 3.2 Reverse Transcription Reaction

The reverse transcription reaction to synthesize cDNA from the starting RNA material can be performed with various priming strategies, enzymes, and experimental conditions [2, 3]. However, in order to compare gene expression data across different experiments or laboratories, these variables should be kept constant, particularly ensuring that the same amount of RNA is added to

each reaction (or that the enzyme/protocol used results in a proportional cDNA yield).

1. Prepare an RT master mix in a 1.5 mL tube according to the following table:

| Component | Volume (per reaction) (μL) |
|---|---|
| Water | 4.2 |
| 10× RT Buffer (1×) | 2 |
| 25× dNTP Mix (100 mM) | 0.8 |
| 10× RT Random Primers | 2 |
| MultiScribe Reverse Transcriptase | 1 |

2. Add 10 μL of mastermix to each individual PCR-tube. Then add 100–1,000 ng of each RNA sample, in a volume of 10 μL. The final reaction volume is 20 μL. No-RT control reaction(s) should be included in the experiment.
3. Briefly centrifuge the tubes to collect the contents and to eliminate any air bubbles.
4. Place the tubes in a thermal cycler using the following conditions:

| | Step 1 | Step 2 | Step 3 | Step 4 |
|---|---|---|---|---|
| Temperature (°C) | 25 | 37 | 85 | 4 |
| Time | 10 min | 120 min | 5 min | ∞ |

5. Store cDNA samples at 4 °C (short term) or at –20 °C (for up to 6 months).

### 3.3 Quantitative Real-time PCR: LightCycler® 480 System

1. Set up your samples:
   (a) Every gene–primer-pair combination used in a qPCR should be tested to calculate primer efficiency (*see* **Note 8**).
   (b) The cDNA samples resulting from the RT reaction may be diluted in water, to obtain a final estimated concentration between 5 and 10 ng/μL (estimation based on the initial amount of RNA used in the RT reaction). This concentration range is ideal for the qRT-PCR. All amplification reactions should have a similar concentration of cDNA.
2. Before loading the PCR plate, and in order to minimize pipetting errors, it is important to prepare master mixes for each primer pair used. The accuracy of qPCR is highly dependent on accurate pipetting and thorough mixing of solutions. To prepare the qPCR Master Mix, add components in the order indicated in the table below. The protocol provided here

uses SYBR® Green I chemistry, but other PCR-product detection chemistries could be used (*see* **Note 9**).

| Component | Volume (per reaction) (μL) for 96-well plate |
|---|---|
| LC480 SYBR® Green I Master (2×) (Roche Diagnostics) | 10 |
| Water | 6.4 |
| Primer Forward (10 μM) | 0.8 |
| Primer Reverse (10 μM) | 0.8 |

3. Loading the plate: Once all master mixes for each pair of primers are prepared, start loading the plate by adding first the Master Mix (18 μL) and then the cDNA samples (2 μL). Avoid producing bubbles. The final reaction volume in each well is 20 μL. Then add the No Template Control (NTC) and no-Reverse Transcription control (no-RT, or RT-) reactions (*see* **Note 10**). Seal the plate with LightCycler® 480 Sealing Foil by pressing it firmly to the plate surface, using your hand or a scraper. Sealing the plate properly is crucial to eliminate evaporation at high temperatures.
4. Place the multiwell plate in a standard swing-bucket centrifuge equipped with a rotor for multiwell plates with suitable adaptors. Balance it with a suitable counterweight (e.g., another multiwell plate). Centrifuge the plate at 1,500 × *g* for 2 min.
5. Load the multiwell plate into the LightCycler® 480 Instrument and set up the qPCR program (annealing temperature in the PCR is primer-dependent):

| | Temperature (°C) | Time | Acquisition |
|---|---|---|---|
| Activation | 95 | 10 min | None |
| PCR (45 cycles) | 95<br>60<br>72 | 10 s<br>30 s<br>30 s | None<br>None<br>Single |
| Melting | 95<br>65<br>95 | 2 s<br>15 s<br>– | None<br>None<br>Continuous |
| Cooling | 40 | 30 s | None |

### 3.4 Quantitative Real-time PCR: BioMark™ System

BioMark System arrays allow for the automatic combination of sets of samples with sets of assays, significantly reducing reaction volume and the number of liquid-handling steps performed during the experiment. For instance, using the 48 × 48 array (as described in this protocol), 48 different samples (e.g., time-points in a time-course experiment) can be tested with up to 48 different assays (e.g., genes).

1. Specific Target Amplification (STA): This step is recommended to increase the number of copies of target DNA.
   (a) STA Primer Mix (500 nM):
   - Pool together 1 μL aliquots of all of the 100 μM primer sets to be included in the STA reaction (up to 100 different assays).
   - Add DNA Suspension Buffer to make the final volume 200 μL.
   - Vortex to mix and briefly spin reaction tube.

   (b) STA Pre-Mix:
   - In a DNA-free hood, prepare a Pre-Mix for the STA reaction according to the following table:

| Component | Volume (per reaction) (μL) |
|---|---|
| TaqMan PreAmp Master Mix | 2.5 |
| 500 nM pooled STA Primer Mix | 0.5 |
| Water | 0.75 |

   - Add 3.75 μL of STA Pre-Mix for each sample in a 96-well plate.
   - Add 1.25 μL of cDNA (at 5–25 ng/μL) to each reaction well, making a final volume of 5 μL. Include a no-PreAmplification control: add water instead of cDNA.
   - Seal the plate properly. Then, vortex and briefly spin the plate.

   (c) STA thermal cycle reaction:
   - Place the plate into the thermal cycler and run the following program (annealing temperature in the PCR is primer-dependent):

| | Activation | 16 cycles | | Hold |
|---|---|---|---|---|
| Temperature (°C) | 95 | 95 | 60 | 4 |
| Time | 10 min | 15 s | 4 min | ∞ |

   - Eliminate the unincorporated primers from the STA amplification reaction. Prepare Exonuclease Mix as follows:

| Component | Per 5 μL sample |
|---|---|
| Water | 1.4 μL |
| Exonuclease I reaction buffer | 0.2 μL |
| Exonuclease I (20 U/μL) | 0.4 μL |

- Add 2 μL of Exonuclease Mix to each 5 μL STA reaction. Vortex, centrifuge, and place in a thermal cycler.

| | Digest | Inactivate | Hold |
|---|---|---|---|
| Temperature (°C) | 37 | 80 | 4 |
| Time | 30 min | 15 min | ∞ |

- Dilute the STA reaction to an appropriate final product concentration, as shown below. A minimum dilution of fivefold should be used.

| Volume of water or TE Buffer | | | |
|---|---|---|---|
| Volume of STA Rx | 5-fold dilution | 10-fold dilution | 20-fold dilution |
| 7 μL | 18 μL | 43 μL | 93 μL |

- Store diluted STA products at −20 °C or use immediately for on-chip PCR.

2. Sample and Assay Mix preparation:
   (a) Prepare Sample mix as shown below:

| Component | Volume per inlet with overage (μL) |
|---|---|
| 2× SsoFast EvaGreen Supermix with low ROX | 3.0 |
| 20× DNA binding dye sample loading reagent | 0.3 |

   (b) In a new 96-well plate aliquot 3.3 μL of Sample mix and add 2.7 μL of each STA and Exo I-treated sample.
   (c) Seal the plate properly. Then, vortex and spin plate. Keep on ice.
   (d) Prior to preparing the Assay mix, combine the two primers of each primer pair making a final concentration of 20 μM.
   (e) Prepare Assay mix as shown below:

| Component | Volume per inlet with overage (μL) |
|---|---|
| 2× Assay loading reagent | 3.0 |
| 1× DNA suspension buffer | 1.5 |

   (f) In a new 96-well plate, aliquot 4.5 μL of Assay mix and add in 1.5 μL of the primer pair mix at 20 μM.
   (g) Seal the plate properly. Then, vortex and spin the plate. Keep on ice.

3. Priming the 48×48 Dynamic Array™ IFC
   (a) Inject control line fluid into each accumulator on the chip. Load the chip within 60 min of priming (refer to instrument manufacturer's instructions for details).
   (b) Remove and discard the blue protective film from the bottom of the chip.
   (c) Place the chip into the IFC controller for the 48×48 Dynamic Array IFC.
   (d) Run the Prime script for the 48×48 Dynamic Array IFC.
   (e) Pipette 5 µL of each assay and 5 µL of each sample into their respective inlets on the chip.
   (f) Place the chip to the IFC controller and run the Load Mix program.
   (g) After the program has run, take out the chip from the IFC controller and remove any dust particle from the chip surface.
   (h) Place the chip in the Biomark System and run the following program (annealing temperature in the PCR is primer-dependent):

| | Activation | 30 Cycles | | Melting | |
|---|---|---|---|---|---|
| Temperature (°C) | 95 | 96 | 60 | 60 | 95 |
| Time | 60 s | 5 s | 20 s | 3 s | 1 °C/3 s |

### 3.5 Data Analysis

Different methodologies can be used for determination of the Quantification Cycle, Cq [16] (previously referred to as Ct/Cp/takeoff point):

- The threshold cycle method measures the Cq at a constant fluorescence level. These constant threshold methods assume that all samples have the same amplicon DNA concentration at the threshold fluorescence. The strength of this method is that it is extremely robust, but the threshold value needs to be adjusted for each experiment.
- The second derivative method calculates Cq as the second derivative maximum of the amplification curve. It is not user-dependent and is widely used.

Before performing the actual analysis, it is important to validate the data according to a variety of criteria (preferably following the Minimum Information for Publication of Real-time PCR Experiments: MIQE guidelines, *see* **Note 11**, ref. 16). In particular:

- Check amplification curves. A normal amplification plot has three distinct phases; linear baseline, exponential and plateau.

- Check controls (RT-, NTC).
- Check that the slope of the standard curve is between −3.2 and −3.5.
- Check technical replicates. They should be within 0.5 Cq of each other.
- Check melting peaks (when using a binding dye, or probes such as Molecular Beacons or Scorpions that are not hydrolyzed during the reaction) to verify that single, specific amplification products have been synthesized in the reaction.

#### 3.5.1 Absolute Quantification

Absolute quantification relies on measurement to a standards curve constructed using the real-time PCR data obtained from amplification of these standards of known concentrations of template. Commonly, standards are derived from purified dsDNA plasmid, in vitro-transcribed RNA or in vitro-synthesized ssDNA. A standard curve (plot of Cq value against log of amount of standard) is generated using different dilutions of the standard. The Cq value of the target is compared with the standard curve, allowing calculation of the initial amount of the target. It is important to select an appropriate standard for the type of nucleic acid to be quantified. This method requires having the same efficiency of amplification in all reactions (reactions with experimental samples and reactions with the external standards). When using absolute quantification for determination of mRNA concentration, it is usual to correct absolute copy number of the specific target relative to absolute copy number of one or more reference genes

#### 3.5.2 Relative Quantification

Relative quantification relies on comparing the expression level of a target gene relative to a reference gene between a control sample and the test samples. Normalization to reference genes is the most common method for controlling for variation in qRT-PCR experiments. It is used to measure the relative change in mRNA expression levels. Many mathematical models are available. Most common relative quantification methods are:

(a) Pfaffl model [17]: combines gene quantification and normalization into a single calculation (Eq. 1). This model adjusts the amplification efficiencies ($E$) from target and reference genes in order to correct differences between the two assays.

$$Ratio = \frac{\left(E_{target}\right)^{\Delta Cq\ target\ (control-sample)}}{\left(E_{reference}\right)^{\Delta Cq\ reference\ (control-sample)}} \quad (1)$$

(b) $2^{-\Delta\Delta Cq}$ method [18]: This is a simpler version of the first model. Target and control amplification efficiency ($E_{\text{target}}$ and $E_{\text{reference}}$) are assumed to be maximum (100 %, i.e., a value of 2, indicating

amplicon doubling during each cycle) (Eq. 2). In addition the relative expression of the target in all test samples is compared to that in a control or calibrator sample

$$Ratio = 2^{-[\Delta Cq\ Sample - \Delta Cq\ control]} \quad (2)$$

## 4 Notes

1. *geNorm* is a widely used algorithm to determine the most stable reference from a given set of candidate genes on the basis of the *M* value (the *M* value is the internal control gene-stability measure, defined as the average pair-wise variation of a particular gene with all other control genes; genes with the lowest *M* values have the most stable expression) [8]. *geNorm* calculates and compares the *M* value of each pair of genes, and eliminates the gene with the highest *M* value, and then repeats this process with the remaining genes until the pair of genes with the lowest *M* value is identified. Thus, the genes forming this pair are considered as optimal reference genes among the initial candidate set.
2. The genome-wide analyses performed by Czechowski et al. led to the identification of many novel reference gene candidates, with purportedly better expression characteristics than traditional reference genes [11]. In these analyses the SD/MV ratio (SD/mean expression value, i.e., the coefficient of variation, or CV) for each gene in all the given experimental conditions (developmental series, abiotic stress series, hormone series, nutrient starvation and re-addition series, diurnal series, light series, and biotic stress series) is calculated. The gene that has the lowest CV value is considered as the gene with the most stable expression, and therefore a potential reference gene. Through these analyses, 25 reference genes, including 20 novel and 5 traditional ones, were recommended [11]. These genes were then validated by qRT-PCR and their expression stability ranked using the *geNorm* algorithm (*see* Table 1).
3. There are specific plates and films for the LC480 system that have been designed to ensure the best heat transfer from the thermal block and minimal autofluorescence, which is important in order to achieve a good signal-to-noise ratio in the detection of amplification products. In this protocol, we suggest using the LC 480 Multiwell Plate 96 from Roche.
4. The RNA preparation should be free of contaminating genomic DNA, so we recommend using a previously tested commercial kit for RNA isolation (*see* **Note 10**).
5. For primer design, it is important to consider the following points: (1) PCR products should be short (the ideal length is

from 70 to 250 bp); (2) The gene-specific forward and reverse primers should have similar melting temperatures (Tm) and length; (3) Primers should be between 15 and 25 nucleotides long and with a G/C content of around 50 %. (4) Primers should have low or no self-complementarity, in order to avoid the formation of primer dimers; (5) For the same reason, avoid pairs of primers that show sequence complementarity at their 3′ ends; (6) Primers that span introns or cross intron/exon boundaries are advantageous because they allow to distinguish amplification from cDNA or from contaminant genomic DNA. Primers should be ordered with desalt purification. Primer stock solutions should be prepared with DNase/RNase-free water. Make aliquots to avoid contamination and repeated freezing/thawing. Original stock of PCR primers should be stored at −20 °C, and working dilutions at 4 °C for up to 2 weeks.

6. The presence of liquid nitrogen inside the microcentrifuge tubes during tissue grinding should be avoided, to prevent potential loss of tissue by nitrogen spill, or by the popping of the tube if closed with liquid nitrogen inside. Tubes can be pre-chilled in liquid nitrogen. As an alternative for grinding the tissue, mortar and pestle could be used instead of pellet pestles and an electric drill.
7. Both fresh and frozen (−80 °C) tissue can be used as starting material, and ground plant material can be stored at −80 °C before RNA purification. However, do not allow the frozen material to thaw before grinding or before the first solution of the RNA purification procedure is added.
8. Make a four-step dilution series (1:4 dilutions) from cDNA samples. In order to evaluate the efficiency of the PCR reaction, it is important to generate at least one standard curve for each primer pair. A standard curve graph is made by plotting the Ct/Cp values on the *y*-axis and the logarithm of the input amounts on the *x*-axis. The slope of the line of this plot will give the efficiency of the reaction according to the equation $E = [10^{(-1/\text{slope})}] - 1$; slope should be between −3.2 and −3.5 and $R^2 > 0.98$.
9. SYBR® Green I and EvaGreen® are the most used dye chemistries, due to cost and simple optimization process. However, these dyes bind to any double-stranded DNA formed in the reaction, including primer-dimers and other nonspecific reaction products, which may result in an overestimation of the target concentration. Other methods, such as hydrolysis probes, may also be used. Probe-based qRT-PCR relies on the sequence-specific detection of a desired PCR product. It utilizes a fluorescently labeled target-specific probe, which results in increased specificity and sensitivity.

10. No template controls (NTC) should be included for each pair of primers tested to ensure that there is no reagent contamination. In these control reactions, water is added instead of sample, so no amplification is expected. In case the NTC reaction shows the synthesis of amplification products (i.e., the presence of a contaminant), measures such as pipette decontamination, using new primers aliquots, or thorough bench cleaning might be necessary. No reverse transcription controls (no-RT, or RT-) are used to detect the presence of contaminant genomic DNA in the RNA samples. If the RT- reaction shows the synthesis of amplification products, the corresponding RNA samples should be treated with DNase prior to their use in the reverse transcription reaction. If the primers were designed to span an intron or an intron/exon boundary, it is not necessary to perform a no-RT control.
11. MIQE Guidelines [16]. The MIQE guidelines were published in response to the recognition that several publications contain little information that describes the qPCR or that gives the reader the opportunity to determine the quality of the experiment. The result of these omissions is that several publications contain misleading conclusions based on inadequate quality control of the technical process. The MIQE guidelines contain a step-by-step guide and checklist, which leads the experimenter through the process of experiment validation. This has the additional function of providing a framework for publication analysis by peer reviewers and journal editors. Several publishing houses are now requiring that MIQE guidelines are followed for papers containing qPCR data.

## Acknowledgements

Work in the authors' laboratory is funded by grants from Spanish Ministerio de Economía y Competividad (BFU2011-22734; and Programa Consolider-Ingenio, CSD2007-00036), and the Agència de Gestió d'Ajuts Universitaris i de Recerca (AGAUR) (grant SGR2009-GRC476). J. J. was supported by a fellowship from the European Molecular Biology Organization (EMBO).

### References

1. Bustin SA, Benes V, Nolan T, Pfaffl MW (2005) Quantitative real-time RT-PCR—a perspective. J Mol Endocrinol 34(3):597–601
2. Kubista M, Andrade JM, Bengtsson M, Forootan A, Jonak J, Lind K, Sindelka R, Sjoback R, Sjogreen B, Strombom L, Stahlberg A, Zoric N (2006) The real-time polymerase chain reaction. Mol Aspects Med 27(2–3):95–125
3. Nolan T, Hands RE, Bustin SA (2006) Quantification of mRNA using real-time RT-PCR. Nat Protoc 1(3):1559–1582
4. Fleige S, Pfaffl MW (2006) RNA integrity and the effect on the real-time qRT-PCR performance. Mol Aspects Med 27(2–3):126–139
5. Nolan T, Hands RE, Ogunkolade W, Bustin SA (2006) SPUD: a quantitative PCR assay for

the detection of inhibitors in nucleic acid preparations. Anal Biochem 351(2):308–310

6. Gutierrez L, Mauriat M, Guenin S, Pelloux J, Lefebvre JF, Louvet R, Rusterucci C, Moritz T, Guerineau F, Bellini C, Van Wuytswinkel O (2008) The lack of a systematic validation of reference genes: a serious pitfall undervalued in reverse transcription-polymerase chain reaction (RT-PCR) analysis in plants. Plant Biotechnol J 6(6):609–618
7. Gutierrez L, Mauriat M, Pelloux J, Bellini C, Van Wuytswinkel O (2008) Towards a systematic validation of references in real-time RT-PCR. Plant Cell 20(7):1734–1735
8. Vandesompele J, De Preter K, Pattyn F, Poppe B, Van Roy N, De Paepe A, Speleman F (2002) Accurate normalization of real-time quantitative RT-PCR data by geometric averaging of multiple internal control genes. Genome Biol 3(7):RESEARCH0034
9. Pfaffl MW, Tichopad A, Prgomet C, Neuvians TP (2004) Determination of stable housekeeping genes, differentially regulated target genes and sample integrity: BestKeeper—Excel-based tool using pair-wise correlations. Biotechnol Lett 26(6):509–515
10. Schmid M, Davison TS, Henz SR, Pape UJ, Demar M, Vingron M, Scholkopf B, Weigel D, Lohmann JU (2005) A gene expression map of *Arabidopsis thaliana* development. Nat Genet 37:501–506
11. Czechowski T, Stitt M, Altmann T, Udvardi MK, Scheible WR (2005) Genome-wide identification and testing of superior reference genes for transcript normalization in Arabidopsis. Plant Physiol 139(1):5–17
12. Chao WS, Dogramaci M, Foley ME, Horvath DP, Anderson JV (2012) Selection and validation of endogenous reference genes for qRT-PCR analysis in leafy spurge (Euphorbia esula). PLoS One 7(8):e42839
13. Caldana C, Scheible WR, Mueller-Roeber B, Ruzicic S (2007) A quantitative RT-PCR platform for high-throughput expression profiling of 2500 rice transcription factors. Plant Methods 3:7
14. Hruz T, Wyss M, Docquier M, Pfaffl MW, Masanetz S, Borghi L, Verbrugghe P, Kalaydjieva L, Bleuler S, Laule O, Descombes P, Gruissem W, Zimmermann P (2011) RefGenes: identification of reliable and condition specific reference genes for RT-qPCR data normalization. BMC Genomics 12:156
15. Wellmer F, Alves-Ferreira M, Dubois A, Riechmann JL, Meyerowitz EM (2006) Genome-wide analysis of gene expression during early Arabidopsis flower development. PLoS Genet 2(7):e117
16. Bustin SA, Benes V, Garson JA, Hellemans J, Huggett J, Kubista M, Mueller R, Nolan T, Pfaffl MW, Shipley GL, Vandesompele J, Wittwer CT (2009) The MIQE guidelines: minimum information for publication of quantitative real-time PCR experiments. Clin Chem 55(4):611–622
17. Pfaffl MW (2001) A new mathematical model for relative quantification in real-time RT-PCR. Nucleic Acids Res 29(9):e45
18. Livak KJ, Schmittgen TD (2001) Analysis of relative gene expression data using real-time quantitative PCR and the 2(-Delta Delta C(T)) Method. Methods 25(4):402–408

*Journal of Experimental Botany*, Vol. 67, No. 6 pp. 1639–1648, 2016
doi:10.1093/jxb/erw058

FLOWERING NEWSLETTER REVIEW

# Genome-wide analyses for dissecting gene regulatory networks in the shoot apical meristem

**Mariana Bustamante[1,*], José Tomás Matus[1,*] and José Luis Riechmann[1,2,†]**

[1] Center for Research in Agricultural Genomics (CRAG) CSIC-IRTA-UAB-UB, Cerdanyola del Vallès, 08193 Barcelona, Spain
[2] Institució Catalana de Recerca i Estudis Avançats (ICREA), Barcelona, 08010, Spain

* These authors contributed equally to this work.
† Correspondence: joseluis.riechmann@cragenomica.es

Received 24 November 2015; Accepted 1 February 2016

Editor: Lars Hennig, Swedish University of Agricultural Sciences

## Abstract

**Shoot apical meristem activity is controlled by complex regulatory networks in which components such as transcription factors, miRNAs, small peptides, hormones, enzymes and epigenetic marks all participate. Many key genes that determine the inherent characteristics of the shoot apical meristem have been identified through genetic approaches. Recent advances in genome-wide studies generating extensive transcriptomic and DNA-binding datasets have increased our understanding of the interactions within the regulatory networks that control the activity of the meristem, identifying new regulators and uncovering connections between previously unlinked network components. In this review, we focus on recent studies that illustrate the contribution of whole genome analyses to understand meristem function.**

**Key words:** Arabidopsis, cell-type specific, shoot apical meristem, stem cell, transcriptome, WUSCHEL.

## Introduction

The shoot apical meristem (SAM) is responsible for generating all postembryonic above-ground organs of a plant, such as stems, leaves and flowers (Barton, 2010; Ha *et al.*, 2010). Established during embryogenesis, the SAM remains active during the entire lifecycle of the plant, providing it with the capacity to generate organs throughout every stage of its development. This capacity relies on a small population of stem cells that are located in the centric region of the meristem, a highly regulated microenvironment termed the stem cell niche (reviewed in Aichinger *et al.*, 2012; Dinneny and Benfey, 2008; Perales and Reddy, 2012; Sablowski, 2007, 2011). A stem cell niche is also present in the root apical meristem (RAM) and both types of meristems share additional organizational characteristics (e.g. organizing centers that maintain their respective stem cell populations and differentiation zones) (Dinneny and Benfey, 2008), as well as similarities in molecular mechanisms [for instance, conserved transcriptional regulators that control plant stem cell function (Sarkar *et al.*, 2007; Zhou *et al.*, 2015)]. However, the SAM and the RAM differ in the effect that specific hormones have upon their activity (e.g. auxin and cytokinin: Dello Ioio *et al.*, 2008; Zhao *et al.*, 2010), and in the fact that the SAM can give rise to a large set of sub-specialized meristems such as inflorescence, flower, sympodial and branch meristems, among others (reviewed in Bartlett and Thompson, 2014). In addition, the SAM possesses the unique characteristic of determining the spatial arrangement of aerial organs around the stem, a process known as phyllotaxis. The regular spacing of lateral organs along stems and branches and flowers (e.g. whorled, clockwise or anticlockwise spiral) differs among

species and it can vary between the embryonic, young and reproductive phases within the same organism (Traas, 2013).

The molecular and cellular mechanisms underlying the organization and activity of the SAM have been extensively studied over the past twenty years, by using sophisticated combinations of genetic, molecular, imaging and modeling approaches. This has resulted in a detailed – although still incomplete – characterization of a molecular regulatory network that operates extensively at the transcriptional level and that also includes hormone signaling and intercellular movement of proteins and microRNAs (Fig. 1). Whereas a majority of our current knowledge on this topic is derived from studies in *Arabidopsis*, genes related to the maintenance and organization of the SAM are highly conserved among different plant species and mutations in key regulators result in comparable severe developmental defects. The mechanisms and regulation of SAM development and function, and of plant stem cell niches and stem cell homeostasis, have been the subject of several recent detailed reviews (Barton, 2010; Gaillochet *et al.*, 2015; Ha *et al.*, 2010; Holt *et al.*, 2014). Here, a short introduction to these topics is provided, but the focus is on the contribution that recent genome-wide analyses have made to our understanding of the SAM and on how they have expanded the interactions and networks characterized through genetics. Genome-wide analyses of meristem function and development were pioneered for the study of the RAM, in particular by the development of methods for root cell type-specific expression profiling (e.g. Birnbaum *et al.*, 2003, 2005; Nawy *et al.*, 2005; Brady *et al.*, 2007). More recently, these and other techniques have been developed for genomic analyses in the SAM and aerial meristems and organs (e.g. Yadav *et al.*, 2009; Jiao and Meyerowitz, 2010; Yadav *et al.*, 2014).

The SAM is a dome-shaped structure that is organized into several clonally distinct cell layers and subdivided into different zones or functional domains (Fig. 1). In dicotyledonous plants such as Arabidopsis, the SAM consists of three cell layers (L1 to L3). An external L1 overlies the L2, both

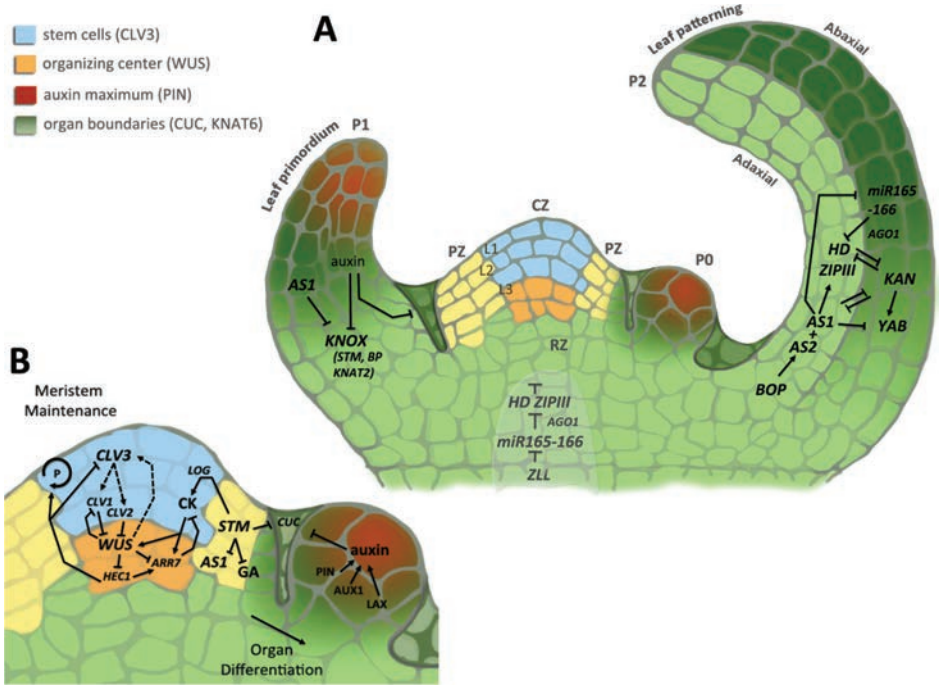


**Fig 1.** General overview of the shoot apical meristem organization and regulation in the context of organ differentiation. (A) Cells from the shoot apical meristem (SAM) are arranged in layers. L1, L2 and L3 represent three clonally distinct cell groups occupying the tunica and corpus. The SAM architecture is organized in a central zone (CZ), encompassing the stem cell niche (SCN) and the organizing center (OC), the peripheral zone (PZ) and the rib zone (RZ). The molecular events determining the maintenance of the SAM are in tight coordination with organ differentiation processes. Leaf primordia are indicated in three different developmental stages (P0, P1, P2). Regulation of boundaries and organ emergence in these primordia begins with auxin peaks and the activity of *ASYMMETRIC LEAVES 1* (*AS1*), both repressing the meristem-promoting activities of *KNOX* genes and cytokinins (CK). *HD-ZIPIII* genes are then induced by AS1, playing an antagonistic role with KANADI (KAN) for promoting leaf differentiation and patterning. The ARGONAUTE family member ZWILLE (*ZLL*) is expressed in the vasculature underlying the SAM and sequesters miR165/166 to prevent the repressing role of *HD-ZIPIII* genes in the shoot meristem primordium, thus promoting stem cell maintenance. (B) Stem cell-regulation machinery in the SAM. A pool of pluripotent stem cells is maintained by a WUSCHEL/CLAVATA3 (WUS/CLV3) negative-feedback loop, maintaining the proper number of stem cells in the SAM. *CLV3*, *CLV1* and *WUS* are expressed in overlapping domains between the SCN and the OC. CLV3 is a mobile glycopeptide ligand perceived by CLV1 and CLV2 for restricting *WUS* to its narrow domain in the L3, conferring a stem cell-restricting signal delivered to the stem OC cells. WUS, as stem cell-promoting protein, migrates from the OC into the SCN (dashed lines), enhancing the expression of *CLV3*. CK provide in the center of the SAM a positional cue to maintain the expression domain of *WUS*. *SHOOT MERISTEMLESS* (*STM*) activates CK biosynthesis through LONELY GUY (LOG), which converts cytokinin riboside 5′-monophosphates (CKRps) into active CK. Higher sensitivity to CK in the OC is achieved by repression of *ARR7*. The bHLH factor HECATE1 (HEC1) is a direct repression target of WUS in the OC. HEC1 activates proliferation (P) through cell-cycle regulators in stem cells. *STM* and related *KNOX* genes also keep cells in an undifferentiated state by repressing *AS1* and gibberellic acid (GA) biosynthesis in stem cells. *CUC* genes are negatively regulated by STM and auxin-dependent signaling, restricting their expression to the boundary region.

growing in a two-dimensional way by anticlinal cell division (originating cell walls are perpendicular to the apex surface) and together comprising the tunica (Barton, 2010; Shapiro *et al.*, 2015). An innermost layer, L3, comprises the corpus and grows in a three-dimensional manner, with both periclinal and anticlinal cell divisions. Each of these histogenic layers gives rise to different tissues. In general, epidermis is formed from the L1 layer while gametes arise from the L2. The pericycle and internal tissue of organs form from the L3 and further corpus cells (Poethig, 1987).

The SAM is also subdivided into three functional domains or zones, which are different from layers (Fig. 1): the central zone (CZ), the peripheral zone (PZ) and the rib zone (RZ). Whereas layers are clearly distinguished in histological sections, zones or domains can be defined by distinct gene expression patterns (Reddy and Meyerowitz, 2005; Yadav *et al.*, 2009), reflecting the transcriptional and developmental programs that are governing each of them. The CZ includes both tunica (L1 and L2) and corpus (L3) cells, and is where the stem cells are located. Underneath the stem cells lies the organizing center (OC), a small group of cells that sustains them. Cells from the CZ divide at a slow rate. Daughter cells are displaced laterally into the PZ, a ring of cells that surround the CZ and that is characterized by a high mitotic activity, or basally into the RZ. Cells in the PZ undergo sequential differentiation gaining distinct identities and giving rise to organ primordia (Reddy *et al.*, 2004; Heisler *et al.*, 2005), whereas the RZ will give rise to the inner tissues of the stem. As cells are passively displaced through these different functional domains by cell division and growth, they need to assess their position relative to the neighboring cells and adjust their fate or identity accordingly, for the SAM to maintain its functional domains. Thus, the dynamic nature of the SAM depends on intercellular communication. Furthermore, organ initiation requires precise spatiotemporal gene activation in coordination with the instructive signal of auxin (also related to phyllotaxis) (Ha *et al.*, 2010; Vernoux *et al.*, 2010, 2011).

Tunica and corpus cells within the CZ are symplasmically interconnected by plasmodesmata (PD) (Rinne and van der Schoot, 1998). The arrangement of PD between the central and peripheral zone gives rise to symplasmic fields, and changes in intercellular signaling achieved by positional closing of PD may shift the developmental phase of the SAM and specify, for instance, the zones of organ differentiation (Sager and Lee, 2014).

Initiation and establishment (patterning) of the Arabidopsis shoot meristem in the embryo, and its activity throughout plant development, relies on the expression in very specific domains of several genes that code for transcription factors (TFs) or signaling proteins. *CUP-SHAPED COTYLEDON1* (*CUC1*), *CUC2* and *CUC3*, encoding partially redundant NAC TFs, are required for SAM initiation and boundary formation (Zadnikova and Simon, 2014): *cuc* double mutants generate a continuous fused cup-shaped cotyledon structure without a SAM (Aida *et al.*, 1997; Takada *et al.*, 2001; Vroemen *et al.*, 2003). The homeodomain TF SHOOT MERISTEMLESS (STM) is also essential for meristem initiation and maintenance, with the latter requiring the right balance between cell proliferation and differentiation. STM promotes proliferation and inhibits cellular differentiation and endoreduplication (Endrizzi *et al.*, 1996; Long *et al.*, 1996; Scofield *et al.*, 2013). Consistent with this, ectopic expression of *STM*-like genes, such as the *KNOTTED* gene in maize, causes the formation of ectopic meristems (Smith *et al.*, 1992).

Within the established SAM, the stem cell population is stably maintained throughout development by the CLAVATA (CLV)/WUSCHEL (WUS) pathway and a mechanism that involves communication between the OC and the CZ (Waites and Simon, 2000; Ha *et al.*, 2010; Gaillochet *et al.*, 2015) (Fig. 1). *WUS*, like *STM*, codes for a homeodomain TF (Mayer *et al.*, 1998) and both factors act in parallel pathways that are connected through cytokinin action (Gaillochet *et al.*, 2015). WUS acts to promote stem cell identity and is required, together with CLV proteins, for the long-term functioning of the SAM (Yadav *et al.*, 2010). WUS expression is localized in a group of cells belonging to the organizing center (OC) found at the L3 (corpus). The CLV3-CLV1 (and -CLV2/CORYNE) ligand-receptor interaction complex was identified from the group of *clavata* (*clv*) mutants that exhibited increases in SAM size and higher number of floral organs (Clark *et al.*, 1997; Fletcher *et al.*, 1999; Jeong *et al.*, 1999). This complex restricts stem cell number and promotes cell differentiation in the SAM in a feedback regulatory loop involving WUS (Brand *et al.*, 2000; Schoof *et al.*, 2000). CLV1, a receptor kinase, and the receptor-like CLV2 and CRN recognize the small protein CLV3 after it is secreted from the tunica and probably diffused throughout PD (Fletcher *et al.*, 1999; Rojo *et al.*, 2002). PD are also important for WUS movement from the OC into the tunica-CZ cells (Daum *et al.*, 2014).

Establishment, patterning and maintenance of the SAM involve many additional factors and interactions among them, which are described in several recent detailed reviews (see Fig 1, and Ha *et al.*, 2010; Perales and Reddy, 2012; Holt *et al.*, 2014; Gaillochet *et al.*, 2015). The brief morphological, organizational and genetic schema outlined above is provided here as background for the genome-wide studies on the Arabidopsis SAM performed over the past few years, which are the main subject of this review. Transcriptomic and other genome-wide studies of SAM initiation and maintenance have uncovered previously unknown links and interactions among different components of the meristem developmental machinery in Arabidopsis (Table 1). Here, we will focus on some novel insights that have been gained through the use of these experimental approaches.

## Gene regulatory networks of central stem cell regulators

Gene expression profiling of the different functional zones and cell types that constitute the SAM was initially hampered by the fact that the respective domains are very small [for instance, the Arabidopsis SAM contains ~35 stem cells (Reddy and Meyerowitz, 2005)]. However, by marking

**Table 1.** *Genome-wide analyses of shoot apical meristem development*

| Process studied | Genomic experimental approach | Plant material | Genome-wide observations | Reference |
|---|---|---|---|---|
| Gene expression map of the SAM | Cell sample-specific gene expression profiling. Protoplast FACS and microarrays. | Four different cell samples of SAMs of *ap1 cal* mutant plants. | ~2500 genes differentially expressed among CZ, RM and PZ cell types. | Yadav *et al.*, 2009 |
| Gene expression map of the SAM | Cell sample-specific gene expression profiling. Protoplast FACS and microarrays. | Ten different cell populations (clonal cell layers and domains) of SAMs of *ap1 cal* mutant plants. | ~2200 genes identified as 'cell population differentially expressed genes' (CPEGs) in the CZ and PZ domain datasets. 1456 CPEGs were identified across the L1, L2 and L3 SAM cell populations; 472 across the CZ, organ primordia, organ boundaries and outer PZ; 1031 in vascular cell populations in comparison with the L2 cell layer; and 292 in meristematic and non-meristematic L1 in comparison with the L2 cell layer. | Yadav *et al.*, 2014 |
| WUS transcriptional network and target genes | WUS-responsive genes; microarrays. Genome-wide identification of chromatin regions bound by WUS; ChIP-chip. | Apices of several genetic backgrounds and lines (microarrays). Apices of 35S:WUS-GR seedlings (ChIP-chip). | 675 WUS-responsive genes and 164 high-confidence chromatin regions bound by WUS *in vivo* (corresponding to 159 genes), were identified. Overlap of the two datasets identified 8 direct and responsive WUS targets. | Busch *et al.*, 2010 |
| WUS transcriptional network and target genes | WUS-responsive genes; microarrays. Computational modeling. | SAMs of 35S:WUS-GR *ap1 cal* plants. | Identification of 641 genes differentially expressed in response to WUS activation; 189 of those identified as direct targets. Results were superimposed onto the cell type-specific SAM gene expression map (Yadav *et al.*, 2009, 2014). | Yadav *et al.*, 2013 |
| HEC1 transcriptional network and target genes | HEC1-responsive genes; microarrays. | Inflorescence apices of *hec1,2,3* triple mutants and of a *HEC1*-inducible line. | 463 HEC1-responsive genes were identified. 80 of these genes responded to both HEC1 and WUS (Busch *et al.*, 2010), in the majority of cases in an antagonistic fashion. | Schuster *et al.*, 2014 |
| Gene expression atlas of the meristem-to-leaf boundary region | Cell type-specific gene expression profiling; TRAP-seq. Genome-wide yeast one-hybrid screens. | Seedling immunopurified polysomes from boundary-region and leaf primordia cels. | 466 up-regulated genes and 868 down-regulated genes in the boundary domain compared to leaf primordia. 103 TFs identified as interacting with the promoter regions of TFs that regulate boundary and axillary meristem formation. | Tian *et al.*, 2014 |
| KAN1 transcriptional network and target genes; REV target genes | KAN1-responsive genes; microarrays. | 35S:KAN1-GR seedlings. | Identification of 265 genes differentially expressed in response to KAN1 activation. | Reinhart *et al.*, 2013 |
| KAN1 transcriptional network and target genes | Genome-wide identification of chromatin regions bound by KAN1; ChIP-seq. KAN1-responsive genes; microarrays. | 35S:FLAG-GR-KAN1 seedlings (ChIP-seq). 35S:KAN-GR seedlings (microarrays). | Identification of 4183 chromatin regions bound by KAN1; 1802 of them contained a conserved motif, corresponding to 3151 potential KAN1 target genes. Identification of 500 KAN1-responsive genes. Overlap of the two datasets identified 211 direct and down-regulated KAN1 targets. | Merelo *et al.*, 2013 |
| KAN1 transcriptional network and target genes | KAN1-responsive genes; microarrays. | 35S:KAN1-GR seedlings. | Identification of 222 genes differentially expressed in response to KAN1 activation; 104 of those identified as direct targets (82 down-regulated and 22 up-regulated). | Huang *et al.*, 2014 |
| KAN1 transcriptional network and target genes | KAN1-responsive genes; RNA-seq | 35S:FLAG-GR-KAN1 seedlings. | Identification of 969 genes down-regulated in response to KAN1 activation; 661 of them are also identified in the ChIP-seq dataset (Merelo *et al.*, 2013). Combination with additional KAN1 gene expression profiling data (Merelo *et al.*, 2013; Reinhart *et al.*, 2013) identifies a set of 72 high-confidence direct targets that are both bound and down-regulated by KAN1. | Xie *et al.*, 2015 |

specific cell types with a fluorescent reporter to allow their isolation by FACS (a methodology pioneered for studies on root development and the RAM, see Birnbaum *et al.*, 2003, 2005; Nawy *et al.*, 2005; Brady *et al.*, 2007) and using the *apetala1 cauliflower* double mutant background (in which there is a massive over-proliferation of inflorescence-like meristems), it was possible to define a gene expression map of the Arabidopsis SAM (Yadav *et al.*, 2009, 2014). This allowed the definition of gene expression profiles for specific cell populations and functional domains of the SAM, and the identification of novel genes with unique expression patterns within the meristem. An interesting finding from these experiments was that among the genes that are differentially expressed (up-regulated) in cells from the *CLV3*-expression domain (that is, in stem cells in the L1 and L2 of the CZ), there is an enrichment of genes involved in DNA metabolism, DNA replication and repair, histone and DNA modifications, and chromosome organization and biogenesis: from *ARABIDOPSIS THALIANA BREAST CANCER SUSCEPTIBILITY1* (*ATBRCA1*), to *TELOMERASE REVERSE TRANCRIPTASE* (ATTERT), to *SIRTUINS* (SIR1, SIR2) (Yadav *et al.*, 2009). A subsequent higher-resolution gene expression map of the SAM indicated that these genes involved in DNA repair pathways and telomere maintenance are specifically expressed in cells of the L2 layer (Yadav *et al.*, 2014). This may reflect a selective pressure for avoiding mutations in the L2 stem cells, from which the germ cells are derived (Yadav *et al.*, 2009, 2014). Another link between the physiology of the meristem and the gene expression map could be established for L1-specific gene expression (i.e. expression in the SAM epidermis), since GO categories or genes that were enriched in the corresponding datasets included those involved in wax biosynthesis and in pathogen defense (Yadav *et al.*, 2014). Finally, gene expression in the L3 layer (corpus) was enriched for GO terms and genes related to photosynthesis, ionic homeostasis, and the response to multiple hormones (Yadav *et al.*, 2014), providing molecular support for the presence of a functional chloroplast machinery in the SAM.

These and other studies have shown that cell-type specific transcriptome analyses display higher sensitivity, in this case when compared to gene expression profiling experiments conducted with whole organs or more complex samples. In particular, there were over 1000 genes for which expression was detected in the cell-type specific SAM datasets, but not in the entire AtGenExpress developmental series of wild-type plants (Schmid *et al.*, 2005): rare transcripts and genes that might be expressed in only a few cells or cell-types of the meristem, as further shown by *in situ* hybridization experiments for selected genes (Yadav *et al.*, 2009). Cell-type specific or spatially-defined unique expression patterns might be indicative of a relevant role in the SAM and therefore the corresponding genes are good candidates for reverse genetics experiments. The abundance of cell-type specific expression within the context of a tissue or structure of varied cell types, as is the SAM, is also indicative of complexity in transcriptional regulation, and >1700 genes were identified as specific to SAM cell types (Yadav *et al.*, 2009). In line with this presumed complexity, expression was detected for >1200 TF-coding genes and ~23% of those showed differential expression among the different SAM cell populations (Yadav *et al.*, 2014).

The gene expression map of the Arabidopsis SAM has also facilitated the characterization and analysis of the transcriptional programs that are directly controlled by WUS, by providing a reference dataset to frame results obtained through other genome-wide approaches and experiments (Busch *et al.*, 2010; Yadav *et al.*, 2013). WUS is the key TF for stem cell specification and maintenance in the SAM and it has been shown to be capable of acting both as an activator and a repressor of transcription (Ikeda *et al.*, 2009). However, until recently very few WUS target genes were known: *AGAMOUS (AG)* (Lenhard *et al.*, 2001; Lohmann *et al.*, 2001), four two-component *Arabidopsis Response Regulator* (*ARR*) genes (Leibfried *et al.*, 2005) and *CLV3* (Yadav *et al.*, 2011). The identification of *ARR*s as targets of WUS provided a mechanistic link between plant hormones (cytokinin) and the CLV/WUS stem cell network, whereby the direct repression by WUS of *ARR5*, *ARR6*, *ARR7* and *ARR15* transcription appears necessary for proper meristem function (*ARR* genes would negatively influence meristem size) (Leibfried *et al.*, 2005). With respect to *CLV3*, it was shown that the WUS protein, synthesized in cells of the OC, migrates into the CZ where it directly activates *CLV3* transcription by binding to its promoter, and computational modeling showed that maintenance of the WUS gradient is essential for regulating stem cell number (Fig. 1) (Yadav *et al.*, 2011). Additional experiments demonstrated that WUS moves to the stem cells in the L2 and L1 via plasmodesmata in a highly regulated fashion, and that this movement is required for WUS function and, thus, stem cell activity (Daum *et al.*, 2014). The direct regulation of *CLV3* by WUS and the importance of WUS gradients – that extend radially into the PZ where stem-cell progeny cells differentiate (Yadav *et al.*, 2011) – are now central tenets of the stem cell regulatory network in Arabidopsis. However, whereas the identification of these direct interactions contributed to understanding the molecular circuitry of the network, they did not fully explain the mechanisms by which WUS controls stem cell homeostasis.

A *35S:WUS-GR ap1 cal* system was used to identify WUS-responsive genes [in this system, WUS is activated through the application of dexamethasone (dex) and direct WUS targets can be identified through the combined application of dex and cycloheximide] (Yadav *et al.*, 2013). The experiments identified over 600 WUS-responsive genes and showed a predominance of repression versus activation. Among the WUS-responsive genes, 49 up-regulated and 140 down-regulated genes were classified as direct WUS targets. The gene expression profiling data could then be correlated with the cell-type gene expression map of the SAM (which was also obtained in an *ap1 cal* background) and it was found that a majority of the WUS-activated genes are expressed in the central parts of the SAM, whereas the majority of WUS-repressed genes are normally expressed in the PZ. In particular, it was observed that WUS represses a large number of differentiation-promoting TF-coding genes, including TFs

involved in promoting lateral organ polarity and differentiation, such as KANADI1 (KAN1), KANADI2 (KAN2), ASYMMETRIC LEAVES 2 (AS2) and YABBY3 (YAB3), TFs involved in cell fate specification and inflorescence stem growth [KNAT1/BREVIPEDICELLUS (BP), BELL1-LIKE HOMEODOMAIN 5 (BLH5)], and others (Yadav *et al.*, 2013), which also correlates with previous lines of evidence suggesting that WUS represses differentiation (Busch *et al.*, 2010; Yadav *et al.*, 2010, 2013).

These results, combined with computational modeling and transient gene manipulations and live imaging, indicated that WUS controls stem cell maintenance in part by directly repressing a group of differentiation-promoting TFs and excluding them from the CZ, thus preventing premature differentiation of stem cells (Yadav *et al.*, 2013). The dual function of WUS in regulating its own level by activating its negative regulator CLV3 and repressing differentiation would lead to a robust homeostatic mechanism that balances stem cell numbers and differentiation rates in a dynamic cellular environment (Yadav *et al.*, 2013). This dual function could involve having different WUS thresholds for CZ and PZ regulation (Yadav *et al.*, 2013), and makes the WUS gradient a central component of the SAM mechanism of function.

The genome-wide regulatory activities of WUS were also studied by transcriptional profiling of shoot apices of *wus* and *clv3* mutant plants, and of WUS- and CLV3-inducible overexpressing lines, together with WUS ChIP-chip experiments (genome-wide DNA binding) (Busch *et al.*, 2010). *CLV1* was identified as a direct target that is repressed by WUS, suggesting that WUS might indirectly sustain its own expression by directly repressing one of its repressors through a regulatory loop that would involve the fine-tuning of expression levels rather than an on/off switch for *CLV1*, given that the expression domains of *WUS* and *CLV1* overlap (Busch *et al.*, 2010). Other direct targets of WUS were three members of the *TOPLESS/TOPLESS-RELATED* (*TPL/TPR*) family of transcriptional corepressors, *TPL*, *TPR1* and *TPR2* (Busch *et al.*, 2010), which are involved in embryonic patterning and auxin signaling (Long *et al.*, 2006; Szemenyei *et al.*, 2008). The regulatory interaction of WUS with this group of genes appears complex, as *WUS* induction resulted in an increase in *TPL* expression and in a reduction for *TPR2*. In addition, *TPR1* and *TPR2* are expressed in the periphery of the SAM but excluded from the *WUS* expression domain, and at the same time strongly expressed in young flowers in domains overlapping with that of *WUS* (Busch *et al.*, 2010). Nevertheless, these results as well as the GO-term analysis of the set of WUS targets suggested that WUS has the potential to influence auxin signaling and that the regulation of the cytokinin/auxin balance may be central to SAM function (Busch *et al.*, 2010). Furthermore, WUS had previously been found to interact with TPL/TPR proteins, and the observation that the WUS C-terminal sequences involved in the interaction were required to complement the *wus-1* mutant, or that ectopic expression of a *WUS* allele lacking them produces a dominant negative phenotype, indicated the importance of this interaction for WUS function (Kieffer *et al.*, 2006; Causier *et al.*, 2012).

*HECATE1* (*HEC1*), which codes for a bHLH TF and was initially described as involved in the development of female reproductive tissues together with the closely related *HEC2* and *HEC3* genes (Gremski *et al.*, 2007), was another gene identified as a WUS repressed direct target (Busch *et al.*, 2010; Schuster *et al.*, 2014). Triple *hec1 hec2 hec3* mutants displayed SAMs that were significantly reduced in size, whereas expressing *HEC1* from the stem cell-specific *CLV3* promoter led to massive SAM expansion, and no phenotypic alteration was caused by expressing *HEC1* in the PZ from the *UFO* promoter. Altogether, these results indicated that HEC1 specifically stimulates proliferation of stem cells (Schuster *et al.*, 2014). HEC1 was found to repress *CLV3* and *WUS* and, conversely, repression of HEC1 in the OC is an essential function of WUS in SAM maintenance, highlighting the opposing functions of these two stem cell regulators (Schuster *et al.*, 2014).

To help dissecting *HEC1* roles in the SAM, gene expression profiling experiments were conducted using apices of *hec1 hec2 hec3* triple mutants and using a *HEC1*-inducible line. Strikingly, these analyses revealed that HEC1 and WUS show very similar functional signatures, evidenced by the enrichment of the same GO-term categories (response to stimulus, metabolic processes, regulation of metabolic processes and transport), suggesting that the coordinated regulation of metabolic processes and hormone signaling are essential functions of these stem cell regulators (Schuster *et al.*, 2014). A vast majority of the genes that were identified as responding to both TFs showed opposite responses (activated by WUS – repressed by HEC1, and vice versa), in line with the antagonistic behavior of WUS and HEC1 in the SAM (Schuster *et al.*, 2014). HEC1 was also found to enhance expression of several cell cycle genes (in agreement with its role in stimulating cell proliferation), as well as of the cytokinin response genes *ARR5*, *ARR7* and *ARR15* (which are repressed by WUS).

Altogether, these results showed functions of HEC1 that are strictly cell-type specific and that the stem cell regulators WUS and HEC1 share, at a global gene-regulatory level, the integration of hormone-related pathways implicated in the correct functioning of the SAM. Moreover, the existence of multiple feedback loops in a SAM regulatory circuitry that is much more complex than previously anticipated through genetic analyses was also highlighted (Schuster *et al.*, 2014).

The central role that *WUS* plays in stem cell and SAM functioning is mirrored in other types of meristems. In particular, the *WUS-RELATED HOMEOBOX 5* (*WOX5*) gene is expressed in the root meristem quiescent center and it is capable of functioning interchangeably with *WUS* in the control of shoot and root stem cell niches (Sarkar *et al.*, 2007; Zhou *et al.*, 2015). Like WUS, WOX5 also represses differentiation of stem cells that are neighboring its domain of expression. WUS, WOX5, and also WOX4, which defines the vascular stem cell niche, all have as conserved interacting cofactors HAIRY MERISTEM (HAM) transcriptional regulators (Zhou *et al.*, 2015). Thus, it appears that WUS/WOX proteins, the interaction with HAM proteins and repression of differentiation programs, are all key features of a conserved

mechanism for the specification and maintenance of stem cells within all plant meristems (Zhou *et al.*, 2015).

## Establishment of organ boundaries between the SAM and axillary meristems in Arabidopsis.

As stem cells from the SAM divide, daughter cells are displaced laterally and might eventually give rise to axillary meristems and lateral organs. This process requires the formation of a meristem-to-organ boundary region, which involves cells located between the SAM and the arising organs stopping growing (Aida and Tasaka, 2006; Rast and Simon, 2008). The genetic programs and regulatory networks that control the processes of organ boundary and axillary meristem formation are not well defined, although some key Arabidopsis TF-coding genes that participate in the process have been identified through genetic analyses, such as *CUC1-3* (see above), *REGULATOR OF AXILLARY MERISTEMS* genes (*RAX1-3*), *LATERAL SUPPRESSOR* (*LAS*) and *REGULATOR OF AXILLARY MERISTEM FORMATION* (*ROX*) (Greb *et al.*, 2003; Keller *et al.*, 2006; Raman *et al.*, 2008; Yang *et al.*, 2012). The fact that organ boundary cells are very low in abundance has also hindered the application of genomic approaches to their study.

Cell-type specific gene expression profiling in the meristem-to-leaf boundary region was recently conducted using the TRAP-Seq method (for information on the method, see: Mustroph *et al.*, 2009; Jiao and Meyerowitz, 2010). A TRAP-Seq line that made use of the *LAS* promoter characterized the translatome of the boundary region, whereas a line using the *ASYMMETRIC LEAVES1* (*AS1*) promoter captured the translatome in emerging leaf primordia but excluding the SAM (Tian *et al.*, 2014). This allowed the identification of >1300 genes that were differentially expressed between the boundary domain and the developing leaf. This genome-wide approach was combined with a yeast one-hybrid screen that interrogated ~1200 Arabidopsis TFs with a set of regulatory regions from genes that are boundary regulators, such as *CUC2* and *LAS*. Integration of these two datasets allowed derivation of a gene regulatory network that links most previously isolated key regulators, by defining new interactions among those factors and also identifying new genes affecting boundary and axillary meristem formation (e.g. *DORNROSCHEN –DRN*- and *SQUAMOSA PROMOTER BINDING PROTEIN-LIKE9*/15 -SPL9/15-). New regulatory relationships between CUC2 and *LAS*, or between RAX1/3 and *CUC2*, were found. This study also revealed a direct interaction between CUC2 and *MiR164c*, a miRNA with boundary-specific expression and that targets *CUC1* and *CUC2* (Baker *et al.*, 2005; Raman *et al.*, 2008; Sieber *et al.*, 2007), suggesting the occurrence of reciprocal regulation between these two key regulators of boundary formation (Tian *et al.*, 2014). ARR1 was also found to directly activate *LAS*, providing a molecular link between axillary meristem initiation and cytokinin signaling. In addition, the organ-boundary cell translatome showed enrichment for several hormone-responsive genes, hinting to participation of additional hormones (brassinosteroids, ethylene, abscisic acid) in boundary-region physiology, beyond the recently described roles of auxin and cytokinin (see Wang *et al.*, 2014*a*, *b*).

## KANADI1 target genes and leaf primordia development

The *KANADI* genes (*KAN1* to *KAN4*), members of the GARP family of TFs, control polarity associated patterning processes and play key roles as regulators of abaxial (the lower side of the leaf) identity and meristem formation in Arabidopsis. *KAN1-4* act antagonistically with the class III homeodomain leucine zipper (HD-ZIPIII) genes *PHABULOSA* (*PHB*), *PHAVOLUTA* (*PHV*) and *REVOLUTA* (*REV*), which promote adaxial (upper side of the leaf) identity in organ primordia (Bowman and Floyd, 2008). During the formation of the Arabidopsis leaf blade (also known as lamina, the flat part of the leaf), KAN1-4 and PHB/PHV/REV maintain a stable abaxial/adaxial boundary and promote growth in a coordinated manner (Fig. 1) (Bowman and Floyd, 2008). Other regulatory genes that are involved in the process of specifying adaxial/abaxial sides include the MYB TF *ASYMMETRIC LEAVES1* (*AS1*), *ASYMMETRIC LEAVES2* (*AS2*), coding for a LOB-domain protein, both promoting adaxial identity, and members of the *YABBY* (*YAB*) gene family and the *AUXIN RESPONSE FACTOR* genes *ARF3* and *ARF4*, for abaxial fate (Merelo *et al.*, 2013). In addition to their role in determining the adaxial/abaxial polarity of leaf primordia, other studies have shown that KAN genes are also capable of repressing the formation of new meristems, whereas HD-ZIPIII genes promote their formation (Talbert *et al.*, 1995; McConnell and Barton, 1998; Kerstetter *et al.*, 2001; Huang *et al.*, 2014).

Until recently, *AS2* was the only known direct target gene of KAN1 (KAN1 represses *AS2* transcription on the abaxial side) (Wu *et al.*, 2008). However, four different genome-wide studies have sought to identify KAN1 targets (Merelo *et al.*, 2013; Reinhart *et al.*, 2013; Huang *et al.*, 2014; Xie *et al.*, 2015). In contrast to the studies described above, the identification of KAN1 target genes was not conducted using shoot apices or cell-type populations, but rather whole seedlings. However, the conclusions may be relevant for KAN1 roles in the patterning of leaf primordia. First, KAN1 directly targets several genes of the adaxial/abaxial polarity network, such as *PHB*, and seems to act primarily as a repressor. Second, KAN1 targets several genes involved in auxin signaling, expanding previous reports that indicated that KAN activity was related to regulation of *PIN-FORMED1* (*PIN1*) expression, possibly influencing auxin movement and acting antagonistically to HD-ZIPIII TFs (Izhaki and Bowman, 2007; Ilegems *et al.*, 2010). In fact, KAN1 was found to regulate genes involved in auxin transport (members of the *PIN* family, *PINOID*, *PLA2A*, *WAG2, AUX1* and others), auxin signaling (*DFL1*, *DFL2*, *WES1*, *ARF3/4* among them) and auxin biosynthesis (*TAA1* and *YUC5*). In addition, it was found that a subset of target genes is oppositely regulated by

KAN1 and by REV – including some of the auxin signaling genes – indicating that one of the possible mechanisms for the antagonistic activities of these two factors in polarity patterning might be the opposite regulation of shared targets, and that through their antagonistic activities they may contribute to the production of auxin gradients that function as positional signals.

## Final remarks

Over 25 years of intense genetic and molecular studies on the Arabidopsis SAM have resulted in the identification of many key regulatory factors that control the establishment, patterning and functioning of the meristem, as well as stem cell homeostasis. These genes soon started to be integrated in gene circuits, feedback mechanisms and small networks to explain SAM properties. Therefore, a suitable genetic mechanistic background was available to start overlying genome-wide approaches to study SAM function, much like it happened, for instance, in the cases of floral development, the floral transition, or root development. The minute nature of the object of study, however, imposed additional technical difficulties for applying genomic methods. However, the combination of cell-type specific genomics approaches, live imaging and mathematical modeling has substantially deepened our understanding of the SAM, while at the same time made clear that there is still much to learn about what arguably is, in E. Meyerowitz's words, 'the most important object on Earth' (Coghlan, 2000). At a mechanistic level, the vast majority of our knowledge on the SAM is derived from Arabidopsis, which particularly in this field has lived up to its role as a 'model system'.

## Acknowledgements

This work was supported by grants from the Spanish Ministerio de Economía y Competitividad (BFU2014-58289-P) and from the Agencia de Gestió d'Ajuts Universitaris I de Recerca (2014 SGR 1406) to JLR.

## References

**Aichinger E, Kornet N, Friedrich T, Laux T.** 2012. Plant stem cell niches. Annual Review of Plant Biology **63,** 615–636.

**Aida M, Ishida T, Fukaki H, Fujisawa H, Tasaka M.** 1997. Genes involved in organ separation in Arabidopsis: an analysis of the cup-shaped cotyledon mutant. Plant Cell **9,** 841–857.

**Aida M, Tasaka M.** 2006. Genetic control of shoot organ boundaries. Current Opinion in Plant Biology **9,** 72–77.

**Baker CC, Sieber P, Wellmer F, Meyerowitz EM.** 2005. The early extra petals1 mutant uncovers a role for microRNA miR164c in regulating petal number in Arabidopsis. Current Biology **15,** 303–315.

**Bartlett ME, Thompson B.** 2014. Meristem identity and phyllotaxis in inflorescence development. Frontiers in Plant Science **5,** 508.

**Barton MK.** 2010. Twenty years on: the inner workings of the shoot apical meristem, a developmental dynamo. Developmental Biology **341,** 95–113.

**Birnbaum K, Jung JW, Wang JY, Lambert GM, Hirst JA, Galbraith DW, Benfey PN.** 2005. Cell type-specific expression profiling in plants via cell sorting of protoplasts from fluorescent reporter lines. Nature Methods **2,** 615–619.

**Birnbaum K, Shasha DE, Wang JY, Jung JW, Lambert GM, Galbraith DW, Benfey PN.** 2003. A gene expression map of the Arabidopsis root. Science **302,** 1956–1960.

**Bowman JL, Floyd SK.** 2008. Patterning and polarity in seed plant shoots. Annual Review of Plant Biology **59,** 67–88.

**Brady SM, Orlando DA, Lee JY, Wang JY, Koch J, Dinneny JR, Mace D, Ohler U, Benfey PN.** 2007. A high-resolution root spatiotemporal map reveals dominant expression patterns. Science **318,** 801–806.

**Brand U, Fletcher JC, Hobe M, Meyerowitz EM, Simon R.** 2000. Dependence of stem cell fate in Arabidopsis on a feedback loop regulated by CLV3 activity. Science **289,** 617–619.

**Busch W, Miotk A, Ariel FD, *et al*.** 2010. Transcriptional control of a plant stem cell niche. Developmental Cell **18,** 849–861.

**Causier B, Ashworth M, Guo W, Davies B.** 2012. The TOPLESS Interactome: A Framework for Gene Repression in Arabidopsis. Plant Physiology **158,** 423–438.

**Clark SE, Williams RW, Meyerowitz EM.** 1997. The CLAVATA1 gene encodes a putative receptor kinase that controls shoot and floral meristem size in Arabidopsis. Cell **89,** 575–585.

**Coghlan A.** 2000. Plants point the way. Trends in Genetics **16** Supp. 1, 30–31.

**Daum G, Medzihradszky A, Suzaki T, Lohmann JU.** 2014. A mechanistic framework for noncell autonomous stem cell induction in Arabidopsis. Proceedings of the National Acadedmy of Sciences, USA **111,** 14619–14624.

**Dello Ioio R, Nakamura K, Moubayidin L, Perilli S, Taniguchi M, Morita MT, Aoyama T, Costantino P, Sabatini S.** 2008. A genetic framework for the control of cell division and differentiation in the root meristem. Science **322,** 1380–1384.

**Dinneny JR, Benfey PN.** 2008. Plant stem cell niches: standing the test of time. Cell **132,** 553–557.

**Endrizzi K, Moussian B, Haecker A, Levin JZ, Laux T.** 1996. The SHOOT MERISTEMLESS gene is required for maintenance of undifferentiated cells in Arabidopsis shoot and floral meristems and acts at a different regulatory level than the meristem genes WUSCHEL and ZWILLE. Plant Journal **10,** 967–979.

**Fletcher JC, Brand U, Running MP, Simon R, Meyerowitz EM.** 1999. Signaling of cell fate decisions by CLAVATA3 in Arabidopsis shoot meristems. Science **283,** 1911–1914.

**Gaillochet C, Daum G, Lohmann JU.** 2015. O cell, where art thou? The mechanisms of shoot meristem patterning. Current Opinion in Plant Biology **23,** 91–97.

**Greb T, Clarenz O, Schafer E, Muller D, Herrero R, Schmitz G, Theres K.** 2003. Molecular analysis of the LATERAL SUPPRESSOR gene in Arabidopsis reveals a conserved control mechanism for axillary meristem formation. Genes & Development **17,** 1175–1187.

**Gremski K, Ditta G, Yanofsky MF.** 2007. The HECATE genes regulate female reproductive tract development in *Arabidopsis thaliana*. Development **134,** 3593–3601.

**Ha CM, Jun JH, Fletcher JC.** 2010. Shoot apical meristem form and function. Current Topics in Developmental Biology **91,** 103–140.

**Heisler MG, Ohno C, Das P, Sieber P, Reddy GV, Long JA, Meyerowitz EM.** 2005. Patterns of auxin transport and gene expression during primordium development revealed by live imaging of the arabidopsis inflorescence meristem. Current Biology **15,** 1899–1911.

**Holt AL, van Haperen JM, Groot EP, Laux T.** 2014. Signaling in shoot and flower meristems of Arabidopsis thaliana. Current Opinion in Plant Biology **17,** 96–102.

**Huang T, Harrar Y, Lin C, Reinhart B, Newell NR, Talavera-Rauh F, Hokin SA, Barton MK, Kerstetter RA.** 2014. Arabidopsis KANADI1 acts as a transcriptional repressor by interacting with a specific cis-element and regulates auxin biosynthesis, transport, and signaling in opposition to HD-ZIPIII factors. Plant Cell **26,** 246–262.

**Ikeda M, Mitsuda N, Ohme-Takagi M.** 2009. Arabidopsis WUSCHEL is a bifunctional transcription factor that acts as a repressor in stem cell regulation and as an activator in floral patterning. Plant Cell **21,** 3493–3505.

**Ilegems M, Douet V, Meylan-Bettex M, Uyttewaal M, Brand L, Bowman JL, Stieger PA.** 2010. Interplay of auxin, KANADI and Class III HD-ZIP transcription factors in vascular tissue formation. Development **137,** 975–984.

**Izhaki A, Bowman JL.** 2007. KANADI and class III HD-Zip gene families regulate embryo patterning and modulate auxin flow during embryogenesis in Arabidopsis. Plant Cell **19,** 495–508.

**Jeong S, Trotochaud AE, Clark SE.** 1999. The Arabidopsis CLAVATA2 gene encodes a receptor-like protein required for the stability of the CLAVATA1 receptor-like kinase. Plant Cell **11,** 1925–1934.

**Jiao Y, Meyerowitz EM.** 2010. Cell-type specific analysis of translating RNAs in developing flowers reveals new levels of control. Molecular Systems Biology **6,** 419.

**Keller T, Abbott J, Moritz T, Doerner P.** 2006. Arabidopsis REGULATOR OF AXILLARY MERISTEMS1 controls a leaf axil stem cell niche and modulates vegetative development. Plant Cell **18,** 598–611.

**Kerstetter RA, Bollman K, Taylor RA, Bomblies K, Poethig RS.** 2001. KANADI regulates organ polarity in Arabidopsis. Nature **411,** 706–709.

**Kieffer M, Stern Y, Cook H, Clerici E, Maulbetsch C, Laux T, Davies B.** 2006. Analysis of the transcription factor WUSCHEL and its functional homologue in *Antirrhinum* reveals a potential mechanism for their roles in meristem maintenance. Plant Cell **18,** 560–573.

**Leibfried A, To JP, Busch W, Stehling S, Kehle A, Demar M, Kieber JJ, Lohmann JU.** 2005. WUSCHEL controls meristem function by direct regulation of cytokinin-inducible response regulators. Nature **438,** 1172–1175.

**Lenhard M, Bohnert A, Jurgens G, Laux T.** 2001. Termination of stem cell maintenance in Arabidopsis floral meristems by interactions between WUSCHEL and AGAMOUS. Cell **105,** 805–814.

**Lohmann JU, Hong RL, Hobe M, Busch MA, Parcy F, Simon R, Weigel D.** 2001. A molecular link between stem cell regulation and floral patterning in Arabidopsis. Cell **105,** 793–803.

**Long JA, Moan EI, Medford JI, Barton MK.** 1996. A member of the KNOTTED class of homeodomain proteins encoded by the STM gene of Arabidopsis. Nature **379,** 66–69.

**Long JA, Ohno C, Smith ZR, Meyerowitz EM.** 2006. TOPLESS regulates apical embryonic fate in Arabidopsis. Science **312,** 1520–1523.

**Mayer KF, Schoof H, Haecker A, Lenhard M, Jurgens G, Laux T.** 1998. Role of WUSCHEL in regulating stem cell fate in the Arabidopsis shoot meristem. Cell **95,** 805–815.

**McConnell JR, Barton MK.** 1998. Leaf polarity and meristem formation in Arabidopsis. Development **125,** 2935–2942.

**Merelo P, Xie Y, Brand L, Ott F, Weigel D, Bowman JL, Heisler MG, Wenkel S.** 2013. Genome-wide identification of KANADI1 target genes. PLoS ONE **8,** e77341.

**Mustroph A, Zanetti ME, Jang CJ, Holtan HE, Repetti PP, Galbraith DW, Girke T, Bailey-Serres J.** 2009. Profiling translatomes of discrete cell populations resolves altered cellular priorities during hypoxia in Arabidopsis. Proceedings of the National Academy of Sciences, USA **106,** 18843–18848.

**Nawy T, Lee JY, Colinas J, Wang JY, Thongrod SC, Malamy JE, Birnbaum K, Benfey PN.** 2005. Transcriptional profile of the Arabidopsis root quiescent center. Plant Cell **17,** 1908–1925.

**Perales M, Reddy GV.** 2012. Stem cell maintenance in shoot apical meristems. Current Opinion in Plant Biology **15,** 10–16.

**Poethig RS.** 1987. Clonal analysis of cell lineage patterns in plant development. American Journal of Botany **74,** 581–594.

**Raman S, Greb T, Peaucelle A, Blein T, Laufs P, Theres K.** 2008. Interplay of miR164, CUP-SHAPED COTYLEDON genes and LATERAL SUPPRESSOR controls axillary meristem formation in *Arabidopsis thaliana*. Plant Journal **55,** 65–76.

**Rast MI, Simon R.** 2008. The meristem-to-organ boundary: more than an extremity of anything. Current Opinion in Genetics and Development **18,** 287–294.

**Reddy GV, Heisler MG, Ehrhardt DW, Meyerowitz EM.** 2004. Real-time lineage analysis reveals oriented cell divisions associated with morphogenesis at the shoot apex of *Arabidopsis thaliana*. Development **131,** 4225–4237.

**Reddy GV, Meyerowitz EM.** 2005. Stem-cell homeostasis and growth dynamics can be uncoupled in the Arabidopsis shoot apex. Science **310,** 663–667.

**Reinhart BJ, Liu T, Newell NR, Magnani E, Huang T, Kerstetter R, Michaels S, Barton MK.** 2013. Establishing a framework for the Ad/abaxial regulatory network of Arabidopsis: ascertaining targets of class III homeodomain leucine zipper and KANADI regulation. Plant Cell **25,** 3228–3249.

**Rinne PL, van der Schoot C.** 1998. Symplasmic fields in the tunica of the shoot apical meristem coordinate morphogenetic events. Development **125,** 1477–1485.

**Rojo E, Sharma VK, Kovaleva V, Raikhel NV, Fletcher JC.** 2002. CLV3 is localized to the extracellular space, where it activates the Arabidopsis CLAVATA stem cell signaling pathway. Plant Cell **14,** 969–977.

**Sablowski R.** 2007. The dynamic plant stem cell niches. Current Opinion in Plant Biology **10,** 639–644.

**Sablowski R.** 2011. Plant stem cell niches: from signalling to execution. Current Opinion in Plant Biology **14,** 4–9.

**Sager R, Lee JY.** 2014. Plasmodesmata in integrated cell signalling: insights from development and environmental signals and stresses. Journal of Experimental Botany **65,** 6337–6358.

**Sarkar AK, Luijten M, Miyashima S, Lenhard M, Hashimoto T, Nakajima K, Scheres B, Heidstra R, Laux T.** 2007. Conserved factors regulate signalling in Arabidopsis thaliana shoot and root stem cell organizers. Nature **446,** 811–814.

**Schmid M, Davison TS, Henz SR, Pape UJ, Demar M, Vingron M, Scholkopf B, Weigel D, Lohmann JU.** 2005. A gene expression map of *Arabidopsis thaliana* development. Nature Genetics **37,** 501–506.

**Schoof H, Lenhard M, Haecker A, Mayer KF, Jurgens G, Laux T.** 2000. The stem cell population of Arabidopsis shoot meristems is maintained by a regulatory loop between the CLAVATA and WUSCHEL genes. Cell **100,** 635–644.

**Schuster C, Gaillochet C, Medzihradszky A, Busch W, Daum G, Krebs M, Kehle A, Lohmann JU.** 2014. A regulatory framework for shoot stem cell control integrating metabolic, transcriptional, and phytohormone signals. Developmental Cell **28,** 438–449.

**Scofield S, Dewitte W, Nieuwland J, Murray JA.** 2013. The Arabidopsis homeobox gene SHOOT MERISTEMLESS has cellular and meristem-organisational roles with differential requirements for cytokinin and CYCD3 activity. Plant J **75,** 53–66.

**Shapiro BE, Tobin C, Mjolsness E, Meyerowitz EM.** 2015. Analysis of cell division patterns in the Arabidopsis shoot apical meristem. Proceedings of the National Academy of Sciences, USA **112,** 4815–4820.

**Sieber P, Wellmer F, Gheyselinck J, Riechmann JL, Meyerowitz EM.** 2007. Redundancy and specialization among plant microRNAs: role of the MIR164 family in developmental robustness. Development **134,** 1051–1060.

**Smith LG, Greene B, Veit B, Hake S.** 1992. A dominant mutation in the maize homeobox gene, Knotted-1, causes its ectopic expression in leaf cells with altered fates. Development **116,** 21–30.

**Szemenyei H, Hannon M, Long JA.** 2008. TOPLESS mediates auxin-dependent transcriptional repression during Arabidopsis embryogenesis. Science **319,** 1384–1386.

**Takada S, Hibara K, Ishida T, Tasaka M.** 2001. The CUP-SHAPED COTYLEDON1 gene of Arabidopsis regulates shoot apical meristem formation. Development **128,** 1127–1135.

**Talbert PB, Adler HT, Parks DW, Comai L.** 1995. The REVOLUTA gene is necessary for apical meristem development and for limiting cell divisions in the leaves and stems of *Arabidopsis thaliana*. Development **121,** 2723–2735.

**Tian C, Zhang X, He J, *et al*.** 2014. An organ boundary-enriched gene regulatory network uncovers regulatory hierarchies underlying axillary meristem initiation. Molecular Systems Biology **10,** 755.

**Traas J.** 2013. Phyllotaxis. Development **140,** 249–253.

**Vernoux T, Besnard F, Traas J.** 2010. Auxin at the shoot apical meristem. Cold Spring Harbor Perspectives in Biology **2,** a001487.

**Vernoux T, Brunoud G, Farcot E, *et al*.** 2011. The auxin signalling network translates dynamic input into robust patterning at the shoot apex. Molecular Systems Biology **7,** 508.

**Vroemen CW, Mordhorst AP, Albrecht C, Kwaaitaal MA, De Vries SC.** 2003. The *CUP-SHAPED COTYLEDON3* gene is required for boundary and shoot meristem formation in Arabidopsis. Plant Cell **15,** 1563–1577.

**Waites R, Simon R.** 2000. Signaling cell fate in plant meristems. Three clubs on one tousle. Cell **103,** 835–838.

**Wang Q, Kohlen W, Rossmann S, Vernoux T, Theres K.** 2014*a*. Auxin depletion from the leaf axil conditions competence for axillary meristem formation in arabidopsis and tomato. Plant Cell **26,** 2068–2079.

**Wang Y, Wang J, Shi B, Yu T, Qi J, Meyerowitz EM, Jiao Y.** 2014*b*. The stem cell niche in leaf axils is established by auxin and cytokinin in Arabidopsis. Plant Cell **26,** 2055–2067.

**Wu G, Lin WC, Huang T, Poethig RS, Springer PS, Kerstetter RA.** 2008. KANADI1 regulates adaxial-abaxial polarity in Arabidopsis by directly repressing the transcription of ASYMMETRIC LEAVES2. Proceedings of the National Academy of Sciences, USA **105,** 16392–16397.

**Xie Y, Straub D, Eguen T, Brandt R, Stahl M, Martinez-Garcia JF, Wenkel S.** 2015. Meta-analysis of Arabidopsis KANADI1 direct target genes identifies a basic growth-promoting module acting upstream of hormonal signaling pathways. Plant Physiology **169,** 1240–1253.

**Yadav RK, Girke T, Pasala S, Xie M, Reddy GV.** 2009. Gene expression map of the Arabidopsis shoot apical meristem stem cell niche. Proceedings of the National Academy of Sciences, USA **106,** 4941–4946.

**Yadav RK, Perales M, Gruel J, Girke T, Jonsson H, Reddy GV.** 2011. WUSCHEL protein movement mediates stem cell homeostasis in the Arabidopsis shoot apex. Genes & Development **25,** 2025–2030.

**Yadav RK, Perales M, Gruel J, Ohno C, Heisler M, Girke T, Jonsson H, Reddy GV.** 2013. Plant stem cell maintenance involves direct transcriptional repression of differentiation program. Molecular Systems Biology **9,** 654.

**Yadav RK, Tavakkoli M, Reddy GV.** 2010. WUSCHEL mediates stem cell homeostasis by regulating stem cell number and patterns of cell division and differentiation of stem cell progenitors. Development **137,** 3581–3589.

**Yadav RK, Tavakkoli M, Xie M, Girke T, Reddy GV.** 2014. A high-resolution gene expression map of the Arabidopsis shoot meristem stem cell niche. Development **141,** 2735–2744.

**Yang F, Wang Q, Schmitz G, Muller D, Theres K.** 2012. The bHLH protein ROX acts in concert with RAX1 and LAS to modulate axillary meristem formation in Arabidopsis. Plant Journal **71,** 61–70.

**Zadnikova P, Simon R.** 2014. How boundaries control plant development. Current Opinion in Plant Biology **17,** 116–125.

**Zhao Z, Andersen SU, Ljung K, Dolezal K, Miotk A, Schultheiss SJ, Lohmann JU.** 2010. Hormonal control of the shoot stem-cell niche. Nature **465,** 1089–1092.

**Zhou Y, Liu X, Engstrom EM, Nimchuk ZL, Pruneda-Paz JL, Tarr PT, Yan A, Kay SA, Meyerowitz EM.** 2015. Control of plant stem cell function by conserved interacting transcriptional regulators. Nature **517,** 377–380.

# References

Adam, Hélène, Mélanie Marguerettaz, Rashad Qadri, Bernard Adroher, Frédérique Richaud, Myriam Collin, Anne-Céline Thuillet, Yves Vigouroux, Patrick Laufs, James W Tregear, and Stefan Jouannic (2011). "Divergent expression patterns of miR164 and CUP-SHAPED COTYLEDON genes in palms and other monocots: implication for the evolution of meristem function in angiosperms." In: *Molecular Biology and Evolution* 28.4, pp. 1439–1454. DOI: 10.1093/molbev/msq328. URL: https://academic.oup.com/mbe/article-lookup/doi/10.1093/molbev/msq328.

Aida, M, T Ishida, and M Tasaka (1999). "Shoot apical meristem and cotyledon formation during Arabidopsis embryogenesis: interaction among the CUP-SHAPED COTYLEDON and SHOOT MERISTEMLESS genes." In: *Development* 126.8, pp. 1563–1570. URL: http://eutils.ncbi.nlm.nih.gov/entrez/eutils/elink.fcgi?dbfrom=pubmed&id=10079219&retmode=ref&cmd=prlinks.

Aida, M, T Ishida, H Fukaki, H Fujisawa, and M Tasaka (1997). "Genes involved in organ separation in Arabidopsis: an analysis of the *cup-shaped cotyledon* mutant." In: *The Plant Cell* 9.6, pp. 841–857. DOI: 10.1105/tpc.9.6.841. URL: http://www.plantcell.org/cgi/doi/10.1105/tpc.9.6.841.

Aida, Mitsuhiro and Masao Tasaka (2006). "Morphogenesis and patterning at the organ boundaries in the higher plant shoot apex." In: *Plant molecular biology* 60.6, pp. 915–928. DOI: 10.1007/s11103-005-2760-7. URL: http://link.springer.com/10.1007/s11103-005-2760-7.

Aida, Mitsuhiro, Teva Vernoux, Masahiko Furutani, Jan Traas, and Masao Tasaka (2002). "Roles of PIN-FORMED1 and MONOPTEROS in pattern formation of the apical region of the Arabidopsis embryo." In: *Development* 129.17, pp. 3965–3974. URL: http://eutils.ncbi.nlm.nih.gov/entrez/eutils/elink.fcgi?dbfrom=pubmed&id=12163400&retmode=ref&cmd=prlinks.

Andrés, Fernando and George Coupland (2012). "The genetic basis of flowering responses to seasonal cues." In: *Nature reviews. Genetics* 13.9, pp. 627–639. DOI: 10.1038/nrg3291. URL: http://eutils.ncbi.nlm.nih.gov/entrez/eutils/elink.fcgi?dbfrom=pubmed&id=22898651&retmode=ref&cmd=prlinks.

Bailly, E and S I Reed (1999). "Functional characterization of rpn3 uncovers a distinct 19S proteasomal subunit requirement for ubiquitin-dependent proteolysis of cell cycle regulatory proteins in . . . " In: *Molecular and cellular biology*. URL: http://mcb.asm.org/content/19/10/6872.short.

Baker, Catherine C, Patrick Sieber, Frank Wellmer, and Elliot M Meyerowitz (2005). "The *early extra petals1* mutant uncovers a role for microRNA *miR164c* in regulating petal number in *Arabidopsis*." In: *Current biology : CB* 15.4, pp. 303–315. DOI: 10.1016/j.cub.2005.02.017. URL: http://linkinghub.elsevier.com/retrieve/pii/S0960982205001132.

Bell, Elizabeth M, Wan-Ching Lin, Aman Y Husbands, Lifeng Yu, Venkateswari Jaganatha, Barbara Jablonska, Amanda Mangeon, Michael M Neff, Thomas Girke, and Patricia S Springer (2012). "Arabidopsis lateral organ boundaries negatively regulates brassinosteroid accumulation to limit growth in organ boundaries." In: *Proceedings of the National Academy of Sciences of the United States of America* 109.51, pp. 21146–21151. DOI: 10.1073/pnas.1210789109. URL: http://www.pnas.org/cgi/doi/10.1073/pnas.1210789109.

Benkova, Eva, Marta Michniewicz, Michael Sauer, Thomas Teichmann, Daniela Seifertová, Gerd Jürgens, and Jirí Friml (2003). "Local, efflux-dependent auxin gradients as a common module for plant organ formation." In: *Cell* 115.5, pp. 591–602. DOI: 10.1038/nrm1302. URL: http://www.nature.com/doifinder/10.1038/nrm1302.

Berckmans, Barbara, Valya Vassileva, Stephan P C Schmid, Sara Maes, Boris Parizot, Satoshi Naramoto, Zoltan Magyar, Claire Lessa Alvim Kamei, Csaba Koncz, Laszlo Bögre, Geert Persiau, Geert De Jaeger, Jiří Friml, Rüdiger Simon, Tom Beeckman, and Lieven De Veylder (2011). "Auxin-dependent cell cycle reactivation through transcriptional regulation of Arabidopsis E2Fa by lateral organ boundary proteins." In: *The Plant cell* 23.10, pp. 3671–3683. DOI: 10.1105/tpc.111.088377. URL: http://eutils.ncbi.nlm.nih.gov/entrez/eutils/elink.fcgi?dbfrom=pubmed&id=22003076&retmode=ref&cmd=prlinks.

Berger, Yael, Smadar Harpaz-Saad, Arnon Brand, Hadas Melnik, Neti Sirding, John Paul Alvarez, Michael Zinder, Alon Samach, Yuval Eshed, and Naomi Ori (2009). "The NAC-domain transcription factor GOBLET specifies leaflet boundaries in compound tomato leaves." In: *Development (Cambridge, England)* 136.5, pp. 823–832. DOI: 10.1242/dev.031625. URL: http://eutils.ncbi.nlm.nih.gov/entrez/eutils/elink.fcgi?dbfrom=pubmed&id=19176589&retmode=ref&cmd=prlinks.

Bergiers, Isabelle, Laure Bridoux, Nathan Nguyen, Jean-Claude Twizere, and Ren Rezs hazy (2013). "The Homeodomain Transcription Factor Hoxa2 Interacts with and Promotes the Proteasomal Degradation of the E3 Ubiquitin Protein Ligase RCHY1". In: *PLoS ONE* 8.11, e80387–12. DOI: 10.1371/journal.pone.0080387. URL: http://dx.plos.org/10.1371/journal.pone.0080387.

Bilsborough, Gemma D, Adam Runions, Michalis Barkoulas, Huw W Jenkins, Alice Hasson, Carla Galinha, Patrick Laufs, Angela Hay, Przemyslaw Prusinkiewicz, and Miltos Tsiantis (2011). "Model for the regulation of Arabidopsis thaliana leaf margin development." In: *Proceedings of the National Academy of Sciences of the United States of America* 108.8, pp. 3424–3429. DOI: 10.1073/pnas.1015162108. URL: http://www.pnas.org/cgi/doi/10.1073/pnas.1015162108.

Blein, Thomas, Amada Pulido, Aurélie Vialette-Guiraud, Krisztina Nikovics, Halima Morin, Angela Hay, Ida Elisabeth Johansen, Miltos Tsiantis, and Patrick Laufs (2008). "A conserved molecular framework for compound leaf development." In: *Science (New York, N.Y.)* 322.5909, pp. 1835–1839. DOI: 10.1126/science.1166168. URL: http://www.sciencemag.org/cgi/doi/10.1126/science.1166168.

Bolger, Anthony M, Marc Lohse, and Bjoern Usadel (2014). "Trimmomatic: a flexible trimmer for Illumina sequence data." In: *Bioinformatics (Oxford, England)* 30.15, pp. 2114–2120. DOI: 10.1093/bioinformatics/btu170. URL: http://eutils.ncbi.nlm.nih.gov/entrez/eutils/elink.fcgi?dbfrom=pubmed&id=24695404&retmode=ref&cmd=prlinks.

Book, Adam J, Jan Smalle, Kwang-Hee Lee, Peizhen Yang, Joseph M Walker, Sarah Casper, James H Holmes, Laura A Russo, Zachri W Buzzinotti, Pablo D Jenik, and Richard D Vierstra (2009). "The RPN5 subunit of the 26s proteasome is essential for gametogenesis, sporophyte development, and complex assembly in Arabidopsis." In: *The Plant cell* 21.2, pp. 460–478. DOI: 10.1105/tpc.108.064444. URL: http://eutils.ncbi.nlm.nih.gov/entrez/eutils/elink.fcgi?dbfrom=pubmed&id=19252082&retmode=ref&cmd=prlinks.

Brand, Arnon, Neti Shirding, Sharona Shleizer, and Naomi Ori (2007). "Meristem maintenance and compound-leaf patterning utilize common genetic mechanisms in tomato." In: *Planta* 226.4, pp. 941–951. DOI: 10.1007/s00425-007-0540-0. URL: http://link.springer.com/10.1007/s00425-007-0540-0.

Brewer, P B (2004). "PETAL LOSS, a trihelix transcription factor gene, regulates perianth architecture in the Arabidopsis flower". In: *Development* 131.16, pp. 4035–4045. DOI: 10.1242/dev.01279. URL: http://eutils.ncbi.nlm.nih.gov/entrez/eutils/elink.fcgi?dbfrom=pubmed&id=15269176&retmode=ref&cmd=prlinks.

Browning, Karen S and Julia Bailey-Serres (2015). "Mechanism of cytoplasmic mRNA translation." In: *The Arabidopsis book* 13, e0176. DOI: 10.1199/tab.0176. URL: http://www.bioone.org/doi/10.1199/tab.0176.

Brukhin, Vladimir, Jacqueline Gheyselinck, Valeria Gagliardini, Pascal Genschik, and Ueli Grossniklaus (2005). "The RPN1 subunit of the 26S proteasome in Arabidopsis is essential for embryogenesis." In: *The Plant Cell* 17.10, pp. 2723–2737. DOI: 10.1105/tpc.105.034975. URL: http://www.plantcell.org/cgi/doi/10.1105/tpc.105.034975.

Bundock, Paul and Paul Hooykaas (2005). "An Arabidopsis hAT-like transposase is essential for plant development." In: *Nature* 436.7048, pp. 282–

284. DOI: 10.1038/nature03667. URL: http://eutils.ncbi.nlm.nih.gov/entrez/eutils/elink.fcgi?dbfrom=pubmed&id=16015335&retmode=ref&cmd=prlinks.

Busch, Wolfgang, Andrej Miotk, Federico D Ariel, Zhong Zhao, Joachim Forner, Gabor Daum, Takuya Suzaki, Christoph Schuster, Sebastian J Schultheiss, Andrea Leibfried, Silke Haubeiss, Nati Ha, Raquel L Chan, and Jan U Lohmann (2010). "Transcriptional Control of a Plant Stem Cell Niche". In: *Developmental Cell* 18.5, pp. 841–853. DOI: 10.1016/j.devcel.2010.03.012. URL: http://linkinghub.elsevier.com/retrieve/pii/S1534580710001516.

Bush, Maxwell S, Natalie Crowe, Tao Zheng, and John H Doonan (2015). "The RNA helicase, eIF4A-1, is required for ovule development and cell size homeostasis in Arabidopsis". In: *The Plant Journal* 84.5, pp. 989–1004. DOI: 10.1111/tpj.13062. URL: http://doi.wiley.com/10.1111/tpj.13062.

Bush, Maxwell S, Olivier Pierrat, Candida Nibau, Veronika Mikitova, Tao Zheng, Fiona M K Corke, Konstantinos Vlachonasios, Laura K Mayberry, Karen S Browning, and John H Doonan (2016). "eIF4A RNA Helicase Associates with Cyclin-Dependent Protein Kinase A in Proliferating Cells and Is Modulated by Phosphorylation". In: *Plant physiology* 172.1, pp. 128–140. DOI: 10.1104/pp.16.00435. URL: http://www.plantphysiol.org/lookup/doi/10.1104/pp.16.00435.

Bustamante, Mariana, José Tomás Matus, and José Luis Riechmann (2016). "Genome-wide analyses for dissecting gene regulatory networks in the shoot apical meristem." In: *Journal of Experimental Botany* 67.6, pp. 1639–1648. URL: http://jxb.oxfordjournals.org/lookup/doi/10.1093/jxb/erw058.

Cheng, Xiaofei, Jianling Peng, Junying Ma, Yuhong Tang, Rujin Chen, Kirankumar S Mysore, and Jiangqi Wen (2012). "NO APICAL MERISTEM (MtNAM) regulates floral organ identity and lateral organ separation in Medicago truncatula." In: *New Phytologist* 195.1, pp. 71–84. DOI: 10.1111/j.1469-8137.2012.04147.x. URL: http://doi.wiley.com/10.1111/j.1469-8137.2012.04147.x.

Cho, Euna and Patricia C Zambryski (2011). "Organ boundary1 defines a gene expressed at the junction between the shoot apical meristem and lateral organs." In: *Proceedings of the National Academy of Sciences of the United States of America* 108.5, pp. 2154–2159. DOI: 10.1073/pnas.1018542108. URL: http://www.pnas.org/lookup/doi/10.1073/pnas.1018542108.

Coen, E S and E M Meyerowitz (1991). "The war of the whorls: genetic interactions controlling flower development." In: *Nature* 353.6339, pp. 31–37. DOI: 10.1038/353031a0. URL: http://www.nature.com/doifinder/10.1038/353031a0.

Cox, Jürgen and Matthias Mann (2008). "MaxQuant enables high peptide identification rates, individualized p.p.b.-range mass accuracies and proteome-wide protein quantification." In: *Nature biotechnology* 26.12, pp. 1367–

1372. DOI: 10.1038/nbt.1511. URL: http://www.nature.com/doifinder/10.1038/nbt.1511.

Cox, Jürgen, Neuhauser, Nadin, Michalski, Annette, Scheltema, Richard A, Olsen, Jesper V, and Mann, Matthias (2011). "Andromeda: a peptide search engine integrated into the MaxQuant environment." In: *Journal of proteome research* 10.4, pp. 1794–1805. DOI: 10.1021/pr101065j. URL: http://eutils.ncbi.nlm.nih.gov/entrez/eutils/elink.fcgi?dbfrom=pubmed&id=21254760&retmode=ref&cmd=prlinks.

Cui, Xia, Falong Lu, Qi Qiu, Bing Zhou, Lianfeng Gu, Shuaibin Zhang, Yanyuan Kang, Xiekui Cui, Xuan Ma, Qingqing Yao, Jinbiao Ma, Xiaoyu Zhang, and Xiaofeng Cao (2016). "REF6 recognizes a specific DNA sequence to demethylate H3K27me3 and regulate organ boundary formation in Arabidopsis." In: *Nature genetics* 48.6, pp. 694–699. DOI: 10.1038/ng.3556. URL: http://www.nature.com/doifinder/10.1038/ng.3556.

Dahmann, Christian, Andrew C Oates, and Michael Brand (2011). "Boundary formation and maintenance in tissue development". In: *Nature Reviews Genetics* 12.1, pp. 43–55. DOI: 10.1038/nrg2902. URL: http://dx.doi.org/10.1038/nrg2902.

Ding, Lian, Shuangshuang Yan, Li Jiang, Wensheng Zhao, Kang Ning, Jianyu Zhao, Xiaofeng Liu, Juan Zhang, Qian Wang, and Xiaolan Zhang (2015). "HANABA TARANU (HAN) Bridges Meristem and Organ Primordia Boundaries through PINHEAD, JAGGED, BLADE-ON-PETIOLE2 and CYTOKININ OXIDASE 3 during Flower Development in Arabidopsis." In: *PLoS genetics* 11.9, e1005479. DOI: 10.1371/journal.pgen.1005479. URL: http://dx.plos.org/10.1371/journal.pgen.1005479.

Ditta, Gary, Anusak Pinyopich, Pedro Robles, Soraya Pelaz, and Martin F Yanofsky (2004). "The SEP4 gene of Arabidopsis thaliana functions in floral organ and meristem identity." In: *Current Biology* 14.21, pp. 1935–1940. DOI: 10.1016/j.cub.2004.10.028. URL: http://linkinghub.elsevier.com/retrieve/pii/S0960982204008152.

Dobin, Alexander, Carrie A Davis, Felix Schlesinger, Jorg Drenkow, Chris Zaleski, Sonali Jha, Philippe Batut, Mark Chaisson, and Thomas R Gingeras (2013). "STAR: ultrafast universal RNA-seq aligner." In: *Bioinformatics (Oxford, England)* 29.1, pp. 15–21. DOI: 10.1093/bioinformatics/bts635. URL: http://eutils.ncbi.nlm.nih.gov/entrez/eutils/elink.fcgi?dbfrom=pubmed&id=23104886&retmode=ref&cmd=prlinks.

Dreni, Ludovico and Dabing Zhang (2016). "Flower development: the evolutionary history and functions of the AGL6 subfamily MADS-box genes." In: *Journal of experimental botany* 67.6, pp. 1625–1638. DOI: 10.1093/jxb/erw046. URL: http://eutils.ncbi.nlm.nih.gov/entrez/eutils/elink.fcgi?dbfrom=pubmed&id=26956504&retmode=ref&cmd=prlinks.

Du, Zhou, Xin Zhou, Yi Ling, Zhenhai Zhang, and Zhen Su (2010). "agriGO: a GO analysis toolkit for the agricultural community." In: *Nucleic acids research* 38.Web Server issue, W64–70. DOI: 10.1093/nar/gkq310. URL: http://eutils.ncbi.nlm.nih.gov/entrez/eutils/elink.fcgi?dbfrom=pubmed&id=20435677&retmode=ref&cmd=prlinks.

Ernst, Heidi A, Olsen, Addie Nina, Larsen, Sine, and Lo Leggio, Leila (2004). "Structure of the conserved domain of ANAC, a member of the NAC family of transcription factors." In: *EMBO reports* 5.3, pp. 297–303. DOI: 10.1038/sj.embor.7400093.

Estornell, Leandro H, Javier Agustí, Paz Merelo, Manuel Talón, and Francisco R Tadeo (2013). "Elucidating mechanisms underlying organ abscission." In: *Plant science : an international journal of experimental plant biology* 199-200, pp. 48–60. DOI: 10.1016/j.plantsci.2012.10.008. URL: http://linkinghub.elsevier.com/retrieve/pii/S0168945212002191.

Favaro, Rebecca, Anusak Pinyopich, Raffaella Battaglia, Maarten Kooiker, Lorenzo Borghi, Gary Ditta, Martin F Yanofsky, Martin M Kater, and Lucia Colombo (2003). "MADS-box protein complexes control carpel and ovule development in Arabidopsis." In: *The Plant Cell* 15.11, pp. 2603–2611. DOI: 10.1105/tpc.015123. URL: http://www.plantcell.org/cgi/doi/10.1105/tpc.015123.

Ferrier, Thilia, José Tomás Matus, Jian Jin, and José Luis Riechmann (2011). "Arabidopsis paves the way: genomic and network analyses in crops". In: *Current Opinion in Biotechnology* 22.2, pp. 260–270. DOI: 10.1016/j.copbio.2010.11.010. URL: http://dx.doi.org/10.1016/j.copbio.2010.11.010.

Friml, Jirí, Anne Vieten, Michael Sauer, Dolf Weijers, Heinz Schwarz, Thorsten Hamann, Remko Offringa, and Gerd Jürgens (2003). "Efflux-dependent auxin gradients establish the apical-basal axis of Arabidopsis." In: *Nature* 426.6963, pp. 147–153. DOI: 10.1038/nature02085. URL: http://www.nature.com/doifinder/10.1038/nature02085.

Furutani, Masahiko, Teva Vernoux, Jan Traas, Takehide Kato, Masao Tasaka, and Mitsuhiro Aida (2004). "PIN-FORMED1 and PINOID regulate boundary formation and cotyledon development in Arabidopsis embryogenesis." In: *Development* 131.20, pp. 5021–5030. DOI: 10.1242/dev.01388. URL: http://dev.biologists.org/cgi/doi/10.1242/dev.01388.

Galbiati, Francesca, Dola Sinha Roy, Sara Simonini, Mara Cucinotta, Luca Ceccato, Candela Cuesta, Maria Simaskova, Eva Benkova, Yuri Kamiuchi, Mitsuhiro Aida, Dolf Weijers, Rüdiger Simon, Simona Masiero, and Lucia Colombo (2013). "An integrative model of the control of ovule primordia formation". In: *The Plant Journal* 76.3, pp. 446–455. DOI: 10.1111/tpj.12309. URL: http://doi.wiley.com/10.1111/tpj.12309.

Gallois, Jean-Luc, Anouchka Guyon-Debast, Alain Lécureuil, Daniel Vezon, Virginie Carpentier, Sandrine Bonhomme, and Philippe Guerche (2009). "The Arabidopsis proteasome RPT5 subunits are essential for gametophyte development and show accession-dependent redundancy." In: *The Plant Cell* 21.2, pp. 442–459. DOI: 10.1105/tpc.108.062372. URL: http://www.plantcell.org/cgi/doi/10.1105/tpc.108.062372.

Gendron, Joshua M, Jiang-Shu Liu, Min Fan, Ming-Yi Bai, Stephan Wenkel, Patricia S Springer, M Kathryn Barton, and Zhi-Yong Wang (2012). "Brassinosteroids regulate organ boundary formation in the shoot apical meristem of Arabidopsis." In: *Proceedings of the National Academy of Sciences*

*of the United States of America* 109.51, pp. 21152–21157. DOI: 10.1073/pnas.1210799110. URL: http://www.pnas.org/cgi/doi/10.1073/pnas.1210799110.

Gómez-Mena, Concepción and Robert Sablowski (2008). "ARABIDOPSIS THALIANA HOMEOBOX GENE1 establishes the basal boundaries of shoot organs and controls stem growth." In: *The Plant Cell* 20.8, pp. 2059–2072. DOI: 10.1105/tpc.108.059188. URL: http://www.plantcell.org/cgi/doi/10.1105/tpc.108.059188.

Gonçalves, Beatriz, Alice Hasson, Katia Belcram, Millán Cortizo, Halima Morin, Krisztina Nikovics, Aurélie Vialette-Guiraud, Seiji Takeda, Mitsuhiro Aida, Patrick Laufs, and Nicolas Arnaud (2015). "A conserved role for CUP-SHAPED COTYLEDON genes during ovule development." In: *The Plant Journal* 83.4, pp. 732–742. DOI: 10.1111/tpj.12923. URL: http://doi.wiley.com/10.1111/tpj.12923.

Grbić, V and A B Bleecker (2000). "Axillary meristem development in Arabidopsis thaliana." In: *The Plant Journal* 21.2, pp. 215–223. URL: http://eutils.ncbi.nlm.nih.gov/entrez/eutils/elink.fcgi?dbfrom=pubmed&id=10743661&retmode=ref&cmd=prlinks.

Greb, Thomas, Oliver Clarenz, Elisabeth Schafer, Dorte Muller, Ruben Herrero, Gregor Schmitz, and Klaus Theres (2003). "Molecular analysis of the LATERAL SUPPRESSOR gene in Arabidopsis reveals a conserved control mechanism for axillary meristem formation." In: *Genes & development* 17.9, pp. 1175–1187. DOI: 10.1101/gad.260703. URL: http://eutils.ncbi.nlm.nih.gov/entrez/eutils/elink.fcgi?dbfrom=pubmed&id=12730136&retmode=ref&cmd=prlinks.

Grubb, C Douglas, Brandon J Zipp, Jutta Ludwig-Müller, Makoto N Masuno, Tadeusz F Molinski, and Steffen Abel (2004). "Arabidopsis glucosyltransferase UGT74B1 functions in glucosinolate biosynthesis and auxin homeostasis." In: *The Plant Journal* 40.6, pp. 893–908. DOI: 10.1111/j.1365-313X.2004.02261.x. URL: http://eutils.ncbi.nlm.nih.gov/entrez/eutils/elink.fcgi?dbfrom=pubmed&id=15584955&retmode=ref&cmd=prlinks.

Grubb, C Douglas, Brandon J Zipp, Jakub Kopycki, Melvin Schubert, Marcel Quint, Eng-Kiat Lim, Dianna J Bowles, M Soledade C Pedras, and Steffen Abel (2014). "Comparative analysis of Arabidopsis UGT74 glucosyltransferases reveals a special role of UGT74C1 in glucosinolate biosynthesis." In: *The Plant Journal* 79.1, pp. 92–105. DOI: 10.1111/tpj.12541. URL: http://eutils.ncbi.nlm.nih.gov/entrez/eutils/elink.fcgi?dbfrom=pubmed&id=24779768&retmode=ref&cmd=prlinks.

Guo, Hui-Shan, Xie, Qi, Fei, Ji-Feng, and Chua, Nam-Hai (2005). "MicroRNA directs mRNA cleavage of the transcription factor NAC1 to downregulate auxin signals for arabidopsis lateral root development." In: *The Plant Cell* 17.5, pp. 1376–1386. DOI: 10.1105/tpc.105.030841.

Ha, Chan Man, Ji Hyung Jun, Hong Gil Nam, and Jennifer C Fletcher (2007). "BLADE-ON-PETIOLE 1 and 2 control Arabidopsis lateral organ fate through regulation of LOB domain and adaxial-abaxial polarity

genes." In: *The Plant Cell* 19.6, pp. 1809–1825. DOI: 10.1105/tpc.107.051938. URL: http://www.plantcell.org/lookup/doi/10.1105/tpc.107.051938.

Hasson, Alice, Anne Plessis, Thomas Blein, Bernard Adroher, Stephen Grigg, Miltos Tsiantis, Arezki Boudaoud, Catherine Damerval, and Patrick Laufs (2011). "Evolution and diverse roles of the CUP-SHAPED COTYLEDON genes in Arabidopsis leaf development." In: *The Plant Cell* 23.1, pp. 54–68. DOI: 10.1105/tpc.110.081448. URL: http://www.plantcell.org/lookup/doi/10.1105/tpc.110.081448.

Heinz, Sven, Christopher Benner, Nathanael Spann, Eric Bertolino, Yin C Lin, Peter Laslo, Jason X Cheng, Cornelis Murre, Harinder Singh, and Christopher K Glass (2010). "Simple combinations of lineage-determining transcription factors prime cis-regulatory elements required for macrophage and B cell identities." In: *Molecular cell* 38.4, pp. 576–589. DOI: 10.1016/j.molcel.2010.05.004. URL: http://linkinghub.elsevier.com/retrieve/pii/S1097276510003667.

Heisler, Marcus G, Ohno, Carolyn, Das, Pradeep, Sieber, Patrick, Reddy, Gonehal V, Long, Jeff A, and Meyerowitz, Elliot M (2005). "Patterns of auxin transport and gene expression during primordium development revealed by live imaging of the *Arabidopsis* inflorescence meristem." In: *Current biology : CB* 15.21, pp. 1899–1911. DOI: 10.1016/j.cub.2005.09.052. URL: http://eutils.ncbi.nlm.nih.gov/entrez/eutils/elink.fcgi?dbfrom=pubmed&id=16271866&retmode=ref&cmd=prlinks.

Hibara, Ken-ichiro, Shinobu Takada, and Masao Tasaka (2003). "*CUC1* gene activates the expression of SAM-related genes to induce adventitious shoot formation." In: *The Plant Journal* 36.5, pp. 687–696. URL: http://eutils.ncbi.nlm.nih.gov/entrez/eutils/elink.fcgi?dbfrom=pubmed&id=14617069&retmode=ref&cmd=prlinks.

Hibara, Ken-ichiro, Karim, Md Rezaul, Takada, Shinobu, Taoka, Ken-ichiro, Furutani, Masahiko, Aida, Mitsuhiro, and Tasaka, Masao (2006). "Arabidopsis CUP-SHAPED COTYLEDON3 regulates postembryonic shoot meristem and organ boundary formation." In: *The Plant Cell* 18.11, pp. 2946–2957. DOI: 10.1105/tpc.106.045716. URL: http://eutils.ncbi.nlm.nih.gov/entrez/eutils/elink.fcgi?dbfrom=pubmed&id=17122068&retmode=ref&cmd=prlinks.

Hu, Xiaomei and Lin Xu (2016). "Transcription Factors WOX11/12 Directly Activate WOX5/7 to Promote Root Primordia Initiation and Organogenesis." In: *Plant physiology* 172.4, pp. 2363–2373. DOI: 10.1104/pp.16.01067. URL: http://eutils.ncbi.nlm.nih.gov/entrez/eutils/elink.fcgi?dbfrom=pubmed&id=27784768&retmode=ref&cmd=prlinks.

Huang, Tengbo, Francesc López-Giráldez, Jeffrey P Townsend, and Vivian F Irish (2012). "RBE controls microRNA164 expression to effect floral organogenesis." In: *Development* 139.12, pp. 2161–2169. DOI: 10.1242/dev.075069. URL: http://dev.biologists.org/cgi/doi/10.1242/dev.075069.

Huang, W, L Pi, W Liang, B Xu, H Wang, R Cai, and H Huang (2006). "The Proteolytic Function of the Arabidopsis 26S Proteasome Is Required for Specifying Leaf Adaxial Identity". In: *The Plant Cell* 18.10, pp. 2479–2492. DOI: 10.1105/tpc.106.045013. URL: http://www.plantcell.org/cgi/doi/10.1105/tpc.106.045013.

Huang, Weihua and Hai Huang (2007). "A Novel Function of the 26S Proteasome in Repressing Class-1 KNOX Genes During Leaf Development." In: *Plant Signaling & Behavior* 2.1, pp. 25–27. DOI: 10.1105/tpc.106.045013.

Hutchins, Andrew P, Gethin R Roberts, Clive W Lloyd, and John H Doonan (2004). "In vivo interaction between CDKA and eIF4A: a possible mechanism linking translation and cell proliferation." In: *FEBS letters* 556.1-3, pp. 91–94. URL: http://eutils.ncbi.nlm.nih.gov/entrez/eutils/elink.fcgi?dbfrom=pubmed&id=14706832&retmode=ref&cmd=prlinks.

Immink, Richard G H, Kerstin Kaufmann, and Gerco C Angenent (2010). "The 'ABC' of MADS domain protein behaviour and interactions." In: *Seminars in cell & developmental biology* 21.1, pp. 87–93. DOI: 10.1016/j.semcdb.2009.10.004. URL: http://eutils.ncbi.nlm.nih.gov/entrez/eutils/elink.fcgi?dbfrom=pubmed&id=19883778&retmode=ref&cmd=prlinks.

Ishida, Tetsuya, Mitsuhiro Aida, Shinobu Takada, and Masao Tasaka (2000). "Involvement of *CUP-SHAPED COTYLEDON* Genes in Gynoecium and Ovule Development in *Arabidopsis thaliana*". In: *Plant and Cell Physiology* 41.1, pp. 60–67. DOI: 10.1093/pcp/41.1.60. URL: http://pcp.oxfordjournals.org/cgi/doi/10.1093/pcp/41.1.60.

Iyer, Lakshminarayan M and L Aravind (2012). "ALOG domains: provenance of plant homeotic and developmental regulators from the DNA-binding domain of a novel class of DIRS1-type retroposons." In: *Biology direct* 7, p. 39. DOI: 10.1186/1745-6150-7-39. URL: http://eutils.ncbi.nlm.nih.gov/entrez/eutils/elink.fcgi?dbfrom=pubmed&id=23146749&retmode=ref&cmd=prlinks.

Kamiuchi, Yuri, Kayo Yamamoto, Masahiko Furutani, Masao Tasaka, and Mitsuhiro Aida (2014). "The CUC1 and CUC2 genes promote carpel margin meristem formation during *Arabidopsis* gynoecium development." In: *Frontiers in Plant Science* 5, p. 165. DOI: 10.3389/fpls.2014.00165. URL: http://journal.frontiersin.org/article/10.3389/fpls.2014.00165/abstract.

Kaplan-Levy, Ruth N, Tezz Quon, Martin O'Brien, Pia G Sappl, and David R Smyth (2014). "Functional domains of the PETAL LOSS protein, a trihelix transcription factor that represses regional growth in Arabidopsis thaliana". In: *The Plant Journal* 79.3, pp. 477–491. DOI: 10.1111/tpj.12574. URL: http://doi.wiley.com/10.1111/tpj.12574.

Kaufmann, Kerstin, Jose M Muiño, Ruy Jauregui, Chiara A Airoldi, Cezary Smaczniak, Pawel Krajewski, and Gerco C Angenent (2009). "Target genes of the MADS transcription factor SEPALLATA3: integration of developmental and hormonal pathways in the *Arabidopsis* flower." In: *PLoS biology* 7.4, e1000090. DOI: 10.1371/journal.pbio.1000090. URL: http:

//biology.plosjournals.org/perlserv/?request=get-document&doi=10.1371/journal.pbio.1000090.

Kaufmann, Kerstin, Jose M Muiño, Magne Østerås, Laurent Farinelli, Pawel Krajewski, and Gerco C Angenent (2010a). "Chromatin immunoprecipitation (ChIP) of plant transcription factors followed by sequencing (ChIP-SEQ) or hybridization to whole genome arrays (ChIP-CHIP)". In: *Nature Protocols* 5.3, pp. 457–472. DOI: 10.1038/nprot.2009.244. URL: http://www.nature.com/doifinder/10.1038/nprot.2009.244.

Kaufmann, Kerstin, Frank Wellmer, Jose M Muiño, Thilia Ferrier, Samuel E Wuest, Vijaya Kumar, Antonio Serrano-Mislata, Francisco Madueño, Pawel Krajewski, Elliot M Meyerowitz, Gerco C Angenent, and José Luis Riechmann (2010b). "Orchestration of floral initiation by APETALA1." In: *Science (New York, N.Y.)* 328.5974, pp. 85–89. DOI: 10.1126/science.1185244. URL: http://www.sciencemag.org/cgi/doi/10.1126/science.1185244.

Keller, Thomas, Jessica Abbott, Thomas Moritz, and Peter Doerner (2006). "Arabidopsis REGULATOR OF AXILLARY MERISTEMS1 controls a leaf axil stem cell niche and modulates vegetative development." In: *The Plant Cell* 18.3, pp. 598–611. DOI: 10.1105/tpc.105.038588. URL: http://www.plantcell.org/cgi/doi/10.1105/tpc.105.038588.

Kempin, S A, B Savidge, and M F Yanofsky (1995). "Molecular basis of the cauliflower phenotype in Arabidopsis." In: *Science (New York, N.Y.)* 267.5197, pp. 522–525. URL: http://eutils.ncbi.nlm.nih.gov/entrez/eutils/elink.fcgi?dbfrom=pubmed&id=7824951&retmode=ref&cmd=prlinks.

Kim, Hyo Jung, Hong Gil Nam, and Pyung Ok Lim (2016). "Regulatory network of NAC transcription factors in leaf senescence." In: *Current opinion in plant biology* 33, pp. 48–56. DOI: 10.1016/j.pbi.2016.06.002. URL: http://linkinghub.elsevier.com/retrieve/pii/S1369526616300851.

Kim, Jeong Im, Whitney L Dolan, Nickolas A Anderson, and Clint Chapple (2015). "Indole Glucosinolate Biosynthesis Limits Phenylpropanoid Accumulation in Arabidopsis thaliana." In: *The Plant cell* 27.5, pp. 1529–1546. DOI: 10.1105/tpc.15.00127. URL: http://eutils.ncbi.nlm.nih.gov/entrez/eutils/elink.fcgi?dbfrom=pubmed&id=25944103&retmode=ref&cmd=prlinks.

Kim, Tae-Wuk and Zhi-Yong Wang (2010). "Brassinosteroid signal transduction from receptor kinases to transcription factors." In: *Annual review of plant biology* 61, pp. 681–704. DOI: 10.1146/annurev.arplant.043008.092057. URL: http://eutils.ncbi.nlm.nih.gov/entrez/eutils/elink.fcgi?dbfrom=pubmed&id=20192752&retmode=ref&cmd=prlinks.

Knip, Marijn, Steven Hiemstra, Afke Sietsma, Marina Castelein, Sylvia de Pater, and Paul Hooykaas (2013). "DAYSLEEPER: a nuclear and vesicular-localized protein that is expressed in proliferating tissues." In: *BMC Plant Biology* 13.1, p. 211. DOI: 10.1186/1471-2229-13-211. URL: http://bmcplantbiol.biomedcentral.com/articles/10.1186/1471-2229-13-211.

Koyama, Tomotsugu, Masahiko Furutani, Masao Tasaka, and Masaru Ohme-Takagi (2007). "TCP transcription factors control the morphology of shoot lateral organs via negative regulation of the expression of boundary-specific genes in Arabidopsis." In: *The Plant Cell* 19.2, pp. 473–484. DOI: 10.1105/tpc.106.044792. URL: http://www.plantcell.org/cgi/doi/10.1105/tpc.106.044792.

Krizek, Beth A, Michael W Lewis, and Jennifer C Fletcher (2006). "RABBIT EARS is a second-whorl repressor of AGAMOUS that maintains spatial boundaries in Arabidopsis flowers." In: *The Plant Journal* 45.3, pp. 369–383. DOI: 10.1111/j.1365-313X.2005.02633.x. URL: http://doi.wiley.com/10.1111/j.1365-313X.2005.02633.x.

Kwon, Chang Seob, Ken-ichiro Hibara, Jennifer Pfluger, Staver Bezhani, Heral Metha, Mitsuhiro Aida, Masao Tasaka, and Doris Wagner (2006). "A role for chromatin remodeling in regulation of CUC gene expression in the Arabidopsis cotyledon boundary." In: *Development* 133.16, pp. 3223–3230. DOI: 10.1242/dev.02508. URL: http://dev.biologists.org/cgi/doi/10.1242/dev.02508.

Lampugnani, Edwin R, Aydin Kilinc, and David R Smyth (2012). "PETAL LOSS is a boundary gene that inhibits growth between developing sepals in Arabidopsis thaliana". In: *The Plant Journal* 71.5, pp. 724–735. DOI: 10.1111/j.1365-313X.2012.05023.x. URL: http://doi.wiley.com/10.1111/j.1365-313X.2012.05023.x.

Laufs, Patrick, Alexis Peaucelle, Halima Morin, and Jan Traas (2004). "MicroRNA regulation of the CUC genes is required for boundary size control in Arabidopsis meristems." In: *Development* 131.17, pp. 4311–4322. DOI: 10.1242/dev.01320. URL: http://eutils.ncbi.nlm.nih.gov/entrez/eutils/elink.fcgi?dbfrom=pubmed&id=15294871&retmode=ref&cmd=prlinks.

Lee, Dong-Keun, Matt Geisler, and Patricia S Springer (2009). "LATERAL ORGAN FUSION1 and LATERAL ORGAN FUSION2 function in lateral organ separation and axillary meristem formation in Arabidopsis." In: *Development* 136.14, pp. 2423–2432. DOI: 10.1242/dev.031971. URL: http://dev.biologists.org/cgi/doi/10.1242/dev.031971.

Lee, Han Woo, Nan Young Kim, Dong Ju Lee, and Jungmook Kim (2009a). "LBD18/ASL20 regulates lateral root formation in combination with LBD16/ASL18 downstream of ARF7 and ARF19 in Arabidopsis." In: *Plant physiology* 151.3, pp. 1377–1389. DOI: 10.1104/pp.109.143685. URL: http://eutils.ncbi.nlm.nih.gov/entrez/eutils/elink.fcgi?dbfrom=pubmed&id=19717544&retmode=ref&cmd=prlinks.

Lee, Myoung-Hoon, Hwi Seong Jeon, Hye Gi Kim, and Ohkmae K. Park (2017). "An Arabidopsis NAC transcription factor NAC4 promotes pathogen-induced cell death under negative regulation by microRNA164". In: *New Phytologist* 214.1. 2016-22559, pp. 343–360. ISSN: 1469-8137. DOI: 10.1111/nph.14371. URL: http://dx.doi.org/10.1111/nph.14371.

Lee, Sang-Sook, Hye Sun Cho, Gyeong Mee Yoon, Joon-Woo Ahn, Hyong-Ha Kim, and Hyun-Sook Pai (2003). "Interaction of NtCDPK1 calcium-dependent protein kinase with NtRpn3 regulatory subunit of the 26S proteasome in Nicotiana tabacum." In: *The Plant Journal* 33.5, pp. 825–840. URL: http://eutils.ncbi.nlm.nih.gov/entrez/eutils/elink.fcgi?dbfrom=pubmed&id=12609025&retmode=ref&cmd=prlinks.

Lee, Woo Yong, Daeyoup Lee, Won-Il Chung, and Chang Seob Kwon (2009b). "Arabidopsis ING and Alfin1-like protein families localize to the nucleus and bind to H3K4me3/2 via plant homeodomain fingers." In: *The Plant Journal* 58.3, pp. 511–524. DOI: 10.1111/j.1365-313X.2009.03795.x. URL: http://doi.wiley.com/10.1111/j.1365-313X.2009.03795.x.

Li, Qunhua, James B Brown, Haiyan Huang, and Peter J Bickel (2011). "Measuring reproducibility of high-throughput experiments". In: *The Annals of Applied Statistics* 5.3, pp. 1752–1779. DOI: 10.1214/11-AOAS466. URL: http://projecteuclid.org/euclid.aoas/1318514284.

Li, Xing Guo, Ying Hua Su, Xiang Yu Zhao, Wei Li, Xin Qi Gao, and Xian Sheng Zhang (2010). "Cytokinin overproduction-caused alteration of flower development is partially mediated by CUC2 and CUC3 in Arabidopsis." In: *Gene* 450.1-2, pp. 109–120. DOI: 10.1016/j.gene.2009.11.003. URL: http://linkinghub.elsevier.com/retrieve/pii/S0378111909005721.

Liao, Yang, Gordon K Smyth, and Wei Shi (2014). "featureCounts: an efficient general purpose program for assigning sequence reads to genomic features." In: *Bioinformatics (Oxford, England)* 30.7, pp. 923–930. DOI: 10.1093/bioinformatics/btt656. URL: http://eutils.ncbi.nlm.nih.gov/entrez/eutils/elink.fcgi?dbfrom=pubmed&id=24227677&retmode=ref&cmd=prlinks.

Lie, Catharine, Corey Kelsom, and Xuelin Wu (2012). "WOX2 and STIMPY-LIKE/WOX8 promote cotyledon boundary formation in Arabidopsis." In: *The Plant Journal* 72.4, pp. 674–682. DOI: 10.1111/j.1365-313X.2012.05113.x. URL: http://doi.wiley.com/10.1111/j.1365-313X.2012.05113.x.

Lindemose, Søren, Michael K Jensen, Jan Van de Velde, Charlotte O'Shea, Ken S Heyndrickx, Christopher T Workman, Klaas Vandepoele, Karen Skriver, and Federico De Masi (2014). "A DNA-binding-site landscape and regulatory network analysis for NAC transcription factors in Arabidopsis thaliana." In: *Nucleic acids research* 42.12, pp. 7681–7693. DOI: 10.1093/nar/gku502. URL: https://academic.oup.com/nar/article-lookup/doi/10.1093/nar/gku502.

Liu, Jingchun, Lihong Sheng, Yingqiang Xu, Jiqin Li, Zhongnan Yang, Hai Huang, and Lin Xu (2014). "WOX11 and 12 are involved in the first-step cell fate transition during de novo root organogenesis in Arabidopsis." In: *The Plant cell* 26.3, pp. 1081–1093. DOI: 10.1105/tpc.114.122887. URL: http://eutils.ncbi.nlm.nih.gov/entrez/eutils/elink.fcgi?dbfrom=pubmed&id=24642937&retmode=ref&cmd=prlinks.

Livak, K J and T D Schmittgen (2001). "Analysis of relative gene expression data using real-time quantitative PCR and the 2(-Delta Delta C(T))

Method." In: *Methods (San Diego, Calif.)* 25.4, pp. 402–408. DOI: 10.1006/meth.2001.1262. URL: http://linkinghub.elsevier.com/retrieve/pii/S1046202301912629.

Long, J and M K Barton (2000). "Initiation of axillary and floral meristems in Arabidopsis." In: *Developmental biology* 218.2, pp. 341–353. DOI: 10.1006/dbio.1999.9572. URL: http://linkinghub.elsevier.com/retrieve/pii/S0012160699995726.

Long, Jeff A, Erich I Moan, June I Medford, and M Kathryn Barton (1996). "A member of the KNOTTED class of homeodomain proteins encoded by the *STM* gene of *Arabidopsis*". In: *, Published online: 04 January 1996; | doi:10.1038/379066a0* 379.6560, pp. 66–69. DOI: 10.1038/379066a0. URL: http://www.nature.com/doifinder/10.1038/379066a0.

Love, Michael I, Wolfgang Huber, and Simon Anders (2014). "Moderated estimation of fold change and dispersion for RNA-seq data with DESeq2." In: *Genome biology* 15.12, p. 550. DOI: 10.1186/s13059-014-0550-8. URL: http://eutils.ncbi.nlm.nih.gov/entrez/eutils/elink.fcgi?dbfrom=pubmed&id=25516281&retmode=ref&cmd=prlinks.

Lu, Falong, Xia Cui, Shuaibin Zhang, Thomas Jenuwein, and Xiaofeng Cao (2011). "Arabidopsis REF6 is a histone H3 lysine 27 demethylase." In: *Nature genetics* 43.7, pp. 715–719. DOI: 10.1038/ng.854. URL: http://www.nature.com/doifinder/10.1038/ng.854.

Maere, Steven, Karel Heymans, and Martin Kuiper (2005). "BiNGO: a Cytoscape plugin to assess overrepresentation of gene ontology categories in biological networks." In: *Bioinformatics (Oxford, England)* 21.16, pp. 3448–3449. DOI: 10.1093/bioinformatics/bti551. URL: http://eutils.ncbi.nlm.nih.gov/entrez/eutils/elink.fcgi?dbfrom=pubmed&id=15972284&retmode=ref&cmd=prlinks.

Mallory, Allison C, Diana V Dugas, David P Bartel, and Bonnie Bartel (2004). "MicroRNA regulation of NAC-domain targets is required for proper formation and separation of adjacent embryonic, vegetative, and floral organs." In: *Current Biology* 14.12, pp. 1035–1046. DOI: 10.1016/j.cub.2004.06.022. URL: http://linkinghub.elsevier.com/retrieve/pii/S0960982204004269.

Marhavý, Peter, Duclercq, Jérôme, Weller, Benjamin, Feraru, Elena, Bielach, Agnieszka, Offringa, Remko, Friml, Jirí, Schwechheimer, Claus, Murphy, Angus, and Benkova, Eva (2014). "Cytokinin controls polarity of PIN1-dependent auxin transport during lateral root organogenesis." In: *Current biology : CB* 24.9, pp. 1031–1037. DOI: 10.1016/j.cub.2014.04.002. URL: http://eutils.ncbi.nlm.nih.gov/entrez/eutils/elink.fcgi?dbfrom=pubmed&id=24768050&retmode=ref&cmd=prlinks.

Maugarny, Aude, Beatriz Gonçalves, Nicolas Arnaud, and Patrick Laufs (2016). "CUC Transcription Factors: To the Meristem and Beyond". In: *Plant Transcription Factors*. Elsevier, pp. 229–247. ISBN: 9780128008546. DOI: 10.1016/B978-0-12-800854-6.00015-4. URL: http://linkinghub.elsevier.com/retrieve/pii/B9780128008546000154.

Merelo, Paz, Xie, Yakun, Brand, Lucas, Ott, Felix, Weigel, Detlef, Bowman, John L, Heisler, Marcus G, and Wenkel, Stephan (2013). "Genome-Wide Identification of KANADI1 Target Genes". In: *PLoS ONE* 8.10, e77341–14. DOI: 10.1371/journal.pone.0077341. URL: http://eutils.ncbi.nlm.nih.gov/entrez/eutils/elink.fcgi?dbfrom=pubmed&id=24155946&retmode=ref&cmd=prlinks.

Morikawa, Tomomi, Masaharu Mizutani, Nozomu Aoki, Bunta Watanabe, Hirohisa Saga, Shigeki Saito, Akira Oikawa, Hideyuki Suzuki, Nozomu Sakurai, Daisuke Shibata, Akira Wadano, Kanzo Sakata, and Daisaku Ohta (2006). "Cytochrome P450 CYP710A encodes the sterol C-22 desaturase in Arabidopsis and tomato." In: *The Plant cell* 18.4, pp. 1008–1022. DOI: 10.1105/tpc.105.036012. URL: http://eutils.ncbi.nlm.nih.gov/entrez/eutils/elink.fcgi?dbfrom=pubmed&id=16531502&retmode=ref&cmd=prlinks.

Murray, James A H, Angharad Jones, Christophe Godin, and Jan Traas (2012). "Systems analysis of shoot apical meristem growth and development: integrating hormonal and mechanical signaling." In: *The Plant Cell* 24.10, pp. 3907–3919. DOI: 10.1105/tpc.112.102194. URL: http://www.plantcell.org/lookup/doi/10.1105/tpc.112.102194.

Nagel, Dawn H, Colleen J Doherty, Jose L Pruneda-Paz, Robert J Schmitz, Joseph R Ecker, and Steve A Kay (2015). "Genome-wide identification of CCA1 targets uncovers an expanded clock network in *Arabidopsis*." In: *Proceedings of the National Academy of Sciences of the United States of America*, p. 201513609. DOI: 10.1073/pnas.1513609112. URL: http://www.pnas.org/lookup/doi/10.1073/pnas.1513609112.

Nahar, Most Altaf-Un, Tetsuya Ishida, David R Smyth, Masao Tasaka, and Mitsuhiro Aida (2012). "Interactions of CUP-SHAPED COTYLEDON and SPATULA genes control carpel margin development in Arabidopsis thaliana." In: *Plant and Cell Physiology* 53.6, pp. 1134–1143. DOI: 10.1093/pcp/pcs057. URL: https://academic.oup.com/pcp/article-lookup/doi/10.1093/pcp/pcs057.

Nikovics, Krisztina, Thomas Blein, Alexis Peaucelle, Tetsuya Ishida, Halima Morin, Mitsuhiro Aida, and Patrick Laufs (2006). "The balance between the MIR164A and CUC2 genes controls leaf margin serration in Arabidopsis." In: *The Plant Cell* 18.11, pp. 2929–2945. DOI: 10.1105/tpc.106.045617. URL: http://www.plantcell.org/cgi/doi/10.1105/tpc.106.045617.

Oh, Eunkyoo, Jia-Ying Zhu, Ming-Yi Bai, Rafael Augusto Arenhart, Yu Sun, and Zhi-Yong Wang (2014). "Cell elongation is regulated through a central circuit of interacting transcription factors in the Arabidopsis hypocotyl". In: *eLife* 3, pp. 601–19. DOI: 10.7554/eLife.03031. URL: http://elifesciences.org/lookup/doi/10.7554/eLife.03031.

Olsen, Addie Nina, Heidi A Ernst, Leila Lo Leggio, and Karen Skriver (2005). "NAC transcription factors: structurally distinct, functionally diverse." In: *Trends in plant science* 10.2, pp. 79–87. DOI: 10.1016/j.tplants.

2004.12.010. URL: http://linkinghub.elsevier.com/retrieve/pii/S1360138504002961.

O'Malley, Ronan C, Shao-shan Carol Huang, Liang Song, Mathew G Lewsey, Anna Bartlett, Joseph R Nery, Mary Galli, Andrea Gallavotti, and Joseph R Ecker (2016). "Cistrome and Epicistrome Features Shape the Regulatory DNA Landscape." In: *Cell* 165.5, pp. 1280–1292. DOI: 10.1016/j.cell.2016.04.038. URL: http://linkinghub.elsevier.com/retrieve/pii/S0092867416304810.

Ó'Maoiléidigh, Diarmuid S, Samuel E Wuest, Liina Rae, Andrea Raganelli, Patrick T Ryan, Kamila Kwasniewska, Pradeep Das, Amanda J Lohan, Brendan Loftus, Emmanuelle Graciet, and Frank Wellmer (2013). "Control of reproductive floral organ identity specification in Arabidopsis by the C function regulator AGAMOUS." In: *The Plant Cell* 25.7, pp. 2482–2503. DOI: 10.1105/tpc.113.113209. URL: http://www.plantcell.org/cgi/doi/10.1105/tpc.113.113209.

Ooka, Hisako, Kouji Satoh, Koji Doi, Toshifumi Nagata, Yasuhiro Otomo, Kazuo Murakami, Kenichi Matsubara, Naoki Osato, Jun Kawai, Piero Carninci, Yoshihide Hayashizaki, Koji Suzuki, Keiichi Kojima, Yoshinori Takahara, Koji Yamamoto, and Shoshi Kikuchi (2003). "Comprehensive analysis of NAC family genes in Oryza sativa and Arabidopsis thaliana." In: *DNA research : an international journal for rapid publication of reports on genes and genomes* 10.6, pp. 239–247. URL: http://eutils.ncbi.nlm.nih.gov/entrez/eutils/elink.fcgi?dbfrom=pubmed&id=15029955&retmode=ref&cmd=prlinks.

Pagnussat, Gabriela C, Hee-Ju Yu, Quy A Ngo, Sarojam Rajani, Sevugan Mayalagu, Cameron S Johnson, Arnaud Capron, Li-Fen Xie, De Ye, and Venkatesan Sundaresan (2005). "Genetic and molecular identification of genes required for female gametophyte development and function in Arabidopsis." In: *Development* 132.3, pp. 603–614. DOI: 10.1242/dev.01595. URL: http://dev.biologists.org/cgi/doi/10.1242/dev.01595.

Pajoro, A, S Biewers, E Dougali, F Leal Valentim, M A Mendes, A Porri, G Coupland, Y Van de Peer, A D J van Dijk, L Colombo, B Davies, and G C Angenent (2014). "The (r)evolution of gene regulatory networks controlling Arabidopsis plant reproduction: a two-decade history". In: *Journal of Experimental Botany* 65.17, pp. 4731–4745. DOI: 10.1093/jxb/eru233. URL: http://jxb.oxfordjournals.org/lookup/doi/10.1093/jxb/eru233.

Pajoro, Alice, Madrigal, Pedro, Muiño, Jose M, Matus, José Tomás, Jin, Jian, Mecchia, Martin A, Debernardi, Juan M, Palatnik, Javier F, Balazadeh, Salma, Arif, Muhammad, Ó'Maoiléidigh, Diarmuid S, Wellmer, Frank, Krajewski, Pawel, Riechmann, José Luis, Angenent, Gerco C, and Kaufmann, Kerstin (2014). "Dynamics of chromatin accessibility and gene regulation by MADS-domain transcription factors in flower development." In: *Genome Biology* 15.3, R41. DOI: 10.1186/gb-2014-15-3-r41. URL: http://eutils.ncbi.nlm.nih.gov/entrez/eutils/elink.fcgi?dbfrom=pubmed&id=24581456&retmode=ref&cmd=prlinks.

Paz-Aviram, Tal, Avital Yahalom, and Daniel A Chamovitz (2008). "Arabidopsis eIF3e interacts with subunits of the ribosome, Cop9 signalosome and proteasome." In: *Plant Signaling & Behavior* 3.6, pp. 409–411. DOI: 10.1111/j.1365-313X.2007.03347.x. URL: http://doi.wiley.com/10.1111/j.1365-313X.2007.03347.x.

Pelaz, S, G S Ditta, E Baumann, E Wisman, and M F Yanofsky (2000). "B and C floral organ identity functions require SEPALLATA MADS-box genes." In: *Nature* 405.6783, pp. 200–203. DOI: 10.1038/35012103. URL: http://www.nature.com/doifinder/10.1038/35012103.

Pinyopich, Anusak, Gary S Ditta, Beth Savidge, Sarah J Liljegren, Elvira Baumann, Ellen Wisman, and Martin F Yanofsky (2003). "Assessing the redundancy of MADS-box genes during carpel and ovule development". In: *Nature* 424.6944, pp. 85–88. DOI: 10.1038/nature01741. URL: http://www.nature.com/doifinder/10.1038/nature01741.

Puranik, Swati, Pranav Pankaj Sahu, Prem S Srivastava, and Manoj Prasad (2012). "NAC proteins: regulation and role in stress tolerance." In: *Trends in plant science* 17.6, pp. 369–381. DOI: 10.1016/j.tplants.2012.02.004. URL: http://eutils.ncbi.nlm.nih.gov/entrez/eutils/elink.fcgi?dbfrom=pubmed&id=22445067&retmode=ref&cmd=prlinks.

Quinlan, Aaron R and Ira M Hall (2010). "BEDTools: a flexible suite of utilities for comparing genomic features." In: *Bioinformatics (Oxford, England)* 26.6, pp. 841–842. DOI: 10.1093/bioinformatics/btq033. URL: http://eutils.ncbi.nlm.nih.gov/entrez/eutils/elink.fcgi?dbfrom=pubmed&id=20110278&retmode=ref&cmd=prlinks.

R Core Team (2017). *R: A Language and Environment for Statistical Computing*. R Foundation for Statistical Computing. Vienna, Austria. URL: https://www.R-project.org/.

Raasi, Shahri and Dieter H Wolf (2007). "Ubiquitin receptors and ERAD: A network of pathways to the proteasome". In: *Seminars in Cell & Developmental Biology* 18.6, pp. 780–791. DOI: 10.1016/j.semcdb.2007.09.008. URL: http://linkinghub.elsevier.com/retrieve/pii/S1084952107001462.

Raman, Smita, Thomas Greb, Alexis Peaucelle, Thomas Blein, Patrick Laufs, and Klaus Theres (2008). "Interplay of miR164, CUP-SHAPED COTYLEDON genes and LATERAL SUPPRESSOR controls axillary meristem formation in Arabidopsis thaliana." In: *The Plant Journal* 55.1, pp. 65–76. DOI: 10.1111/j.1365-313X.2008.03483.x. URL: http://doi.wiley.com/10.1111/j.1365-313X.2008.03483.x.

Rast, Madlen I and Rüdiger Simon (2008). "The meristem-to-organ boundary: more than an extremity of anything." In: *Current opinion in genetics & development* 18.4, pp. 287–294. DOI: 10.1016/j.gde.2008.05.005. URL: http://linkinghub.elsevier.com/retrieve/pii/S0959437X08000713.

Riechmann, J L, J Heard, G Martin, L Reuber, C Jiang, J Keddie, L Adam, O Pineda, O J Ratcliffe, R R Samaha, R Creelman, M Pilgrim, P Broun, J Z Zhang, D Ghandehari, B K Sherman, and G Yu (2000). "Arabidopsis transcription factors: genome-wide comparative analysis among eukaryotes." In: *Science (New York, N.Y.)* 290.5499, pp. 2105–2110. URL:

http://eutils.ncbi.nlm.nih.gov/entrez/eutils/elink.fcgi?dbfrom=pubmed&id=11118137&retmode=ref&cmd=prlinks.

Ritchie, Matthew E, Belinda Phipson, Di Wu, Yifang Hu, Charity W Law, Wei Shi, and Gordon K Smyth (2015). "limma powers differential expression analyses for RNA-sequencing and microarray studies." In: *Nucleic acids research* 43.7, e47. DOI: 10.1093/nar/gkv007. URL: http://eutils.ncbi.nlm.nih.gov/entrez/eutils/elink.fcgi?dbfrom=pubmed&id=25605792&retmode=ref&cmd=prlinks.

Rogers, Kestrel and Xuemei Chen (2013). "Biogenesis, turnover, and mode of action of plant microRNAs." In: *The Plant cell* 25.7, pp. 2383–2399. DOI: 10.1105/tpc.113.113159. URL: http://eutils.ncbi.nlm.nih.gov/entrez/eutils/elink.fcgi?dbfrom=pubmed&id=23881412&retmode=ref&cmd=prlinks.

Rubin, D M, M H Glickman, C N Larsen, S Dhruvakumar, and D Finley (1998). "Active site mutants in the six regulatory particle ATPases reveal multiple roles for ATP in the proteasome." In: *The EMBO journal* 17.17, pp. 4909–4919. DOI: 10.1093/emboj/17.17.4909. URL: http://emboj.embopress.org/cgi/doi/10.1093/emboj/17.17.4909.

Sadanandom, Ari, Mark Bailey, Richard Ewan, Jack Lee, and Stuart Nelis (2012). "The ubiquitin-proteasome system: central modifier of plant signalling". In: *New Phytologist* 196.1, pp. 13–28. DOI: 10.1111/j.1469-8137.2012.04266.x. URL: http://doi.wiley.com/10.1111/j.1469-8137.2012.04266.x.

Sakai, H, L J Medrano, and E M Meyerowitz (1995). "Role of SUPERMAN in maintaining Arabidopsis floral whorl boundaries." In: *Nature* 378.6553, pp. 199–203. DOI: 10.1038/378199a0. URL: http://www.nature.com/doifinder/10.1038/378199a0.

Schwab, Rebecca, Javier F Palatnik, Markus Riester, Carla Schommer, Markus Schmid, and Detlef Weigel (2005). "Specific effects of microRNAs on the plant transcriptome." In: *Developmental Cell* 8.4, pp. 517–527. DOI: 10.1016/j.devcel.2005.01.018. URL: http://linkinghub.elsevier.com/retrieve/pii/S1534580705000225.

Shannon, Paul, Andrew Markiel, Owen Ozier, Nitin S Baliga, Jonathan T Wang, Daniel Ramage, Nada Amin, Benno Schwikowski, and Trey Ideker (2003). "Cytoscape: a software environment for integrated models of biomolecular interaction networks." In: *Genome research* 13.11, pp. 2498–2504. DOI: 10.1101/gr.1239303. URL: http://eutils.ncbi.nlm.nih.gov/entrez/eutils/elink.fcgi?dbfrom=pubmed&id=14597658&retmode=ref&cmd=prlinks.

Sieber, Patrick, Frank Wellmer, Jacqueline Gheyselinck, José Luis Riechmann, and Elliot M Meyerowitz (2007). "Redundancy and specialization among plant microRNAs: role of the *MIR164* family in developmental robustness." In: *Development* 134.6, pp. 1051–1060. DOI: 10.1242/dev.02817. URL: http://dev.biologists.org/cgi/doi/10.1242/dev.02817.

Smaczniak, Cezary, Richard G H Immink, Jose M Muiño, Robert Blanvillain, Marco Busscher, Jacqueline Busscher-Lange, Q D Peter Dinh, Shujing Liu, Adrie H Westphal, Sjef Boeren, François Parcy, Lin Xu, Cristel C Carles, Gerco C Angenent, and Kerstin Kaufmann (2012a). "Characterization of MADS-domain transcription factor complexes in *Arabidopsis* flower development." In: *Proceedings of the National Academy of Sciences of the United States of America* 109.5, pp. 1560–1565. DOI: 10.1073/pnas.1112871109. URL: http://www.pnas.org/cgi/doi/10.1073/pnas.1112871109.

Smaczniak, Cezary, Na Li, Sjef Boeren, Twan America, Walter van Dongen, Soenita S Goerdayal, Sacco de Vries, Gerco C Angenent, and Kerstin Kaufmann (2012b). "Proteomics-based identification of low-abundance signaling and regulatory protein complexes in native plant tissues". In: *Nature Protocols* 7.12, pp. 2144–2156. DOI: 10.1038/nprot.2012.129. URL: http://dx.doi.org/10.1038/nprot.2012.129.

Smalle, Jan and Richard D Vierstra (2004). "THE UBIQUITIN 26S PROTEASOME PROTEOLYTIC PATHWAY". In: *Annual review of plant biology* 55.1, pp. 555–590. DOI: 10.1146/annurev.arplant.55.031903.141801. URL: http://www.annualreviews.org/doi/10.1146/annurev.arplant.55.031903.141801.

Smyth, D R, J L Bowman, and E M Meyerowitz (1990). "Early flower development in Arabidopsis." In: *The Plant Cell* 2.8, pp. 755–767. DOI: 10.1105/tpc.2.8.755. URL: http://eutils.ncbi.nlm.nih.gov/entrez/eutils/elink.fcgi?dbfrom=pubmed&id=2152125&retmode=ref&cmd=prlinks.

Smyth, Gordon K and Terry Speed (2003). "Normalization of cDNA microarray data". In: *Methods* 31.4, pp. 265–273. DOI: 10.1016/s1046-2023(03)00155-5.

Souer, E, A van Houwelingen, D Kloos, J Mol, and R Koes (1996). "The no apical meristem gene of Petunia is required for pattern formation in embryos and flowers and is expressed at meristem and primordia boundaries." In: *Cell* 85.2, pp. 159–170. URL: http://eutils.ncbi.nlm.nih.gov/entrez/eutils/elink.fcgi?dbfrom=pubmed&id=8612269&retmode=ref&cmd=prlinks.

Spinelli, Silvana V, Ana Paula Martin, Ivana L Viola, Daniel H Gonzalez, and Javier F Palatnik (2011). "A mechanistic link between STM and CUC1 during Arabidopsis development." In: *Plant physiology* 156.4, pp. 1894–1904. DOI: 10.1104/pp.111.177709. URL: http://www.plantphysiol.org/cgi/doi/10.1104/pp.111.177709.

Takada, S, K Hibara, T Ishida, and M Tasaka (2001). "The *CUP-SHAPED COTYLEDON1* gene of *Arabidopsis* regulates shoot apical meristem formation." In: *Development* 128.7, pp. 1127–1135. URL: http://dev.biologists.org/content/128/7/1127.abstract.

Takeda, Seiji, Noritaka Matsumoto, and Kiyotaka Okada (2004). "RABBIT EARS, encoding a SUPERMAN-like zinc finger protein, regulates petal development in Arabidopsis thaliana." In: *Development (Cambridge, England)* 131.2, pp. 425–434. DOI: 10.1242/dev.00938. URL: http://eutils.

ncbi.nlm.nih.gov/entrez/eutils/elink.fcgi?dbfrom=pubmed&id=14681191&retmode=ref&cmd=prlinks.

Takeda, Seiji, Keiko Hanano, Ayano Kariya, Satoko Shimizu, Li Zhao, Minami Matsui, Masao Tasaka, and Mitsuhiro Aida (2011). "CUP-SHAPED COTYLEDON1 transcription factor activates the expression of LSH4 and LSH3, two members of the ALOG gene family, in shoot organ boundary cells." In: *The Plant Journal* 66.6, pp. 1066–1077. DOI: 10.1111/j.1365-313X.2011.04571.x. URL: http://doi.wiley.com/10.1111/j.1365-313X.2011.04571.x.

Taoka, Ken-ichiro, Yoshiko Yanagimoto, Yasufumi Daimon, Ken-ichiro Hibara, Mitsuhiro Aida, and Masao Tasaka (2004). "The NAC domain mediates functional specificity of CUP-SHAPED COTYLEDON proteins." In: *The Plant Journal* 40.4, pp. 462–473. DOI: 10.1111/j.1365-313X.2004.02238.x. URL: http://doi.wiley.com/10.1111/j.1365-313X.2004.02238.x.

Theissen, G and H Saedler (2001). "Plant biology. Floral quartets." In: *Nature* 409.6819, pp. 469–471. DOI: 10.1038/35054172. URL: http://eutils.ncbi.nlm.nih.gov/entrez/eutils/elink.fcgi?dbfrom=pubmed&id=11206529&retmode=ref&cmd=prlinks.

Tian, C, X Zhang, J He, H Yu, Y Wang, B Shi, Y Han, G Wang, X Feng, C Zhang, J Wang, J Qi, R Yu, and Y Jiao (2014). "An organ boundary-enriched gene regulatory network uncovers regulatory hierarchies underlying axillary meristem initiation". In: *Molecular systems biology* 10.10, pp. 755–755. DOI: 10.15252/msb.20145470. URL: http://msb.embopress.org/cgi/doi/10.15252/msb.20145470.

Topisirovic, Ivan, Alex Kentsis, Jacqueline M Perez, Monica L Guzman, Craig T Jordan, and Katherine L B Borden (2005). "Eukaryotic translation initiation factor 4E activity is modulated by HOXA9 at multiple levels." In: *Molecular and cellular biology* 25.3, pp. 1100–1112. DOI: 10.1128/MCB.25.3.1100-1112.2005. URL: http://eutils.ncbi.nlm.nih.gov/entrez/eutils/elink.fcgi?dbfrom=pubmed&id=15657436&retmode=ref&cmd=prlinks.

Tweneboah, Solomon and Sang-Keun Oh (2017). "Biological roles of NAC transcription factors in the regulation of biotic and abiotic stress responses in solanaceous crops". In: *Journal of Plant Biotechnology* 44.1, pp. 1–11. DOI: 10.5010/JPB.2017.44.1.001. URL: http://www.kspbtjpb.org/journal/view.html?doi=10.5010/JPB.2017.44.1.001.

Vain, Philippe, Vera Thole, Barbara Worland, Magdalena Opanowicz, Max S Bush, and John H Doonan (2011). "A T-DNA mutation in the RNA helicase eIF4A confers a dose-dependent dwarfing phenotype in Brachypodium distachyon." In: *The Plant journal : for cell and molecular biology* 66.6, pp. 929–940. DOI: 10.1111/j.1365-313X.2011.04555.x. URL: http://eutils.ncbi.nlm.nih.gov/entrez/eutils/elink.fcgi?dbfrom=pubmed&id=21457366&retmode=ref&cmd=prlinks.

Vidal, Elena A, Tomás C Moyano, Eleodoro Riveras, Orlando Contreras-López, and Rodrigo A Gutiérrez (2013). "Systems approaches map regulatory networks downstream of the auxin receptor AFB3 in the nitrate response of Arabidopsis thaliana roots." In: *Proceedings of the National Academy of Sciences of the United States of America* 110.31, pp. 12840–12845. DOI: 10.1073/pnas.1310937110. URL: http://www.pnas.org/cgi/doi/10.1073/pnas.1310937110.

Vroemen, Casper W, Andreas P Mordhorst, Cathy Albrecht, Mark A C J Kwaaitaal, and Sacco C de Vries (2003). "The CUP-SHAPED COTYLEDON3 gene is required for boundary and shoot meristem formation in Arabidopsis." In: *The Plant cell* 15.7, pp. 1563–1577. URL: http://eutils.ncbi.nlm.nih.gov/entrez/eutils/elink.fcgi?dbfrom=pubmed&id=12837947&retmode=ref&cmd=prlinks.

Wang, Quan, Wouter Kohlen, Susanne Rossmann, Teva Vernoux, and Klaus Theres (2014). "Auxin Depletion from the Leaf Axil Conditions Competence for Axillary Meristem Formation in Arabidopsis and Tomato." In: *The Plant cell* 26.5, pp. 2068–2079. DOI: 10.1105/tpc.114.123059. URL: http://eutils.ncbi.nlm.nih.gov/entrez/eutils/elink.fcgi?dbfrom=pubmed&id=24850851&retmode=ref&cmd=prlinks.

Wang, Quan, Alice Hasson, Susanne Rossmann, and Klaus Theres (2015). "*Divide et impera*: boundaries shape the plant body and initiate new meristems." In: *New Phytologist*, n/a–n/a. DOI: 10.1111/nph.13641. URL: http://doi.wiley.com/10.1111/nph.13641.

Weir, Irene, Jianping Lu, Holly Cook, Barry Causier, Zsuzsanna Schwarz-Sommer, and Brendan Davies (2004). "CUPULIFORMIS establishes lateral organ boundaries in Antirrhinum." In: *Development (Cambridge, England)* 131.4, pp. 915–922. DOI: 10.1242/dev.00993. URL: http://eutils.ncbi.nlm.nih.gov/entrez/eutils/elink.fcgi?dbfrom=pubmed&id=14757643&retmode=ref&cmd=prlinks.

Wellmer, Frank, Márcio Alves-Ferreira, Annick Dubois, José Luis Riechmann, and Elliot M Meyerowitz (2006). "Genome-wide analysis of gene expression during early Arabidopsis flower development." In: *PLoS genetics* 2.7, e117. DOI: 10.1371/journal.pgen.0020117.eor. URL: http://dx.plos.org/10.1371/journal.pgen.0020117.

Welner, Ditte H, Farah Deeba, Leila Lo Leggio, and Karen Skriver (2015). *NAC Transcription Factors: From Structure to Function in Stress-Associated Networks*. Elsevier Inc. DOI: 10.1016/B978-0-12-800854-6/00013-0. URL: http://dx.doi.org/10.1016/B978-0-12-800854-6/00013-0.

Wikström, N, V Savolainen, and M W Chase (2001). "Evolution of the angiosperms: calibrating the family tree." In: *Proceedings. Biological sciences* 268.1482, pp. 2211–2220. DOI: 10.1098/rspb.2001.1782. URL: http://rspb.royalsocietypublishing.org/cgi/doi/10.1098/rspb.2001.1782.

Winter, Cara M, Ryan S Austin, Servane Blanvillain-Baufumé, Maxwell A Reback, Marie Monniaux, Miin-Feng Wu, Yi Sang, Ayako Yamaguchi, Nobutoshi Yamaguchi, Jane E Parker, François Parcy, Shane T Jensen,

Hongzhe Li, and Doris Wagner (2011). "LEAFY target genes reveal floral regulatory logic, cis motifs, and a link to biotic stimulus response." In: *Developmental Cell* 20.4, pp. 430–443. DOI: 10.1016/j.devcel.2011.03.019. URL: http://linkinghub.elsevier.com/retrieve/pii/S1534580711001250.

Winter, Debbie, Ben Vinegar, Hardeep Nahal, Ron Ammar, Greg V Wilson, and Nicholas J Provart (2007). "An "Electronic Fluorescent Pictograph" browser for exploring and analyzing large-scale biological data sets." In: *PloS one* 2.8, e718. DOI: 10.1371/journal.pone.0000718. URL: http://eutils.ncbi.nlm.nih.gov/entrez/eutils/elink.fcgi?dbfrom=pubmed&id=17684564&retmode=ref&cmd=prlinks.

Wuest, Samuel E, Diarmuid S Ó'Maoiléidigh, Liina Rae, Kamila Kwasniewska, Andrea Raganelli, Katarzyna Hanczaryk, Amanda J Lohan, Brendan Loftus, Emmanuelle Graciet, and Frank Wellmer (2012). "Molecular basis for the specification of floral organs by APETALA3 and PISTILLATA." In: *Proceedings of the National Academy of Sciences of the United States of America* 109.33, pp. 13452–13457. DOI: 10.1073/pnas.1207075109. URL: http://www.pnas.org/cgi/doi/10.1073/pnas.1207075109.

Yahalom, A, T H Kim, E Winter, B Karniol, A G von Arnim, and D A Chamovitz (2001). "Arabidopsis eIF3e (INT-6) associates with both eIF3c and the COP9 signalosome subunit CSN7." In: *The Journal of biological chemistry* 276.1, pp. 334–340. DOI: 10.1074/jbc.M006721200. URL: http://www.jbc.org/lookup/doi/10.1074/jbc.M006721200.

Yekutieli, Daniel and Yoav Benjamini (2001). "The control of the false discovery rate in multiple testing under dependency". In: *The Annals of Statistics* 29.4, pp. 1165–1188. DOI: 10.1214/aos/1013699998. URL: http://dx.doi.org/10.1214/aos/1013699998.

Yen, Hsueh-Chi S, Colin Gordon, and Eric C Chang (2003). "Schizosaccharomyces pombe Int6 and Ras homologs regulate cell division and mitotic fidelity via the proteasome." In: *Cell* 112.2, pp. 207–217. URL: http://eutils.ncbi.nlm.nih.gov/entrez/eutils/elink.fcgi?dbfrom=pubmed&id=12553909&retmode=ref&cmd=prlinks.

Yoshida, Akiko, Takuya Suzaki, Wakana Tanaka, and Hiro-Yuki Hirano (2009). "The homeotic gene long sterile lemma (G1) specifies sterile lemma identity in the rice spikelet." In: *Proceedings of the National Academy of Sciences of the United States of America* 106.47, pp. 20103–20108. DOI: 10.1073/pnas.0907896106. URL: http://eutils.ncbi.nlm.nih.gov/entrez/eutils/elink.fcgi?dbfrom=pubmed&id=19901325&retmode=ref&cmd=prlinks.

Žádníková, Petra and Rüdiger Simon (2014). "How boundaries control plant development." In: *Current opinion in plant biology* 17, pp. 116–125. DOI: 10.1016/j.pbi.2013.11.013. URL: http://linkinghub.elsevier.com/retrieve/pii/S1369526613001866.

Zhang, Yong, Tao Liu, Clifford A Meyer, Jérôme Eeckhoute, David S Johnson, Bradley E Bernstein, Chad Nusbaum, Richard M Myers, Myles

Brown, Wei Li, and X Shirley Liu (2008). "Model-based analysis of ChIP-Seq (MACS)." In: *Genome biology* 9.9, R137. DOI: 10.1186/gb-2008-9-9-r137. URL: http://eutils.ncbi.nlm.nih.gov/entrez/eutils/elink.fcgi?dbfrom=pubmed&id=18798982&retmode=ref&cmd=prlinks.

Zhang, Zhonghui, Xiuying Liu, Xinwei Guo, Xiu-Jie Wang, and Xiuren Zhang (2016). "Arabidopsis AGO3 predominantly recruits 24-nt small RNAs to regulate epigenetic silencing." In: *Nature Plants* 2.5, p. 16049. DOI: 10.1038/nplants.2016.49. URL: http://www.nature.com/articles/nplants201649.

Zhu, Tingting, Eviatar Nevo, Dongfa Sun, and Junhua Peng (2012). "Phylogenetic analyses unravel the evolutionary history of NAC proteins in plants." In: *Evolution; international journal of organic evolution* 66.6, pp. 1833–1848. DOI: 10.1111/j.1558-5646.2011.01553.x. URL: http://doi.wiley.com/10.1111/j.1558-5646.2011.01553.x.

Zimmermann, Roman and Wolfgang Werr (2005). "Pattern formation in the monocot embryo as revealed by NAM and CUC3 orthologues from Zea mays L." In: *Plant molecular biology* 58.5, pp. 669–685. DOI: 10.1007/s11103-005-7702-x. URL: http://eutils.ncbi.nlm.nih.gov/entrez/eutils/elink.fcgi?dbfrom=pubmed&id=16158242&retmode=ref&cmd=prlinks.